Department of Imaging and Applied Physics

Centre for Marine Science and Technology

Recognition and assessment of seafloor vegetation using a single beam echosounder

Yao-Ting Tseng

This thesis is presented for the Degree of
Doctor of Philosophy
of
Curtin University of Technology

February 2009

Declaration

To the best of my knowledge and belief this thesis contains no material previously published by any other person except where due acknowledgment has been made. This thesis contains no material which has been accepted for the award of any other degree or diploma in any university.

Signature:

Date:

Dedicate to Chien-Youh, Yi-Yen, Jun-Sen, Yu-Cheng

and

Fu-Chen

Acknowledgments

In this study, I firstly give my great thanks to emeritus professor John Penrose. It is him who provided an opportunity for me to secure a scholarship for this study. Secondly, my major supervisor, Professor Alexander Gavrilov, is the one who had generously provided his support for my study. His knowledge and expertise in marine acoustics provided me with a living reference resource.

Persons who had provided helps on this study all should be acknowledged. They include Dr. Alec Duncan, Dr. Rob McCauley, Dr. Gary Kendrick from University of Western Australia, Dr. Justy Siwabessy, and Mr. Andrew Woods. They were the key members involved in my study. Besides these, technicians such as Mr. Frank Thomas, Mr. Malcolm Perry, and Mr. Amos Maggi deserve mention for their great support for the project-related tasks. Thanks also go to the Centre's administration secretary Mrs. Ann Smith.

Colleagues such as Susan Rennie, Chris van Etten, Iain Parnum, Miles Parsons, Matthew Legg, and many friends had provided their helpful comments on my study. Their company in the office and their encouragement provided invaluable help for me to complete this study.

Key members from the Cooperative Research Centre for Coastal Zone, Estuary and Waterway Management (Coastal CRC) deserve thanks for their great support of my research work. They include Chief Executive Officer Dr. Rob Fearon, Executive Assistant Mr. Paul Pinjuh, and Post Graduate Student Coordinator Ms Theresa Leijten. During my study period, the scholarship support from the Coastal CRC provided me great opportunities to engage with the Coastal Water Habitat Mapping project and to participate in many national and international academic activities. The knowledge and experience acquired from these engagements will definitely bring advantages and advancements for my future development. In concluding this work, Mr. Brett Grobaski provided his help on the tedious proofreading task. I appreciate his support when he was also preparing for his wedding in Taiwan.

For the completion of chapter five, I would like to express my gratitude to Michael Harwerth from Germany, Sara Silva from Portugal, Peter Day and Helen Gray from UK, Erick Cantu-Paz from Lawrence Livermore National Laboratory, Ruixiang Sun from China, and many experts from the Genetic Programming community in providing helpful suggestions for me to commence the study of Genetic Programming. Thanks to the major author of GPLAB and many experts in this area in generously providing their comments for the application of GP on this particular study. Through their invaluable comments, I was finally able to have some Genetic Programming study results for marine science and make this study different.

Taiwanese friends in Western Australia provided help for me to better adapt to Australia's culture. Thanks for the enthusiastic help from the Taiwanese Chamber of Commerce of Western Australia and the Curtin Taiwanese Students Association. It was a very warm experience from the engagements with those friends in practicing the same cultural activities. I heartily appreciate their supports and cares during our living in Western Australia.

I extend my acknowledgment to Miss Christine Cooper in Brisbane for her suggestion that I could have my study in Australia. Without her suggestion, I wouldn't have this chance to start this study.

Lastly, I would like to express my gratitude to my family members. My children stayed most of time with me in the study period from 2003 till the end of 2005 in Australia. They were the core of my daily life. We shared the same joys and disappointments within this study period. Through the daily engagement, they gained their invaluable experiences from their stay and studies in Australia. Instead of the author, it is them who had given me much help in dealing with the daily life so that I was able to concentrate my whole energy on my study. Lastly but surely not the least, my wife is the person who has greatly supported me so that I could restart my study again after 15-year's leave from the university. Thanks go to her encouragement and her endurance of our long term separation during this study. She deserves my most gratitude.

Abstract

This study focuses on the potential of using a single beam echosounder as a tool for recognition and assessment of seafloor vegetation. Seafloor vegetation is plant benthos and occupies a large portion of the shallow coastal bottoms. It plays a key role in maintaining the ecological balance by influencing the marine and terrestrial worlds through interactions with its surrounding environment. Understanding of its existence on the seafloor is essential for environmental managers.

Due to the important role of seafloor vegetation to the environment, a detailed investigation of acoustic methods that can provide effective recognition and assessment of the seafloor vegetation by using available sonar systems is necessary. One of the frequently adopted approaches to the understanding of ocean environment is through the mapping of the seafloor. Available acoustic techniques vary in kinds and are used for different purposes. Because of the wide scope of available techniques and methods which can be employed in the field, this study has limited itself to sonar techniques of normal incidence configuration relative to seafloors in selected regions and for particular marine habitats. For this study, a single beam echosounder operating at two frequencies was employed. Integrated with the echosounder was a synchronized optical system. The synchronization mechanism between the acoustic and optical systems provided capabilities to have very accurate groundtruth recordings for the acoustic data, which were then utilized as a supervised training data set for the recognition of seafloor vegetation.

In this study, results acquired and conclusions made were all based on the comparison against the photographic recordings. The conclusion drawn from this investigation is only as accurate as within the selected habitat types and within very shallow water regions.

In order to complete this study, detailed studies of literature and deliberately designed field experiments were carried out. Acoustic data classified with the help of the synchronized optical system were investigated by several methods. Conventional methods such as statistics and multivariate analyses were examined. Conventional

methods for the recognition of the collected data gave some useful results but were found to have limited capabilities. When seeking for more robust methods, an alternative approach, Genetic Programming (GP), was tested on the same data set for comparison. Ultimately, the investigation aims to understand potential methods which can be effective in differentiating the acoustic backscatter signals of the habitats observed and subsequently distinguishing between the habitats involved in this study.

Table of contents

Acknowledgments i
Abstract iii
Table of contents v
List of figures x
List of tables xx
Glossary of symbols xxii

Chapter 1 Introduction 1
1.1 Background and significance 1
1.2 Research objectives 3
1.3 Thesis structure 3

Chapter 2 Historical studies of seafloor vegetation and the substrate 5
2.1 Acoustic studies of seafloor vegetation 5
2.1.1 Introduction of marine benthos 5
2.1.2 Animal benthos 6
2.1.3 Plant benthos 8
2.1.3.1 *Hydrilla* and *Lyngbya*: a historical study ... 8
2.1.3.2 A modelling study for algae 9
2.1.3.3 Areal studies for seagrass and macro algae 11
2.1.3.3.1 Australia 12
2.1.3.3.2 Canada 13
2.1.3.3.3 France 15
2.1.3.3.4 Italy 16
2.1.3.3.5 Japan 19
2.1.3.3.6 Poland 20
2.1.3.3.7 Spain 24
2.1.3.3.8 USA 26
2.2 Seagrass in Western Australia 29
2.2.1 Coverage and diversity 30
2.2.2 Biological features of *P. sinuosa* and *P. australis* 32
2.2.2.1 Meadow and canopy structure 33

2.2.2.2 Leaf area index and pollination features .. 35
2.2.2.3 Anatomy of seagrass 37
2.3 Acoustic studies of seafloor substrates 39
2.3.1 Relevance of seafloor substrates to this study 39
2.3.2 Classification techniques developed 40
2.4 Acoustics used in various problem related tasks..... 41
2.5 Commercial classification techniques..... 42
2.5.1 RoxAnn 43
2.5.2 QTC..... 44
2.5.3 BioSonics 45
2.5.3.1 B1 method 45
2.5.3.2 B2 method 46
2.5.3.3 B3 method 47
2.5.3.4 B4 method 50
2.6 Observations of seafloor backscatter characteristics at different frequencies 52
2.7 Concluding remarks 52

Chapter 3 Instrumentation and data collections..... 54
3.1 The Epi-benthic Scattering Project (ESP)..... 54
3.2 Instrumentation 55
3.2.1 Development of data collection facilities..... 56
3.2.1.1 The ESP structure..... 56
3.2.1.2 The TAPS..... 59
3.2.1.3 The ESP data collection system 59
3.2.1.4 The wet end box and the cameras 61
3.2.1.5 The acoustic sub-system: EQ60 63
3.2.1.5.1 Characteristics of EQ60 64
3.2.2 Synchronization of the optical and acoustic systems.. 65
3.3 Field trials and data collections..... 67
3.3.1 The first field trial 68
3.3.1.1 Field deployment..... 68
3.3.1.2 Samples collected..... 71
3.3.1.3 Biological features of observed seagrasses75

3.3.2 The second field trial 77
3.3.2.1 Field deployment 77
3.3.2.2 Samples collected..... 78
3.3.3 The third field trial..... 83
3.3.3.1 Strategic changes and investigations of depth dependence..... 84
3.3.3.2 Samples collected..... 85
3.4 Differences between 38 and 200 kHz 88
3.5 Data conversion 88
3.6 Classification methodology 90
3.6.1 Photographic classification 90
3.6.1.1 Issues due to the system configuration 92
3.6.2 Classified acoustic data..... 95
3.7 Summary 95

Chapter 4 Conventional study results 96
4.1 Study considerations 96
4.1.1 Applicability of backscatter theory to seafloor vegetation..... 96
4.1.2 Waveform analysis 97
4.1.3 Location of the bottom from the waveform analysis.. 98
4.2 Cockburn Sound 2004..... 100
4.2.1 Characterization parameters 100
4.2.1.1 Bottom backscatter strength..... 100
4.2.1.2 Echo-average backscatter strength..... 103
4.2.1.3 Effective pulse width 104
4.2.1.4 Hurst exponent and fractals 109
4.2.2 Detection abilities of the 38 and 200 kHz sonars 112
4.2.3 Detection of seagrass canopy..... 114
4.3 Owen Anchorage and Parmelia Bank 2005 116
4.3.1 Sea squirts..... 116
4.3.2 Classification performance for only sand and seagrass117
4.3.3 Dependence of characterization parameters on range121
4.3.4 Range difference (RD) and seagrass canopy height . 123

4.3.5 Differences between dense and sparse dispositions.. 127
4.4 Multivariate approach 130
4.4.1 Correlations among statistics 130
4.4.2 Principal components analysis 135
4.4.2.1 Kaiser's rule 136
4.4.2.1.1 Input parameters: Statistics . 137
4.4.2.1.2 Input parameters: Statistics and EPW 141
4.4.3 Linear discriminant analysis 148
4.5 Summary 152

Chapter 5 Application of Genetic Programming 155
5.1 Study motivation 155
5.2 A novel approach for feature extraction..... 156
5.2.1 Supervised training for classification..... 156
5.3 Introduction of GP..... 157
5.3.1 Genetic evolution of computing programs..... 158
5.3.1.1 Tree-based GP individuals 159
5.3.1.2 Reproduction 160
5.3.1.3 Crossover..... 161
5.3.1.4 Mutation 162
5.3.1.5 Why best-so-far 162
5.4 Design of the Fitness Function for classification 163
5.5 A MATLAB toolbox for GP, GPLAB 166
5.6 Implementation of GP 167
5.6.1 Terminal and non-terminal nodes 167
5.6.2 Symbolic regression..... 167
5.6.3 Result 168
5.7 Limitations of GP 175
5.8 Summary 176

Chapter 6 Discussion 178
6.1 The experimental platform: the ESP structure 178
6.2 Conventional investigation results 179

6.2.1 Strengths and weeknesses of the characterization parameters and techniques used 181
6.3 Application of GP algorithm to classification tasks 181

Chapter 7 Conclusions and Recommendations 183
7.1 Literature review 184
7.2 Experimental materials 185
7.3 Data analysis results 186

References 189
Appendices 211

List of figures

Figure 2-1 Performance comparisons of three parameters (c, d and e) along with the echogram (a), plant height (b) and results of cluster analysis (f) over the sandy bare bottoms and plant-covered meadows presented in the work by Tęgowski, Gorska, and Klusek (Tęgowski, Gorska *et al.* 2003). 23

Figure 2-2 An experimental setup for the observations of acoustic backscatter when the macro algae was placed in the wire basket and when removed (Riegl, Purkis *et al.* 2005) 27

Figure 2-3 Recorded echograms of backscatter from eelgrass, *Zostera marina*. A and B indicate the bottom coverage of 100% and 80% by eelgrass respectively (Spratt 1989) 29

Figure 2-4 Location of Success Bank, Parmelia Bank, Owen Anchorage, and Cockburn Sound offshore of the capital of WA, Perth. The inset shows the approximate position of the areas on the Australia contour. 32

Figure 2-5 Images of *P. sinuosa* meadows from (a) a previous study (Smith and Walker 2002) showing apparent bare sand channels in rows, and from (b) the author's video record showing similar row pattern but having denser shoot cover with almost all the shoots bent horizontally. 34

Figure 2-6 Images of *P. australis* meadows from (a)[§] a previous study (Smith and Walker 2002) and from (b) the author's video record showing an apparent open canopy structure when comparing to Figure 2-5b. Areas indicated by the arrows are the spaces in the canopy where a bare sand seafloor is visible. 34

Figure 2-7 Measurements of the leaves of seagrass *P. sinuosa* with a ruler of 30 cm in length. The longest extended leaf length was over 50 cm. The leaves were collected near the Garden Island in Cockburn Sound in 2004. 35

Figure 2-8 Distribution of (a) leaf area, and (b) leaf biomass of shoots in situ in the *P. sinuosa* and *P. australis* canopies (Smith and Walker 2002) 36

Figure 2-9 Stacked distribution of the occupied areas of the "Of bent section", "At flower height", and "Below bent section" on the meadows of *P. sinuosa* and *P. australis*, and their total leaf area cover indexes according to Smith and Walker's measurement readings. 37

Figure 2-10 Transverse cross section of a portion of a *P. australis* leaf blade with air-lucuna marked by A and the cuticle on skin with porous structure (Kuo 1978). 38

Figure 2-11 Transverse cross section of a portion of a *P. sinuosa* leaf blade with air-lucuna marked by A and the cuticle on skin without porous structure (Cambridge and Kuo 1982). 38

Figure 2-12 An illustration of the scenario when acoustic backscatter is collected from a combined effect with targets in the insonified acoustic cone, including the vegetation and the sediment. 40

Figure 2-13 The first bottom echo envelopes from soft and hard bottoms illustrating the approach used in the BioSonics B1 method: (a) envelopes of the echo amplitude and (b) cumulative energy after integrating the squared echo amplitude within a certain time interval (Burczynski 2001). 46

Figure 2-14 E1 and E2 parameters used in BioSonics's B2 method for classifying different bottom types (Burczynski 2001). 47

Figure 2-15 Three successive phases of an echo showing the insonified areas on the sea bottom (Burczynski 2001). In Phase 1, the insonified area increases with time. In Phase 2, the insonified area is ring-like and increasing in diameter with time. In the last phase, the ring width rapidly decreases with time until it disappears. 48

Figure 2-16 Simulation result showing the contribution from bottom surface reverberation (short dash line) and bottom volume reverberation (long dash line) to the collected echo (solid line). 49

Figure 2-17 Numerical simulation results for the echo backscattering from fine sand (solid line), sand (short dashed line), gravel (long dashed line) and rock (alternate long and short dashed line) made by Burczynski. The shoulder at the tail of the echo gradually appeared as the bottom types varied from fine sand to rock, which indicates the contribution of the bottom volume reverberation from different types of sea bottoms. 50

Figure 3-1 Three views of the ESP data collection rig as deployed in 2005, showing its major optical and acoustic components. 57

Figure 3-2 A conceptual diagram (not to scale) showing the ESP structure when deployed in the field. This diagram has been significantly simplified in showing the integrated stereoscopic camera set and the sonar components installed in the ESP frame. 58

Figure 3-3 A simplified block diagram showing the data flow directions and the components of the ESP data collection system. 60

Figure 3-4 Internals of the wet-end box, showing wet end micro-controller, video switch board, tri-axial accelerometer, and two 5-mega-pixel digital still cameras. 62

Figure 3-5 The underwater housing components, showing its (a) back cover, (b) housing cylinder, (c) front cover, and the installed housing (d) without and (e) with the front cover on the ESP frame. 63

Figure 3-6 Data availability of each sensing component when lined up against the time. This data set was collected from the first field trial in 2004. . 67

Figure 3-7 A seagrass coverage map of Cockburn Sound, WA, showing the remaining seagrass coverage (18%) in 1999 after the decline from 1967 (Kendrick, Aylward *et al.* 2002)..... 69

Figure 3-8 Site locations of the first ESP field trial in Cockburn Sound in 2004.. 71

Figure 3-9 Photographic pair and acoustic backscatter waveforms of a typical sand class sample..... 72

Figure 3-10 Photographic pair and acoustic backscatter waveforms of a typical seagrass species *P. sinuosa* class sample. 73

Figure 3-11 Photographic pair and acoustic backscatter waveforms of a typical seagrass species *P. australis* class sample..... 73

Figure 3-12 Photographic pair and acoustic backscatter waveforms of a typical rocky reef class sample..... 74

Figure 3-13 Photographic pair and acoustic backscatter waveforms of a typical macro algae class sample. 74

Figure 3-14 Canopy appearances and characteristics of *P. sinuosa* and *P. australis* recorded in Cockburn Sound 2004. 76

Figure 3-15 Site locations of the second ESP field trial according to the GPS data overlaying on a map of year 1999 seagrass species distribution of 95% likelihood of presence on Success and Parmelia Banks. 78

Figure 3-16 Photographic pair and acoustic backscatter waveforms of a typical sand class sample collected from site 1 of the second field trial..... 80

Figure 3-17 Photographic pair and acoustic backscatter waveforms of a typical *Posidonia* seagrass class sample collected from site 1..... 80

Figure 3-18 Photographic pair and acoustic backscatter waveforms of a typical sea squirts class sample collected from site 2. 81

Figure 3-19 Photographic pair and acoustic backscatter waveforms of a typical macro algae class sample collected from site 4..... 81

Figure 3-20 Photographic pair and acoustic backscatter waveforms of a typical mussel class sample collected from site 5. 82

Figure 3-21 Photographic pair and acoustic backscatter waveforms of a typical coral class sample collected from site 2. 82

Figure 3-22 Site locations of the final ESP field trial according to the GPS data overlain on a map of year 1999 seagrass species distribution of 99% likelihood of presence of Success and Parmelia Banks on the east banks of Owen Anchorage. 84

Figure 3-23 Photographic pair and acoustic backscatter waveforms of a typical sand class sample from the third field trial..... 86

Figure 3-24 Photographic pair and acoustic backscatter waveforms of a typical *Posidonia* seagrass class sample from the third field trial. 87

Figure 3-25 Photographic pair and acoustic backscatter waveforms of a typical *Amphibolis* class sample from the third field trial. 87

Figure 3-26 A particular case showing how the study targets (fish and seafloor) were recorded by the Left camera (no fish), Right camera (fish appeared), and the two-frequency echosounder due to the configuration of the detection components and the relative position of the fish under the detection components. Those marked by @, ©, and ® indicate the possible positions where fish may be observed on the photographs while no indications of fish can be observed from the acoustic signals. 94

Figure 4-1 Typical waveforms at two frequencies of EQ60 backscattered from a densely populated seagrass meadow of *P. australis* showing several peaks in the 200-kHz waveform with backscatter levels comparable to the maximum value (Max). 99

Figure 4-2 Bottom backscatter strength as a function of grazing angle for four different bottom types: shellfish covered sand, *Posidonia Oceanica* seagrass covered sand, medium sand, and mud observed by Lyons and Abraham. 101

Figure 4-3 Histogram of the maximum backscatter strength obtained at 38 kHz from various classes where samples were collected from the first field trial. 102

Figure 4-4 Histogram of the maximum backscatter strength obtained at 200 kHz from various classes where samples were collected from the first field trial. 103

Figure 4-5 Histograms of echo-average backscatter strength obtained at 200 kHz for five classes where samples were collected from the first field trial (cf. Figure 4-25)..... 104

Figure 4-6 Time interval for the summation to be made over for the first bottom return in equation 4-1 and the reference points used to derive the parameters used in this study..... 105

Figure 4-7 Histogram of EPW of five pure habitat types where samples were collected from the first field trial (cf. Figure 4-14). 107

Figure 4-8 Histogram of EPW of four non-pure habitat types where samples were collected from the first field trial (cf. Figure 4-15). 108

Figure 4-9 Log-log plot of the rescaled range (R/S) vs. the sub-series length n of a typical echo from bare sand and its least mean square linear fit. The slope is the Hurst exponent. 111

Figure 4-10 Histograms of the estimated Hurst exponent of five pure habitat types where samples were collected from the first field trial..... 112

Figure 4-11 Histogram of detected bottom range based on the peak location of the echo waveform at 38 kHz for sand and two seagrass species combined. 113

Figure 4-12 Histogram of bottom ranges measured from the front location of the waveform at 200 kHz for sand and two seagrass species combined... 114

Figure 4-13 Histogram of the RD values for five pure classes where samples were collected from the first field trial..... 115

Figure 4-14 Histograms of the EPW of five pure habitat types where samples were collected from the second field trial (cf. Figure 4-7)..... 116

Figure 4-15 Histograms of the EPW of five non-pure habitat types where samples were collected from the second field trial (cf. Figure 4-8)..... 117

Figure 4-16 Histograms of EPW values of the two pure classes observed in the final field trial (cf. Figure 5-8). 118

Figure 4-17 Distributions of the pure class samples derived from the classification results made by visual observation (left) and acoustic method with the EPW parameter (right) over sites of the final field trial. Note the coordinates are omitted here. 120

Figure 4-18 Measurements of the characterization parameters versus range to the bottom and their linear fits for pure sand samples collected from the final field trial. 121

Figure 4-19 Measurements of the characterization parameters versus range to the bottom and their linear fits for pure seagrass samples collected from the final field trial. 122

Figure 4-20 RD vs. bottom range and the linear fits for pure sand and seagrass samples collected from the final field trial. 124

Figure 4-21 Distributions of the sand and seagrass samples classified by EPW with the corrected RD values shown in colour designated for seagrass canopy height at site 4 of the final ESP field trial (cf. Figure 4-30, Figure 4-34, Figure 4-38, Figure 4-46, and Figure 5-10)..... 125

Figure 4-22 Histograms of the estimated seagrass canopy height obtained after removing the average sand RD value of 0.17 m from the RD measured for seagrass at each site of the final ESP field trial. 126

Figure 4-23 An instance of the second peak in the 38-kHz first bottom return from sand which has a higher amplitude than the first one causing an uncommonly large RD value when comparing to the normal RD values. 127

Figure 4-24 Histograms of EPW for the densely and sparsely populated *P. sinuosa* seagrass observed in the final field trial. 128

Figure 4-25 Histograms of echo-average backscatter strength for the densely and sparsely populated *P. sinuosa* seagrass samples collected from the final field trial (cf. Figure 4-5). 129

Figure 4-26 Matrix plot of pairs of five statistics derived from the backscatter envelope of the first bottom return from sand class samples collected from the final field trial and their respective distribution histograms on the main diagonal where scales and units are omitted. 131

Figure 4-27 Matrix plot of pairs of five statistics derived from the backscatter envelope of the first bottom return from *Posidonia* seagrass class samples collected from the final field trial and their respective distribution histograms on the main diagonal where scales and units are omitted. 132

Figure 4-28 Histograms of five statistics derived from the first bottom echoes for sand and *Posidonia* classes obtained from the final field trial where units are omitted here. 133

Figure 4-29 Histograms of skewness values of the two pure classes observed in the final field trial with a boundary value of 4.25 used to discriminate the two class samples. 134

Figure 4-30 Distribution of the sand and *Posidonia* seagrass samples identified by the skewness variable with the corrected RD values shown in colour designated for seagrass canopy height at site 4 of the final ESP field trial (cf. Figure 4-21, Figure 4-34, Figure 4-38, Figure 4-46, and Figure 5-10). 135

Figure 4-31 Eigenvalues obtained from the five normalized statistics as used in section 4.4. The threshold value for the selection of PCs is based on Kaiser's rule (Kaiser 1960). 137

Figure 4-32 Scatter plot of the sand and *Posidonia* class samples on the top-two-PCs space (upper panel) and the partitioning result for two clusters with their respective centroids using K-means (lower panel). 138

Figure 4-33 Scatter plot of two-cluster data on the top-two-PCs space with the misclassified samples marked by circles and squares. 139

Figure 4-34 Distribution of the sand and seagrass samples identified by the PCA and K-means method with the corrected RD values shown in colour designated for seagrass canopy height at site 4 of the final ESP field trial (cf. Figure 4-21, Figure 4-30, Figure 4-38, Figure 4-46, and Figure 5-10). 140

Figure 4-35 Same as Figure 4-31, but with the inclusion of the EPW parameter... 141

Figure 4-36 Scatter plot of the sand and *Posidonia* class samples on the top-two-PCs space (upper panel) and the partitioning result of two clusters with their respective centroids using K-means (lower panel) resulted from the inclusion of the EPW. 142

Figure 4-37 Scatter plot of two-cluster data on the top-two-PCs space with the misclassified data points marked by circles and squares after including the EPW. 143

Figure 4-38 Same as Figure 4-34 but after the inclusion of the EPW (cf. Figure 4-21, Figure 4-30, Figure 4-46, and Figure 5-10). 144

Figure 4-39 Same as the upper panel of Figure 4-36 but after the inclusion of the third PC. 145

Figure 4-40 Same as the bottom panel of Figure 4-36 but after the inclusion of the third PC. 146

Figure 4-41 Same as Figure 4-37 but after the inclusion of the third PC. 146

Figure 4-42 Same as Figure 4-38 but after the inclusion of the third PC (cf. Figure 4-21 and Figure 5-10). 147

Figure 4-43 Projection value *Zp* of point *P* (upper panel) and histograms (lower panel) of the two classes observed on the new axis *Z* expressed by the DF. 149

Figure 4-44 Plot of Fisher's ratio *F* versus angle θ with the maximum *F* ratio value of 281 at an angle of -0.3 degree pointed by the arrow. 150

Figure 4-45 A LDA discrimination result for the data collected from the final ESP field trial using Fisher's criterion with an error rate of 0.097. 151

Figure 4-46 Map of the sand and seagrass samples identified by the LDA with the corrected RD values shown in colour designated for seagrass canopy height at site 4 of the final ESP field trial (cf. Figure 4-21, Figure 4-30, Figure 4-34, Figure 4-38, and Figure 5-10). 152

Figure 5-1 A tree-based GP individual expression equivalent to (√F1) x (F2 – F3)..... 160

Figure 5-2 A sample genetic evolution process of reproduction. 161

Figure 5-3 A sample genetic evolution process of crossover operating on a node.161

Figure 5-4 Two sample genetic evolution processes of mutation operated on an operator and terminal respectively. 162

Figure 5-5 An ideal case of two separated classes with their samples being transformed by a candidate GP individual and mapped on a normalized solution space. The separation between different classes' median values and the maximum fluctuation range within each class combined is one of the measures for the performance of the GP individuals. 165

Figure 5-6 The GP-tree of the best-so-far solution found by the GP system with the fitness function given in equation 5-1. 169

Figure 5-7 Solution values of the 2-class samples after being mapped on a 1-dimensional solution space by the best-so-far solution program for which the statistics at the GP-tree terminals were derived from the same data collected from the final field trial as investigated in section 4.4. 170

Figure 5-8 Histograms of GP solution values of the 2-class samples as used for Figure 5-7. 171

Figure 5-9 Fitness value, number of levels and nodes for the best individuals resulted from each generation vs 10 consecutive generations for the final solution program shown in Figure 5-6. The final fitness value is about 162.1. 172

Figure 5-10 Distributions of the sand and seagrass samples classified by the GP result with the corrected RD values shown in colour designated for seagrass canopy height at site 4 of the final ESP field trial (cf. Figure 4-21, Figure 4-30, Figure 4-34, Figure 4-38, and Figure 4-46). 174

List of tables

Table 3-1 Major characteristics of EQ60 and selected settings. 65

Table 3-2 A classification table of two digits used in combination for the assignments of the habitat types (1st digit) and the distribution attributes (2nd digit) of the observed study targets on the photographs for the first ESP field trial in 2004..... 91

Table 4-1 Confusion matrix for all pure class samples collected from all sites of the final field trial based on the EPW boundary value of 0.12 ms (cf. Table 4-5, Table 4-6, Table 4-7, Table 4-8, Table 4-9, and Table 5-2). Note samples of the *Amphibolis griffithii* and *Posidonia* classes are combined as a single class. 119

Table 4-2 Confusion matrix for pure class samples collected at site 1 and 2. 119

Table 4-3 Confusion matrix for pure class samples collected at site 3. 119

Table 4-4 Confusion matrix for pure class samples collected at site 4. 119

Table 4-5 Confusion matrix for all pure class samples collected from all sites of the final field trial based on the skewness boundary value of 4.25 (cf. Table 4-1, Table 4-6, Table 4-7, Table 4-8, Table 4-9, and Table 5-2). 134

Table 4-6 Confusion matrix of all the pure sand and *Posidonia* class samples with their statistics as the input parameters for the PCA and partitioned by K-means as discussed in the text for the data collected from the final ESP field trial (cf. Table 4-1, Table 4-5, Table 4-7, Table 4-8, Table 4-9, and Table 5-2). 139

Table 4-7 Confusion matrix of all the pure sand and *Posidonia* class samples determined by K-means after including the EPW for the data collected from the final ESP field trial (cf. Table 4-1, Table 4-5, Table 4-6, Table 4-8, Table 4-9 and Table 5-2). 143

Table 4-8 Confusion matrix of all the pure sand and *Posidonia* class samples determined by K-means after the inclusion of EPW and the third PC for the data collected from the final ESP field trial (cf. Table 4-1, Table 4-5, Table 4-6, Table 4-7, Table 4-9, and Table 5-2)..... 147

Table 4-9 Confusion matrix of all the pure sand and *Posidonia* samples determined by LDA with the EPW and skewness variables using Fisher's criterion for the data collected from the final ESP field trial (cf. Table 4-1, Table 4-5, Table 4-6, Table 4-7, Table 4-8, and Table 5-2). 151

Table 5-1 Major GP parametric settings, main historical parameter values, and characteristics used for finding the GP-tree solution program in Figure 5-6. 173

Table 5-2 Confusion matrix of all the pure sand and *Posidonia* class samples based on the boundary of the GP result determined from Figure 5-8 for the data collected from all four sites of the final ESP field trial in 2005 (cf. Table 4-1, Table 4-5, Table 4-6, Table 4-7, Table 4-8, and Table 4-9). 174

Glossary of symbols

Sv	Volume backscatter strength (dB)
TS	Target strength (dB)
R	Range (m)
Pr	Received power (dB re 1W)
Pt	Transmitted power (W)
α	Attenuation coefficient (dB/m)
G_0	Transducer peak gain (non-dimensional, Sv or TS gain as appropriate) - EchoView* calculates G_0 as $10\text{^}(G_0'/10)$ where G_0' is the Sv gain or TS gain respectively.
λ	Wavelength (m)
c	Speed of sound (m/s) - Author assumed this value as 1500 m/s everywhere in this study.
τ	Transmit pulse duration (s) - also known as the pulse length
Ψ	Equivalent two-way beam solid angle (Steradians) - EchoView calculates Ψ as $10\text{^}(\Psi/10)$.
S_a	Filter corrections as defined by SIMRAD - SonarData provided different correction values for different EchoView versions.

* EchoView is a product of SonarData Pty Ltd based in Tasmania, Australia.

Chapter 1 Introduction

1.1 Background and significance

This study investigates the potential of using a single beam echosounder as a tool for recognition and assessment of seafloor vegetation. The expected outcome of this study is useful acoustic techniques which can be applied for habitat mappings of seafloor vegetation. The seafloor vegetation investigated in this study includes mainly seagrass and macro algae populations on the shallow coastal sea bottoms near the capital of Western Australia, Perth, in 2004 and 2005.

Significant progress in the acoustic study of seafloor vegetation has been made due to military requirements for the understanding of acoustic characteristics of buried mines deployed amongst the marine vegetation along coastlines (Richardson, Valent *et al.* 2001; Caruthers and Fisher 2002). Although the focus of the mine burial projects was not on the plant benthos, the plant benthos did play critical roles by affecting the sonar's detection abilities of the buried objects on the shallow coastlines (Elmore, Richardson *et al.* 2005). The impact of plant benthos on the detection of buried mines can be seen from a case study in which an Italian-made Manta mine simulator was deployed among the vegetation on a seabed to simulate the mine burial detection scenario (McCarthy and Sabol 2000). Mainly the drive of the studies above is due to the fact that seafloor vegetation strongly affects the mine-hunting capabilities such that sonars are unable to effectively detect the target mines.

Knowledge and techniques originally being developed for military needs are often transferred to commercial uses. A typical case of such a transfer is the technique acquired by BioSonics Incorporated in the USA from the Engineer Research and Development Center (ERDC) of the US Army Corps of Engineers. One of its current products EcoSAV was developed from the original processing technique called SAVEWS (Submersed Aquatic Vegetation Early Warning System)

(McCarthy and Sabol 2000; Burczynski 2001; Burczynski, Hoffman *et al.* 2001; Sabol and Johnston 2001; Hoffman, Burczynski *et al.* 2002; Sabol, Burczynski *et al.* 2002). This shows that recognition of seafloor vegetation is critical to the military requirements.

Beyond military needs, civilian and scientific requirements for using acoustics as an effective means for the exploration of underwater vegetation drove further developments of the acoustic tools to more challenging scenarios (Caddell 1998; Berntsen, Hovem *et al.* 1999; Chu, Wiebe *et al.* 2000; Bett 2001; Galloway 2001; Caruthers and Fisher 2002; Brehmer, Gerlotto *et al.* 2003; Godlewska, Swierzowski *et al.* 2004). After these developments, acoustic techniques have been gradually called upon as the indispensable tools for monitoring seafloor habitats (Davies, Foster-Smith *et al.* 1997; Bett 2001).

Vegetation's acoustic backscatter properties are still far from fully understood. This can be seen from common practices that a variety of methods are frequently used and combined in order to provide useful outcomes. These methods include air borne surveys, and direct measurements such as the costly and labour intensive diver's measurements. Advancements of acoustic identification abilities can significantly reduce the needs for the expensive methods, which is one of the advantages which acoustic tools can outperform other methods in observing the seabed.

As revealed in previous studies, there are still some areas in which researchers can improve the skills and knowledge to better understand the acoustic properties of seafloor vegetation. Among plant benthos, seagrass has been frequently studied and used as a major health indicator of water conditions (Cavazza, Immordino *et al.* 2000; Piazzi, Acunto *et al.* 2000; Wood and Lavery 2000; Linton and Warner 2003; Lee, Short *et al.* 2004; Marba, Santiago *et al.* 2006). Hence the study of seagrass's acoustic properties occupied a great portion of this work despite the fact that other plants such as macro algae also belong to plant benthos. Besides seagrass and macro algae, limited species of animal benthos and a variety of seafloor substrates were also observed. In order to have a detailed insight into the acoustic backscatter characteristics of seafloor vegetation for recognition purposes, small scale areas near the author's study base were selected.

1.2 Research objectives

This study aims at the following objectives:

- Investigation of acoustic parameters which can efficiently characterize the seafloor vegetation,
- Development of feasible acoustic techniques for the recognition of seafloor vegetation,
- Development of acoustic means which can provide useful quantitative measures of seafloor vegetation by using a single beam echosounder operated at two frequencies.

For the above objectives, several acoustic techniques used for the identification of seafloor vegetation were investigated. Techniques developed in this study are expected to be useful for the classification of seafloor habitats. Through robust classification performance, a person is able to better understand the precise conditions of the seafloor, which in turn can contribute to the better management of coastal environments.

1.3 Thesis structure

The thesis is divided into seven chapters.

The second chapter presents previous studies related to the seafloor vegetation and the seafloor substrate. It provides an overview of our level of understanding of seafloor vegetation by acoustics. It points out the weakness of the previous studies and presents what are brought into focus in this study. In the end, it introduces some of the commercially developed techniques and recommendations made by researchers.

In chapter 3, instrumentation and data collection details are presented. It presents how the field trials were planned and carried out, and details of the data collections. It includes a description of the methods chosen for collecting and classifying the data, and the areas where data were collected. Finally it presents the scope of the collected data and their limitations for use.

Chapter 4 presents the data processing results for each particular field data. These sites include Cockburn Sound surveyed in 2004, and Parmelia Bank and Owen Anchorage of Western Australia surveyed in 2005. The results include the capabilities of the acoustic parameters investigated by conventional techniques and their limitations in characterizing the seafloor vegetation.

In chapter 5, Genetic Programming (GP) is introduced. It introduces the basic theory of the GP algorithm, a prerequisite for the understanding of the application results, and illustrates how GP is applied to this particular acoustic study. In this chapter, it includes an introduction of a MATLAB toolbox for GP used in this study. Also presented are the design of a Fitness Function, the improvement of the classification performance after the adoption of GP, and the limitations of the GP algorithm applied on the case studies.

In chapter 6, discussions are given for the use of the experimental tools, traditional techniques used in the data processing, and the study results after the application of the GP system.

Finally, Chapter 7 presents the author's conclusions and recommendations of his investigation results for the recognition and assessment of seafloor vegetation by using a single beam echosounder operated at two frequencies.

Chapter 2 Historical studies of seafloor vegetation and the substrate

This chapter reviews some of the historical studies of seafloor vegetation relevant to the acoustic backscatter properties. Comments on previous works are provided, including the shortcomings, limitations, and recommendations where possible.

2.1 Acoustic studies of seafloor vegetation

There have been several studies made for the understanding of the acoustic backscatter properties of seafloor vegetation. The historical records showed either the importance of acoustic tools for the management of seafloor habitats or the interesting acoustic features of some seafloor vegetation species. Literature also provided evidences that the presence of some seafloor vegetation affected the effective use of acoustic devices. Following are the major acoustic studies focusing on the animal and plant benthos respectively.

2.1.1 Introduction of marine benthos

Marine benthos can be roughly divided into two categories: plant benthos such as algae and seagrass, and animal benthos such as corals and clams. While benthos can be differentiated by the bodies of water they live in, i.e. marine and freshwater, they can also be differentiated by the size, i.e. micro and macro. Due to the huge number of species which can be included in the benthic community, it is unrealistic to investigate all of them. In this study, only a few species of seafloor

vegetation are investigated such as seagrass and macro algae, and animal benthos such as sea squirts.

2.1.2 Animal benthos

Since animal benthos are not the focus of this study, only brief introductions of some of the typical works are introduced in the following, which highlight the use of acoustics as an important tool for the understanding of animal benthos:

- An observation for the common epi-benthos conducted with a sidescan device and followed up with coring and photography in the Atlantic Ocean (Bett 2001).
- A test for the influence of macrofaunal activities on the low-angle acoustic backscatter from seafloor sediment by a special measurement at both 40 and 300 kHz for the known species at sea (Self, A'Hearn *et al.* 2001).
- A benthic habitat mapping program for the prawns, clams, scallops crabs, rockfish, etc. conducted with an echosounder at 38 and 200 kHz during February 2001 in the Strait of Georgia (Galloway 2001).
- A study of the multibeam data collected from Browns Bank, Canada, between Nova Scotia and Cape Cod in 1996 and 1997 for the understanding of the relationship between the acoustic backscatter intensity and the giant scallop abundance (Kostylev, Courtney *et al.* 2003).
- An investigation of the RoxAnn classification technique for the estimation of shellfish abundance in the Newfoundland and Labrador area (Naidu and Seward 2003).
- An acoustically based observation for the identification of scallop seabed carried out by a variety of acoustic devices and various analysis algorithms in the St. Lawrence Canada in 2002 and 2003 (Hutin, Simard *et al.* 2005).

- An investigation of sandeels ecology by the use of an echosounder for the understanding of interrelationships of sandeels to their predators and fishing activity (Freeman, Mackinson *et al.* 2004).
- A mapping program for the oyster reefs and oyster bottom of Galveston Bay Texas carried out with a tow fish of Datasonics DFT-210 at 22 and 300 kHz in 1990 (Simons, Soniat *et al.* 1992).
- A mapping program for oyster habitat in Chesapeake Bay, Maryland, by the use of assorted sonar systems (Smith and Greenhawk 1998; Smith, Bruce *et al.* 2001).
- A monitoring program of mussel cultures by using sonar devices along the Mediterranean coastline (Brehmer, Gerlotto *et al.* 2003).
- The use of a variety of sidescan sonars and high-resolution seismic reflection profilers for the detection of bivalve reefs in the Bay of Fundy, Canada, in 1995 (Wildish, Fader *et al.* 1998).
- An observation for the bioherms in Chesapeake Bay, USA, by sidescan sonars and divers (Wright, Prior *et al.* 1987).
- An observation of enhanced acoustic backscatter from sand dollars (*Dendraster excentricus*) in water depths between 16 and 24 metres in the vicinity of Humboldt Bay, California (Fenstermacher, Crawford *et al.* 2001).
- A study seeking an effective seafloor classification technique for the mapping of coral reef benthic classes conducted in Negros Occidental, within the Visayas region of the Philippine Archipelago in October 1997 (White, Harborne *et al.* 2003).
- A investigation of the interrelationships between the acoustic backscatter signals and the sediment types and animal benthos for the characterization of seafloor habitats on the western continental shelf of India (Chakraborty, Mahale *et al.* 2007).

2.1.3 Plant benthos

2.1.3.1 *Hydrilla* and *Lyngbya*: a historical study

In the USA, the earliest study of plant benthos investigated by acoustics was accomplished by Maceina and Shireman (Maceina and Shireman 1980). They took advantages of a primitive acoustic system, a depth-recording fathometer DE-719 made by Raytheon Marine Co., to estimate the distribution and biomass of *Hydrilla*, which was regarded as the most problematic aquatic plant found in all types of water in the United States. Although *Hydrilla* was the predominant macrophyte in the surveyed areas, its acoustic tracing patterns were not unique enough to be used as a reliable feature for identification purposes, especially when other aquatic plants coexisted and mixed with it.

Mentioned in their study was another observed nuisance plant, *Lyngbya*, which is also known by its common names such as Mermaid Hair and Fire Weed. It is a filamentous blue-green algae found worldwide (Moreton Bay Waterways and Catchments Partnership 2002). The *Lyngbya* can infest the water mass and attach on plant benthos when environmental conditions permit. Since the algae tissues were so fine when comparing to their attached plants, it was anticipated that the existence of this filamentous vegetation would be hardly distinguishable by their acoustic system. To their surprise, Maceina and Shireman mentioned that the recorded patterns of this aquatic plant were 'distinguishable in the summer and fall' and 'recorded as a low flat mound as it characteristically grows 0.1-0.2 m in height above the hydrosoil' (Maceina and Shireman 1980, p. 35). However, *Najas*, *Nitella* and *Chara* of *Hydrilla*, which also have become troublesome aquatic weeds in lakes, streams, and reservoirs, were found in a variety of areas (Langeland 1996), and distinct differences in tracing patterns were not detected. Moreover, when the winter came and submerged vegetation was near the bottom, the detectable *Lyngbya* (in summer) was not detected anymore. Obviously the observation of the submerged plants with the acoustic tools was disturbed by the plants' physical characteristics and seasonal

factors. The effectiveness of an acoustic tool for the characterization of the vegetation targets was also limited by its coexistence with other vegetation.

This pioneer trial of utilizing acoustic tools for the estimatation of the distribution and biomass of submerged vegetation represented a historical record in showing that sonar systems provided advantages of savings in time and manpower for vegetation surveys, especially when comparing to other conventional labour intensive methods such as diver's measurements. However, their observation of the distinguishable vegetation was derived from visual inspections of the acoustic recordings recorded on the paper. There were no specific acoustic characteristics provided as the quantitative measures for the distinguishable vegetation in their study.

2.1.3.2 A modelling study for algae

Up to date, there has been only one work published on physical models of acoustic backscatter from marine plants (Shenderov 1998). Three physical models were developed by Shenderov to describe acoustic backscattering from algae. The algae were simulated by a three-dimensional system of bent elastic bodies. The backscattered sound pressure from algae was regarded as sound diffraction on semitransparent bent plates and rods corresponding to algae leaves and stems. Ultimately it aimed at the provision of a relationship between the scattered sound wave amplitude and the algae biomass as a basis for estimating underwater vegetation biomass on the seafloor. For this purpose, the three models have to simulate the real world algae. The first model considers acoustic backscattering from a single leaf of three typical conditions: predominantly horizontal disposition, uniform distribution, and predominantly vertical disposition. Then sound reflection and backscattering are modelled for dense dispositions of plants on the bottom by simulating a system of layers with random distances between them. The third model simulates sound scattering by algae with curved intertwined stems.

By comparing his theoretic predictions with previous experimental recordings, Shenderov found that the experimental values of reflection coefficient were mostly within the calculated boundary values. Shenderov showed that the backscattering cross section increased with increasing frequency under the condition of sparse

dispositions of plants, and concluded that the reflected signal intensity was dependent on biomass and the intensity was able to give the estimate of biomass under a condition of appropriate calibration. For a very dense distribution of plants, in contrast, 'the reflected signal depends only slightly on the biomass' (Shenderov 1998, p. 800).

The important result of his study is that 'the backscattering cross section after averaging over the angles of inclination is not dependent on the geometrical parameters of the leaves and the stems bending' (Shenderov 1998, p. 800). In other words, a stable estimate of biomass is expected even if the parameters of the shape are unknown. For the first time, Shenderov provided theoretic models for researchers to understand how physical characteristics of algae influence the acoustic response and consequently the estimated biomass as a result.

From Shenderov's calculations, the equivalent radius of the backscattering cross section from a leaf of area 0.25 m^2 at high frequency is about 2 cm. (The relationship between the equivalent radius a_{sph} and the backscattering cross section σ_0 defined by Shenderov is $\sigma_0 = a_{sph}^2 / 4$.) Noticeably, the equivalent radius of a fish of 0.2-m long is approximately the same. This suggests that there could be an ambiguity in differentiating the acoustic backscatter from two different objects when they hold the above conditions.

For jellyfish, the equivalent radius is about 0.15-0.4 cm. In other words, the acoustic backscatter from small fish and algae is stronger than that from jellyfish and hence algae and fish are more easily detected by the sonars, which is reasonable because their backscatter strength differs approximately 10 times. This also indicates that the jellyfish is nearly acoustically transparent.

For dense distributions of plants on the bottom, an example given by Shenderov showed that the calculated equivalent radius of leaves was about 8 cm. By comparing to the example for the sparse disposition model, this value is relatively large. That is, the backscatter level from dense plants is at least one magnitude higher than that from sparse plants. If this is true, this finding will be a very useful clue for researchers to differentiate sparse and dense distribution of plants. However, this model did not provide suggestions for how to distinguish different plants such as seagrass and algae with similar backscatter strength.

In the more complex model of sound scattering from a system of curved and intertwined stems, the derived cross section in the high-frequency approximation is independent of the specific geometric parameters of the plant curve. In the example provided by Shenderov, the equivalent radius from this model is approximately 6 cm, which is about the same order as that obtained in the sparse disposition model. Noticeably, the model developed by Shenderov is only applicable at frequencies when the product of frequency and leaf thickness is from about 300 to 500 kHz-mm. For an algae leaf of 2 mm in thickness, the applicable frequency range will be about 150-250 kHz. Beyond this frequency range, the model is unable to provide a good description of acoustic backscattering from algae. Sonar systems operating at such frequencies are expected to be capable of predicting the algae biomass when this condition is met.

At lower frequencies, acoustic backscatter still depends on the algae's physical parameters, which limits the application of the model. All in all, Shenderov's study was the first attempt to physically model acoustic backscatter from algae in order to provide quantitative relations between acoustic backscatter characteristics and biomass of algae. Although there are possibly some other acoustic methods capable of estimating the biomass of marine vegetation, 'the results of an approximate estimation will be useful for choosing operation modes of echosounders and analysis of results' (Shenderov 1998, p. 800), concluded Shenderov.

2.1.3.3 Areal studies for seagrass and macro algae

Since seagrass is among other plant benthos representing one of the best indicators of the health conditions of water bodies (Linton and Warner 2003; Lee, Short *et al.* 2004; Marba, Santiago *et al.* 2006), it is particularly focused on in this study. Influences and impact of underwater vegetation to the detection and understanding of its surrounding background had been noticed at a very early date (van der Heijden, Claessen *et al.* 1983). From a review of literature, there have been some studies of seafloor vegetation specifically carried out by means of acoustics. Provided in Appendix A is a list of the major acoustic studies of seagrass or algae

sorted according to the geographic localities. Following are those experimental studies described for each major geographic location in alphabetical order.

2.1.3.3.1 Australia

Australia is renowned for its prominent effort in the protection of its natural environment. Its endeavour extends from the land territory to its legitimate ocean environment. An early attempt at using echosounders for the investigation of the underwater habitats was made by the Offshore Scientific Pty Ltd in Narrabeen Lagoon, NSW, in April 1994 (Hundley and Denning 1994; Hundley, Zabloudil *et al.* 1994). The targeted seagrass was the species *Zostera capricorni*. The study aimed at the evaluation of the acoustic technique's ability to map the density and location of seagrass beds. The advantages of using an acoustic system claimed by the survey company and by the acoustic device supplier, BioSonics Inc., were the insensitivity to water turbidity, near real-time depth availability, data resolution, wide area coverage, and reduced reliance on manpower (BioSonics Inc. 1994).

In the Narrabeen Lagoon mapping project, the evaluation work of using the acoustic system was divided into three phases. The first phase involved ground-truthing areas of seagrass for comparison with the acoustic results. Phase two was to calibrate acoustic systems in order to relate the acoustic characteristics to the seagrass biomass. In the last phase, the researchers used the calibrated acoustic system to carry out acoustic mapping of the seagrass in areas having been ground-truthed. According to the statements published on the sonar supplier's web site (BioSonics Inc. 1994), they claimed that 'this study shows the success of this method for obtaining seagrass bed location and density' and the 'application has been shown to provide high quality, quantitative measures of the characteristics of seagrass beds on a variety of scales.'

However, there was no evidence capable of showing that the quantitative measures were robust enough and able to characterize the seagrass-covered meadows, nor was it able to identify the existence of the seagrass. There are still problems requiring further investigations in order to achieve the goal of obtaining quantitative

measures for the seagrass meadows. This point can be witnessed by a report made by an Australian authority a few years later, which is discussed in the next paragraph.

In 1998, a report to the Great Barrier Reef Marine Park Authority provided a summary of their investigation of the use of a sidescan sonar for the mapping of tropical seagrass habitats (Lee Long, McKenzie *et al.* 1998). According to their preliminary trials, they pointed out that the acoustic techniques 'cannot be used for determining above-ground seagrass biomass in these habitats' and there were some cases where 'seagrass sites were not interpreted as seagrass with the acoustic technique' (Lee Long, McKenzie *et al*. 1998, p. iii). They suggested that the refinement of the acoustic technique was required before it was possible to discern low-biomass seagrass habitat from bare substrate. Except for the advantages of acoustic techniques in time, and labour saving and spatial resolution over traditional sediment grab sampling methods, they found that the relation of acoustic signals to the absolute biomass measures had limited potential, and summarized that dive-based sampling was always required.

From the above points, it is understandable that the acoustic techniques adopted in that time period did not provide satisfactory results for the Australian authority. Nevertheless, there was a major drawback in their study: the relative acoustic backscatter intensity divided into several levels at an interval of 10 dB was used as a measure for the detection and estimate of the seagrass biomass. The use of the acoustic backscatter intensity as a sole parameter for the characterization of seagrass has a limited effect. In a complex environment, like the benthic habitats, a detailed description of the study targets may need more than one parameter. Other possible problems found in their study are the capabilities of the sonar system used. Since every acoustic device has its limited abilities, the sidescan used by them might not be quite suitable for the measurements of the benthic communities such as the seagrass meadows investigated by the Australian authority.

2.1.3.3.2 Canada

An acoustic tracing technique firstly employed by Maceina and Shireman (Maceina and Shireman 1980) was used to estimate the aboveground biomass of

submerged macrophytes in lakes (Duarte 1987). Duarte used an equation to estimate the biomass from the vegetation stand height and plant growth form. Basically, 'the height of the stand sampled was estimated from the echosounder chart' (Duarte 1987, p. 733) while the growth form and the biomass were obtained by SCUBA diver's sampling analysis. Through linear regression, a best fit equation to estimate the mean biomass was derived. In the equation, height and growth form of the macrophytes were used as the variables for estimating the biomass. The results calculated from the equation were compared to those directly obtained by the SCUBA divers through direct observation. Duarte concluded that 'the echosounder-based method is limited to stands growing at depths greater than 70 cm with plants taller than 20 cm' (Duarte 1987, p. 732).

There are two major points which can be further discussed: the way of measuring the plant height from the acoustic recordings and the process of assessing the biomass. The criteria used to measure the plant heights from the acoustic recordings and the accuracy and appropriateness of the plant growth form used as the key feature for the biomass estimate should be reconsidered. Usually, physical shapes and orientations of seagrass and algae leaves in the water are often affected by the current. The plant growth form recorded by the divers is often different from the actual conditions sampled by the echosounder. Considering the typical footprint size of 'about 80 cm in diameter' in Duarte's study (Duarte 1987, p. 733), it would be very difficult for the divers to exactly locate the right place and measure the right height and actual size of the vegetation. A statistical analysis of the dependence of height and growth form on time should be considered.

In another survey, where water depth varied from 0.6 to 14 metres, a Precision Survey fathometer DE-719 was used for the survey of submerged aquatic vegetation in Lake Saint-Pierre, Canada (Fortin, Saint-Cyr *et al.* 1993). The dominant plant species were pondweed (*Potamogeton richardsonii*), water celery (*Vallisneria americana*), and stonewort (*Nitella* sp.). The researchers observed three basic acoustic patterns corresponding to different vegetation structures, or phytoacoustic facies. These three patterns are echo returns appearing 1) near the water surface, 2) in the water column well below the water surface, and 3) a series of echoes located near the lake bottom. Each was respectively associated to 1) tall plants, 2) shorter species, and 3) plants near lake bottoms respectively. The

researchers claimed that 'underwater data collected with SCUBA show good agreement between the basic phytoacoustic facies and the three dominant plant species identified in Lake Saint-Pierre' (Fortin, Saint-Cyr *et al*. 1993, p. 232). However, the determination of the submerged aquatic vegetation density was determined by the use of a numerical code system representing the acoustic signatures of each vegetation cover appearing on the echograms. There was no quantative assessment for how the three acoustic patterns were determined.

Basically, the observation of the submerged aquatic vegetation was limited by the capability of the analogue echosounder, which relied on the acoustic images recorded by an analog recorder. There are many possibilities that the three patterns can be associated to different biological organisms. Nevertheless, this study represents one of the excellent trials when scientists were trying to take advantages of the acoustic devices in mapping the distribution and coverage of underwater vegetation in the early stage.

2.1.3.3.3 France

A combined approach of using a sidescan sonar and aerial photography for the assessment of the seagrass (*P. oceanica*) distribution was examined off the Island of Corsica (Pasqualini, Pergent-Martini *et al.* 1998). Although the researchers used the Principal Components Analysis (PCA) applied to the digitalized image for mapping the seagrass distribution, they did not provide any useful information of the acoustic backscatter characteristics of seagrass. Nevertheless, they found that 'the upper limit of *P. oceanica* seagrass beds rarely exceeds depths of 10 m' and 'the lower limit of *P. oceanica* seagrass beds ranges from 13 m to 42 m' (Pasqualini, Pergent-Martini *et al*. 1998, p. 362).

Recently, a single beam echosounder EQ60 was deployed in the Mediterranean Sea by Semantic-TS, aiming to develop a method for detecting and characterizing vegetation on the seabed (Noel, Viala *et al.* 2006). The researchers asserted that 'the presence of reverberation peaks before the bottom echo in the case of bottom covered with *Posidonia*' provided acoustic signatures for the differentiation of assorted bottom types and offered 'feasibility of the acoustic

detection of the *Posidonia* land' (Noel, Viala *et al*. 2006, p. 1). In addition, they argued that the 'comparison between depth of the canopy echo, and depth of bottom interface echo allows to estimate plants height' (Noel, Viala *et al*. 2006, p. 1). This conclusion raises the question of how to locate the depth of the vegetation canopy and the depth of the bottom interface when the bottom is covered by vegetation. Most importantly, before the detection of vegetation's canopy, it is firstly necessary to understand how to determine whether the echo is backscattered from the vegetation or not. An obvious instance challenging the above suggestion is the presence of other epi-benthos which may also exhibit acoustic signatures similar to those from the vegetation.

2.1.3.3.4 Italy

Italy has been traditionally a key player in underwater acoustics research in the European Union. The once named SACLANT Undersea Research Centre (SACLANTCEN) since 1959 (now changed into NATO Undersea Research Centre (NURC) after 2004 to reflect a much broader mission and range of products than the original Centre) is located in La Spezia, Italy. Bazzano and Siccardi of this Centre conducted a series of experiments to study acoustic backscatter from the seagrass *Posidonia oceanica* (Bozzano and Siccardi 1997; Siccardi, Bozzano *et al.* 1997; Bozzano, Castellano *et al.* 1998; Bozzano, Mantovani *et al.* 1998; Siccardi and Bozzano 2000; Bozzano, Mantovani *et al.* 2002). They conducted measurements of the acoustic backscatter strength of reference objects (ping-pong balls filled with assorted materials) and seagrass in the laboratory water tank and at sea with a controllable device to lower the echosounder in the water. In their measurements, the sonar head was approximately one metre above the targets. The measurements were made for the target strength, reflected beam pattern, and the acoustic return profiles for different settings of sonar gain at the frequency of 2 MHz in order to understand the acoustic characteristics of the abundant Mediterranean seagrass, *P. oceanica*. Although they made several acoustic measurements for the seagrass, no quantitative measures were effective in characterizing the seagrass.

Later Lyons and Pouliquen investigated the acoustic scattering properties of *P. oceanica* within the same research institute, SACLANTCEN (Lyons and Pouliquen 1998). They used sidescan, single beam and parametric sonar to investigate the dependence of scattering strength on grazing angle and frequency. The operational frequency ranged from 30 to 110 kHz. They made a number of experiments in a wide range of grazing angles at several sites near the islands of Elba and Sardinia, Italy, and in Saros Bay, Turkey. From their measurements at sea, they found that the maximum scattering strength from the seagrass was high with the average values between -20 and -26 dB. They speculated that the high scattering strength could be 'due to the gas pockets found in individual *Posidonia* leaves which behave as a line array of bubbles' or 'the carbonate material commonly found on mature leaves' (Lyons and Pouliquen 1998, p. 1628). They also found 'weak dependence on grazing angle' and 'no dependence of scattering strength on frequency' (Lyons and Pouliquen 1998, p. 1628) over the frequency range examined. Although Lyons and Pouliquen's study was on seagrass instead on algae, the last observation is contradictory to some extent to the results predicted by the physical backscatter model for algae made by Shenderov described in section 2.1.3.2. Finally, Lyons and Pouliquen suggested future work on modelling seagrass beds as a volume of randomly oriented bubble line arrays in order to understand the grazing angle and frequency dependence of scattering strength for seagrass bottoms.

In a different approach, a sidescan sonar and an airborne Visual Infra Red Scanner (VIRS) were used to investigate the extension of seagrass (*P. oceanica*) beds and the epiphytic algal assemblage distribution around Elba Island in 1994 and 1995 (Piazzi, Acunto *et al.* 2000). For calibration purposes, direct observations by SCUBA divers and a remote operated vehicle (ROV) were used. There is not much description for the acoustic properties of seagrass or algae in their study. The only helpful information related to this thesis is that 'the distribution of the seagrass was affected by the morphology of the bottom' (Piazzi, Acunto *et al*. 2000, p. 342). But, no information is available for whether this observation is based on the findings from the airborne device or the sidescan sonar.

Around the Island of Ischia and in its adjacent waters, an attempt was made to build an updated and detailed map of the *Posidonia* beds and to monitor their evolution in the areas after 50 years when the first seagrass map was produced by

Funk in 1927 (Colantoni, Gallignani *et al.* 1982). According to the recorded *Posidonia* depth limits in the areas, the seagrass distributed from 0 to 50 m with an average distribution at 15 m. In order to understand the seagrass distribution in an effective way, the investigators decided to use both acoustic systems and other complementary sampling methods for this task. They deployed a low frequency (3.5 kHz) echosounder and a sidescan sonar in their preliminary cruise in 1977, which could be the earliest documented record of the use of sonar systems for the mapping of vegetation-covered seabeds. They found that 'low-frequency echosounding proved to be rather ineffective as it did not discriminate the acoustic character of *Posidonia* beds from those of rocky and sandy bottoms' (Colantoni, Gallignani *et al*. 1982, p. 56). On the other hand, 'the side scan sonar was very satisfactory' (Colantoni, Gallignani *et al*. 1982, p. 57). They claimed that the sidescan 'produces sonographs similar to aerial oblique views' and can 'discriminate the different types of bottom with an excellent degree of accuracy' (Colantoni, Gallignani *et al*. 1982, p. 57). Moreover, they commented that '*Posidonia* beds were remarkably well recognized and their limits, as well as their main features correctly identified in most cases' (Colantoni, Gallignani *et al*. 1982, p. 57). Therefore, the sidescan sonar was utilized throughout the whole rest of the seagrass mapping course in 1977 and 1978. Except for the sonographs produced by the sidescan sonar and presented in their work, there are no quantitative measures examined for the acoustic assessment of the seagrass. Obviously the identification of the so-called patterns of the seagrass was based on the researchers' visual observation of the sonographs and their recognition abilities and scientific experience. No important acoustic features of the seagrass can be learned from the study. However, the ineffective low frequency echosounder used by the researchers may imply that frequencies as low as to the range of 3.5 kHz are not suitable for the detection of marine vegetation like the seagrass *Posidonia*. Hence, sonar systems selected for the detection of seagrass or algae should operate at frequencies higher than at least 3.5 kHz.

2.1.3.3.5 Japan

In the Seto Inland Sea, a 200 kHz Kaijo PS-11E single beam echosounder was used for the mapping of the seagrass *Zostera marina* in 1991 (Komatsu and Tatsukawa 1998). In the study, the authors claimed that 'the echo-sounder recorded clearly vertical distributions of *Z. marina* plants as shading and height pattern on echograms' (Komatsu and Tatsukawa 1998, p. 39). Although they claimed that 'the above-ground biomass of *Z. marina* could be roughly estimated based on a relation between the shading of echo traces of plants and above-ground biomass obtained by quadrat samplings' (Komatsu and Tatsukawa 1998, p. 39), there were no indications of how the recognition of the seagrass *Z. marina* and the differentiation of different seagrass species were achieved.

Later in 2001, the same research group adopted a more advanced 455 kHz multibeam (RESON SeaBat 9001) system for the mapping of seagrass *Zostera caulescens* in Otsuchi Bay on the Sanriku Coast of Japan (Komatsu, Igarashi *et al.* 2003). Basically, the study was an introduction of a methodology for estimating seagrass biomass through the use of processing software (Hypack Max). Using the software, the seagrass signals were compared against the echoes backscattering from the bare substrate in order to obtain a topographic profile of the bottom. After determining the bottom depth difference between the topographic profiles with and without the seagrass, a 3-D seagrass volume was obtained. By the verification of the quadrat samplings, a relationship associating the seagrass volume to the biomass was obtained.

Again, no quantitative assessment of the backscatter characteristics was made to demomstrate how the recognition of the seagrass was made, except the observation that the seagrass signals 'sticked out upward from the base line on the hydrography software' and 'these signals were echo reflecting from the leaves or stems of seagrass on the bottom' (Komatsu, Igarashi *et al*. 2003, p. 225). Cautions should be made that there was a finding in the literature that 'the echo produced by the rhizome and root systems buried up to 10 cm deep have an intensity seven times higher at 100 kHz than at 500 kHz' (Siljeström, Moreno *et al*. 2002, p. 2874). This means that if the determination of the base line is based on the backscatter at 100

kHz, there is a danger of picking up the wrong base line for the true bottom depth and as a consequence leading to an overestimate of the seagrass biomass. A more detailed description of the study results by the Spanish group will be introduced in the following Spain section. Nevertheless, the Japanese researchers reported an interesting finding that seagrass 'blade length was proportional to bottom depth' (Komatsu, Igarashi *et al*. 2003, p. 228). They suggested that 'beam frequencies above 200 kHz are necessary to detect seagrass beds,' and concluded that 'multi-beam sonar is a very useful apparatus for mapping seagrass beds and visualizing the underwater landscape' (Komatsu, Igarashi *et al*. 2003, p. 229). This suggestion is indirectly supported by a study in which a low frequency echosounder of 3.5 kHz was not capable of distinguishing the *P. oceanica* beds from the bare seafloor (Colantoni, Gallignani *et al.* 1982).

Usually but not always, the maximum amplitude of an echo return is considered as an indicator of the sea bottom or the seagrass canopy from which the acoustic signal is backscattered. However, the Spanish research group observed that higher intensity echoes were backscattered from the rhizome and root systems instead from the seagrass canopy at a lower frequency. Because of this consideration, an overview of the biological characteristics of some typical seagrass species found in Western Australia is given in section 2.2.

2.1.3.3.6 Poland

In order to assess the spatial distribution and biomass of underwater vegetation and to identify their species composition, a 208 kHz BioSonics DT 4200 echosounder was used in Puck Bay of the southern Baltic Sea (Tęgowski, Gorska *et al.* 2003). The data collection was carried out over the seabed of a homogeneous sandy bottom with dominant seagrass species of *Zostera marina*, *Zanichellia* sp. and *Potamogeton* sp. within a mean water depth of 1.7 metres. The brown filamentous algae *Pilayella* sp. observed by the Polish scientists is able to populate and attach on the seagrass leaves in eutrophic coastal areas due to its competitive ability in tolerance of polluted waters over the perennial vegetation. Air bubbles trapped in the algae clouds can alter the echoes from the covered seagrass. This acoustic feature

was also observed by Maceina and Shiremand (see section 2.1.3.1). Besides this consideration, the aim of the study by the Polish scientists was to investigate potential parameters that could be used to effectively differentiate the bare sand seafloor from seagrass covered meadows, including the algae.

By examining the echo envelopes, the Polish scientists chose three parameters for characterizing the underwater vegetation. These three parameters are the moment of inertia, spectral width, and fractal dimension derived from the echo envelopes (see Chapter 4 for definitions). The authors compared the classification abilities of the selected parameters in identifying the bare seafloor and the plant-covered meadows. The study targets included the brown filamentous algae *Pilayella* sp. in the polluted and eutrophic waters of Puck Bay. However, the final results were only given for the differentiation of bare sand seafloor and the plant-covered meadows.

The Polish researchers did not agree with some algorithms implemented in Sabol's classification algorithm (Sabol and Johnston 2001; Sabol, Burczynski *et al.* 2002), which will be discussed in more detail in section 2.5.3. They argued that 'the depth of the sharpest rise of the echo envelope cannot be used to localise a vegetation-covered sea floor' (Tęgowski, Gorska *et al*. 2003, p. 216). They observed that 'in the majority of echoes from a vegetated bottom the highest echo level corresponds to backscattering from the water-bottom boundary' (Tęgowski, Gorska *et al*. 2003, p. 216). To examine such arguments, an investigation of several acoustic data sets groundtruthed by synchronized stereo camera footages has been carried out in this PhD study, which will be discussed in the next chapter.

In order to assess the efficiency of these three parameters in distinguishing the bare sand seafloor and the plant-covered meadows, the Polish researchers used some criteria in the performance assessment procedure. Among these cirteria, suitable thresholds were used to divide echoes into two groups according to the parameter variability range. These two groups correspond to the covered and uncovered bottom conditions. In their algorithm, pings for which the parameter was larger than the threshold were classified as plant ones. The overall classification performance of each parameter groundtruthed by visual inspection was assessed by false alarm and misdetection rates. Figure 2-1, taken from their work, shows how these three parameters performed over the sandy bare bottoms and the plant-covered

meadows. The researchers concluded that the moment of inertia parameter gave the best performance and the fractal dimension parameter the poorest. They suggested that the use of just one parameter was not sufficient to detect vegetation under the conditions provided.

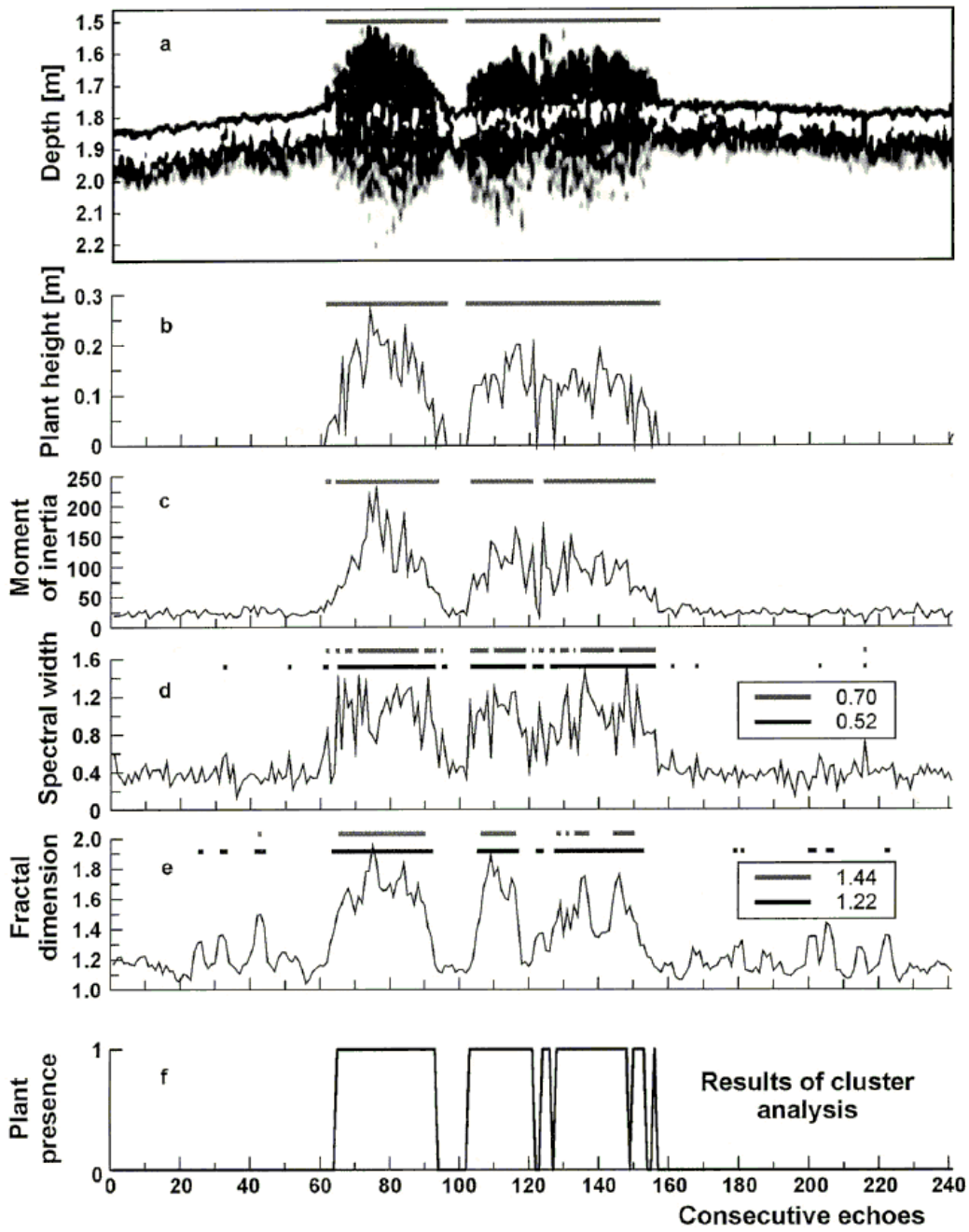

Figure 2-1 Performance comparisons of three parameters (c, d and e) along with the echogram (a), plant height (b) and results of cluster analysis (f) over the sandy bare bottoms and plant-covered meadows presented in the work by Tęgowski, Gorska, and Klusek (Tęgowski, Gorska *et al.* 2003).[†]

[†] Reprinted from Aquatic Living Resources, Vol 16, Jarosław Tęgowski, "Statistical analysis of acoustic echoes from underwater meadows in the eutrophic Puck Bay (southern Baltic Sea)", pages 215-221, copyright (2003), with permission from EDP Sciences.

2.1.3.3.7 Spain

In the earlier stage of a project aiming at characterization of phanerogam communities of *Posidonia oceanica* and *Cymodocea nodosa*, a sidescan sonar was used in the Cabrera Archipelago in the Mediterranean Sea south of Spain (Siljeström, Rey *et al.* 1996). The acoustic data were firstly recorded in an analog form on paper and then scanned to covert them into a digital data format. From the sidescan images collected at two operational frequencies, they found that the '100 kHz band is usually noisier than the 500 kHz one' but 'the definition of the meadow structure is better than that of the 500 kHz image' (Siljeström, Rey *et al*. 1996, p. 311). After applying the K-means algorithm, an enhancement of image classification had been achieved only for the images of dense areas of *Posidonia*. The authors assumed that this could be 'due to the strong structure of the vegetation and to the detailed scale' (Siljeström, Rey *et al*. 1996, p. 312). When the same procedure was applied to the data collected from *Cymodocea*, the classification result from the 100 kHz data 'displays no characteristic structural pattern' but 'a faint dendritic pattern' was discerned when the authors inspected the later images (Siljeström, Rey *et al*. 1996, p. 314). Finally the authors concluded that the use of high resolution sidescan sonar could be a cost-effective solution for the monitoring of these submarine areas. However, no specific acoustic features of seagrass were provided as a basis for the identification of marine vegetation.

Interestingly in a later study on the same experimental data (Siljeström, Moreno *et al.* 2002), the researchers presented a hypothesis to justify the selective response of *Cymodocea nodosa* at two frequencies: 100 and 500 kHz. After proper pre-processing of the two-frequency sidescan images, they found that the 'monospecific plant community presents a very strong acoustic response in 100 kHz' while 'the same vegetation is almost transparent using 500 kHz' (Siljeström, Moreno *et al*. 2002, p. 2872). The authors proposed two possible scenarios to interpret what they had found. The two hypotheses are: 1) air canals in leaves, and 2) air contained in the rhizomes and root systems. Based on their understanding of acoustic theory, they asserted that 'the echo intensity should be higher at 500 kHz than at 100 kHz' (Siljeström, Moreno *et al*. 2002, p. 2874). According to the predicted result from the

theory, the first hypothesis is contradictory to their findings. In their second hypothesis, it 'supposes that the high intensity echo (100 kHz) and the low intensity one (500 kHz) are produced by the rhizome and root systems of *Cymodocea nodosa*' (Siljeström, Moreno *et al*. 2002, p. 2874). From seagrass's anatomy, one can assume that the rhizome and root system can contain air, which might result in high-level echoes at both 100 and 500 kHz. According to the authors' estimate after considering the penetration abilities of the two frequencies in soft sediments, 'the echo produced by the rhizome and root systems buried up to 10 cm deep have an intensity seven times higher at 100 kHz than at 500 kHz' (Siljeström, Moreno *et al*. 2002, p. 2874), which was consistent to their observation. As a result, their second hypothesis was supported. That is, the strong acoustic response at 100 kHz is 1) closely related to the anatomical structure of the plant in that the air can be contained in the dense rhizome and root systems, and 2) related to the 100-kHz's better penetration abilities in sediments than the 500 kHz. This is an important finding. The observation found here can be a useful feature for identification of the seagrass species of *C. nodosa*.

In a different experiment, detailed measurements of the scattering coefficient were made in a laboratory water tank for a thick layer of *Gelidium* seaweed covering a sandy bottom (Carbó and Molero 1997). *Gelidium* is a genus of red algae covering a very wide geographic range. It has long been the major ingredient used as a chemical thickener in the food industry. So there is a strong commercial demand for the information on its geographic distribution needed for harvesting. However, in contrast to the study result made by Maceina and Shireman (Maceina and Shireman 1980), Carbó and Molero were unable to find any unique backscatter characteristics of the *Gelidium* for detection purposes. Using various echosounders with operational frequencies at 102, 201, and 527 kHz in a normal incidence configuration, they found that 'target strength of each individual seaweed front is very weak,' and 'the average value of the bottom scattering strength is found to be between -26 and -34 dB' (Carbó and Molero 1997, p. 343). In the end, the authors concluded that there were difficulties in using echosounder systems to detect the *Gelidium* seaweed layer on a sandy bottom. This shows that the use of echosounders to reliably detect algae such as the *Gelidium* is not a straight-forward procedure. Investigations of study targets and selections of suitable operational frequencies need to be firstly considered before an effective estimate of underwater vegetation by acoustic methods is possible.

2.1.3.3.8 USA

Among many studies, the major acoustic studies of plant benthos in the United States were mostly supported or carried out by a military unit, U.S. Army Engineer Waterways Experimental Station (WES) before the 1990s. They originally investigated various sampling techniques for the assessment and harvesting of the 'submersed aquatic vegetation' (SAV) (Sabol 1984). Later acoustic tools were investigated and developed for the detection and mapping of the SAV in many studies (Sabol and Melton Jr. 1995; Sabol and Burczinski 1998; McCarthy and Sabol 2000; Burczynski, Hoffman *et al.* 2001; Sabol and Johnston 2001; Sabol 2002; Sabol, Burczynski *et al.* 2002; Sabol, Melton *et al.* 2002; Sabol, Shafer *et al.* 2005; Sabol 2005; Sabol and Stewart 2005). The evolution of acoustic techniques was finally developed into a Submersed Aquatic Vegetation Early Warning System (SAVEWS) for the detection and mapping of SAV by the WES (Sabol and Melton Jr. 1995; Sabol and Johnston 2001; Sabol, Burczynski *et al.* 2002; US Army Engineer Research and Development Center 2005). This technique was later transferred to BioSonics Inc., a US hydroacoustic system supplier. One of the products of BioSonics Inc., EcoSAV, was based on SAVEWS patented as a processing technique (Schneider, Burczynski *et al.* 2001). Its methodology will be discussed in section 2.5.3.

Besides the studies carried out by BioSonics and WES in the USA, a unique experimental structure (see Figure 2-2) constructed at a university marina was used for differentiation of the pure acoustic backscatter features of macro algae from that of bare substratum (Riegl, Purkis *et al.* 2005). The experimental setup mainly consisted of a wire basket that can accommodate study targets, such as macro algae or seagrass, and was suspended under an echosounder in the water for measurements. By measuring the acoustic backscatter strength under two different conditions - when the study targets were put into the basket and when removed, the researchers were able to estimate the difference of acoustic backscatter from algae and the sandy substrate. Through this process, the researchers expected to observe the acoustic backscatter characteristics of algae in order to distinguish it from the bare sand seafloor. Although the difference of backscatter intensity between the two conditions

was small, this experiment presented a good scientific approach for the understanding of the acoustic backscatter differences between marine plants and bare sediments.

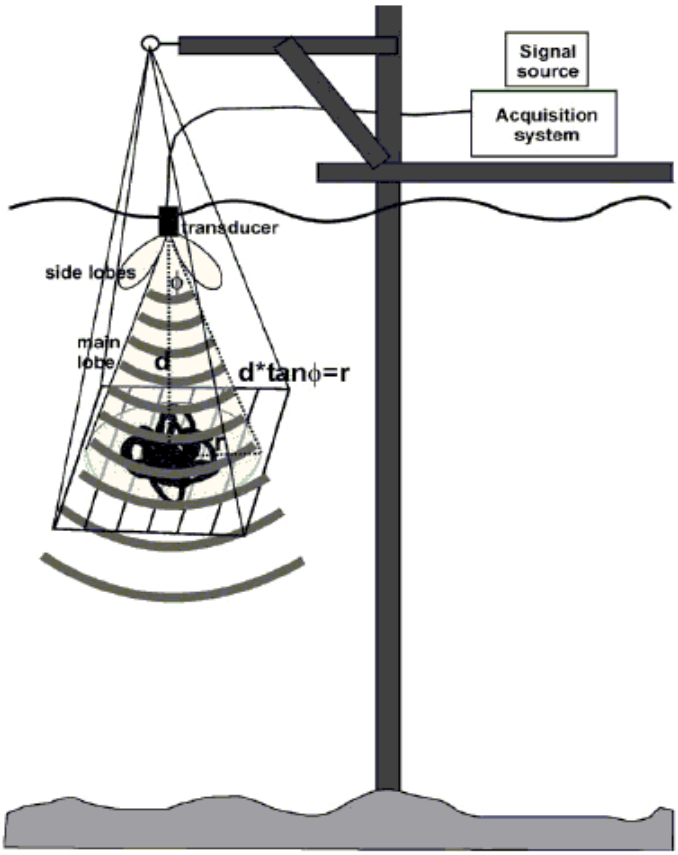

Figure 2-2 An experimental setup for the observations of acoustic backscatter when the macro algae was placed in the wire basket and when removed (Riegl, Purkis *et al.* 2005).‡

In addition to the observations of the macro algae described above, the above study also aimed to assess the effectiveness of various acoustic ground discrimination systems (AGDS), including the RoxAnn algorithm, QTC View and ECHOplus (see section 2.5), on the data collected from macro algae and seagrass in the Indian River Lagoon areas in Florida. The authors used two single beam

‡ Reprinted from Journal of Experimental Marine Biology and Ecology, Vol 326, Riegl *et al.*, "Distribution and seasonal biomass of drift macroalgae in the Indian River Lagoon (Florida, USA) estimated with acoustic seafloor classification (QTCView, Echoplus)", pages 89-104, copyright (2005), with permission from Elsevier.

echosounders at 50 and 200 kHz for the measurements of the acoustic backscatter from areas within the Lagoon in different seasons. By comparing the backscatter characteristics obtained from different locations in different seasons, the authors concluded that the study results 'indicate high spatial and temporal variability in biomass and distribution of macrophyte biomass in the Indian River Lagoon' (Riegl, Purkis *et al*. 2005, p. 90). They also found a dependence of algal biomass on depth and season. This dependence of biomass on sea depth detected by the AGDS systems was also observed by Hutin (Hutin, Simard *et al.* 2005). However, no comments were given for what had caused the depth dependence.

In 1987 and 1988, acoustics was used for mapping the eelgrass *Zostera marina* in Tomales Bay, California (Spratt 1989). Spratt used a Lowrance Truline LRG-1510 fathometer for the determination of eelgrass distribution and a vegetation sampler for groundtruth purposes. The determination of the percent of bottom covered by eelgrass on each transect was measured from acoustic chart recordings (see Figure 2-3). Although the determination of the existence of eelgrass was based on the researcher's visual observation of the recorded echograms, it is still remarkable that acoustics had been recognized as an effective tool for the mapping of eelgrass, especially when reliable quantitative measures of the eelgrass' acoustic features were unavailable in the early days. However, due to the poor performance of the fathometer used, the determination of the eelgrass biomass and its distribution greatly relied on direct sampling tools in order to provide the final eelgrass distribution map for the California Department of Fish and Game.

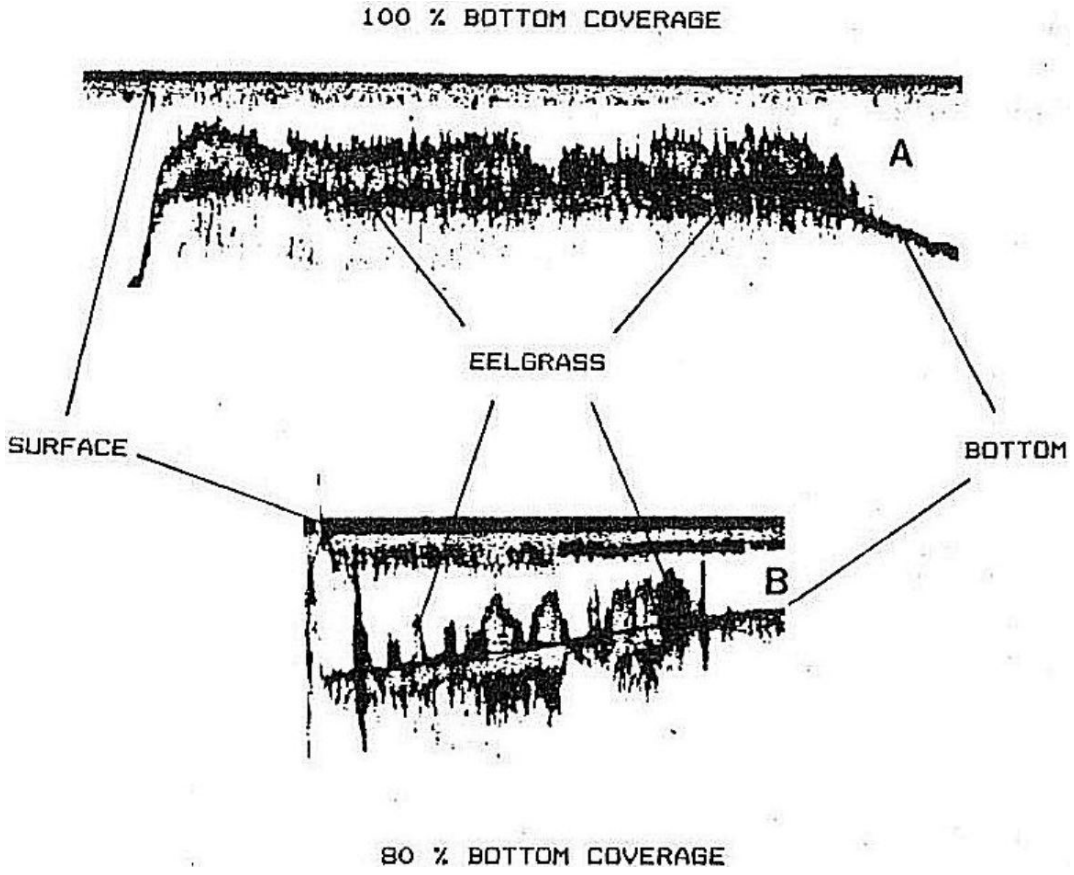

Figure 2-3 Recorded echograms of backscatter from eelgrass, *Zostera marina*. A and B indicate the bottom coverage of 100% and 80% by eelgrass respectively (Spratt 1989).

2.2 Seagrass in Western Australia

In Western Australia (WA) alone, various studies have been made for the understanding of seagrass on the following topics:

- new species (Cambridge and Kuo 1979)
- monitoring of changes in areal coverage (Kendrick, Eckersley *et al.* 1999; Kendrick, Hegge *et al.* 2000; Kirkman and Kirkman 2000; Kendrick, Aylward *et al.* 2002)

- decline of seagrass (Cambridge and McComb 1984; Cambridge, Chiffings *et al.* 1986; Silberstein, Chiffings *et al.* 1986; Walker, Lukatelich *et al.* 1989; Walker and McComb 1992; Hastings, Hesp *et al.* 1995)
- physical factors such as light, temperature, depth, polluted waters, storms, and geological locations affecting seagrass's biological behaviour and distribution (Cambridge 1975; Kirkman 1985; Kirkman and Kuo 1990; Gordon, Grey *et al.* 1994; Masini, Cary *et al.* 1995)
- morphology, anatomy and histochemistry (Kuo 1978; Kuo and Cambridge 1978; Cambridge and Kuo 1982; Kuo, Iizumi *et al.* 1990; Kuo and Kirkman 1990; Kuo 1993)
- canopy structure and pollination biology (Smith and Walker 2002)
- variation of biomass below and above ground (Paling and McComb 2000)
- mechanical transplantation development (Kirkman 1999; Paling, van Keulen *et al.* 2001)
- sedimentation and fauna diversity (Brearley and Walker 1995; Jernakoff and Nielsen 1998; MacArthur and Hyndes 2001; Keulen and Borowitzka 2003)
- association of biomass productivity to the water nutrients (McMahon and Walker 1998)
- ecological significance for the local communities (Walker, Hillman *et al.* 2001)

To provide a background for this research project, the major biological features and distributions of seagrass in WA found in the course of this study are discussed in the following subsections.

2.2.1 Coverage and diversity

Studies of seagrass in WA were mainly limited to areas of shallow waters within 10 m depth offshore of the capital of WA, Perth. The seafloor areas around Cockburn Sound, and Success and Parmelia Banks around Owen Anchorage offshore of the port of Fremantle have been frequently selected as the seagrass study sites. A map showing these areas is given in Figure 2-4. Previous mapping methods included

SCUBA divers' measurement, aerial photography, and satellite imaging. These areas are located within a coastline of 200 km, which is far less than 1 % of the total WA coastline length. Other areas studied also include Warnbro Sound (Walker, Lukatelich *et al.* 1989; Cambridge and Hocking 1997; Smith and Walker 2002), Safety Bay (Keulen and Borowitzka 2003), Rottnest Island (Walker, Lukatelich *et al.* 1989; Brearley and Walker 1995; Hastings, Hesp *et al.* 1995), Shark Bay (Walker and McComb 1988; Marbà and Walker 1999), Geographe Bay (McMahon and Walker 1998), and Two People Bay in Albany (Kendrick, Waycott *et al.* 1997). Australia's coastal waters contain the world's highest diversity of seagrass species, and WA is home to the most diverse seagrass species in Australia (Kirkman 1997; Butler and Jernakoff 1999). It has been estimated that there are over 11 genera and 26 species in WA alone (Kirkman 1997). From the recent observation (van Keulen 2005), the number of species found has increased. There are currently about 58 species recognized of which Australia is home to 30. For the genus *Posidonia*, nine species are currently recognised, of which eight are found in Australia. All eight Australian species occur in WA (Kuo and McComb 1989). The frequently observed and studied seagrass species are *Posidonia sinuosa* Cambridge and Kuo, and *Posidonia australis* Hook. *f.* named after the finders' name (Cambridge and Kuo 1979).

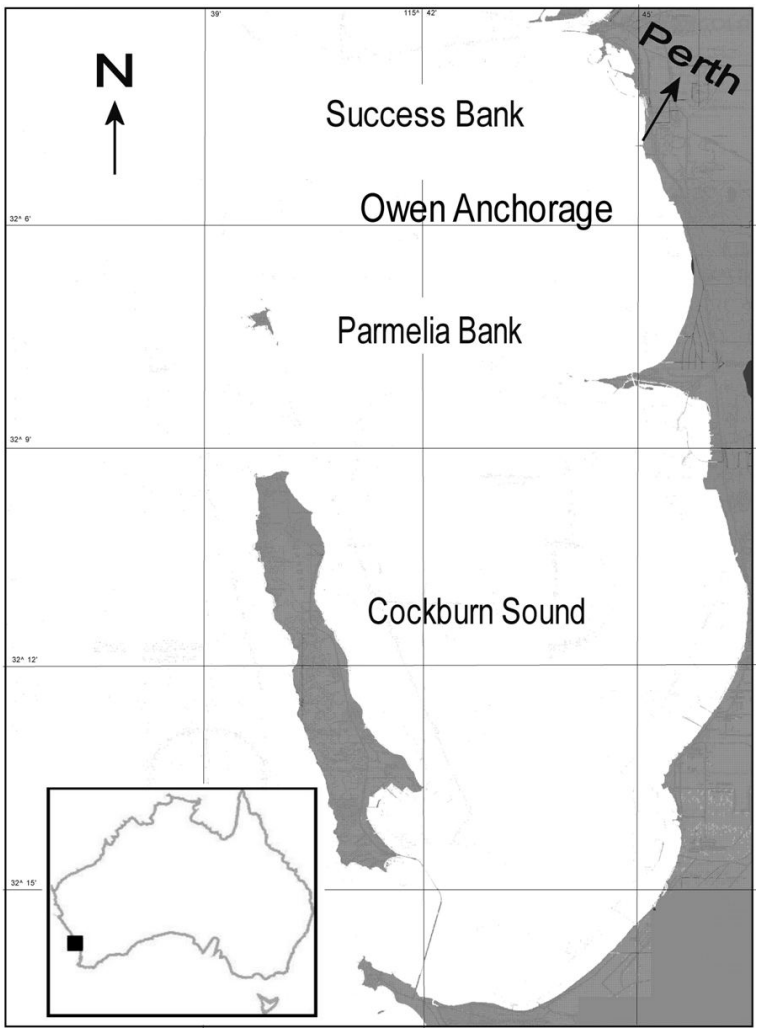

Figure 2-4 Location of Success Bank, Parmelia Bank, Owen Anchorage, and Cockburn Sound offshore of the capital of WA, Perth. The inset shows the approximate position of the areas on the Australia contour.

2.2.2 Biological features of *P. sinuosa* and *P. australis*

Below is a brief discussion of the major biological features of *P. sinuosa* and *P. australis* observed around Cockburn Sound. These features could have effects on the acoustic backscatter and need a thorough understanding.

2.2.2.1 Meadow and canopy structure

According to the samples taken at Warnbro Sound by the biologists (Smith and Walker 2002), meadows of *P. australis* are comparatively smaller (approximately 20-50 m^2) than those of *P. sinuosa* which can extend for hundreds of square metres. *P. sinuosa* shoots often grow in rows (approximately 50 cm wide) and alternate with bare sand channels of similar width (see Figure 2-5a) while *P. australis* shoots grow in an apparently random pattern (see Figure 2-6a). The canopy structure of *P. sinuosa* viewed from above is described as an 'enclosed umbrella-like' canopy while the shoots of *P. australis* have bare spaces between them and may be thought as an 'open' canopy (Smith and Walker 2002, p. 61). From the image data, similar features were also observed on these two seagrass species. Their appearance difference can be observed by comparing Figure 2-5b and Figure 2-6b. Although these two species have somewhat different canopy structure, their canopy heights have little differences. In comparison to the world's longest seagrass *Zostera caulescens* Miki having lengths of up to 7 metres (Aioi, Komatsu *et al.* 1998), the canopy height of these two species is small and ranges from 35 to 45 cm observed by the biologists. These values are different from those observed in the ESP project (around 25 cm) although the extended leaf length can be actually larger than these numbers (see Figure 2-7).

In this study, it was hoped that the acoustic backscatter from seagrass meadows can reveal clues of canopy patterns as one can see from the images. It was believed by the author that the substrate covered by seagrass was more probably detectable by the sonar system if the seagrass canopy is of open canopy pattern rather than closed. This issue is discussed in detail in Chapter 3.

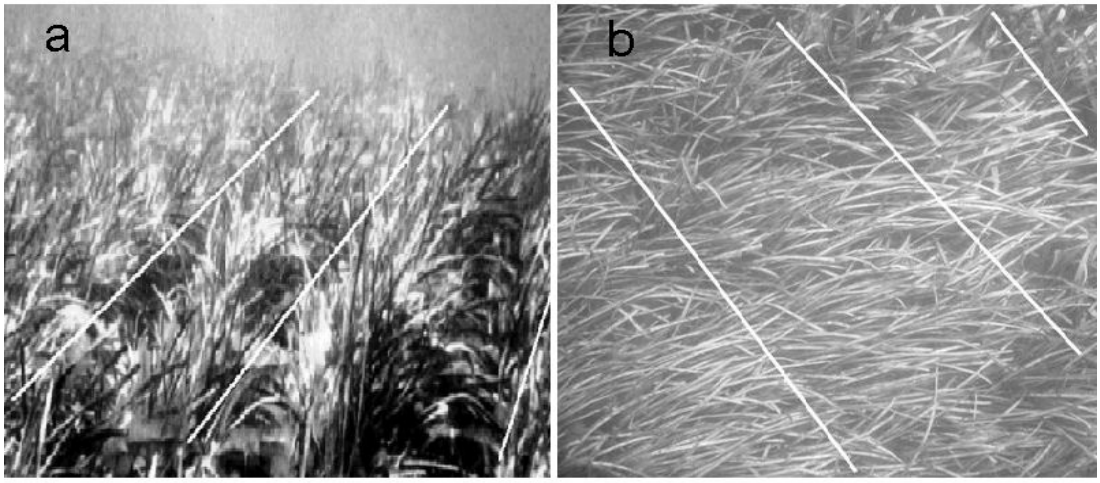

Figure 2-5 Images of *P. sinuosa* meadows from (a)[§] a previous study (Smith and Walker 2002) showing apparent bare sand channels in rows, and from (b) the author's video record showing similar row pattern but having denser shoot cover with almost all the shoots bent horizontally.

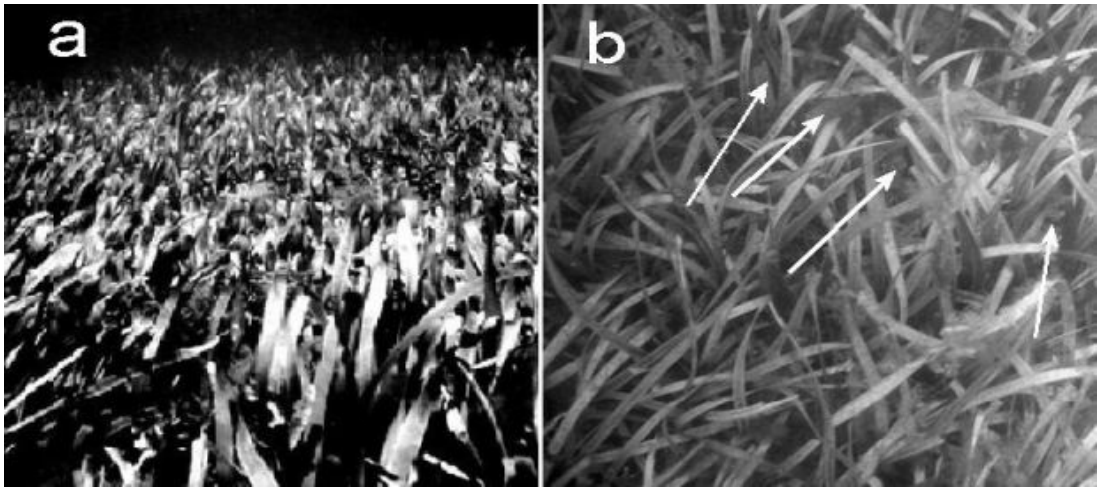

Figure 2-6 Images of *P. australis* meadows from (a)[§] a previous study (Smith and Walker 2002) and from (b) the author's video record showing an apparent open canopy structure when comparing to Figure 2-5b. Areas indicated by the arrows are the spaces in the canopy where a bare sand seafloor is visible.

[§] Reprinted from Aquatic Botany, Vol 74, Smith & Walker, "Canopy structure and pollination biology of the seagrasses *Posidonia australis* and *P. sinuosa* (Posidoneaceae)", pages 57-70, copyright (2002), with permission from Elsevier.

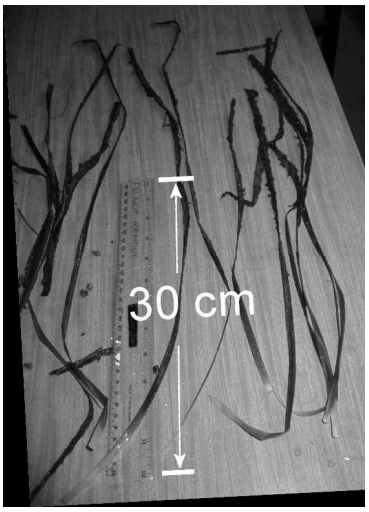

Figure 2-7 Measurements of the leaves of seagrass *P. sinuosa* with a ruler of 30 cm in length. The longest extended leaf length was over 50 cm. The leaves were collected near the Garden Island in Cockburn Sound in 2004.

2.2.2.2 Leaf area index and pollination features

P. sinuosa and *P. australis* differ not only in the meadow and canopy structure but also in shoot density, leaf area, and pollination features. The measured mean shoot density of *P. sinuosa* and *P. australis* is 1475 (m^{-2}) and 913 (m^{-2}) respectively (Smith and Walker 2002). Hence the shoot density of *P. sinuosa* is almost twice as high as that of *P. australis*. This suggests that sonar systems above *P. sinuosa* seagrass meadows will have fewer chances to observe the substrate than above seagrass meadows of *P. australis*.

Smith and Walker observed that leaf area index at flower height in the *P. sinuosa* canopy was significantly higher than that in the *P. australis* canopy. This implies that flowers are better protected in *P. sinuosa*'s meadows due to the higher leaf area index than that of *P. australis*. This means that the sonars will have fewer chances to "see" the flowers and fruits from *P. sinuosa* than from *P. australis*. Questions from this understanding are whether there will be any effective acoustic characteristics that can be observed and related to this biological feature, and if the

sonar systems are effective enough in telling this delicate feature from the vegetation's pollination strategies for survival.

The mean leaf area index is a relative value of the horizontal cross-section of leaves at certain height above the seafloor. A chart showing the distribution of the mean leaf area index and the mean leaf biomass of these two seagrass species at different heights is provided in Figure 2-8. Based on Smith and Walker's measurements, the leaf area distribution in Figure 2-8a can be represented by a chart (see Figure 2-9) indicating the contribution of each leaf cross-section area to the acoustic shielding of the substrate. From Figure 2-9, it is obvious that *P. sinuosa* is more effective than *P. australis* in hiding the substrate from acoustic observation. For *P. sinuosa*, the contribution of the leaf area covering is dominated by the "Of bent section" and the "Below bent section". For *P. australis*, the major contribution comes from the "Below bent section". The "At flower height" sections of both seagrass species contribute little effect to the area covering. This implies that the contribution of the "At flower height" of both seagrass species to the acoustic shielding of the substrate has little difference.

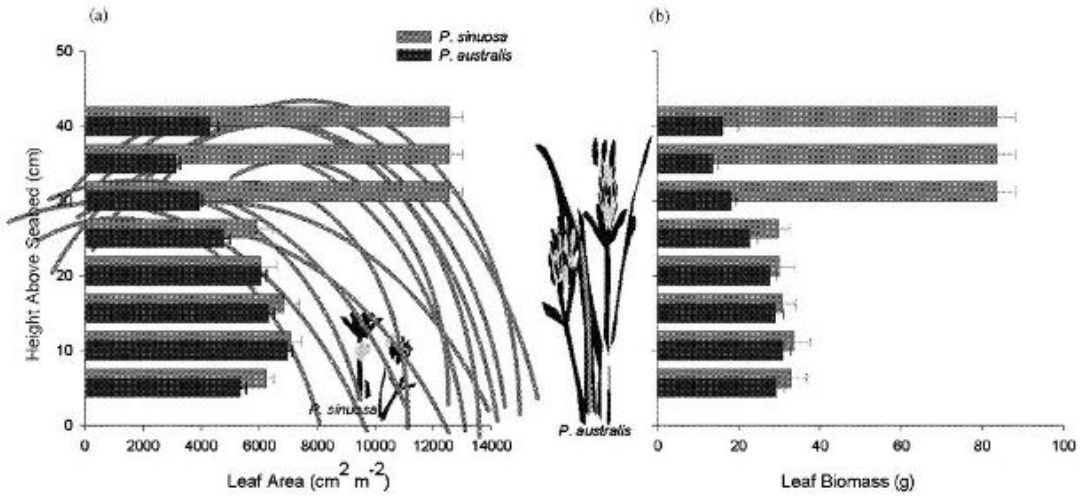

Figure 2-8 Distribution of (a) leaf area, and (b) leaf biomass of shoots in situ in the *P. sinuosa* and *P. australis* canopies (Smith and Walker 2002)**

** Reprinted from Aquatic Botany, Vol 74, Smith & Walker, "Canopy structure and pollination biology of the seagrasses *Posidonia australis* and *P. sinuosa* (Posidoneaceae)", pages 57-70, copyright (2002), with permission from Elsevier.

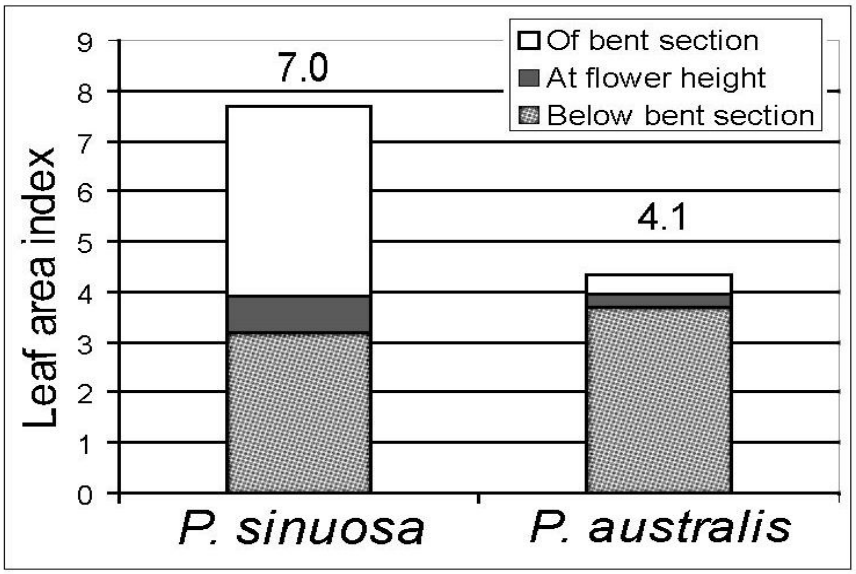

Figure 2-9 Stacked distribution of the occupied areas of the "Of bent section", "At flower height", and "Below bent section" on the meadows of *P. sinuosa* and *P. australis*, and their total leaf area cover indexes according to Smith and Walker's measurement readings.

2.2.2.3 Anatomy of seagrass

According to biologists' observation, both *P. australis* (Kuo 1978) and *P. sinuosa* (Cambridge and Kuo 1982) leaf blade has large air-lacuna (see Figure 2-10 and Figure 2-11). There is no significant difference in the size of the air-lacuna in the inner portion of leaf blade between these two species. However, there is a significant difference on the cuticle (a continuously structural layer on leaf surface). In contrast to *P. australis*, the leaf cuticle of *P. sinuosa* is not porous in appearance (see Figure 2-11). It is unknown if the porous structure of the leaf cuticle of *P. australis* contains air or not. If the porous structure contains air, this may explain why *P. australis* is more capable of standing upward than *P. sinuosa*.

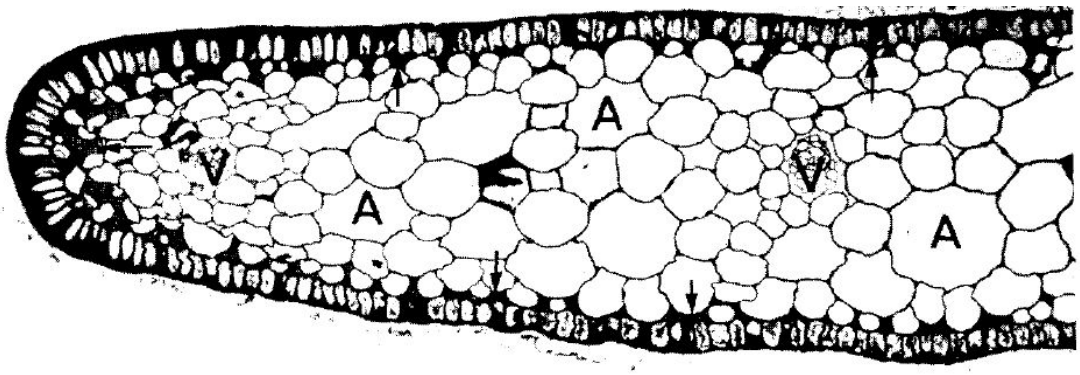

Figure 2-10 Transverse cross section of a portion of a *P. australis* leaf blade with air-lucuna marked by A and the cuticle on skin with porous structure (Kuo 1978).††

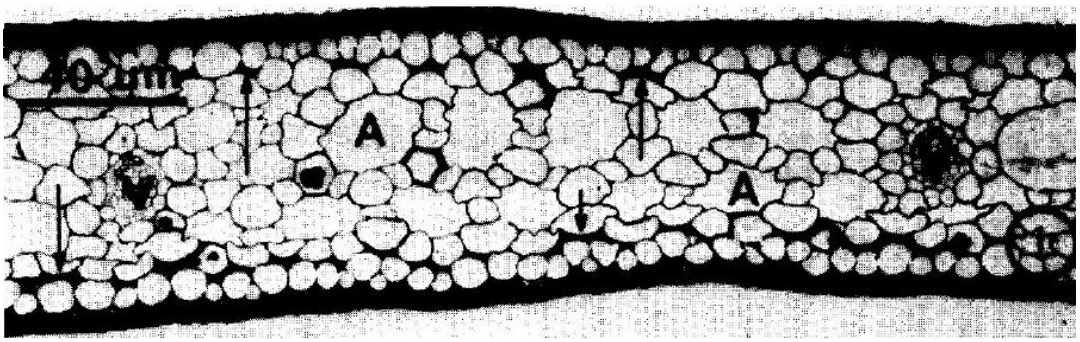

Figure 2-11 Transverse cross section of a portion of a *P. sinuosa* leaf blade with air-lucuna marked by A and the cuticle on skin without porous structure (Cambridge and Kuo 1982).‡‡

Larger leaf area coverage by *P. sinuosa* may physically cover the sand bottoms and contribute superior masking effects than *P. australis* for the undercovered sand bottoms from being observed by sonar systems above. However,

†† Reprinted from Aquatic Botany, Vol 5, Kuo, "Morphology, anatomy and histochemistry of the Australian seagrasses of the genus *Posidonia* könig (posidoniaceae). I. Leaf blade and leaf sheath of *Posidonia australis* Hook. *f.*", pages 171-190, copyright (1978), with permission from Elsevier.

‡‡ Reprinted from Aquatic Botany, Vol 14, Cambridge and Kuo, "Morphology, anatomy and histochemistry of the Australian seagrasses of the genus *Posidonia* könig (posidoniaceae). III. *Posidonia sinuosas* Cambridge & Kuo.", pages 1-14, copyright (1982), with permission from Elsevier.

if the porous structure of the leaf cuticle of *P. australis* contains air, it may contribute more substantial effects to the sonar systems than *P. sinuosa*'s larger leaf area.

Besides the above mentioned features, the seagrass's assembly features, such as the row pattern of *P. sinuosa* meadows, might be possibly observable and used for seafloor characterization by acoustic systems. The presence and the biological features of seagrass may affect acoustic backscattering from the seafloor, which was one of the major focuses of this study that predetermined the selection of instrumentation and data analysis methods implemented in the project. These effects are discussed in more detail in Chapter 3 and Chapter 4.

2.3 Acoustic studies of seafloor substrates

2.3.1 Relevance of seafloor substrates to this study

Most of acoustic studies of the seafloor made to date have primarily been focusing on mappings of seafloor substrates rather than marine benthos (Dalachartre, Vray *et al.* 1992; Thorne, Hardcastle *et al.* 1994; Andrieux, Delachartre *et al.* 1995; Beaujean 1995; Clarke, Danforth *et al.* 1997; Dyer, Murphy *et al.* 1997; Walter, Lambert *et al.* 1997; Taylor, Vincent *et al.* 1998; Thorne, Hardcastle *et al.* 1998; Caiti 2000; Brandes, Silva *et al.* 2001; Chakraborty, Kaustubha *et al.* 2001; Thorsos, Williams *et al.* 2001; Bentrem, Sample *et al.* 2002; Caruthers and Fisher 2002; Chotiros, Lyons *et al.* 2002; Thorne and Hanes 2002; Walter, Lambert *et al.* 2002; Atallah and Smith 2003; Preston, Parrott *et al.* 2003; Carle, Bloomer *et al.* 2004; Collier and Brown 2005; Tęgowski 2005). The substrate here means the sediments, reefs and rocks constituting the seabeds on which the benthos resides. Seafloor substrates may consist of sand, mud, rocky rubble, coral reefs, or a mixture of these. The reason of examining the acoustic backscatter properties of substrates is that backscatter from the target seafloor vegetation may also contain effects from the substrates. In order to extract the "pure" acoustic backscatter features of the seafloor vegetation only, it is essential to understand the influence of the background signals

backscattering from the substrate, i.e. the seafloor without vegetation. Figure 2-12 illustrates this idea in a simplified manner. In the scenario shown in Figure 2-12, the recorded echo comprises backscatter from everything within the cone under the echosounder, including mainly but not exclusively the seagrass and the sediment. This is the main reason why the acoustic backscatter properties of the seafloor free of vegetation is an essential part of the vegetation's acoustic study.

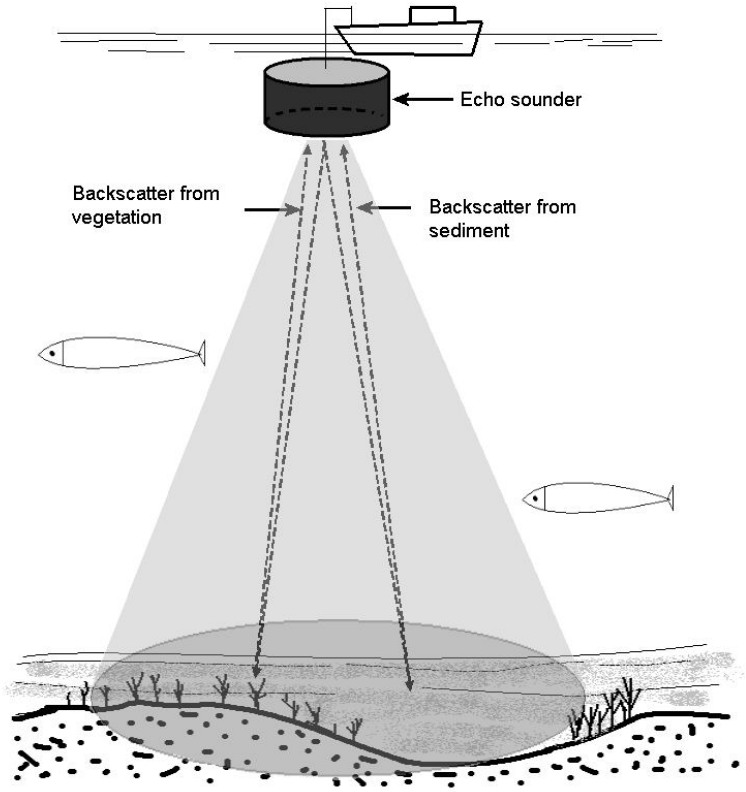

Figure 2-12 An illustration of the scenario when acoustic backscatter is collected from a combined effect with targets in the insonified acoustic cone, including the vegetation and the sediment.

2.3.2 Classification techniques developed

Caruthers and Fisher provided a comprehensive overview of the acoustic systems used for sediment classification tasks (Caruthers and Fisher 2002).

Classification systems were divided into two categories: sonar systems of vertical- and oblique-incidence configurations. Among these systems, vertical-incidence systems occupied the major portion of their reviews although they also discussed sidescan sonar systems which belong to the oblique-incidence category. They investigated many classification systems, such as RoxAnn, QTC View, ECHOplus, BioSonics' classification system, and Automated Seafloor Classification System. The classification systems were reviewed to assess their effectiveness in classifying the sediment types. Among these systems, RoxAnn, QTC View, and BioSonics have been frequently investigated with respective to their effectiveness in classification tasks (Brown, Mitchell *et al.* 2005). A brief overview of these classification techniques will be briefly given in section 2.5.

2.4 Acoustics used in various problem related tasks

In recent years, several research programs were carried out in order to develop techniques for effective mappings of the plant benthos. For instance, a project for mapping the nuisance macro algae (*Ulva* genus) for effective harvesting was carried out in Delaware's inland bays (Rehoboth Bay, Indian River and Little Assawoman) in 2000 (Seaman, Finkbeiner *et al.* 2000; NOAA Coastal Services Center 2005). The observations were made by deploying a 200 kHz echosounder system in deeper parts of the bays of turbid areas and a conventional colour aerial photographic technique in clear and shallow waters. The acoustic data were processed by a GroundMaster RoxAnn signal processor combined with RoxMap software for the RoxAnn's roughness (E1) and hardness (E2) analysis. With the classified habitat map based on RoxAnn's technique, the researchers claimed that 'they identified vegetated areas and preliminary results indicate RoxAnn may be able to distinguish between *Gracilaria* and *Ulva* accumulations' (Seaman, Finkbeiner *et al*. 2000, p. 1704). Although it is not evident from the paper in showing how the macro algae were identified and classified into subgroups, this project demonstrated that acoustic systems were effective tools for mapping vegetation in areas where photographic techniques were ineffective.

Acoustic techniques have gradually been improved and applied to various tasks related to studies of the seafloor. Besides studies of seagrass, acoustic techniques have also been employed for the following tasks which are related to seafloor vegetation:

- determination of depth-related distribution and abundance of seastars (Howell, Billett *et al.* 2002);
- lake bottom recognition (Andrieux, Delachartre *et al.* 1995);
- measurements of detritus (Di Massa and Bosma 2000);
- measurements of oxygen synthesis by seagrass (Hermand, Nascetti *et al.* 1998; Hermand, Nascetti *et al.* 1999; Hermand 2004b; Hermand 2004a);
- shellfish abundance estimation (Smith and Greenhawk 1998; Wildish, Fader *et al.* 1998; Naidu and Seward 2003);
- and many seabed-related acoustic studies (Orr and Rhoads 1982; Libicki, Bedford *et al.* 1989; Panda, LeBlanc *et al.* 1994; Beaujean 1995; Bentrem, Sample *et al.* 2002; Walter, Lambert *et al.* 2002).

The reason for considering the above mentioned topics is the frequent presence of organisms or objects close to, on or beneath the seabed. The presence of these creatures can bring impacts to the effective detection of actual study targets.

2.5 Commercial classification techniques

The studies presented in this section include commercial classification techniques which are primarily software products, although some commercial classification techniques include both hardware and software tools as a whole package. Since the methods used for acoustic classification of the seafloor play an important role in providing habitat maps for end users, it is necessary to understand the algorithms embedded in the commercial products. An overview of such products is given in the following subsections. As can be seen from results of several studies, there are both significant achievements and shortcomings in the application of the discrimination techniques to the marine habitat mapping (Schlagintweit 1993; Magorrian, Service *et al.* 1995; Greenstreet, Tuck *et al.* 1997; Sotheran, Foster-Smith

et al. 1997; Caddell 1998; Pinn and Robertson 1998; Pinn, Robertson *et al.* 1998; Hamilton, Mulhearn *et al.* 1999; Kloser, Bax *et al.* 2001; Pinn and Robertson 2001; Siwabessy 2001; Caruthers and Fisher 2002; Fodale, Bronte *et al.* 2003; Foster-Smith and Sotheran 2003; Freitas, Rodrigues *et al.* 2003; Freitas, Silva *et al.* 2003; Pinn and Robertson 2003; White, Harborne *et al.* 2003; Wilding, Sayer *et al.* 2003; Foster-Smith, Brown *et al.* 2004; Humborstad, Nottestad *et al.* 2004; Madsen 2004; Brown, Mitchell *et al.* 2005; Collier and Brown 2005). Since full descriptions of each product have been provided by each respective manufacturer, only the major features of those classification systems and dissimilarities in their classification approach will be outlined in the following subsections.

2.5.1 RoxAnn

RoxAnn's classification technique is probably one of the most common methods familiar to researchers. It uses two parameters derived from the acoustic backscattered pulses as a measure of the seafloor's roughness and hardness. Practical applications of this method and some theoretical issues of the algorithm have been thoroughly investigated in several works (Chivers, Emerson *et al.* 1990; Schlagintweit 1993; Heald and Pace 1996; Greenstreet, Tuck *et al.* 1997; Hamilton, Mulhearn *et al.* 1999; Siwabessy 2001; Caruthers and Fisher 2002; Wilding, Sayer *et al.* 2003; Humborstad, Nottestad *et al.* 2004). Theoretical grounds of the method were made as early as in 1984 (Orłowski 1984). The method developed by Orłowski was also specifically highlighted in Hamilton's report for the Defence Science and Technology Organisation (DSTO) (Hamilton 2001).

The roughness and hardness are exclusively used as the only parameters characterising each echo from the seafloor (Chivers, Emerson *et al.* 1990; Heald and Pace 1996). Once acoustic samples are represented in a two dimensional space of roughness and hardness, various criteria can then be used to cluster the samples into different classes. Different clusters of samples represent different classes of seafloor habitat types. The criteria used for clustering is mainly based on groundtruth recordings or subjective considerations. There is no universal approach to the selection criteria. Ultimately, the method aims at the optimal results that can provide

distinctive habitat maps such as a colour coded map of different seafloor habitat types.

Empirical factors and subjective decisions often determine the number of classes defined in the roughness and hardness space. When two or more clusters overlap each other, it is often a difficult problem for the determination of the appropriate number of distinctive classes. In this two dimensional space, overlapping of two different classes is highly probable.

Questions have been raised in a few studies on whether acoustic classification tools are capable of distinguishing details of the real habitats, such as the differences between seagrass and macro algae or even the morphologic differences of the same vegetation group (Maceina and Shireman 1980; Colantoni, Gallignani *et al.* 1982). So the classification task does not just involve the technical issues only but also the decision regarding the final resolution of the habitat maps with respect to different classes. This point was also highlighted by many researchers. For instance, the classification algorithm can be adapted to ignore minor classes and keep the predominant classes in order to show the major habitat types on the map (Brown, Mitchell *et al.* 2005).

Comparing to other methods, RoxAnn's technique may have different classification results in certain circumstances. For instance, Collier and Brown mentioned that 'the RoxAnn roughness index E1 compared well with the sidescan, whilst the RoxAnn hardness index E2 did not' (Collier and Brown 2005, p. 431).

2.5.2 QTC

Quester Tangent provides a series of commercial products for sonar data acquisition and post-processing. Especially suitable for single beam echosounders, QTC Impact provides the function that can determine effective acoustic parameters for differentiating the seabed features using only the first echo return from the seabed. The use of the first echo return only is different from the RoxAnn technique where both the first and second echo returns are utilized. It is understood that characterization parameters extracted from the samples or records are presented in a Q space. Through a principal component analysis, prominent Q parameters

contributing most to the spatial variations are selected to characterize the whole data set. Clustering is then applied to the samples distributed in the selected Q space. Both supervised and unsupervised data training schemes can be adopted in the QTC system. The QTC classification ability is comparable to other techniques although some differences have been found in certain cases (Smith and Greenhawk 1998; Galloway 2001; Smith, Bruce *et al.* 2001; Hutin, Simard *et al.* 2005; Moyer, Riegl *et al.* 2005). A detailed discussion of the QTC technique for acoustic bottom classification is available from Legendre's report (Legendre 2002).

2.5.3 BioSonics

In addition to the above mentioned classification techniques, there are also ECHOplus, the Automated Sediment Classification System (ASCS) and other techniques developed for classification of sonar data and examined by many researchers (Lambert, Walter *et al.* 1998; Bates and Whitehead 2001; Caruthers and Fisher 2002; Riegl, Purkis *et al.* 2005).

In BioSonics's sonar processing and classification packages, each of their four methods except the B1 method developed for seafloor discrimination extracts a pair of parameters from the backscatter signals (Burczynski 2001). In these four methods, the parameters are extracted either from the first echo only or from both the first and second echoes. The following subsections give a brief description of these four methods and the parameters determined in each of them.

2.5.3.1 B1 method

This method basically follows Pouliquen and Lurton's idea (Pouliquen and Lurton 1992). In this method, it is assumed that soft sea bottoms tend to produce flatter echo returns than the harder ones (see Figure 2-13a). By integrating the squared echo amplitude within a certain time interval, the cumulative energy is obtained (see Figure 2-13b). After acquiring the bottom echoes from each known bottom type, a database comprising distinctive bottom classes is built. It is also

assumed in this method that each distinctive bottom class has its own distinctive cumulative energy profile. By using a curve fitting algorithm along with the groundtruthed database, unknown bottom echoes can be identified and classified into distinctive classes. This is the so called B1 method in the VBT[§§] software.

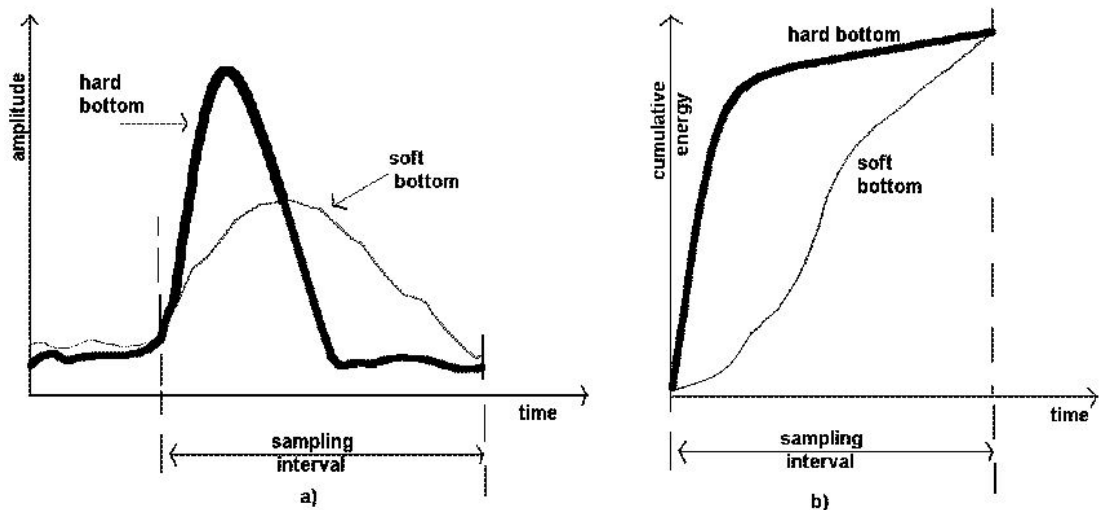

Figure 2-13 The first bottom echo envelopes from soft and hard bottoms illustrating the approach used in the BioSonics B1 method: (a) envelopes of the echo amplitude and (b) cumulative energy after integrating the squared echo amplitude within a certain time interval (Burczynski 2001).[***]

2.5.3.2 B2 method

This method is an exact replica of the RoxAnn's algorithm. Figure 2-14 demonstrates the classification scheme according to the clustering of the backscatter data in the E1 (roughness) and E2 (hardness) space.

[§§] A software package developed by BioSonics for bottom classification and sediment analysis.

[***] Figure reused with permission from Janusz Burczynski with the BioSonics Inc., 4027 Leary Way NW, Seattle WA 98107, USA.

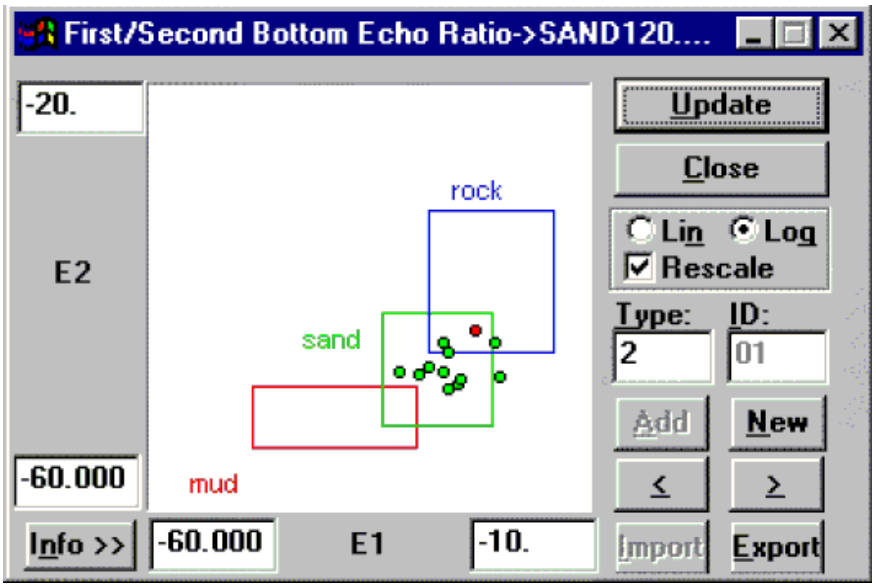

Figure 2-14 E1 and E2 parameters used in BioSonics's B2 method for classifying different bottom types (Burczynski 2001).[†††]

2.5.3.3 B3 method

The B3 method uses only the first bottom return to determine the modified roughness and the modified hardness parameters. The modified roughness parameter defined in this method is almost the same one as that used in the RoxAnn's algorithm for estimating the roughness feature. To illustrate the idea of this method, a drawing demonstrating the evolution of the insonified areas on the bottom with time is shown in Figure 2-15. It shows the development of the insonified area in its three phases. The following is the description of the three phases:

[†††] Figure reused with permission from Janusz Burczynski with the BioSonics Inc., 4027 Leary Way NW, Seattle WA 98107, USA.

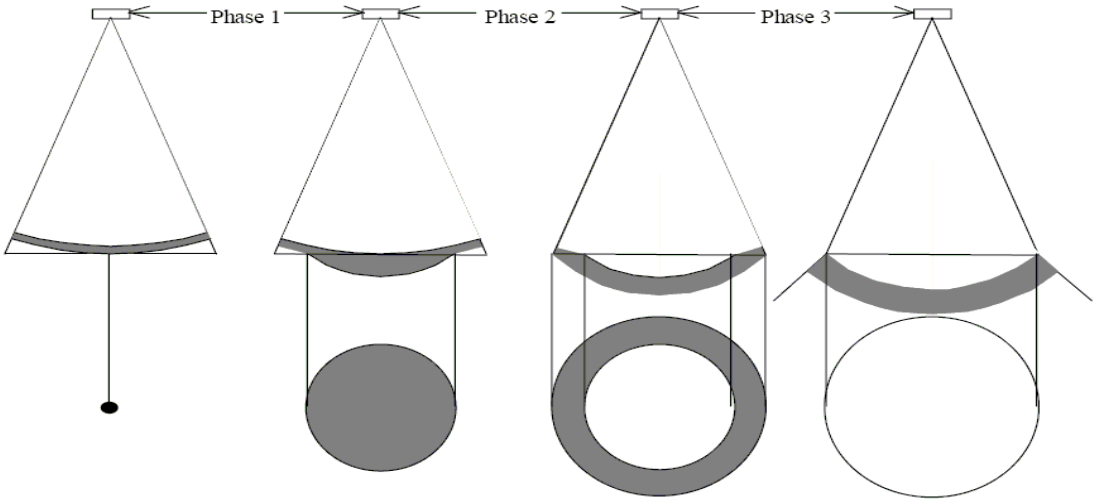

Figure 2-15 Three successive phases of an echo showing the insonified areas on the sea bottom (Burczynski 2001). In Phase 1, the insonified area increases with time. In Phase 2, the insonified area is ring-like and increasing in diameter with time. In the last phase, the ring width rapidly decreases with time until it disappears.‡‡‡

Phase 1 – Attack - It starts from the moment when the front of the transmitted pulse at the specular angle touches the bottom and lasts for approximately the length of the transmitted pulse.

Phase 2 – Decay - It starts from the end of Phase 1 to the moment when the edge of the footprint is insonified.

Phase 3 – Release - It starts from the end of Phase 2 and lasts until the moment when the end of the transmitted pulse insonifies the edge of the footprint.

It is assumed that the remaining portion after the last phase is mainly caused by the reverberation due to bottom volume inhomogenity. To illustrate this model, Burczynski numerically simulated the effects of bottom surface reverberation and

‡‡‡ Figure reused with permission from Janusz Burczynski, BioSonics Inc., 4027 Leary Way NW, Seattle WA 98107, USA.

bottom volume reverberation contributing to the resulting echo received by the echosounder (see Figure 2-16). The plot shows that the major contribution to the echo after the last phase is primarily from the bottom volume reverberation. Figure 2-17 shows how different types of sea bed, from fine sand to rock, affect the echo tail appearing as a shoulder.

In this method, the first bottom return is divided into two parts. The first part starts from the echo front and ends in a time interval equal to the transmitted pulse width. The second part starts right after the first part and lasts three times longer than the transmitted pulse width. The modified roughness parameter in this method is defined as the energy of the second part. The modified hardness parameter is the energy of the first part of the first bottom echo, which is different from the hardness determined in the RoxAnn algorithm.

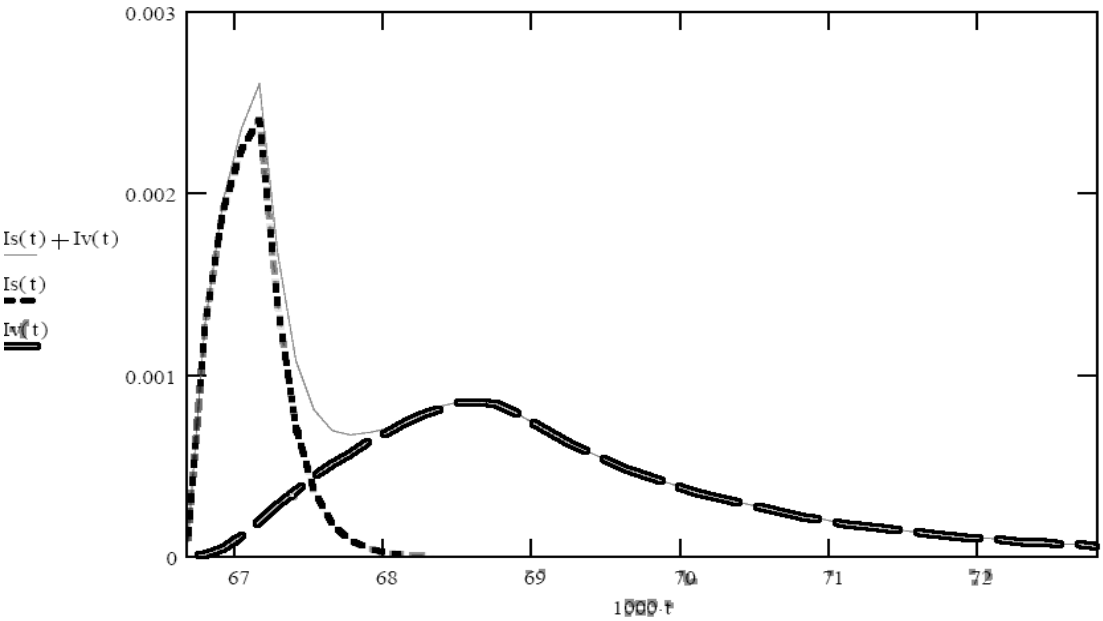

Figure 2-16 Simulation result showing the contribution from bottom surface reverberation (short dash line) and bottom volume reverberation (long dash line) to the collected echo (solid line).[§§§]

[§§§] Figure reused with permission from Janusz Burczynski with the BioSonics Inc., 4027 Leary Way NW, Seattle WA 98107, USA.

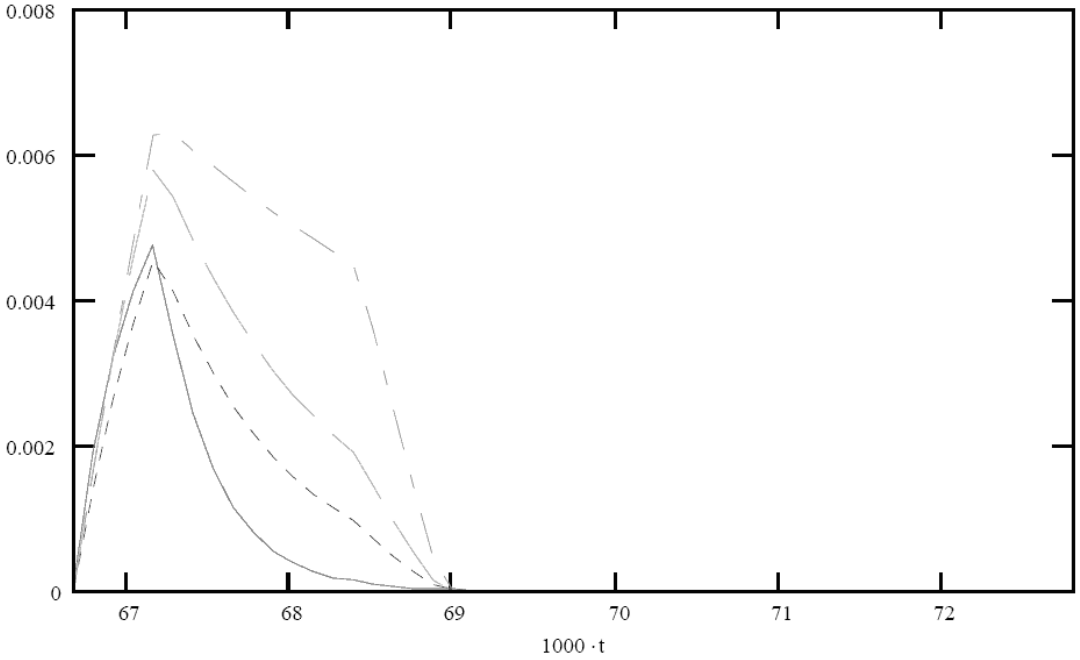

Figure 2-17 Numerical simulation results for the echo backscattering from fine sand (solid line), sand (short dashed line), gravel (long dashed line) and rock (alternate long and short dashed line) made by Burczynski. The shoulder at the tail of the echo gradually appeared as the bottom types varied from fine sand to rock, which indicates the contribution of the bottom volume reverberation from different types of sea bottoms.[****]

2.5.3.4 B4 method

The fractal dimension parameter (see section 4.2.1.4 for the definition of fractal dimension) is used in the B4 method, in addition to the roughness parameter (E1) which is determined in the same way as that in the previous methods and in the RoxAnn algorithm. The effectiveness of using the fractal dimension parameter of the first bottom echo for characterizing the seafloor types has been explored by Tęgowski, Gorska and Klusek (Tęgowski, Gorska *et al.* 2003) who concluded that

[****] Figure reused with permission from Janusz Burczynski with the BioSonics Inc., 4027 Leary Way NW, Seattle WA 98107, USA.

the poorest parameter was the fractal dimension when compared with two more effective parameters, the moment of inertia and the spectral width.

Both Sabol's reports (Sabol and Johnston 2001; Sabol, Burczynski *et al.* 2002) for the US Army Corps and Engineers and Caruthers and Fisher's report (Caruthers and Fisher 2002) provided a clear explanation of BioSonics's classification algorithms developed for seafloor characterization. As to the choice of the method most suitable for seafloor characterization in any particular conditions, there is little information and discussion available from the reports.

BioSonics also suggested a method for detecting seagrass and estimating its height (Sabol and Johnston 2001). The method is based on an assumption that the leading edge of the echo signal corresponds to backscatter from the top of the seagrass canopy, while the "true" bottom, i.e. the sediment substrate, can be determined from the time of the trailing edge crossing a threshold of certain level (relative to the maximum backscatter) corrected for the transmitted pulse length. Sabol *et al*. suggested a threshold of –50 dB. At high frequencies, such as 200 kHz, the leading edge of the echo signal backscattered from seagrass is usually distinctive enough to be observed, so that the range estimate to the seagrass canopy determined by the moment of threshold crossing is reasonably accurate, which is discussed in detail in section 4.2.3 of the thesis.

In contrast to the canopy top, detection of the substrate by the threshold crossing of the trailing edge, as used in the BioSonics' method, is much more ambiguous. As demonstrated in Chapter 4, the echo signal backscattered from seagrass consists commonly of multiple peaks with highly variable amplitudes. The later arrival peaks strongly distort the trailing edge in a fairly random manner, and hence the moment of threshold crossing at a fixed amplitude level also strongly varies from one echo signal to another, even if the sea depth does not change. Consequently, the range estimates by the trailing edge contain large random errors.

2.6 Observations of seafloor backscatter characteristics at different frequencies

Unique backscatter characteristics from benthos have been noticed by researchers. Mackinson's research group observed stronger backscatter intensity at 120 kHz than that at 38 kHz for sandeels (Mackinson, Turner *et al.* 2005). Similar observations with the employment of a sidescan sonar also found that the acoustic seafloor images from the 100 kHz band were usually noisier than the 500 kHz (Siljeström, Rey *et al.* 1996). However, Siljeström's research group also noticed that the definition of the meadow structure derived from the 100 kHz was better than that from the 500 kHz. From the above observations, it shows that the use of different frequencies presents different information about the study targets. From the studies of the *Posidonia* seagrass, historical records indicated that higher frequencies gave more details than the lower ones.

2.7 Concluding remarks

It is obvious that acoustic studies of seafloor vegetation comprise a wide scope of knowledge. The acoustic backscatter from seafloor vegetation depends on the vegetation's biological features, sediment properties, and technical characteristics and measurement settings of the sonar systems. Issues involved include many technical issues and environmental constraints as well. Acoustically determined results need to be compared to groundtruth measuremnts such as video recordings or direct samplings in order to provide accuracy assessment. In this study, the acoustic observation was verified by comparing to the optical recordings.

In this thesis, basic quantitative assessments are provided. Although not exhaustive, it is hoped that this study can provide some basic ideas of the acoustic properties of the seafloor vegetation for further research needs.

Among a large variety of seafloor vegetation, only a limited number of species have been acoustically studied before. No matter whether they are animal or plant benthos, the acoustic backscatter characteristics are still not fully understood.

Since there is a need for using acoustics as a means to effectively characterize and monitor the vegetation on seafloors, potential methods for the above purpose were investigated in this study.

There is a potential by the use of sonar systems with different frequencies to characterize the study targets. The use of two frequencies in providing quantitative assessments of seagrass canopy height will be illustrated in section 4.3.4.

Chapter 3 Instrumentation and data collections

Based on the understanding of the literature discussed in Chapter 2, instrumentation and data collection aim to support the following requirements:

- To collect groundtruth recordings (videos and photographs) that can reflect the actual situation of the study targets as accurately as possible so that the groundtruth recordings can provide the best support for the identification of the acoustic data.
- In addition to seafloor vegetation, to collect data from bare sea bottoms such as pure sand bottoms so that the backscatter characteristics can be compared to that of seafloor vegetation.
- To collect high resolution acoustic data in the hope that morphological features of underwater vegetation can be revealed.
- To develop and build a composite data collection system which can collect groundtruth recordings (videos and photographs) and acoustic data simultaneously.

In order to fulfil the above requirements, the instrumental systems and the experimental setup were designed and built, and will be introduced below.

3.1 The Epi-benthic Scattering Project (ESP)

The ESP project is part of the Coastal Water Habitat Mapping (CWHM) project of the Cooperative Research Centre for Coastal Zone, Estuary and Waterway Management (Coastal CRC). It was initiated within the CWHM project, with one of its goals being to provide support for the author's study needs. It ran from the end of

2003 until the beginning of 2006. It was mainly supported by the Coastal CRC, with additional resources provided by Curtin University of Technology.

'The aim of this project is to develop innovative acoustic techniques as a tool for seafloor habitat mapping,' as was stated in the beginning of its first milestone report (Woods 2004). In order to achieve this aim, several steps were taken:

- Development of a test rig: This enabled a direct comparison of acoustic backscatter with stereoscopic imagery from a range of benthic habitats, including those with substantial communities of seagrasses and macro algae,
- Investigation of the relationship between a plant's physical characteristics and acoustic backscatter: This provided opportunities to find useful acoustic parameters that can be used to characterize the epi-benthic plants,
- Development of appropriate processing techniques: The techniques developed can be used as effective tools to distinguish the seafloor vegetation from other habitat types observed in this study.

In order to fulfil the above requirements, the ESP project was divided into three stages. Each stage involved a field experiment with its own goal and is introduced in section 3.3.

3.2 Instrumentation

The ESP data collection mainly included the use of two echosounders and an optical sub-system. The acoustic system included the SIMRAD EQ60, a single beam echosounder operating at 38 and 200 kHz, and the TAPS (Tracor Acoustic Profiling System), a six-frequency echosounder. The optical system mainly contained a pair of digital cameras. These two cameras were controlled by a custom electronic circuit board. The development of the design and the use of the composite system are introduced in the following subsections.

3.2.1 Development of data collection facilities

3.2.1.1 The ESP structure

The ESP test rig is shown in Figure 3-1. A diagram in Figure 3-2 illustrates the basic experimental conditions of the concluded ESP project. The structure can accommodate the optical and acoustic components for the simultaneous data collection and can be deployed and operated from a small boat. The triggering of the two data collection components was synchronized. Due to the synchronization ability, each echo can be accurately identified by the examination of the corresponding stereoscopic photographs. After calibration, the stereoscopic camera system is capable of measuring the seagrass canopy height for comparisons with the the acoustic recordings.

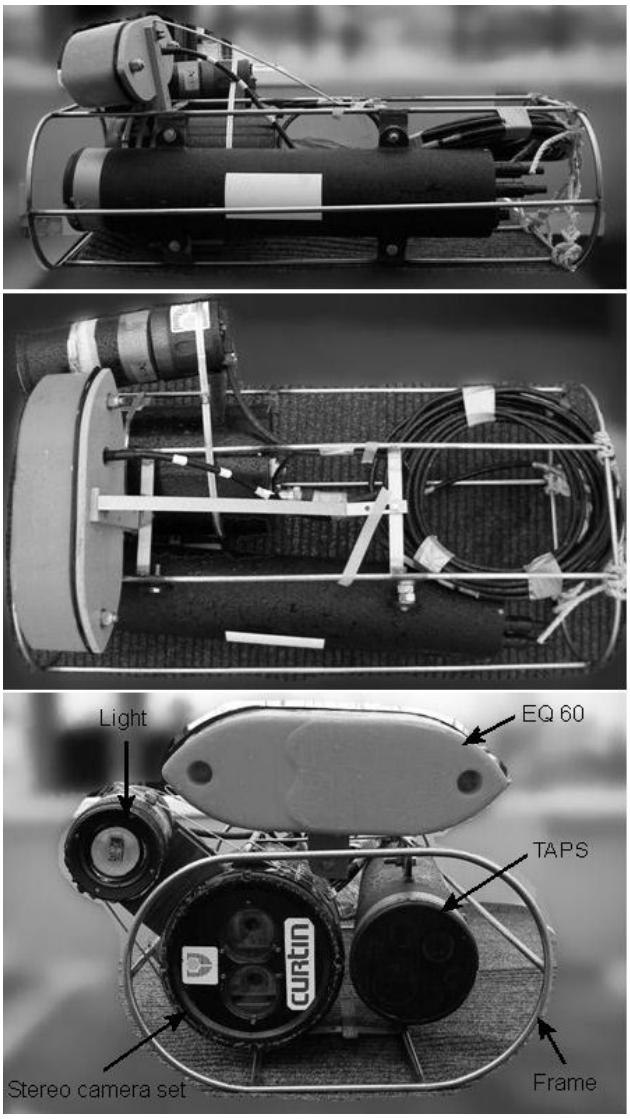

Figure 3-1 Three views of the ESP data collection rig as deployed in 2005, showing its major optical and acoustic components.[††††]

[††††] Mr. Malcolm Perry carried out the mechanic work necessary to integrate the ESP components together.

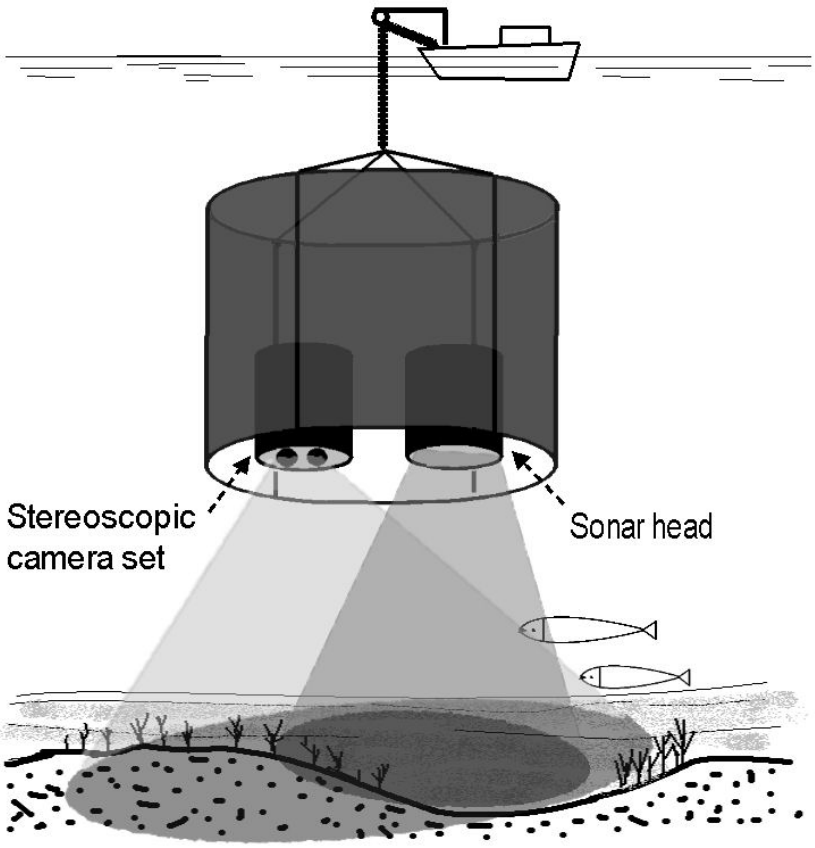

Figure 3-2 A conceptual diagram (not to scale) showing the ESP structure when deployed in the field. This diagram has been significantly simplified in showing the integrated stereoscopic camera set and the sonar components installed in the ESP frame.

The whole structure can be lowered into the water and supported by ropes from a boat. Attached to the ropes are the data cables responsible for the transmission of control signals and delivering of the collected data back to computers on the boat. Since the whole structure was designed to be able to freely move with the currents, there were occasions when the sonar head was not actually looking vertically downward. In these situations, the acoustic backscatter was not from the normal incidence direction, which was an undesirable situation in this project. An inclinometer was used to measure the orientation. Along with the optical and acoustic components, there was a light installed adjacent to the optical components to provide additional illumination when there was insufficient natural light.

3.2.1.2 The TAPS

The six-frequency scientific echosounder TAPS was installed as one of the acoustic components in the integrated data collection system. It has six frequencies at 265, 420, 700, 1100, 1850, and 3000 kHz. As it stated in the product manual (BAE Systems): TAPS is a self-contained oceanographic instrument that measures acoustic backscatter (volume scattering strength, *Sv*) at six frequencies along with depth, temperature, and date/time. The major advantage of TAPS was its six-frequency capability, providing opportunities to understand the dependence of acoustic backscatter on frequency. This was expected to be helpful in determining the frequency ranges most suitable for the monitoring of seafloor vegetation.

The major drawback of TAPS is its fixed range bin length of 12.5 cm, especially when comparing to a much better range resolution of the EQ60 of 1.88 cm. Problems were also experienced with the relatively large amplitude reflections from the seabed saturating the receiver, which made it impossible to produce useful measurements for further analysis. Attempts to overcome the saturation problem by fitting an attenuating mask to the instrument were only partially successful. Because of these problems, the experimental recordings from TAPS were finally discarded from further analysis and are not considered further in this thesis.

3.2.1.3 The ESP data collection system

The ESP data collection system comprised several components. A simplified system block diagram showing the data flow directions and the components is provided in Figure 3-3. A more detailed system block diagram made by other project team members is provided in Appendix B.

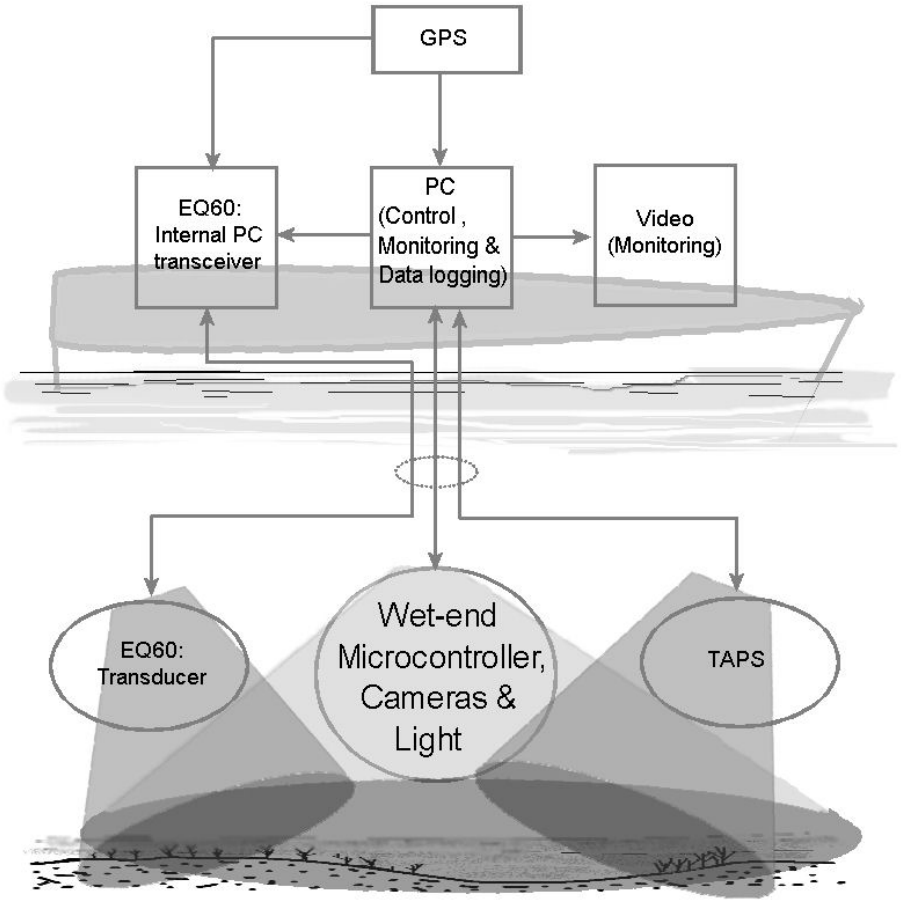

Figure 3-3 A simplified block diagram showing the data flow directions and the components of the ESP data collection system.

3.2.1.4 The wet end box and the cameras

In the hardware system, the wet end box is the major component that was completely designed and installed by the ESP project members. Installed in the box were two 5-Mega-pixel digital still cameras, a micro-controller, a video switch board, and a tri-axial accelerometer, which can sense the orientation angles of the device. Figure 3-4 shows the components without the underwater housing. Figure 3-5 shows the major underwater housing components and the completed wet end box on the ESP frame. A schematic diagram of the wet end micro-controller is provided in Appendix C.

The wet end micro-controller (WEM) is mainly a bridge between the two cameras in the wet end box and the personal computer (PC) on the boat. It synchronizes the two cameras and is responsible for delivering the trigger signals from the PC to the cameras. It also controls the video switch board and samples the signals from the accelerometers. The recorded digital photographs were stored on the memory cards in the cameras. It was necessary to retrieve the wet end box back onto the boat and upload the recorded photographs to the PC when the memory cards were fully loaded. A real-time view of the seabed from one of the cameras was provided via the video switch board. Through the video monitoring of the seabeds in real time, operators were able to maintain well focused field views for the optical system. Tilt angles sensed by the tri-axial accelerometer were transmitted digitally to the PC by the wet end micro-controller. The data communications between the dry-end PC and the wet end box were via a bidirectional RS422 serial data link.

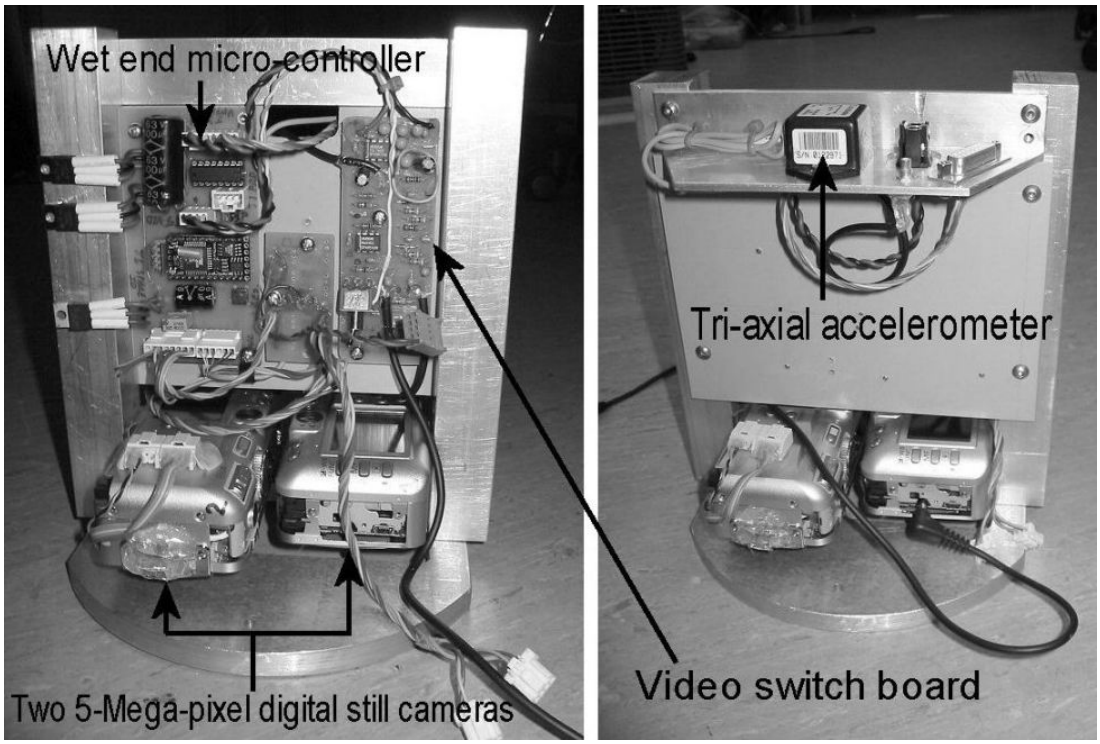

Figure 3-4 Internals of the wet-end box, showing wet end micro-controller, video switch board, tri-axial accelerometer, and two 5-mega-pixel digital still cameras.[‡‡‡‡]

[‡‡‡‡] Design, testing, and construction of the stereoscopic camera system were carried out by Mr. Andrew Woods. Software for the wet-end microcontroller was written by Dr. Alec Duncan.

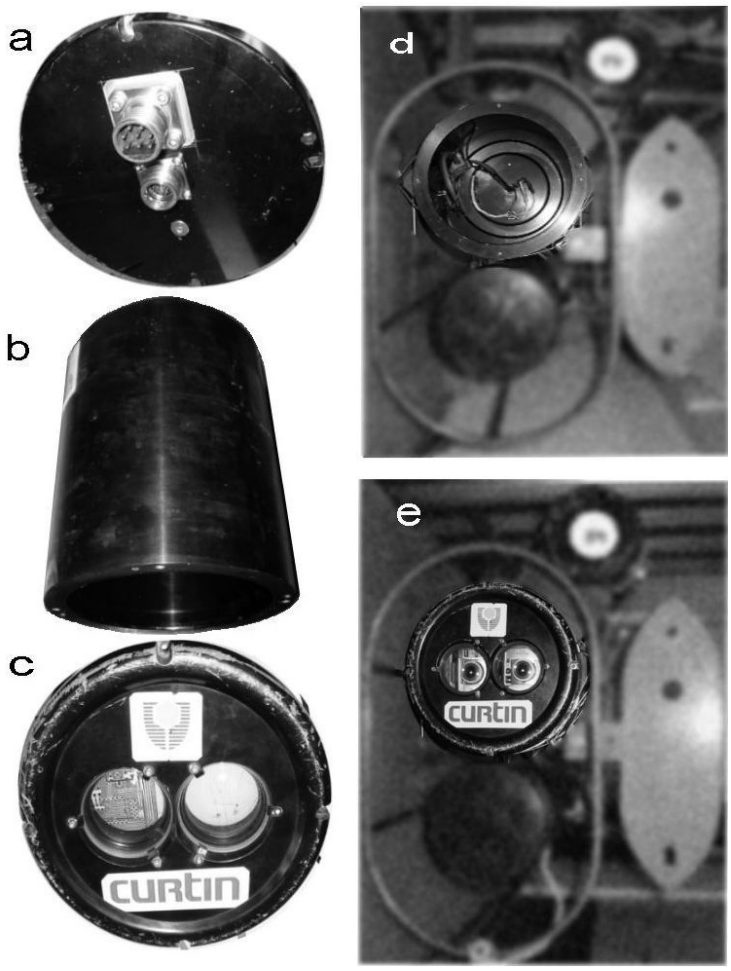

Figure 3-5 The underwater housing components, showing its (a) back cover, (b) housing cylinder, (c) front cover, and the installed housing (d) without and (e) with the front cover on the ESP frame.

3.2.1.5 The acoustic sub-system: EQ60

The SIMRAD EQ60 is a self-contained echosounder, which can be deployed for a variety of tasks. It can operate at either 38 or 200 kHz individually, or at both these frequencies simultaneously. For the ESP project, both frequencies were used and the EQ60 was switched to the "external triggering" mode so that the control software (ESPañolito) on the PC was able to provide a proper timing for the triggering of every sensing component.

The EQ60 received not only the triggering signals from PC but also the position data from the GPS receiver according to the position of the antenna. The GPS data were stored on its computer hard disc.

The EQ60 is a very mature acoustic product, and can be easily installed on small boats. For the ESP project, the sonar head (which contains the two acoustic transducers) was installed along with the TAPS and the wet end box on the ESP frame. The sonar head was connected through an independent cable to the EQ60's dedicated computer where the signals were digitised and stored on a hard disc. After the completion of the field trials, the logged data were transferred to the author's PC for analysis.

Since the acoustic components were firmly installed on the ESP frame, the direction of the transmitted beams was completely governed by the movements of the ESP frame. When the frame was deflected away from a vertical orientation by strong currents, the EQ60 was also tilted away from vertical incidence angles. The strategy used in the field was to look for ideal sites that can minimise the undesirable tilt effect.

3.2.1.5.1 Characteristics of EQ60

The EQ60's beam patterns at the 38 and 200 kHz frequencies are provided in Appendix D. The major characteristics of EQ60 extracted from the product manual (Simrad) are provided in Table 3-1.

Table 3-1 Major characteristics of EQ60 and selected settings.

Operational frequencies (kHz)		38.08	198.864
Parameters	Band width (kHz)	3.8	10.0
	Nominal beam width (degree) (see Appendix D)	15.2	7.2
	Sample interval (μs)	Selected: 126	Selected: 25
	Absorption coefficient (dB/m)	0.0098	0.0523
	Maximum ping rate (1/sec)	10	10
Adjustable	Transmit power (W)	Selected : 100	Selected : 100
	Pulse length (μs)	Selected: 256~1024	Selected: 100~1024

3.2.2 Synchronization of the optical and acoustic systems

The purpose of simultaneously collecting each optical and acoustic sample pair was for the purpose that each acoustic sample could be attributed to a proper habitat type by identifying the corresponding optical sample.

Synchronization was achieved by the ESPañolito program which controlled the triggering of all the components. This program was developed by a project member, Mr. Amos Maggi. It provided interfaces for the control and management of the data collection in the field. It was installed in a Windows environment, and can be easily adapted to the field requirements.

In the ESP hardware system, there were seven clocks that needed to be corrected. These clocks controlled Camera 1, Camera 2, WEM, TAPS, EQ60, GPS, and the PC itself. The correction of these seven clock times was accomplished by considering the time offset differences relative to a reference clock and by considering the frequency differences from different clocks. The two camera clocks exhibited some variations although over 95% of the variations were within 0.02 seconds. Considering the common time separation between two consecutive data

samplings, these variations did not cause significant problems. After this step, each acoustic sample was referred to its correct photographic pair. A database containing the corrected optical and acoustic records was ready for the optical classification task, which was the next step.

Figure 3-6 shows the data availability of each component when lined up against the time (day number). The optical recordings were essential records used to identify habitat types. Without the optical recordings, an accurate correspondence of the acoustic signals to the correct habitat types is unachievable in this case study. Figure 3-6 was produced from a data set collected from the first field trial in 2004. From this figure, one is able to find out that not every optical recording has its corresponding acoustic recordings, and vice versa.

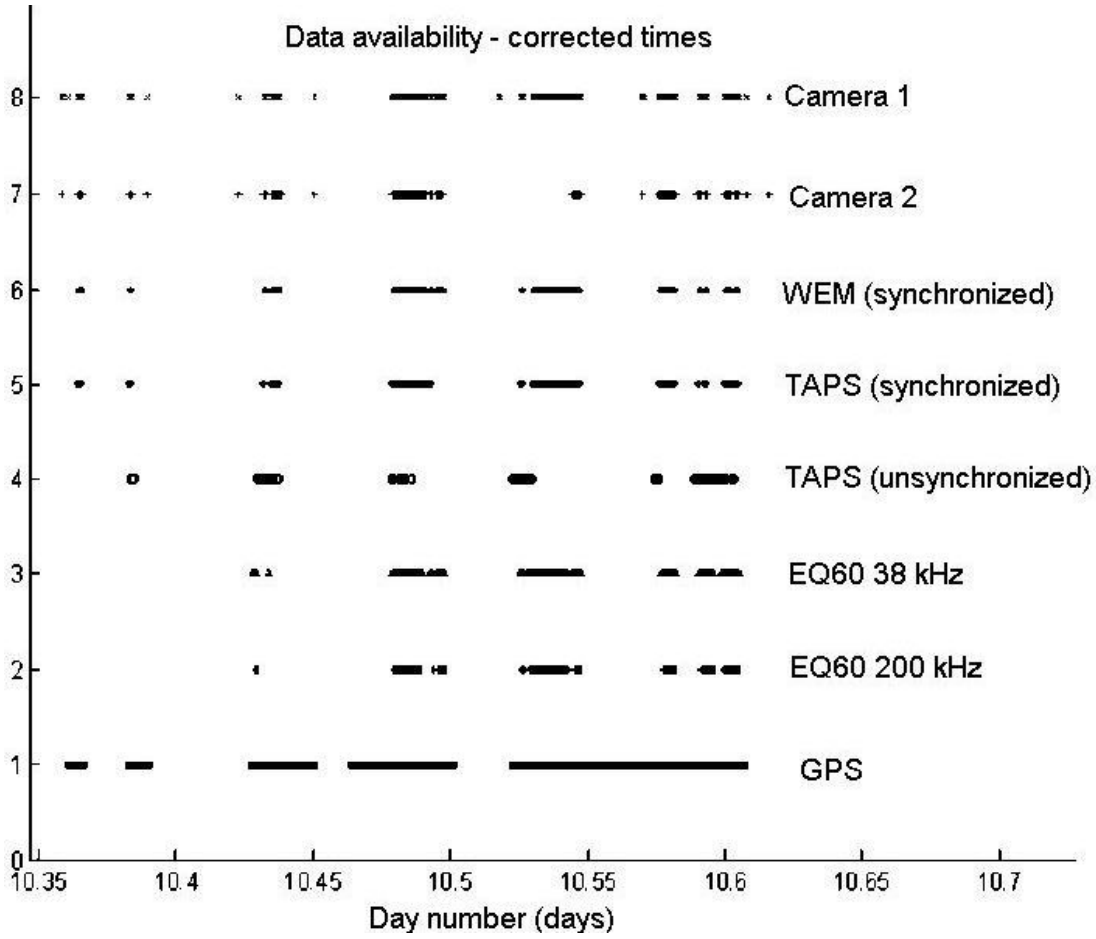

Figure 3-6 Data availability of each sensing component when lined up against the time. This data set was collected from the first field trial in 2004.

3.3 Field trials and data collections

Data were collected from several field trials held in shallow coastal waters near the capital of Western Australia, Perth. There were three field trials implemented specifically for the ESP project. The three ESP field trials were carried out on 10 August 2004, 1 June 2005, and 26 October 2005. The experimental conditions are introduced in the following subsections.

3.3.1 The first field trial

On 10th of August 2004, the ESP project carried out its first field trial off Woodman Point in Cockburn Sound, Western Australia. The Sound is a coastal shelf region bounded partly by Garden Island to the west. Due to the protection from the open ocean provided by Garden Island and the blocking effects of a causeway to the south connecting the island to the mainland, the water in the Sound provided a calmer environment than those outside the Sound and was suitable for field trials.

3.3.1.1 Field deployment

In Cockburn Sound, there were only very few seagrass meadows still existing, mainly on shallow banks on the northern areas near Parmelia Banks, on narrow strips of banks near Garden Island, and on comparatively larger areas of banks at the southern part of the Sound near the causeway. Figure 3-7 shows the seagrass distributions compiled by a group of seagrass specialists (Kendrick, Aylward *et al.* 2002). From this figure, the author was able to plan the field deployment locations in order to cover both seagrass meadows and bare sand seafloors.

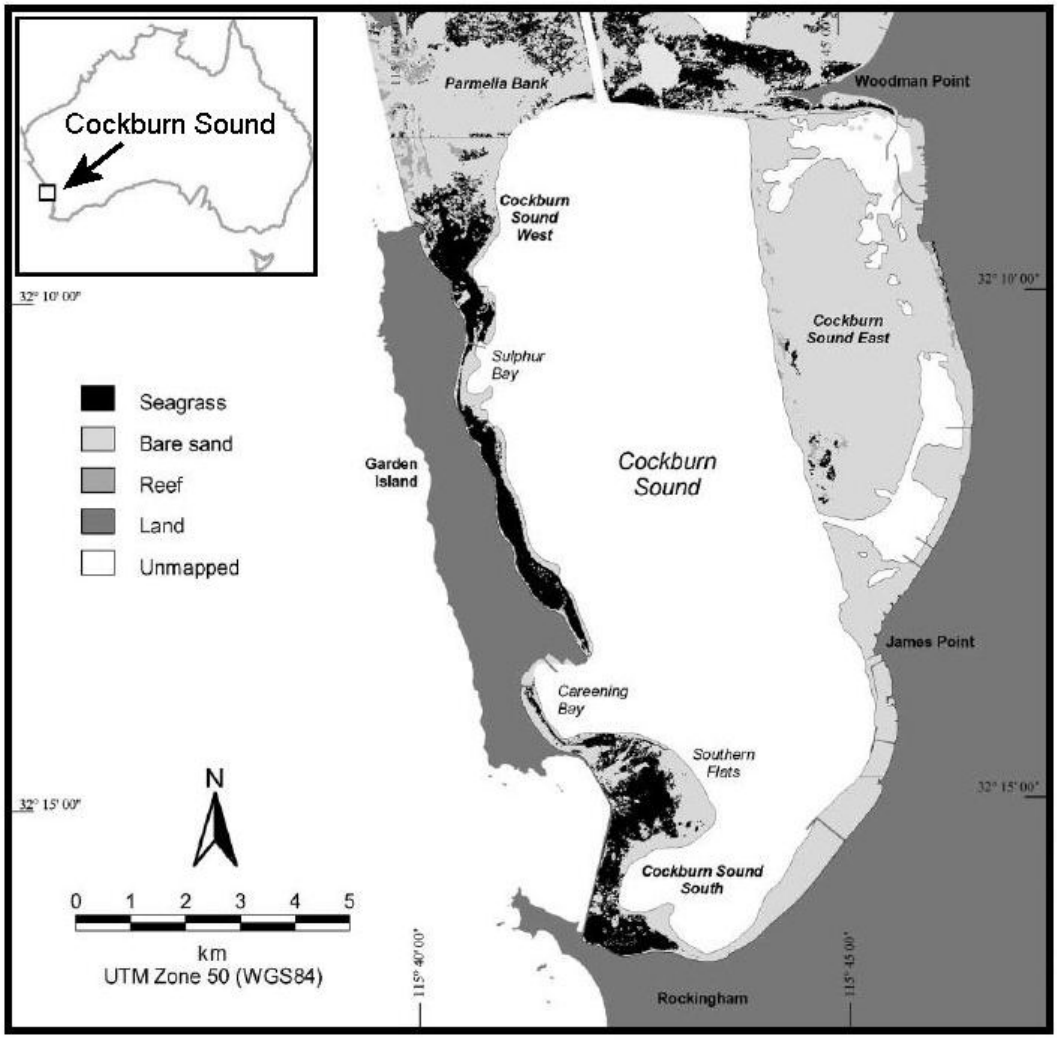

Figure 3-7 A seagrass coverage map of Cockburn Sound, WA, showing the remaining seagrass coverage (18%) in 1999 after the decline from 1967 (Kendrick, Aylward *et al.* 2002).[§§§§]

The water depths of the planned transects were all less than 10 metres except in an area near the centre of the Sound where depths beyond 10 metres were observed. The aims of the first sea trial were to test the equiment and deployment techniques and to obtain acoustic echoes from a variety of seabeds – particularly sand and seagrass.

[§§§§] Reprinted from Aquatic Botany, Vol. 73, Kendrick, Aylward *et al*., "Changes in seagrass coverage in Cockburn Sound, Western Australia between 1967 and 1999", p75-87, copyright (2002), with permission from Elsevier.

Since seagrass uses sunlight as the source of energy to undergo photosynthesis, it can only survive in shallow areas where the sunlight conditions are acceptable. Although 99% of the seagrass in the world is in depths less than 50 metres and a depth limit of 90 metres is predicted by a model (Duarte 1991), the seagrasses recorded in Cockburn Sound were mainly limited to water depths less than 10 metres. From this field trial, there were no seagrass meadows observed at depths more than 10 m. However, since the surveyed areas were bounded in very limited areas, the observation result does not imply that it is impossible to find seagrass meadows in unsurveyed areas of the Sound.

Considering the need to collect samples from the seagrass meadows and for the safety of the boat, field sites were chosen from areas where seagrass had been reported and the depths were deep enough and safe for the boat to sail. When the ESP structure was deployed in the field, it was supported by a rope and hung from a simple derrick used to lower the structure into the water for measurements. The derrick was made by Dr. Rob McCauley, the leader of the CWHM project and also a member of the ESP project. According to the plan, the ESP structure should be maintained at a fixed distance above the seabed at each site. Because of the different water depth at each site this meant that the draft of the instrument (i.e. depth of sonar head below water surface) was different at each site. The draft can be easily determined by measuring the height of the ESP structure and the lengths of the rope in advance and marking the rope with colour tapes at every equal distance. By observing the mark on the rope which appears above the water surface level, one was able to have a good estimate of the sonar's actual draft.

Unfortunately, the weather conditions were often unpredictable. Occasional strong winds did happen and the drafts were not always properly recorded. The actual drafts of the ESP structure at the three sites were not reliable. Consequently, the ESP device can not be used to measure water depth.

However, distance readings from the sonar and from the videos did provide real-time information that allowed the ESP structure to be maintained at an appropriate distance above the seafloor for suitable optical focusing and operations of the acoustic system. The boat was anchored at each site. However, the winds and currents generated relative motions between the ESP system and the seabed. This was not a significant problem when ambient lighting conditions were good and the

exposure times needed were short enough to take clear photographs. But the relative motions did in some cases result in motion blurring of photographs taken under poor lighting conditions – for example when the seabed was in the shadow of the boat.

Data were collected from three sites, which covered five major habitat types in the Sound. In Figure 3-8, seabeds in "Site 1" were predominantly pure sand and seagrass meadows while those seen at "Site 2" were predominantly sand, reef, and algae. Data collected from "Site 3" were excluded from further analysis due to problems with the poor quality data collected. The analysis results of the data collected from this field trial are given in Chapter 4.

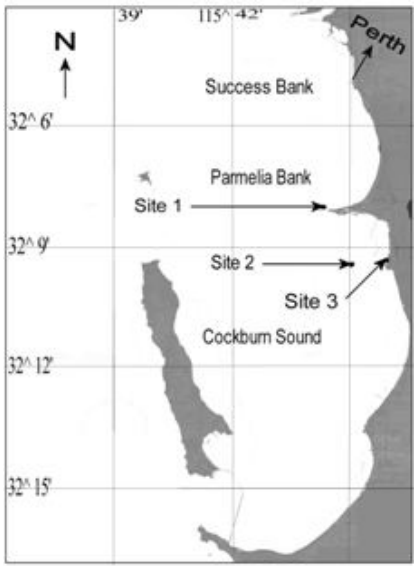

Figure 3-8 Site locations of the first ESP field trial in Cockburn Sound in 2004.

3.3.1.2 Samples collected

In this field trial, synchronized data from the EQ60, TAPS, stereo image cameras, and GPS were acquired. A total of 1232 sample pairs of both echoes and still images were acquired. Further examination of the images and the echoes revealed that 540 samples were fully intact and 300 of these samples were selected as standard representatives of 5 pure classes. Pure classes are defined here for those groups of sample collected from seafloors with single species of seafloor vegetation or sole substrate observed from the optical images. Typical class samples of

photographic pairs and acoustic backscatter waveforms of these 5 pure classes are provided in figures from Figure 3-9 to Figure 3-13. In these figures, the markers X on the photographic pairs are the centres of 38 and 200 kHz beams, and circles around them are the estimated -3dB level locations of their major lobes based on the range of 1.5 metres. Predominant habitat types in the areas within these two circles determined what habitat types the samples would be classified into. The number of samples within each of these classes were 81, 10, 8, 21 and 180 respectively for the pure sand, seagrass 1 (*Posidonia sinuosa*), seagrass 2 (*Posidonia australis*), rocky reef, and macro algae.

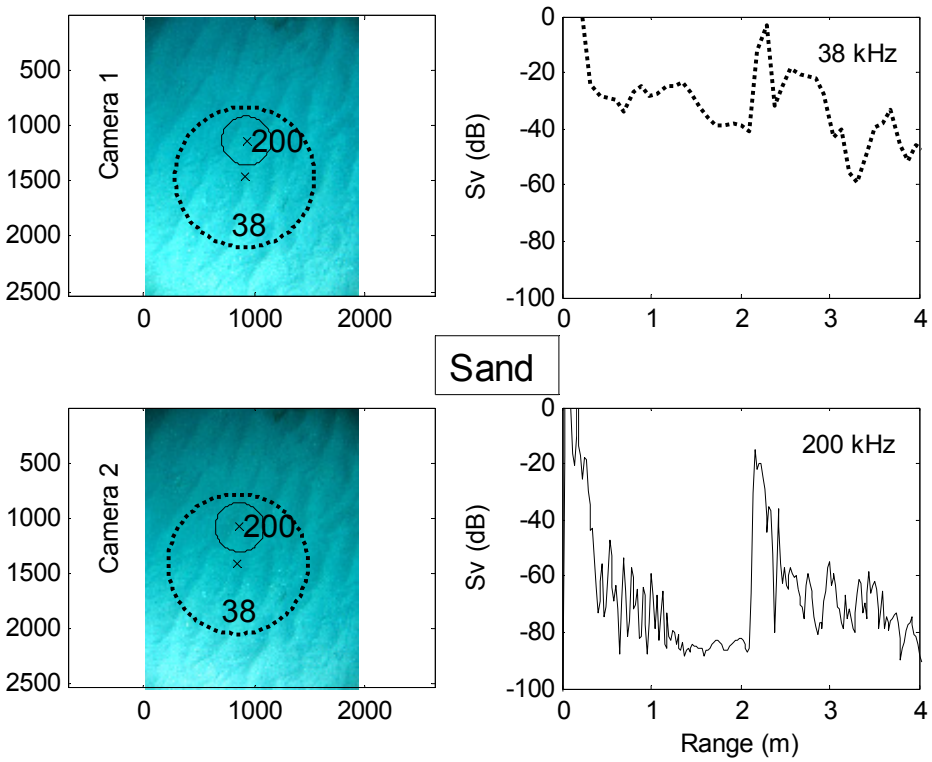

Figure 3-9 Photographic pair and acoustic backscatter waveforms of a typical sand class sample.

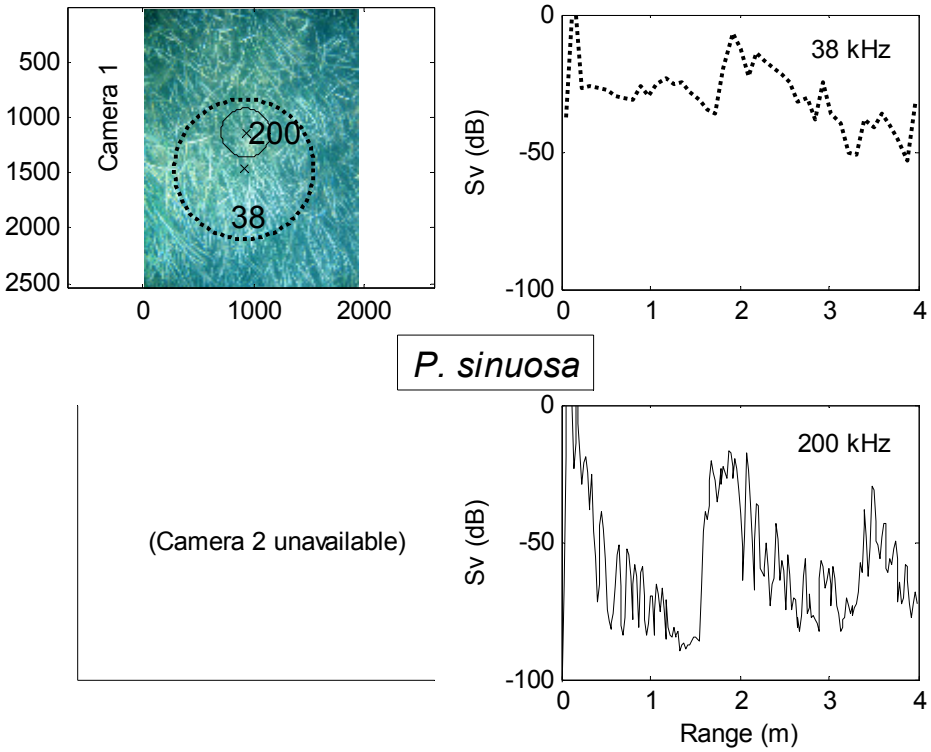

Figure 3-10 Photographic pair and acoustic backscatter waveforms of a typical seagrass species *P. sinuosa* class sample.

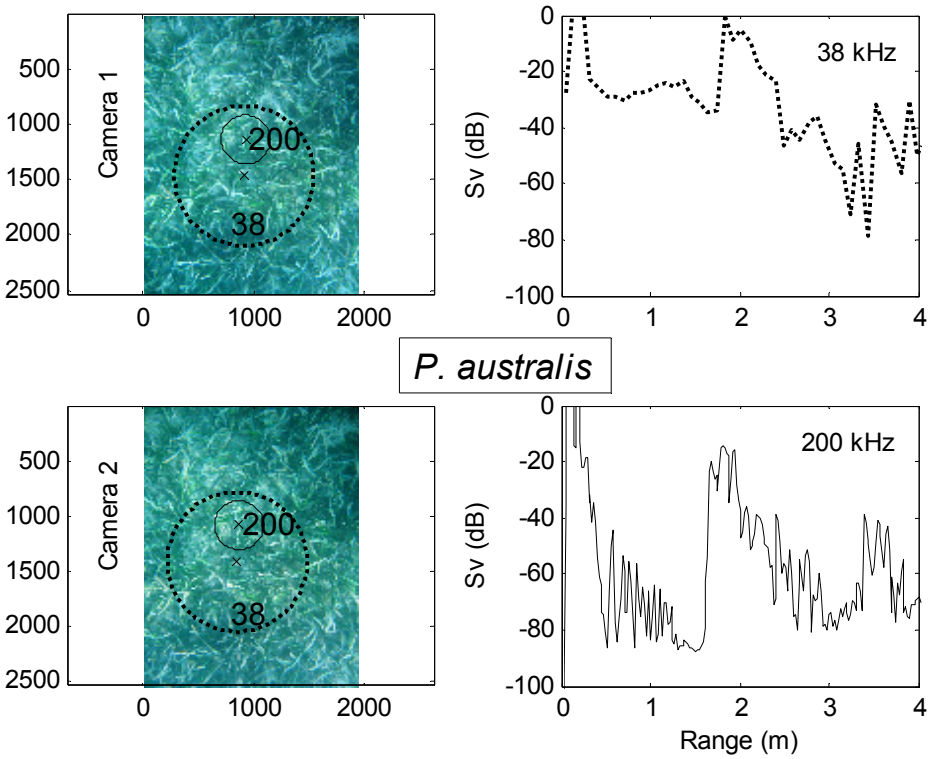

Figure 3-11 Photographic pair and acoustic backscatter waveforms of a typical seagrass species *P. australis* class sample.

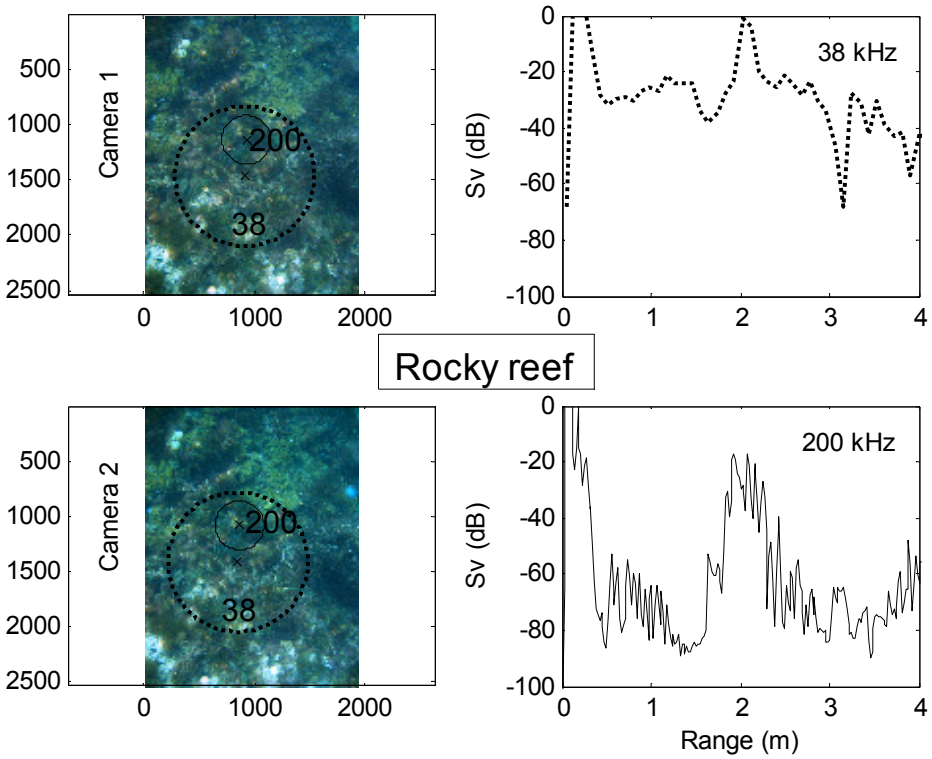

Figure 3-12 Photographic pair and acoustic backscatter waveforms of a typical rocky reef class sample.

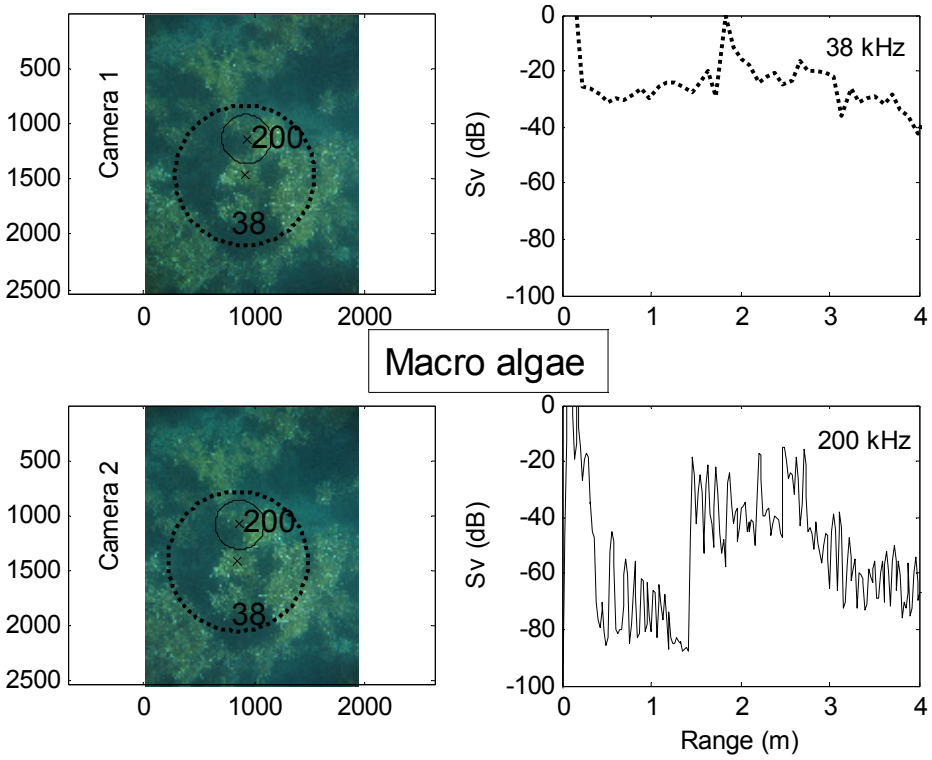

Figure 3-13 Photographic pair and acoustic backscatter waveforms of a typical macro algae class sample.

3.3.1.3 Biological features of observed seagrasses

The observed major seagrass species in Cockburn Sound were *P. sinuosa* and *P. australis*. An overview of the historical seagrass distribution in the Sound can be seen from Figure 3-7. Contrary to the historical data, the collected seagrass samples at Cockburn Sound in 2004 were dominated by *P. australis*. The typical appearances of the dense seagrass species observed in this field trial are shown in Figure 3-14. The seagrass species on the upper part of the photograph in the figure is *P. sinuosa* while the lower part is *P. australis*. The 25 cm canopy height on both sides of the figure was estimated from the seagrass illustration by Phillips and Meñez (Phillips and Meñez 1988). This number was reasonably within the scope of the measurements observed in the ESP project. As has been described in section 2.2.2.2, the "Of bent section" of *P. sinuosa* can be observed directly from above the seagrass meadows while the "Below bent section" is not possibly seen from the photograph. From Figure 3-14, a distinct canopy pattern difference between these two seagrasses can be easily observed.

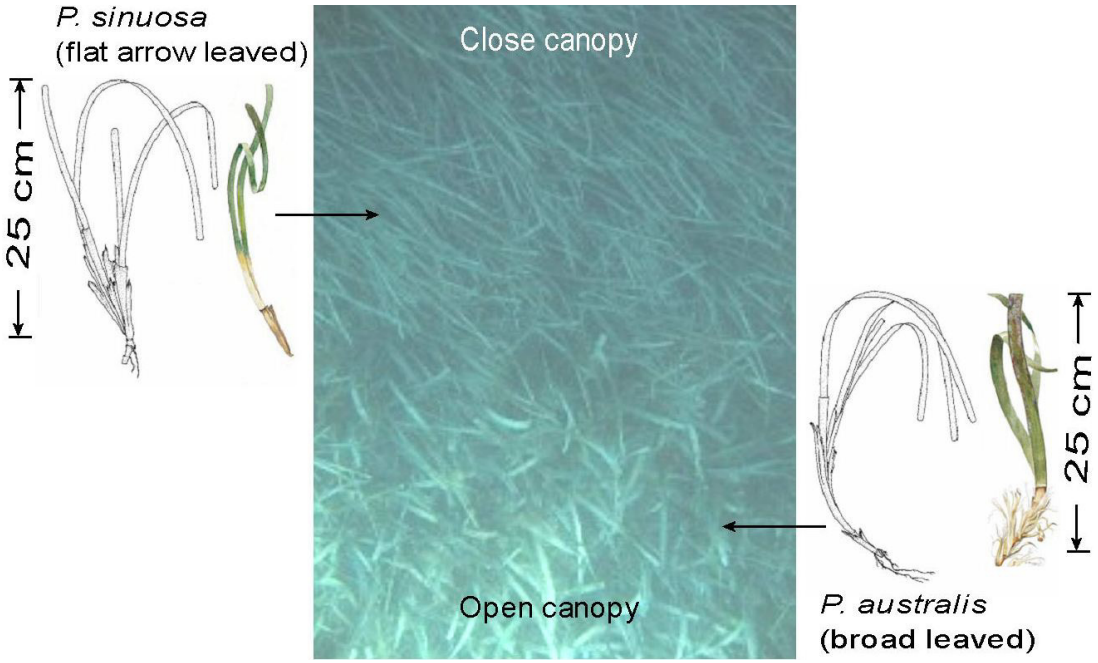

Figure 3-14 Canopy appearances and characteristics of *P. sinuosa* and *P. australis* recorded in Cockburn Sound 2004.*****

The historical seagrass recordings of *P. sinuosa* and *P. australis* for the average canopy height observed by Smith and Walker were between 35 and 45 cm (Smith and Walker 2002), and were about 25 cm from the estimate of the diagrams depicted by Phillips and Meñez (Phillips and Meñez 1988). The vegetation in water can wave along with the currents such that the detected canopy height of the plants can vary from one moment to the next moment. The average canopy height can also change at different seasons through their life cycles. The changing behaviour of the canopy height due to seasonal changes was observed and documented by McKenzie (McKenzie 1994). In McKenzie's observation, the observed canopy height varied even more for the seagrass species of *Zostera capricorni* Aschers where the canopy height was the greatest between October and February (maximum 53.4 cm) and the

***** The seagrass diagrams on both sides of the seagrass photograph in Figure 3-14 were extracted from the publications by Government of South Australia (Coast Protection Board. (2004). "Seagrasses of South Australia." 2004, from www.environment.sa.gov.au.), and (Phillips, R. C. and E. G. Meñez (1988). "Seagrasses." Smithsonian contributions to the marine sciences **34**: 85-89.). The identification of the seagrass species was supported and advised by the author's associate supervisor, Associate Prof. Gary Kendrick at the Department of Botany of the University of Western Australia.

lowest around mid year (minimum 4.4 cm) on the Northern Queensland coastlines in Australia.

3.3.2 The second field trial

3.3.2.1 Field deployment

During the second ESP field trial on first of June 2005, measurements were made at Owen Anchorage to the north, west Parmelia Bank to the west, and Jervoise Bay harbour in the Cockburn Sound to the south. Shallow banks are divided by a shipping channel into west and east banks which are densely populated by seagrasses. More seagrass species are found in these areas than in Cockburn Sound. Site locations of the second field trial are shown in Figure 3-15 overlain on a map of the year 1999 seagrass species distribution at Success and Parmelia Banks. The seagrass distribution map was a result of the extrapolation of the sampled data by the kriging method and was done by Dr. Karen Holmes at the University of Western Australia. The figure shows how the estimated seagrass species were scattered in the Sound, and the field site locations where the data were collected.

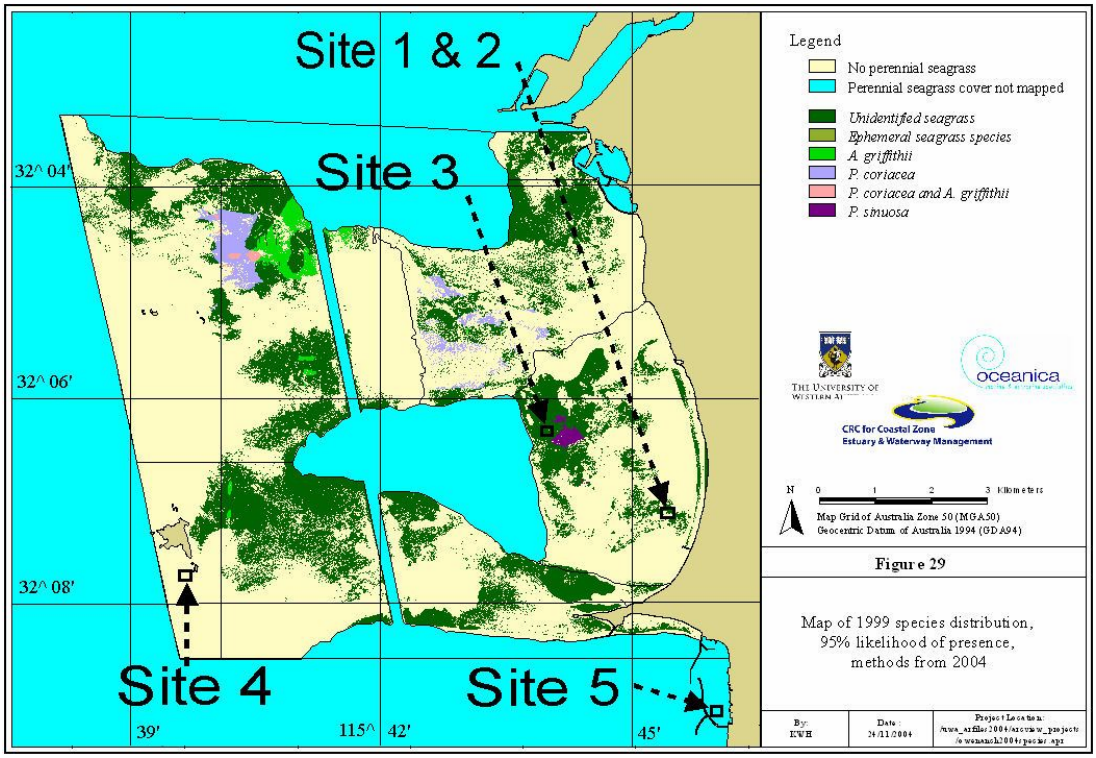

Figure 3-15 Site locations of the second ESP field trial according to the GPS data overlaying on a map of year 1999 seagrass species distribution of 95% likelihood of presence on Success and Parmelia Banks.[†††††]

3.3.2.2 Samples collected

At site 1, the predominant *Posidonia* seagrass was observed with much cleaner leaf surface conditions than those observed in Cockburn Sound in the first field trial. Flat and pure sand bottoms were almost identical to those observed in the first field trial.

At site 2, sea squirts populated the major areas on rubble bottoms with patchy seagrass and wrack mixed together. Surprisingly hard corals were observed at a few spots. This site was unique for its rough bottom surface due to the wide spread assemblage of sea squirts in this area. On a few photographs, oval-shaped plate profiles of unknown organisms projected from the bottom.

[†††††] The seagrass distribution map was provided by Dr. Karen Holmes of the University of Western Australia.

At site 3, dense *Posidonia* species covered the whole area. Since no physical samples of the seagrass were collected from this field trial, it was not possible to definitively determine the seagrass species. However, since the *P. australis* possesses the open canopy structure and an open canopy structure was also clearly observed from positions above the seagrass meadows in the field, it is possible that the seagrass meadows were predominantly occupied by seagrass species with the same open canopy structure, including *P. australis*. But it is uncertain for whether the seagrass in this site is definitely *P. australis* or not. Although the historical records showed that *P. sinuosa* is the predominant seagrass species to be observed around this site, the photographs did not provide any validation of the historical observations. In the whole area, flat and uniformly distributed seagrass meadows can be the only descriptor in characterizing the sea bottom at this site.

After moving on to site 4 just south of Carnac Island, clear water, and a variety of macro algae and the common tall kelp species of *Ecklonia radiata* were observed. Occasionally covered by hard shell benthos, the sea bottoms were basically fine sands and rocky reefs with a lot of macro algae growing on them. Tall algae and rocky reefs were the common scenes at this site. Very flat and pure sand bottoms were observed on the last few photographs.

After a strong wind built up in the afternoon, the field trial was moved on to site 5 within the Jervoise Bay harbour. Calm water and muddy sand are the major features of this site. Due to the low ambient light levels at this site, the light was turned on for the optical system. No vegetation was found at this site. This may be due to the human activities frequently carried on within the harbour. In a few photos, mussel shells covered the sea bottom.

Due to insufficient separations between the sonar head and the sea bottom at site 5, there were overlaps between the ringing of the acoustic tranducers and the first bottom returns. In view of this issue, the samples collected from this site were discarded from further analysis.

Typical photographic pairs and acoustic backscatter signals from each habitat type are provided in figures from Figure 3-16 to Figure 3-21. A few coral samples as shown in Figure 3-21 were collected from site 2.

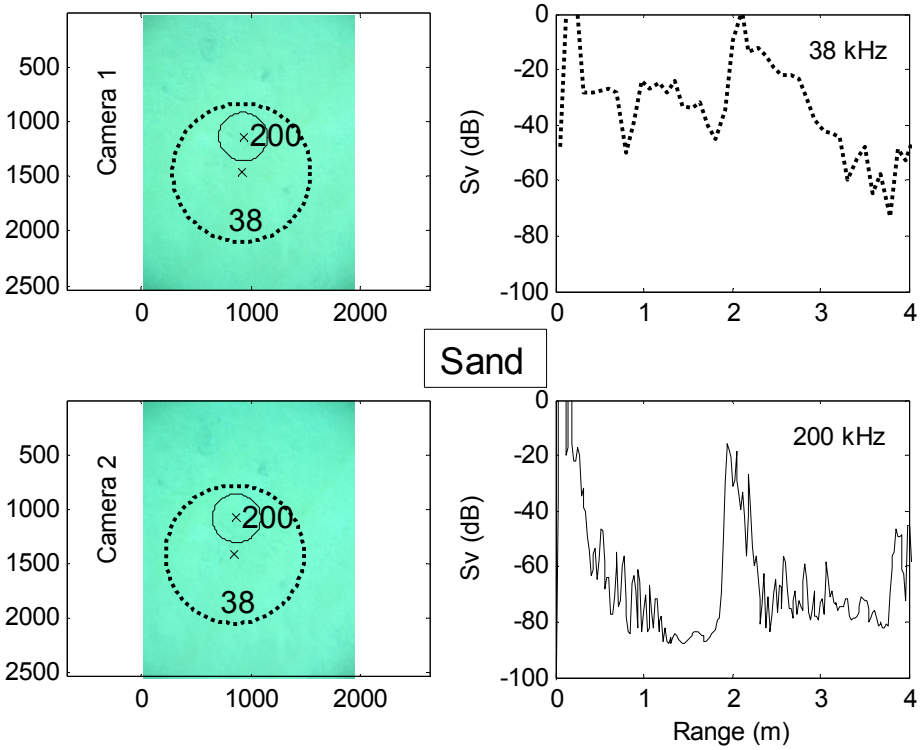

Figure 3-16 Photographic pair and acoustic backscatter waveforms of a typical sand class sample collected from site 1 of the second field trial.

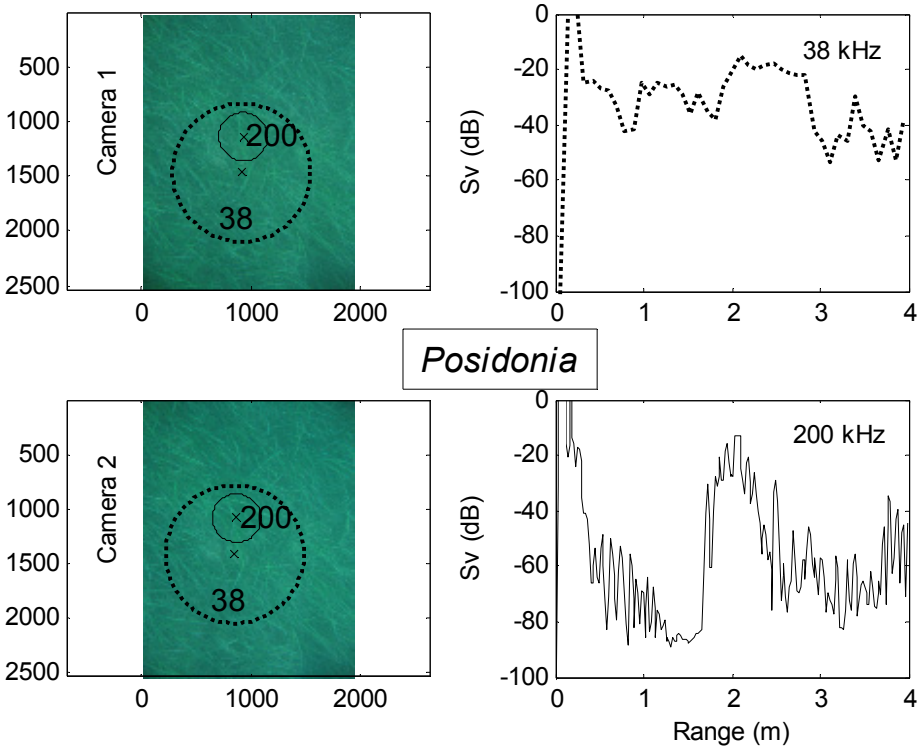

Figure 3-17 Photographic pair and acoustic backscatter waveforms of a typical *Posidonia* seagrass class sample collected from site 1.

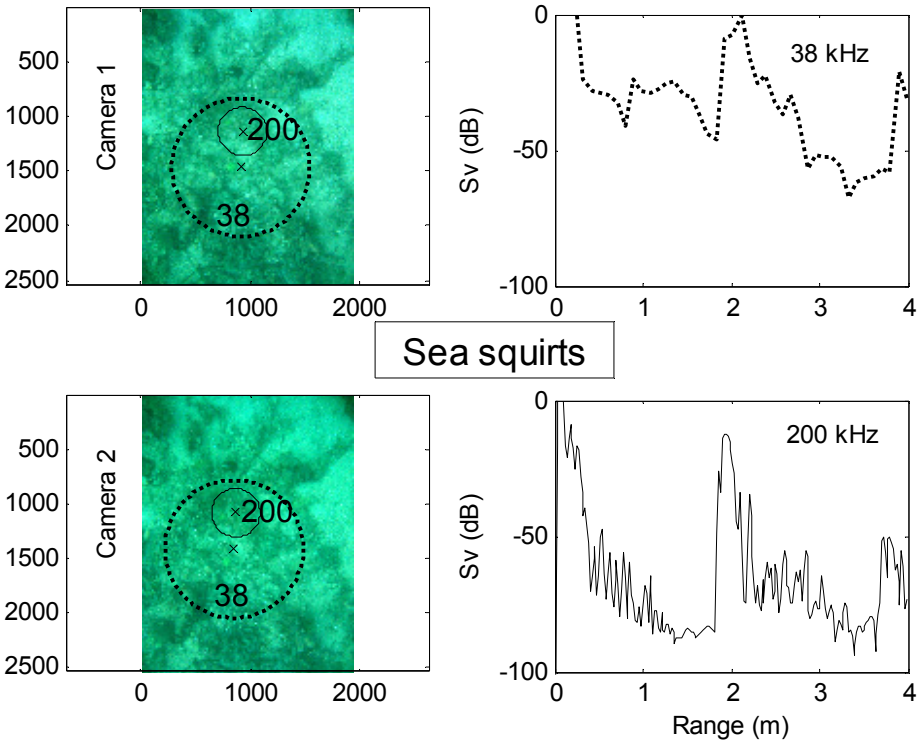

Figure 3-18 Photographic pair and acoustic backscatter waveforms of a typical sea squirts class sample collected from site 2.

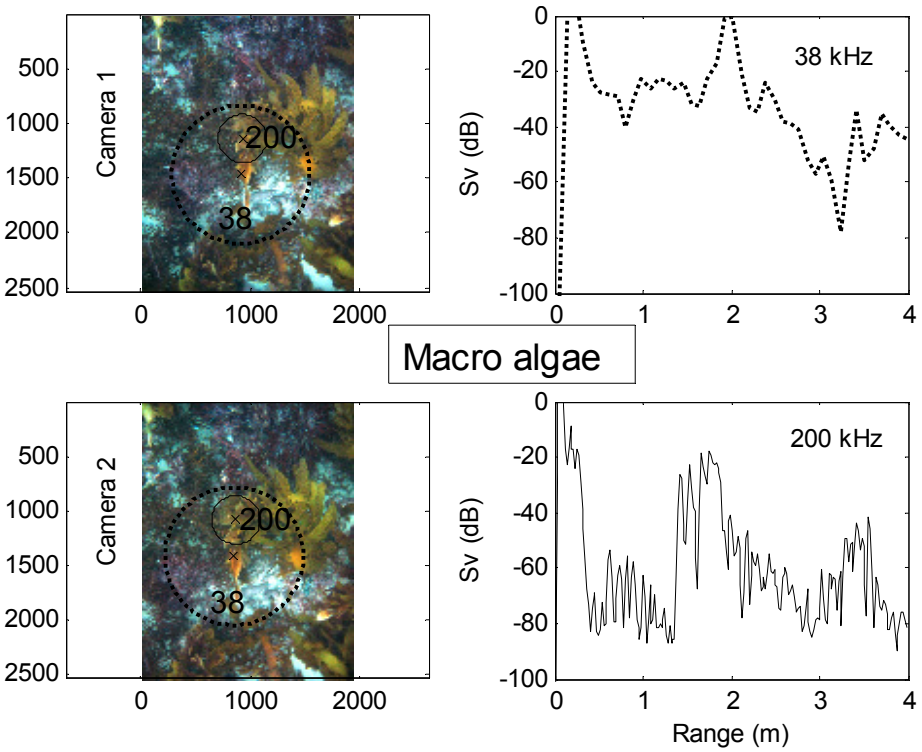

Figure 3-19 Photographic pair and acoustic backscatter waveforms of a typical macro algae class sample collected from site 4.

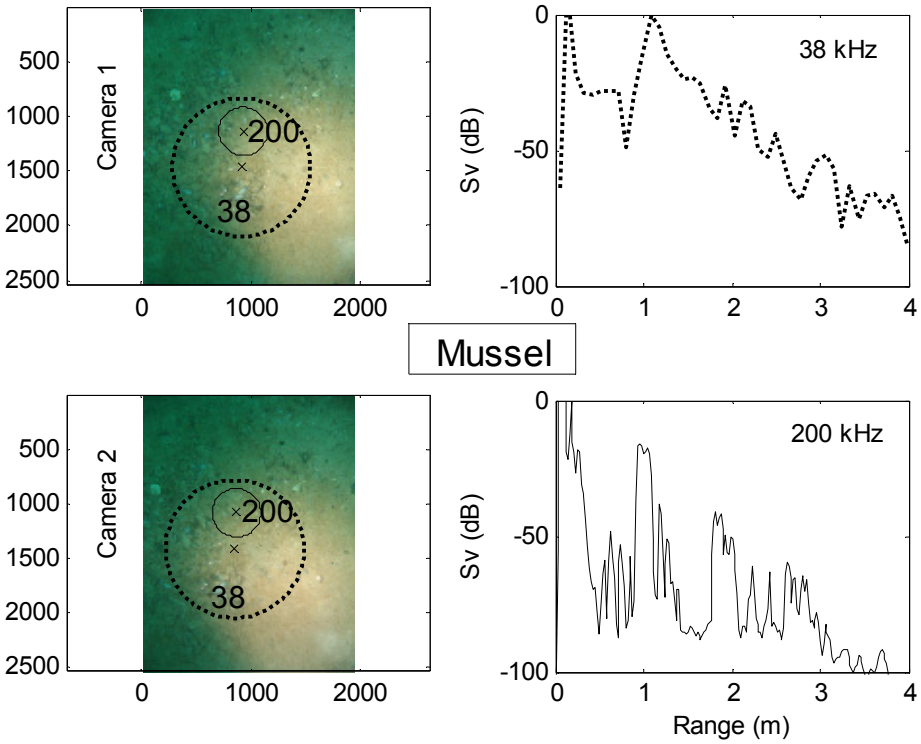

Figure 3-20 Photographic pair and acoustic backscatter waveforms of a typical mussel class sample collected from site 5.

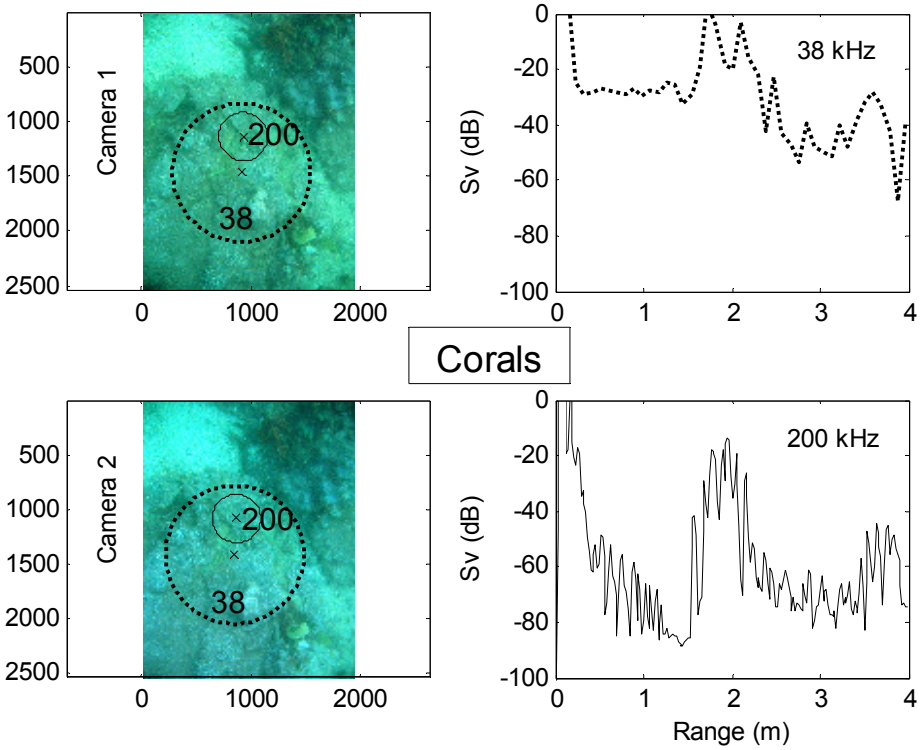

Figure 3-21 Photographic pair and acoustic backscatter waveforms of a typical coral class sample collected from site 2.

3.3.3 The third field trial

On the 26th of October 2005, the ESP project completed its final field trial. It was a rainy day but fortunately with comparatively calm weather suitable for the experiment. Like the previous trials, the journey started from Woodman Point in Cockburn Sound and went straight to the planned field sites. After arrival at the designated sites, the ESP wet end system was deployed over the side of the boat on a davit. The experiment was limited to a smaller area than before on the east bank of Owen Anchorage. The site locations of this trial are shown in Figure 3-22.

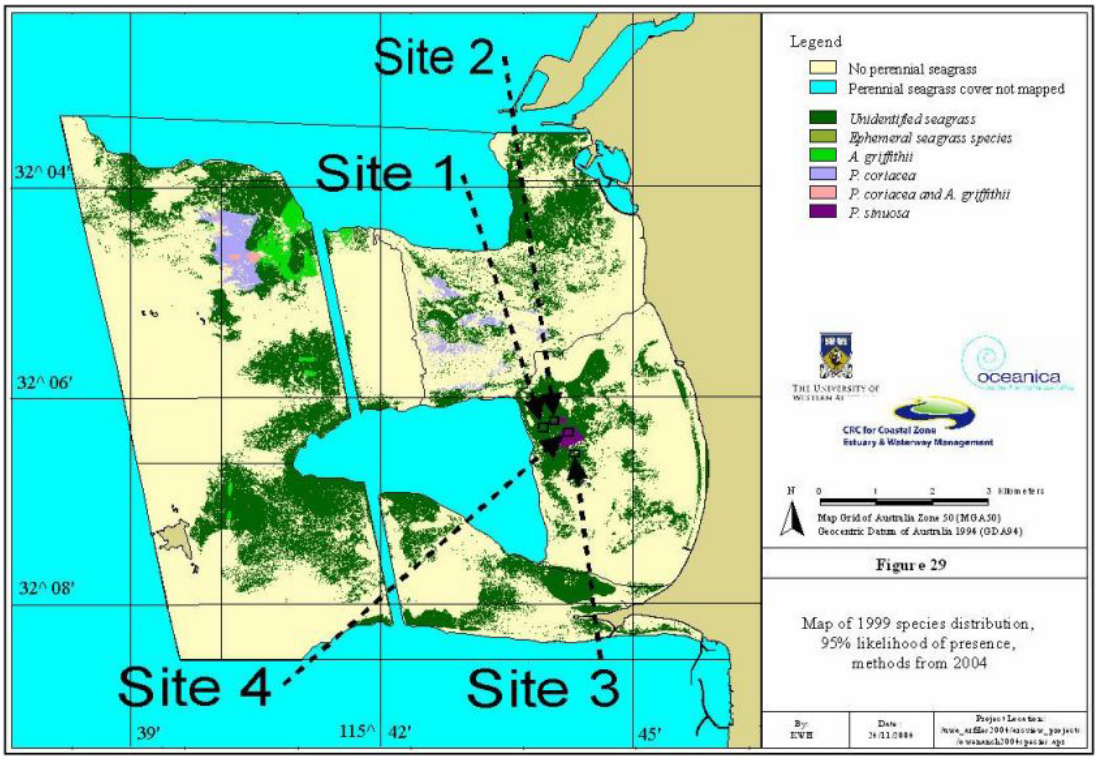

Figure 3-22 Site locations of the final ESP field trial according to the GPS data overlain on a map of year 1999 seagrass species distribution of 99% likelihood of presence of Success and Parmelia Banks on the east banks of Owen Anchorage.[‡‡‡‡‡]

3.3.3.1 Strategic changes and investigations of depth dependence

The field sites of the final field trial had been investigated and documented for the seagrass species and distribution by biologists (Kendrick, Hegge *et al.* 2000). Habitat types were known to be limited to only a few species and their respective locations were supposedly accurate enough to be determined from the seagrass distribution map shown in Figure 3-22. Based on this understanding, the plan was to deploy the ESP system over areas where the observation ranges were to be made beyond the operational limit of the optical system such that the seagrass meadow

[‡‡‡‡‡] The seagrass distribution map was provided by Dr. Karen Holmes of the University of Western Australia.

types can be only determined from the seagrass distribution map provided in Figure 3-22. The major motivation was to understand the acoustic backscatter variation at ranges larger than the operational limit of the optical system. For this reason, part of the acoustic data collected in this field trial was unable to be accurately identified through the assistance of optical recordings. As a consequence, the determination of the associated meadow types of these echoes can not be as accurate as those made in the previous field trials. An inherent assumption in these measurmeents is therefore that the habitat types did not vary significantly at each site.

3.3.3.2 Samples collected

Due to the strategy adopted in this field trial, the samples' species could not always be accurately identified. The seagrass species was roughly identified as the *Posidonia* seagrass group. Since no physical seagrass samples were collected from the meadows, the identification of this *Posidonia* seagrass group was purely based on the canopy appearance on the photographs being similar to the *Posidonia* group. *Posidonia* alone is believed to have at least 8 species in Western Australia (Kuo and McComb 1989). The dense seagrass shown in Figure 3-24 had comparatively narrower blades and longer leaves than those observed in the previous field trials, and higher plant density patterns than those of the other *P. sinuosa* and *P. australis* meadows that were observed at different sites.

Comparatively shorter leaved *Amphibolis* meadows were observed for the first time in this ESP project. This seagrass species was loosely dispersed in the meadows. Bottom substrate can be clearly observed from above the canopy and the canopy height is much shorter than that of *Posidonia*. It is anticipated that it will be a difficult task to differentiate this *Amphibolis* meadow (Figure 3-25) from the sand class (Figure 3-23) if purely based on the observation of the acoustic backscatter.

According to the cover homogeneity, seagrass classes were further differentiated into subclasses to account for the density difference. Since the seagrass species were not accurately identified, it would be more realistic to differentiate the density differences than to tell the differences of seagrass species by acoustics. An

investigation of possible acoustic signatures for the density differences is provided in section 4.3.5.

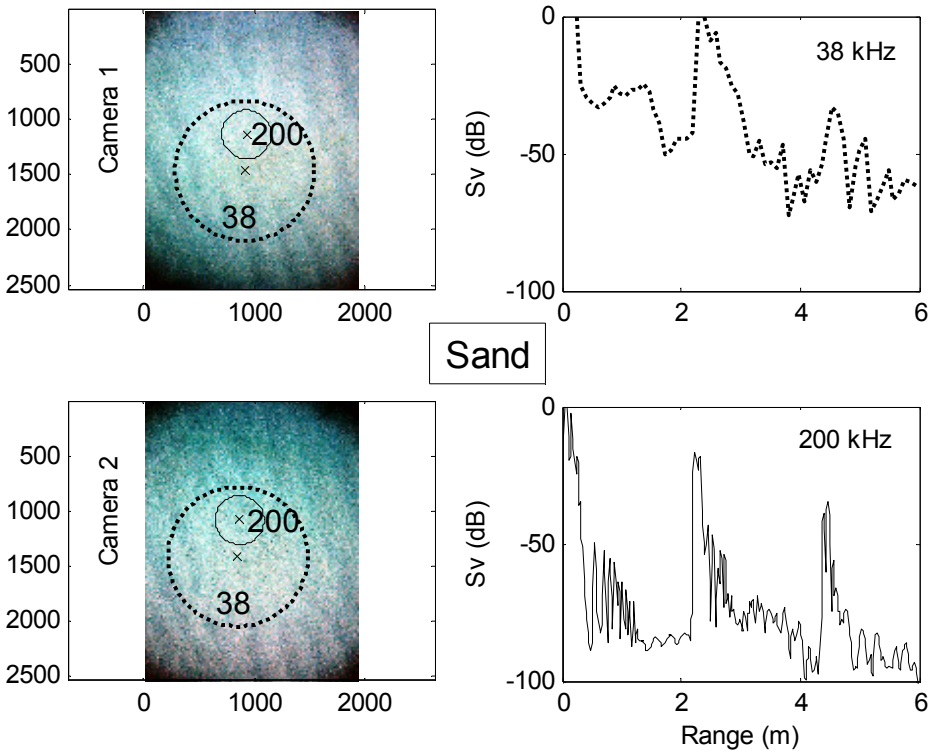

Figure 3-23 Photographic pair and acoustic backscatter waveforms of a typical sand class sample from the third field trial.

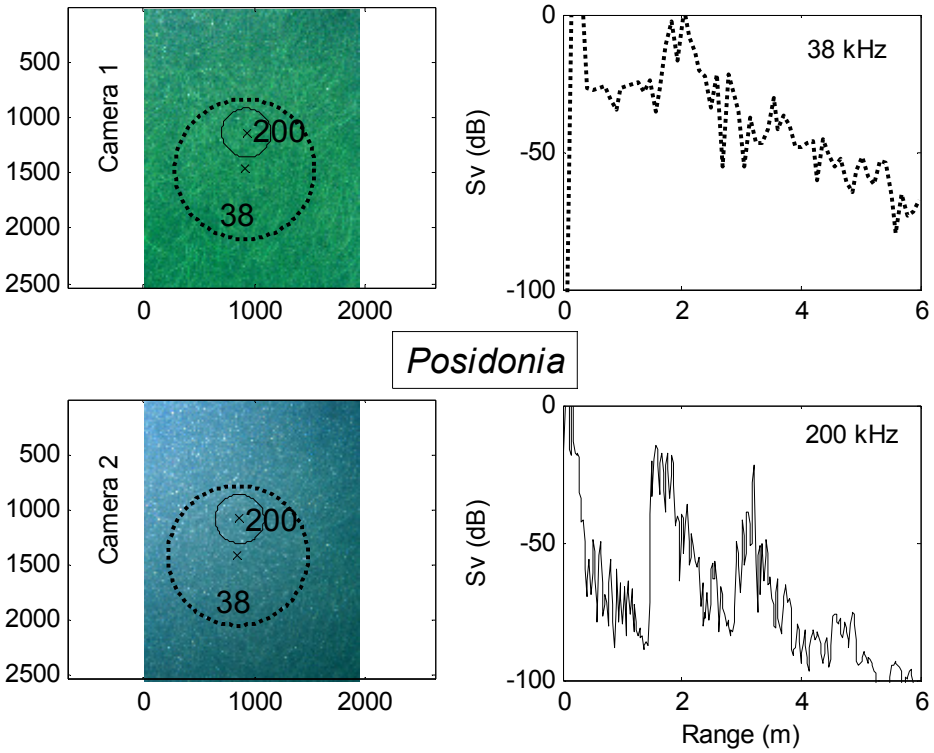

Figure 3-24 Photographic pair and acoustic backscatter waveforms of a typical *Posidonia* seagrass class sample from the third field trial.

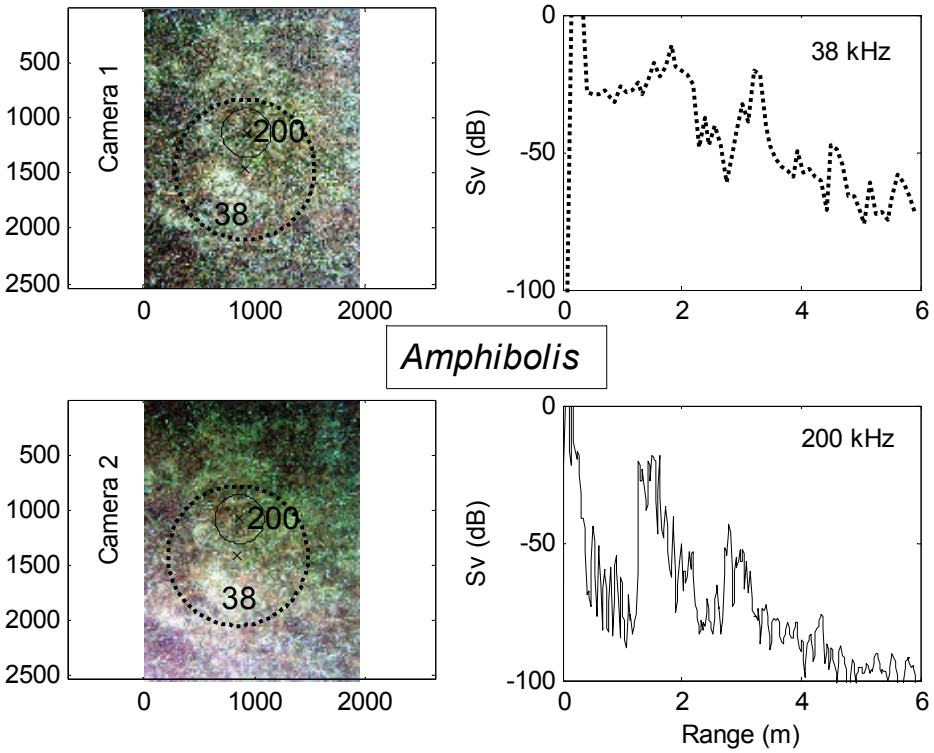

Figure 3-25 Photographic pair and acoustic backscatter waveforms of a typical *Amphibolis* class sample from the third field trial.

3.4 Differences between 38 and 200 kHz

The 200 kHz sounder with the sampling interval of 25 micro-seconds provides better resolution than the 38 kHz sounder. A narrower beam and consequently smaller footprint size at 200 kHz results in a smaller seafloor area sampled at 200 kHz than that at 38 kHz. From the author's observation, the 200-kHz was more sensitive than the 38-kHz to the existence of marine vegetation. Therefore it was proposed in this study that the 38-kHz echo could be a steady indicator for the localization of the water-sediment interface, no matter whether there is vegetation on the bottoms or not. Based on the assumption that each echo was collected from a flat footprint and the operation modes did not change significantly, the author investigated the effectiveness of using the 38-kHz backscatter signal as a reference for the bottom localization and as a base by comparing against the 200-kHz signal for the estimate of vegetation canopy height (see sections 4.2.2, 4.2.3, and 4.3.4).

3.5 Data conversion

Raw data values were logged by the SIMRAD EQ60 acquisition program. The raw data were then exported to values of the volume backscatter strength *Sv* into MATLAB format by SonarData's EchoView software (version 3.10.139.8). According to SonarData's manual, the volume backscatter strength *Sv* is obtained for the range R and received signal level P_r according to:

$$Sv(R,P_r) = P_r + 20\log R + 2\alpha R - 10\log(\frac{P_t G_0^2 \lambda^2 c\tau\psi}{32\pi^2}) - 2S_a \qquad 3\text{-}1$$

where α (in dB/m) is the acoustic attenuation coefficient in sea water, P_t is the transmitted signal power at 1 m from the sonar head, G_0 is receive gain (in relative units), c (in m/s) is the sound speed, τ (in second) is the transmitted pulse width, and ψ (in steradian) is the sonar beamwidth expressed in terms of the solid angle.

It should be noted that SonarData used different formulae in different EchoView versions for defining *Sv*. The formula given in (3-1) was taken from version 3.10.139.8. The up-to-date version provides a different correction term for

$2S_a$. The default input value of S_a in the data processing algorithm is zero. The values of the volume backscatter strength used in this study are derived from the formula defined in equation 3-1.

For the description of the seafloor surface backscatter properties, the volume backscatter strength *Sv* automatically calculated in EchoView and then exported into MATLAB was converted into the received acoustic power P_r, using equeation 3-1, and then the surface backscattering coefficient was calculated according to Medwin and Clay's formulation provided in section 13.3.2 in (Medwin and Clay 1998). The surface backscatter coefficient *s* can be expressed as:

$$s = \frac{\left\langle p_r{}^2 \right\rangle}{p_0{}^2} \frac{R^4 \exp(2\beta R)}{R_0{}^2 A} \qquad 3\text{-}2$$

where $<p_r^2>$ is the mean squared pressure of the received signal, p_0^2 is the squared pressure of the transmitted signal at the reference distance R_0 (R_0= 1m), R is the distance between the sonar head and the seafloor, $\beta = \alpha / 20\log(e)$ is the sound attenuation coefficient in sea water in nepers, and A is the seafloor insonification area.

For the pulse width used and sea depth observed in all experimental measurements in this study, the insonification area was always limited by the sonar beam footprint on the seafloor, which can be expressed in dBs as follows:

$$SCT \equiv 10\log(A) = 10\log\left\{\pi\left(R\tan\left(\frac{\psi}{2}\right)\right)^2\right\} \qquad 3\text{-}3$$

where ψ is the –3-dB width of the main lobe of the sonar directivity pattern expressed in radians. To simplify the calculation, the sonar beams at both frequencies of EQ60 were assumed to be rotationally symmetrical, although it is slightly asymmetrical at 38 kHz (see Appendix D).

Once the received signal level is retrieved from the *Sv* value, the surface backscatter strength *S* can be calculated from:

$$S \equiv 10\log(s) = \left\langle P_r \right\rangle - 10\log\left\langle P_t \right\rangle - 10\log R_0{}^2 + 40\log R + 2\alpha R - SCT \qquad 3\text{-}4$$

In contrast to the definition of the seafloor backscatter strength through the mean level of backscattered signals, as in Equation 3-4, the instantaneous backscatter level P_r is used in this study to estimate "instantaneous" samples of *S*, which, for simplicity, will be referred to as seafloor (or surface) backscatter strength. This

quantity is used to represent the seafloor backscatter value wherever it is considered in the text below, if not mentioned otherwise.

3.6 Classification methodology

Ultimately, the classification aimed at the provision of a classified acoustic database in which each acoustic sample was assigned to a specific bottom type by the examination of the corresponding optical sample. Different field trials observed different bottom types and population differences. For different field trials, classification criteria therefore had to adapt to the bottom types encountered. A habitat type found in one field trial is not necessary to be found in other field trials. Nevertheless, seagrass and flat sand bottoms were observed in every field trial and were the major habitat types exhibiting distinct acoustic backscatter features.

3.6.1 Photographic classification

The assignment of each photographic pair to a distinct habitat type was carried out manually. Before the collected optical data were classified, the photographs had to be previewed in order to understand how many habitat types were in each collected data set. Based on the biological features that appeared on the photographs, a table of tentative habitat types for the collected data was generated.

A typical table of habitat types used for the image classification from the first field trial is given in Table 3-2. In the table, the habitat types assigned for the images were based on the predominant species or bottom types appearing on the photographs and occupying the greatest portion of the areas on the photographs. In the assignments, the attribute of each photographic sample was represented by a combination of two digits.

Table 3-2 A classification table of two digits used in combination for the assignments of the habitat types (1st digit) and the distribution attributes (2nd digit) of the observed study targets on the photographs for the first ESP field trial in 2004.

Assigned NO	1st digit: Habitat types	2nd digit: Distribution attributes
1	Sand	Uniform
2	(Not used)	Non-uniform
3	Reef	Dense
4	Macro algae	Sparse
5	Seagrass 1 (*P. sinuosa*)	Epiphytes attached on seagrass
6	Seagrass 2 (*P. australis*)	Gas bubbles appeared
7	Mixture of 2 seagrasses	
8	Fish appeared	
9	Coarse sand	

For example, a classification of "62" indicates that the predominant species observed from the image pair is seagrass species *P. australis*, and the seagrass photographed is not uniformly distributed on the bottoms. Note that the "80", "05", "06", and "00" are exclusively reserved for the fish observed within the footprints, epiphytes attached on seagrass, gas bubbles, and unrecognizable photographs respectively.

Area cover differences of a species on the photographs were observed. The distribution of a predominant species may vary in extent from dense, medium, to sparse disposition. Areas covered by the predominant species may also occupy only part of the photograph while the other part is totally occupied by different habitat types. In order to accomplish the task of assigning an appropriate habitat type to each

photographic pair, circle plots of the estimated insonified areas for each frequency of the echosounders were plotted on the corresponding photographs.

The circle plots were based on the EQ60's beam patterns (see Appendix D) and laboratory measurements of the beam width at the -3 dB backscatter level at each frequency made in a water tank[§§§§§]. The centre of each circle was also determined.

As one can see in the previous figures such as Figure 3-25, the enclosed areas varied from one frequency to another and hence the habitat type assigned to each sample may have an ambiguity depending on the frequency choice. In this study, the identification of seafloor habitats was primarily based on the areas enclosed by the EQ60 footprint at 200 kHz.

There were occasions when the same optical samples were assigned to different habitat types at different classification attempts. One of the reasons was that there were situations in which the predominant species on the photographs was not distinctive. The other reason was that two or more species were observed in the same photograph.

In order to prevent ambiguities arising from the above issues, data were classified into data sets with different confidences. The highest confidence data sets consist of bottom types of pure sand seafloor and single seagrass species meadows uniformly distributed on the insonified areas. Lower confidence data sets consist of data in which two or more species may appear simultaneously on the images or the species is not uniformly distributed.

3.6.1.1 Issues due to the system configuration

Figure 3-26 shows how a fish appearing within the insonified cone in the water column affected the optical (left and right camera photographs) and acoustic data collected. In this particular case, it shows that there were occasions when the acoustic backscatter data could not be properly interpreted unless a comparison was made for the optical and acoustic samples taking into account the actual

[§§§§§] The laboratory measurements of each frequency's -3 dB backscatter level were mainly supported by Dr. Alec Duncan and assisted by Mr. Andrew Woods.

configuration of the system components. This also shows that objects appearing in the water column can impact on the collected data. This is also why in Table 3-2 there is a category particularly reserved for samples when fish appeared on the photographs.

In Figure 3-26, the 200-kHz echo revealed the fish by exhibiting a sharp peak well above the detected bottom while the 38-kHz echo signal was not sensitive to the presence of the fish. In order to avoid the influence of in-water backscatterers on the acoustic classification of seafloor vegetation, the samples containing fish and gas bubbles were excluded from this study. After this screening, a classified acoustic data set was obtained. It contained classes of 1) pure sand bottoms, 2) pure seagrass 1 (*P. sinuosa*), 3) pure seagrass 2 (*P. australis*), 4) mixed seagrasses, 5) rocky reefs, 6) macro algae, and 7) other non-uniformly distributed species of the above classes.

When fish appeared at positions such as those marked by @, ©, and ® in Figure 3-26 and was actually outside the acoustic cone of the sonar beam, the acoustic samples collected under such conditions might be incorrectly classified into the fish class in spite of the fact that echoes were actually backscattered from fish-free seafloors. If a similar observation system is to be used, one needs to carefully understand the configuration-induced issues in order to prevent such a misclassification possibility.

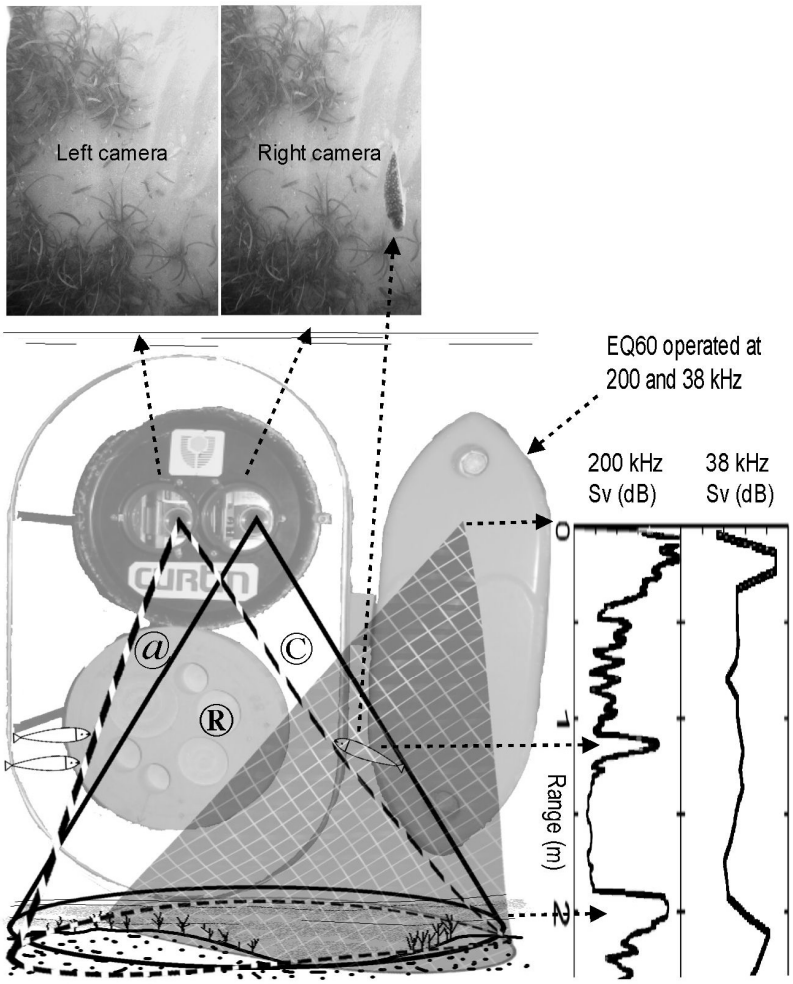

Figure 3-26 A particular case showing how the study targets (fish and seafloor) were recorded by the Left camera (no fish), Right camera (fish appeared), and the two-frequency echosounder due to the configuration of the detection components and the relative position of the fish under the detection components. Those marked by @, ©, and ® indicate the possible positions where fish may be observed on the photographs while no indications of fish can be observed from the acoustic signals.

3.6.2 Classified acoustic data

The synchronization of the optical and acoustic systems allowed classification of the acoustic data set into appropriate habitat types using the above mentioned procedure. After this step, a very accurately identified acoustic data set became available for supervised training of classification algorithms, which was one of the major advantages of the ESP project.

3.7 Summary

In conclusion, the synchronization mechanism between the optical and acoustic systems provided a perfect platform to obtain an accurately classified acoustic data set for further needs including the supervised training requirements of the acoustic classification methods. According to different levels of data confidence, data were divided into the so-called “pure” samples and “non-pure” samples.

With the accurately identified acoustic data, there are chances we can resolve some of the doubts about the relationship between characteristics of the acoustic waveform and the seafloor properties, and use the acoustic features identified from the comparative analysis of acoustic and visual data to develop methods for the acoustic assessment of seafloor vegetation.

Chapter 4 Conventional study results

This chapter illustrates the results of analysis of the acoustic data by some conventional methods. The analysis aims to understand the acoustic backscatter characteristics of some typical vegetation species by comparing their backscatter features against those from the bare sand seafloors. In the three field trials, the study targets varied, the field sites changed, the operational procedures were adapted to the actual conditions, and the data collection system was adjusted accordingly. However, the settings of the EQ60 sonar were kept the same in order to provide a fair comparison between different field trials.

In view of the frequent use of the terminology "feature" and "parameter" in the following text, they are defined below for their specific meanings used in this work.

- Parameter - some measured characteristic of the signal. (e.g., EPW in section 4.2.1.3)
- Feature - the result of some combination of one or more parameters that is then used for classification purposes. (e.g., those PCA components in section 4.4.2 and GP individuals in Chapter 5)

4.1 Study considerations

4.1.1 Applicability of backscatter theory to seafloor vegetation

There have been several theoretical studies made for the estimates of the seafloor roughness defined by various statistical parameters (Isakovich 1969; Akal and Hovem 1978; Berkson and Matthews 1983; Fox and Hayes 1985; Pace, Al-

Hamdani *et al.* 1985; Stanton 1985; Jackson, Winebrenner *et al.* 1986; Ogilvy 1987; Thorsos 1988; Ogilvy 1991; Stanton, Chu *et al.* 1991; Jackson and Briggs 1992; Michalopoulou, Alexandrou *et al.* 1994; Bilgen and Rose 1997; Ivakin 1998; Lyons, Pouliquen *et al.* 1998; Novarini and Caruther 1998; Thomas, Rosen *et al.* 1999; Keiffer and Novarini 2000; Johnson 2002; Liu, Huang *et al.* 2002; Johnson and Burkholder 2004; Liu, Tsai *et al.* 2004). According to Stanton's study (Stanton 1984), if the scale of seafloor roughness is much smaller than the acoustic wavelength, the roughness parameters, such as the root mean square (RMS) roughness height and the roughness correlation length, can be estimated from the acoustic echo envelope and then used for characterizing various bottom types. However, the theory developed by Stanton is only applicable to a limited range of backscatter scenarios depending on the acoustic frequencies and the bottom types. He applied his model to numerically predict acoustic backscatter from several bottom types, including sand ripples, nodules, or rubble beds. For bottom types, such as those covered with seagrass or macro algae, acoustic backscattering at higher frequencies is subject to shadowing effects and multiple reflections from leaves and the substrate and hence the classical acoustic backscatter models, such as the small perturbation model and small slope approximation, are no longer applicable. The Kirchhoff approximation commonly used for acoustic scattering modelling is not applicable to simulating backscattering from the vegetation-covered seabeds. With the only appropriate theoretical models suitable for the vegetation-covered seabeds being a few models made by Shenderov (Shenderov 1998), which are applicable to certain simplified scenarios of backscattering from seafloor plants, the author of this thesis carried out an analysis of the waveform characteristics from an empirical point of view. The attempt here was made to find if there were any acoustic parameters suitable for effective characterization of some typical habitat types in order to provide capabilities for the recognition and assessment of seafloor vegetation by using the available single beam echosounder.

4.1.2 Waveform analysis

For waveform analysis, there are several ways to extract seabed information from backscatter data of multi-frequency sonar systems. It can be the waveform

analysis at a single frequency or a comparison between different frequencies (two frequencies for EQ60). Since the time resolution at the lower frequency (38 kHz) of the EQ60 sonar is coarser than that at 200 kHz, it was mainly the 200 kHz backscatter data which were used for characterizing the seabeds. Due to the 38 kHz's poor sampling resolution (see Table 3-1), extraction of additional useful reference points from the 38 kHz's echo envelope is almost impossible except the maximum backscatter level. The 38 kHz data were only used for its steady indication of the water-sediment interface location by using its maximum backscatter level.

The waveforms of acoustic signals backscattered from bare sediments and from bottoms covered with vegetation are different. Different frequencies also presented different sensitivities to the study targets. Physical properties of the interface between the seafloor substrate and water are the key factors that may influence the returned waveforms. A flat sandy seafloor can be regarded as an ideal flat interface which is unique and different from vegetation-covered seabeds. The existence of vegetation on the water-sediment interface can be regarded as a perturbation of the bare bottom condition. To understand the variation of the backscatter from different bottom types, the author investigated the echo envelopes of the pure sand seafloor and the seagrass-covered seabeds. The results are given in the following sections.

4.1.3 Location of the bottom from the waveform analysis

Illustrated in Figure 4-1 are the typical acoustic waveforms at 38 and 200 kHz for backscattering from a densely populated seagrass meadow of *P. australis* (see Figure 3-9 as a contrast for backscattering from the bare sand bottom). There was a discussion among scientists (e.g., (Sabol, Melton *et al.* 2002) and (Tęgowski, Gorska *et al.* 2003)) about the appropriate reference point on the waveform which could be assigned to the true water-sediment interface location. The true bottom location refers to the interface between the water and the sediment on which the vegetation is accommodated. When an echo backscatters from a flat and bare sand seafloor, the returned waveform is quite sharp and the water-sediment interface can be easily located. When an echo is backscattered from vegetation-covered seabeds, the returned waveform is generally elongated and consists of several peaks of

comparable levels, which is clearly seen at 200 kHz in Figure 4-1. The amplitude of those peaks varies considerably from one transmission to another one. When the echoes are backscattered from very dense seagrass meadows (see Figure 3-17) or tall macro algae (see Figure 3-19), the later arrival peaks distort the echo tail such that it is generally impossible to appropriately determine the range to the bottom by the decay of the backscatter level. If the maximum level can be used to refer to the water-sediment interface location, it is seen in the 38-kHz waveform Figure 4-1 that there is only one peak which can be definitely selected for this assignment (see sections 4.2.2 and 4.2.3 for further investigation results). However, it is evident from the 200-kHz waveform that there are several peaks in the waveform at 200 kHz which could be assigned to the water-sediment interface location if the maximum level were used.

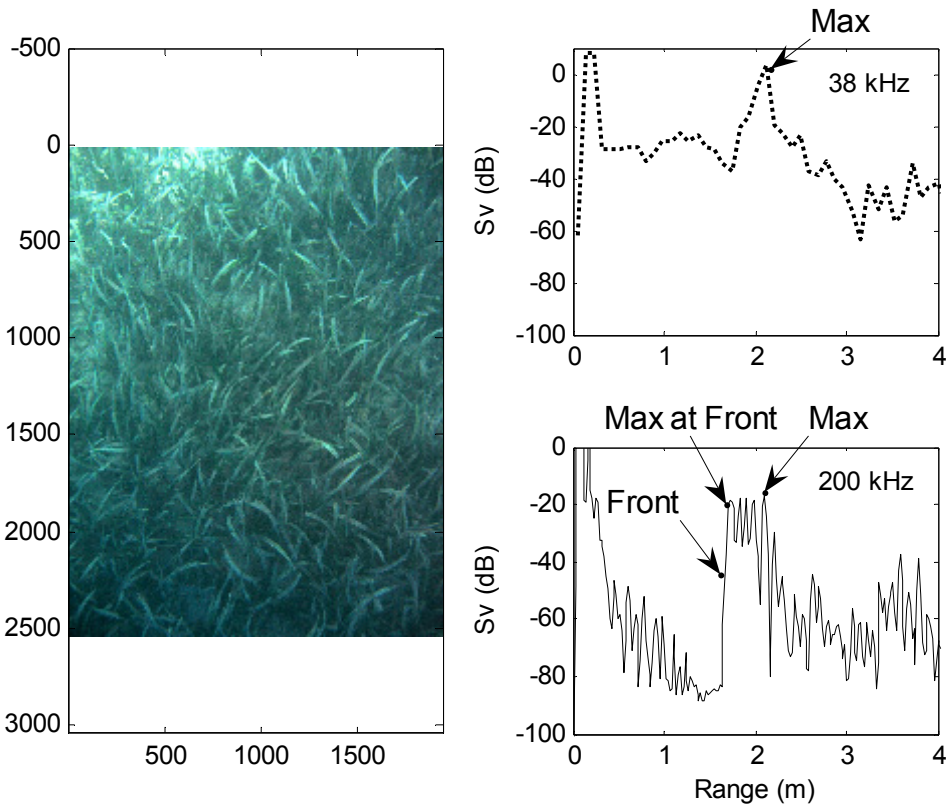

Figure 4-1 Typical waveforms at two frequencies of EQ60 backscattered from a densely populated seagrass meadow of *P. australis* showing several peaks in the 200-kHz waveform with backscatter levels comparable to the maximum value (Max).

The maximum fluctuation between the backscatter peaks at 200 kHz as shown in Figure 4-1 is over 30 cm. The multiple peaks of similar height on the 200 kHz bottom return make the location of the maximum level an unreliable parameter because statistical fluctuations in the heights of the individual peaks will lead to large changes in position of the maximum. When this fluctuation is comparable to the size of the study target, it is a critical issue in considering the designation of an appropriate reference point on the waveform for the correct bottom interface location. To show the effect of the above issue, the author provided the investigation results of this problem in sections 4.2.2 and 4.2.3.

In the following sections, the observations and analysis results of the data collected by the EQ60 from each field trial are provided.

4.2 Cockburn Sound 2004

4.2.1 Characterization parameters

4.2.1.1 Bottom backscatter strength

Lyons and Abraham used the mean backscattering strength (BSS) in dB as a measure for the characterization of different seafloor covers including *Posidonia oceanica* seagrass meadows. The BSS's angular dependence for four bottom types is shown in Figure 4-2 (Lyons and Abraham 1999). From Figure 4-2, the BSS of the *P. oceanica* near the grazing angle of 80 deg is around -20 dB. Lyons and Abraham observed that the mean scattering strength measured in their study did not correlate well with the bottom types. They suggest that any classification scheme needs to consider not just the mean scattering strength but also other parameters to improve characterization results.

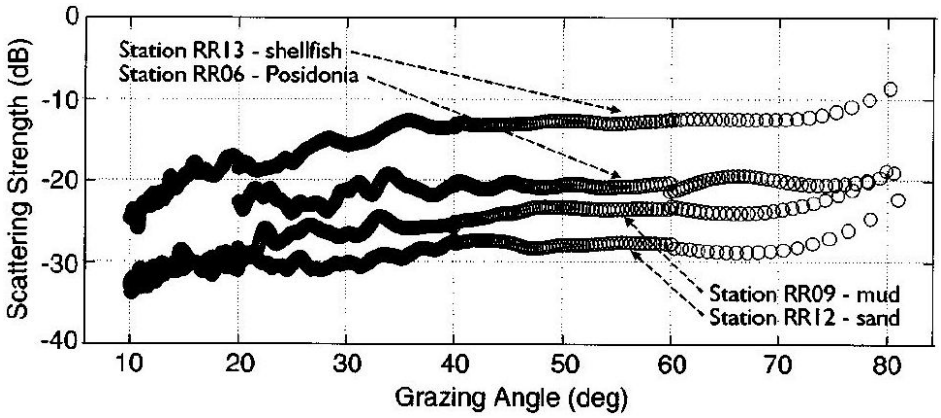

Figure 4-2 Bottom backscatter strength as a function of grazing angle for four different bottom types: shellfish covered sand, *Posidonia Oceanica* seagrass covered sand, medium sand, and mud observed by Lyons and Abraham.******

Instead of using BSS, the author investigated the potential of the maximum backscatter level expressed in terms of surface backscatter strength as a descriptor for the recognition of the bottom types observed in the first field trial. The histograms of the maximum S value for various bottom types observed at two frequencies are shown in Figure 4-3 and Figure 4-4. The results showed that the maximum backscatter strength obtained for each particular class fluctuated over 20 dB at both frequencies. Although the variations of the maximum backscatter strength at 200 kHz were smaller than those at 38 kHz, the maximum backscatter strength also could not be used as a sole characteristic for distinguishing all the classes.

****** Reprinted with permission from The Journal of the Acoustical Society of America, Vol 106, Iss 3, Lyons, A. P. and D. A. Abraham, "Statistical characterization of high-frequency shallow-water seafloor backscatter", pages 1307-1315, copyright (1999), Acoustical Society of America.

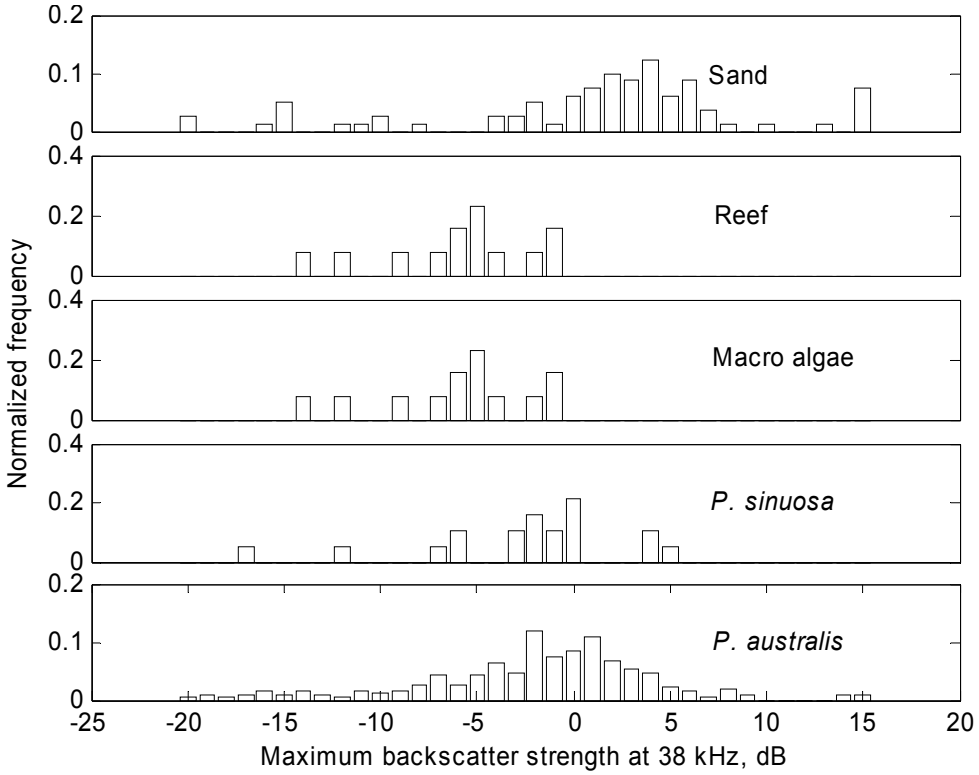

Figure 4-3 Histogram of the maximum backscatter strength obtained at 38 kHz from various classes where samples were collected from the first field trial.

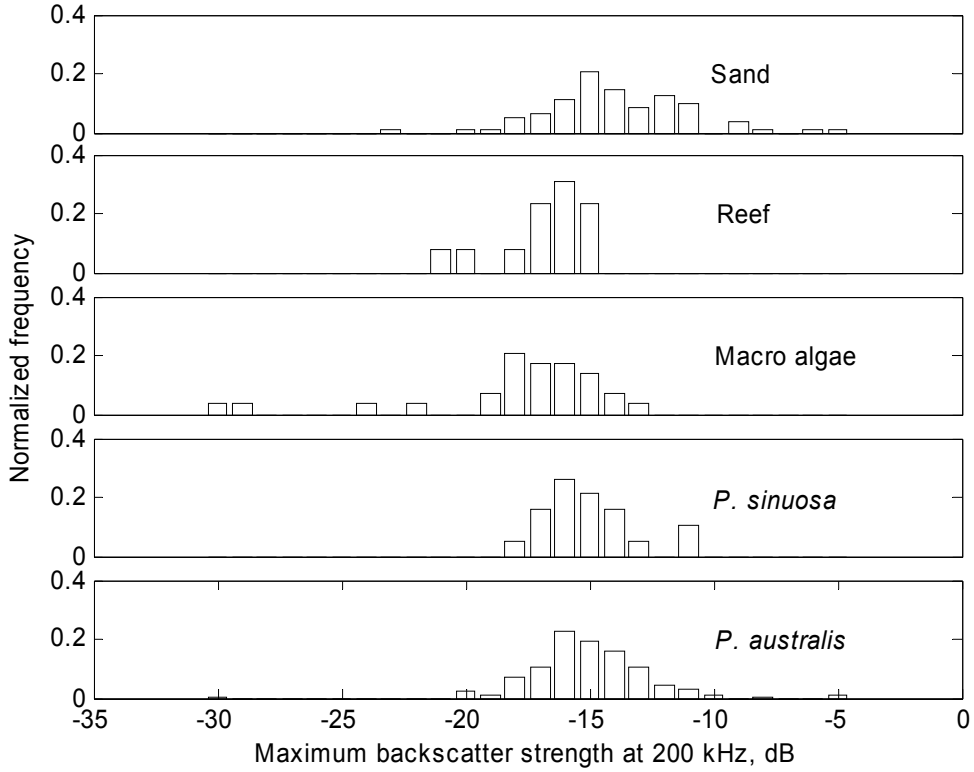

Figure 4-4 Histogram of the maximum backscatter strength obtained at 200 kHz from various classes where samples were collected from the first field trial.

4.2.1.2 Echo-average backscatter strength

A parameter called integral backscattering strength (IBS) has been investigated by Tęgowski (Tęgowski 2002) for recognition of bottom sediments in the southern Baltic Sea. It was defined as an integral of the instantaneous surface backscatter strength S derived from the echo envelope within a depth interval. Instead of using the IBS defined by Tęgowski, the author divided the IBS by the depth interval as an average backscatter strength value for each echo so that the echo-average backscatter strength is independent of the depth interval. As shown in Figure 4-5, the echo-average backscatter strength does not perform better than the maximum backscatter strength in distinguishing the classes discussed in the previous section.

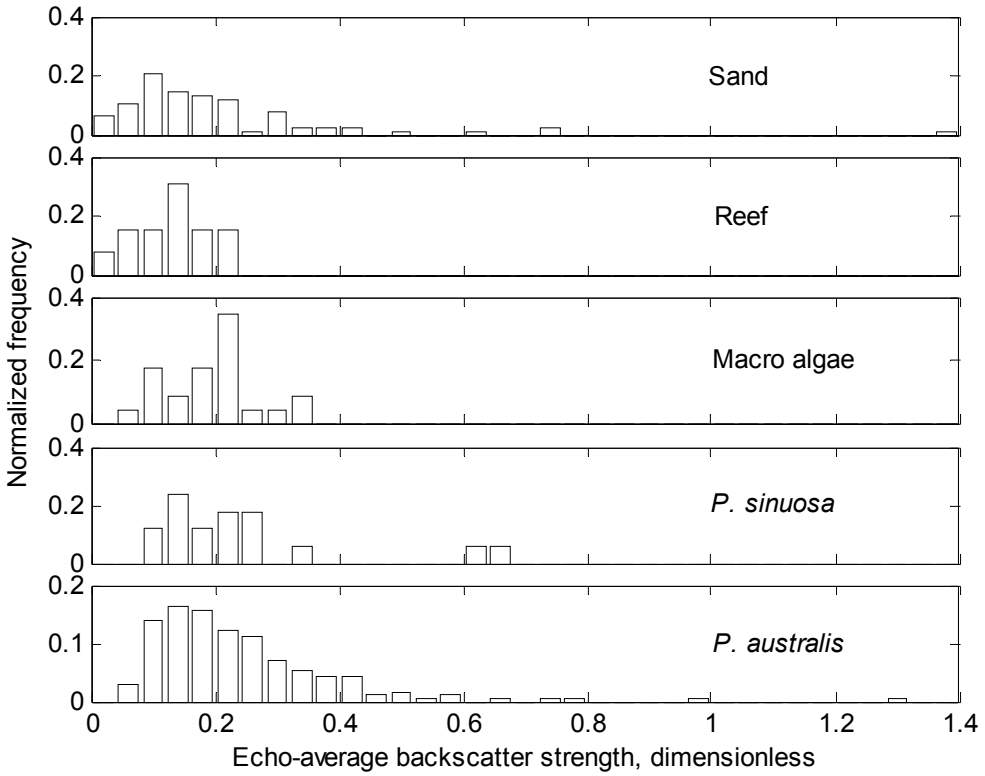

Figure 4-5 Histograms of echo-average backscatter strength obtained at 200 kHz for five classes where samples were collected from the first field trial (cf. Figure 4-25).

4.2.1.3 Effective pulse width

As was discussed in section 2.1.3.3.6, Tęgowski, Gorska and Klusek used the moment of inertia (MI) of the backscatter pulse as a parameter for differentiation of seagrass meadows from flat sandy bottoms (Tęgowski, Gorska *et al.* 2003). MI is the same in concept as the effective pulse width (EPW) discussed below. The EPW is a product of the sampling interval and the square root of MI. Both MI and EPW are based on the determination of the "Center of Mass" (Denbigh 1989) of the backscattered pulse waveforms (Tęgowski, Gorska and Klusek used the term "Centre of Gravity" instead). To calculate the EPW, it is necessary first to determine the centre of mass (CM) of the backscatter return impulse.

The mathematical definition for the CM is

$$i_c(j) = Int\left\{\sum_i i \cdot f_i(j) \Big/ \sum_i f_i(j)\right\} \qquad 4\text{-}1$$

where $f_i(j)$ is the pulse amplitude of the j-th sonar ping number at index i and Int denotes the integer function. For discrete pulse signals of backscatter echoes, the amplitude $f_i(j)$ is the squared acoustic pressure of the backscattered signal. It is essential that the summation in equation 4-1 is made over an interval which contains entirely the first bottom return, i.e. starts before the front of the first bottom echo and ends before the second bottom return. The selected summation time interval is shown in Figure 4-6.

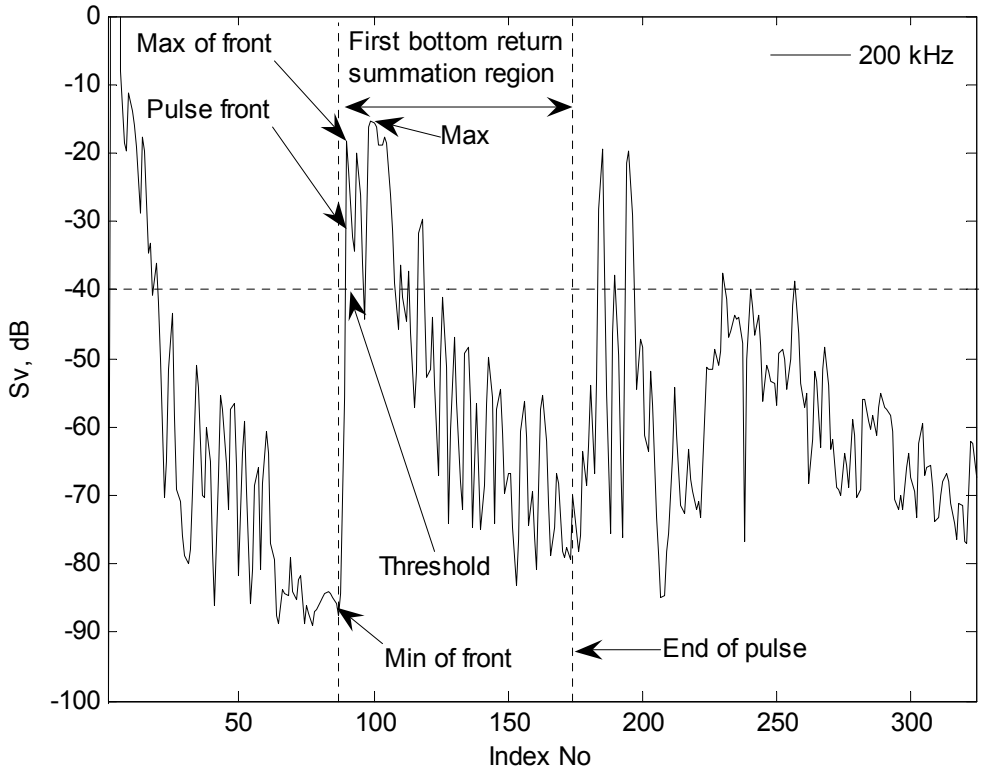

Figure 4-6 Time interval for the summation to be made over for the first bottom return in equation 4-1 and the reference points used to derive the parameters used in this study.

All the parameters used in this study were derived from the first backscatter echo as indicated in Figure 4-6, in contrast to the RoxAnn technique (see section 2.5.1). The summation region starts from the index corresponding to the minimum of the pulse front and ends at the index which is twice the starting index.

In order to determine an appropriate time interval containing the entire signal of the first bottom echo, the maximum backscatter level has to be firstly located. Searching for the maximum level should start from a predefined range from the sonar head to avoid false localization due to acoustic ringing of the transducer decaying for a certain time after transmission of the sonar impulse. Backscatter peaks comparable in level to the first bottom return may appear before the first bottom return if fish or any object of high backscatter target strength, such as gas bubbles, appears in the insonified cone. Those signals backscattering from in-water objects should be manually removed in order to make sure that the characterization parameters are correctly extracted from the first bottom echo. Once the maximum point in the first bottom return is determined, the other reference points such as the "Front" (determined from the selected threshold of the backscatter level), "Min of front", "Max of front" (determined by comparing neighbour backscatter level), and "End" of the first bottom return can be easily determined (see Figure 4-6).

There is a major drawback of this selection for the first bottom return. The farther the study target, the longer the time duration will be considered in the calculation for the first bottom return, which could result in range dependence for the extracted characterization parameters.

EPW of an acoustic backscatter signal can be expressed as

$$EPW(j) = \delta t \sqrt{I(j)} \tag{4-2}$$

where

$$I(j) = \sum_i (i - i_c)^2 \cdot f_i(j) \Big/ \sum_i f_i(j) \tag{4-3}$$

is the MI of the j-th sonar ping and δt is the sampling interval.

By investigating the value of the EPW, it is possible to distinguish a few acoustically distinct seabeds, but not all. In one of the previous study results (Siwabessy, Tseng *et al.* 2004), EPW gives the best performance against other parameters in differentiating various seabed types.

A comparison of the EPW measured for several data sets is provided in Figure 4-7 and Figure 4-8. The data illustrated in Figure 4-7 come from the homogeneous habitat types (pure classes) while those in Figure 4-8 represent the inhomogeneous classes containing mixed seafloor covers within the acoustic

footprint with one major class dominating the others (non-pure classes). Since *P. sinuosa* was not observed in the non-pure classes, it was not included in Figure 4-8.

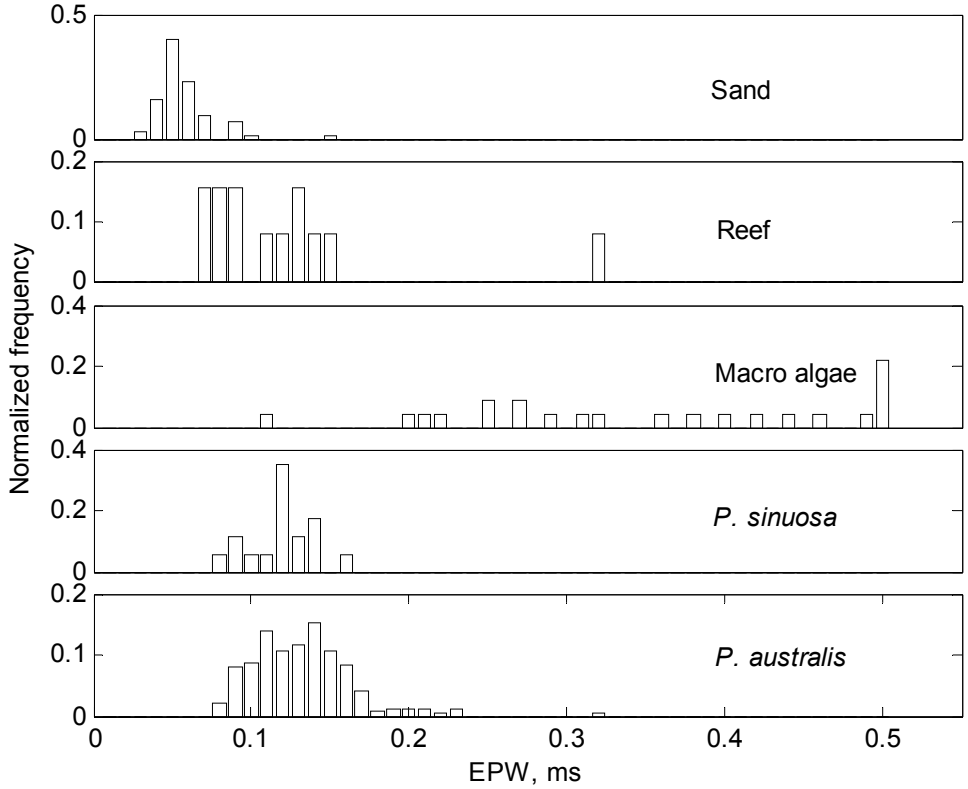

Figure 4-7 Histogram of EPW of five pure habitat types where samples were collected from the first field trial (cf. Figure 4-14).

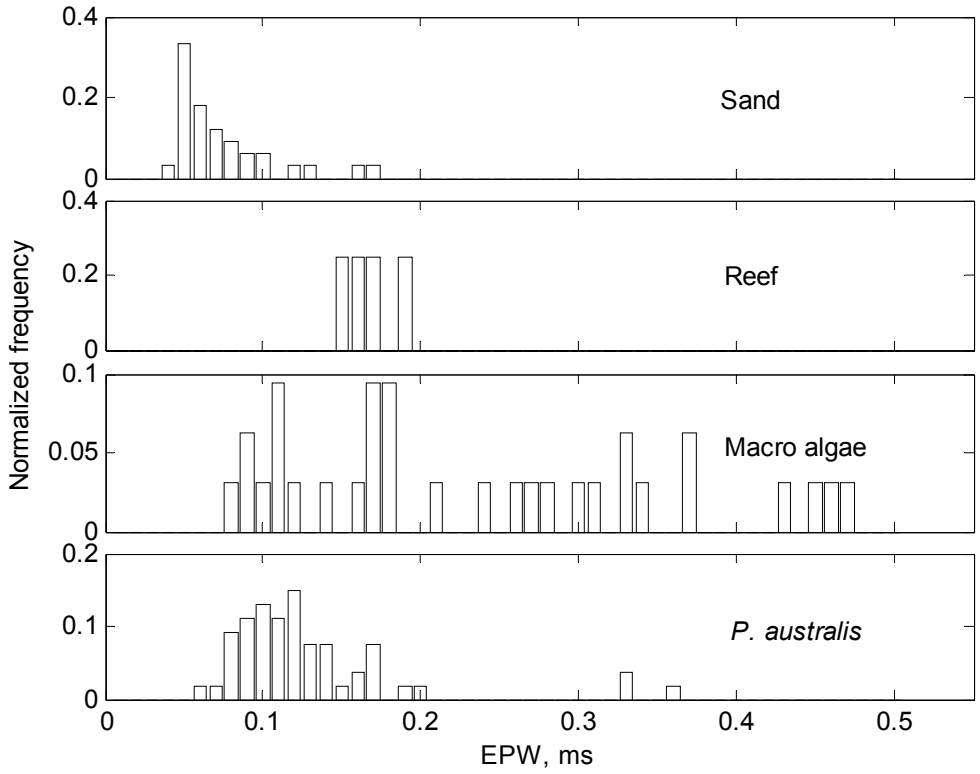

Figure 4-8 Histogram of EPW of four non-pure habitat types where samples were collected from the first field trial (cf. Figure 4-15).

It is seen from Figure 4-7 and Figure 4-8 that the macro algae class exhibits the highest EPW values while the sand class has the lowest EPW values. Overlaps of the EPW distributions between different non-pure classes as shown in Figure 4-8 are considerably larger than those in Figure 4-7. This is most likely due to the mixed habitat types of the non-pure classes with analogous properties between different classes. For example, if the non-pure sand class is mixed with seagrass, the sand class will have EPW values approaching the seagrass's EPW distribution range.

If there are only two classes involved, it is possible to choose an optimal EPW threshold to discriminate the two different classes with the minimum misclassification rate. However, overlapping is inevitable and the condition of more than two classes observed in this study does not allow perfect segmentation of those classes by using the EPW parameter only.

As described in section 3.3.2.2, macro algae, such as the common kelp species of *Ecklonia radiate*, were observed in the field trials. High and prominent shoot profiles were their common feature. Their higher EPW values than other classes may be due to this unique profile feature.

The EPW of backscatter echoes from the seagrass meadows was generally larger than that from flat sandy bottoms. It is still unknown whether the longer tail of the backscatter pulse from seagrass is a consequence of reverberations in the seagrass mass or multiple reflections between the vegetation and the bottom substrate. Large EPW values were also observed from the backscattering from rocky reefs, macro algae and other habitats, such as coral reefs, which make the seafloor surface noticeably rougher than the pure and fine sediments, such as sand and silt.

4.2.1.4 Hurst exponent and fractals

Fractals introduced in topology for the first time by Mandelbrot (Mandelbrot 1967; Mandelbrot 1984) are defined as phenomena exhibiting patterns of self-similarity or self-affinity and are independent of scaling (Hastings and Sugihara 1993). Seagrass canopies of the *P. sinuosa* species exhibit patterns analogous to fractals in scales when viewing from a distance (see Figure 2-5a for the parallel growing patterns periodically separated by the sand channels) and from a closer range (see Figure 2-5b for the parallel inclination of the leaves).

Fractal dimension (FD) of the echo envelope has been used by Tęgowski, Gorska and Klusek as one of the parameters for discriminating bare sand and vegetation-covered seabeds (Tęgowski, Gorska *et al.* 2003). Although they concluded that the accuracy of classification by FD was noticeably worse than that by MI (or EPW in this study), it is worthwhile to examine the robustness of the FD parameter again for the classification of the sonar data collected in this study. To understand this, the author conducted a study of the correlation between the fractal dimension and some distinct habitat types.

The Hausdorff dimension (Hausdorff 1918) and Hurst exponent (Hurst 1951; Hurst 1952) are often used to determine the FD which characterizes the roughness of a geometrical object and long-memory dependence of fractal time series respectively (Gneiting and Schlather 2003). Under certain assumptions, the FD can be related to the Hurst exponent through a linear function (Barton and Poor 1988; Molz, Liu *et al.* 1997).

The Hurst exponent H is a scaling parameter of self-similarity. Its linear relationship with the FD can be expressed by

$$D = C - H \tag{4-4}$$

where D is the FD and C is a constant (Mandelbrot and Wheeler 1983; Feder 1988). Hence, the FD can be determined from the Hurst exponent through the above equation.

According to Hurst's study (Hurst 1951), the Hurst exponent can be estimated by calculating the mean value of the so-called rescaled ranges. A detailed mathematical formulation for estimating the Hurst exponent can be found in (Peters 1994; Weron 2002). The calculation of the Hurst exponent is briefly illustrated by the following procedures.

Firstly the whole length N of an echo envelope is divided into d contiguous sub-series of length n, where $d*n$=N. Next for each sub-series $m = 1,\ldots,d$

1) find each sub-series mean $\langle f \rangle_m$ and standard deviation S_m

$$\langle f \rangle_m = \frac{1}{n}\sum_{i=1}^{n} f_i(m) \tag{4-5}$$

$$S_m = \sqrt{\frac{1}{n}\sum_{i=1}^{n}\left(f_i - \langle f \rangle_m\right)^2} \tag{4-6}$$

2) normalize each sub-series $f_i(m)$ by removing the sub-series mean $\langle f \rangle_m$

$$f_i'(m) = f_i(m) - \langle f \rangle_m, \qquad 1 \le i \le n \tag{4-7}$$

3) calculate a series of cumulative sums for each normalized sub-series data

$$F_i(m) = \sum_{j=1}^{i} f_j'(m) \qquad i = 1,\ldots,n \tag{4-8}$$

One can then easily obtain the so-called "rescaled range" R_m / S_m where

$$R_m = \underset{1\le i\le n}{Max}\{F_i(m)\} - \underset{1\le i\le n}{Min}\{F_i(m)\} \tag{4-9}$$

Finally the mean value of the rescaled range for all sub-series of length n is obtained by

$$\left(\frac{R}{S}\right)_n = \frac{1}{d}\sum_{m=1}^{d}\frac{R_m}{S_m} \tag{4-10}$$

The Hurst exponent H, and hence FD through equation 4-4, can be obtained by taking the logarithm of the mean $(R/S)_n$ through the general relationship:

$$\left(\frac{R}{S}\right)_n = C' \cdot n^H \tag{4-11}$$

Since it is the relative value of the H among the different habitat types that is relevant for the differentiation purpose, one can assign the constant C' to be unity. Following the above formulation, the estimated Hurst exponent H values can be calculated from the slope of a log-log plot of R/S against n. A typical example for a pure sand echo envelope is plotted in Figure 4-9.

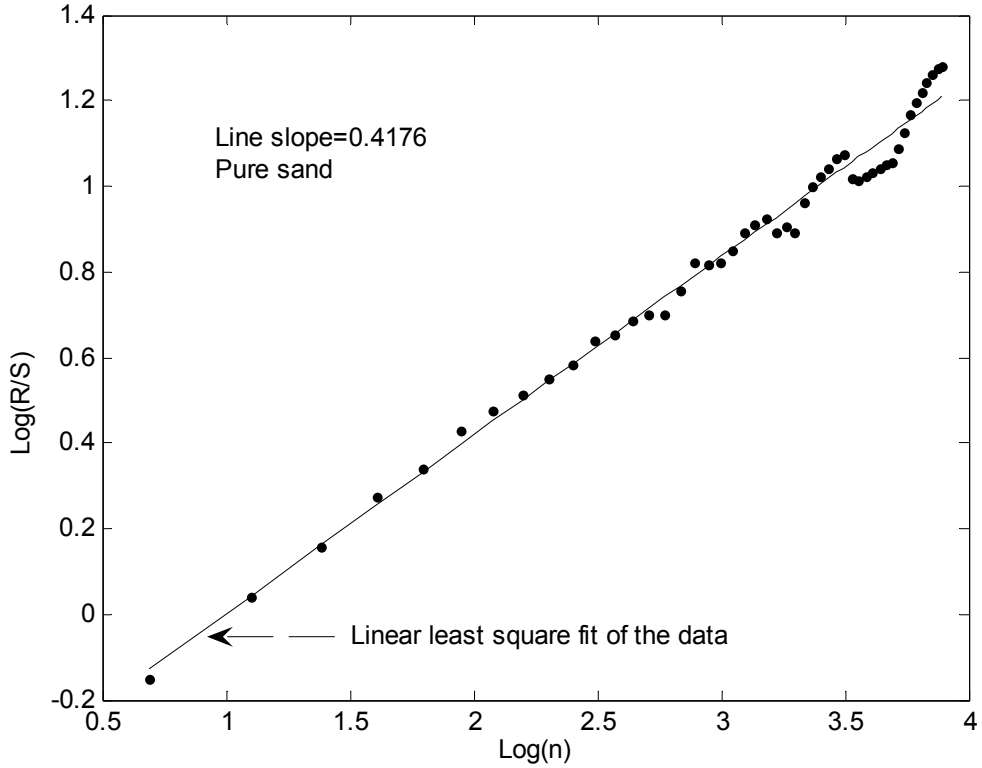

Figure 4-9 Log-log plot of the rescaled range (R/S) vs. the sub-series length n of a typical echo from bare sand and its least mean square linear fit. The slope is the Hurst exponent.

It is noticeable that the rescaled range (R/S) deviates more from the linear fit as the sub-series length n increases. This is because the average value is calculated for fewer available number of d sub-series data sets. The histograms of the Hurst exponent estimated for the echo signals from five pure classes are plotted together in Figure 4-10. Large overlaps of the Hurst exponent distributions obtained for different seafloor classes reveal that the Hurst exponent is not robust enough for using it as a single parameter for distinguishing those five habitat types.

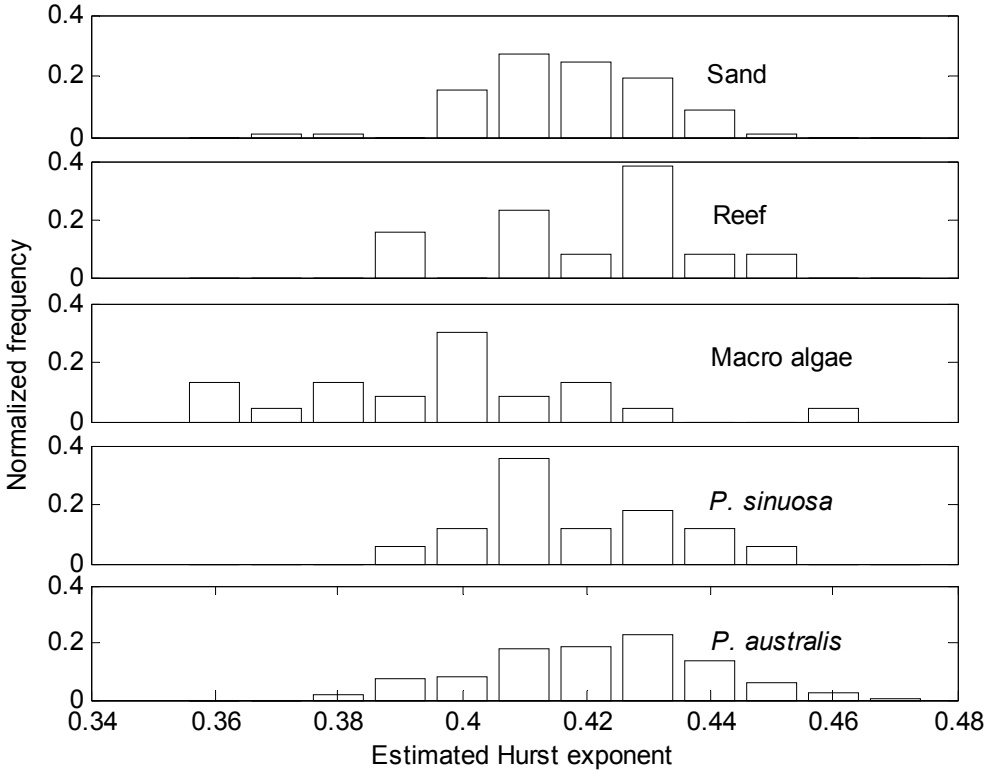

Figure 4-10 Histograms of the estimated Hurst exponent of five pure habitat types where samples were collected from the first field trial.

The Hurst exponent's inability to distinguish the five pure habitat types may be due to the limited sampling ability of the sonar system used. Other possible reasons could be that fractal patterns might not actually exist in the echo envelope or the relationship between Hurst exponent and FD is not a linear one like equation 4-4.

4.2.2 Detection abilities of the 38 and 200 kHz sonars

As discussed in sections 3.4 and 4.1.3, the 38 kHz sonar is expected to be primarily sensitive to the substrate and insensitive to the existence of vegetation on seabeds. To examine this assumption, let us consider a case for samples only selected within a small and bounded area assuming flat sea bottoms. By selecting the maximum amplitude on the 38 kHz waveform (see Figure 4-1) as the indicator for the bottom, there is no obvious evidence from Figure 4-11 that the 38 kHz is sensitive to the existence of seagrass on seabeds. Conversely, the bottom ranges for

the same pings, determined from the front of the 200 kHz echo (see Figure 4-12), exhibited an obvious difference between the sand and the seagrass meadows. It is evident that the 200-kHz echo signal is more sensitive than the 38 kHz in detecting the existence of the vegetation on the seafloor. The limited ability of low frequencies for detecting seagrass habitats was also noticed by a group of Italian researchers (Colantoni, Gallignani *et al.* 1982) and discussed in section 2.1.3.3.4. It is consequently reasonable to expect that the differneces between the ranges determined at these two frequencies may be useful for estimating canopy height.

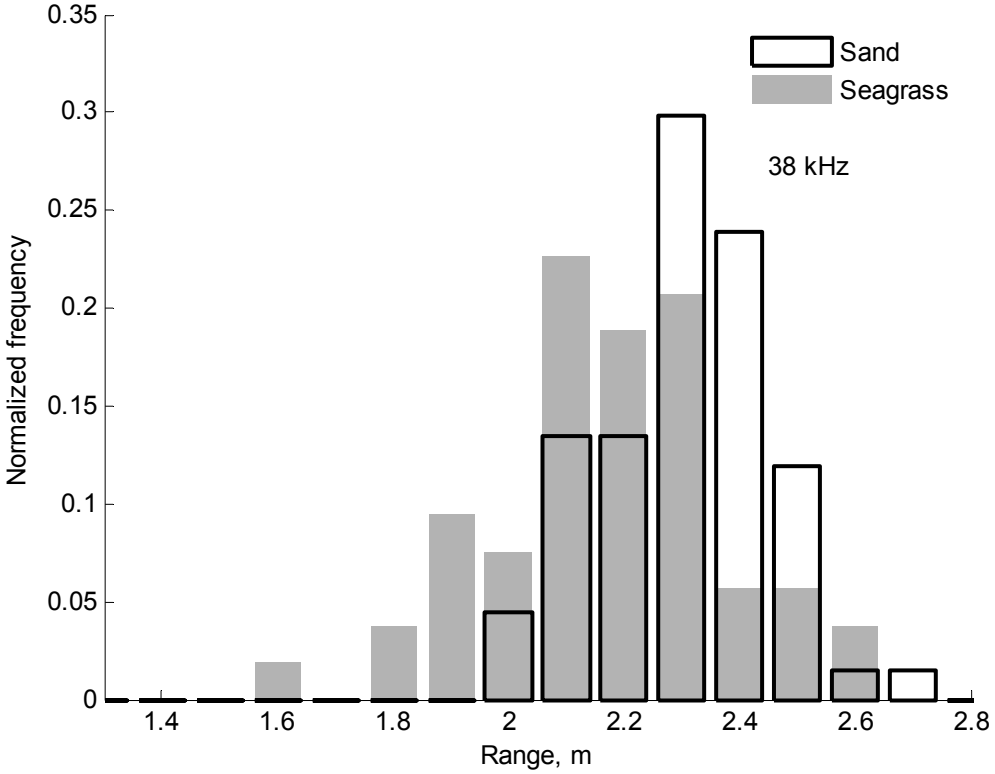

Figure 4-11 Histogram of detected bottom range based on the peak location of the echo waveform at 38 kHz for sand and two seagrass species combined.

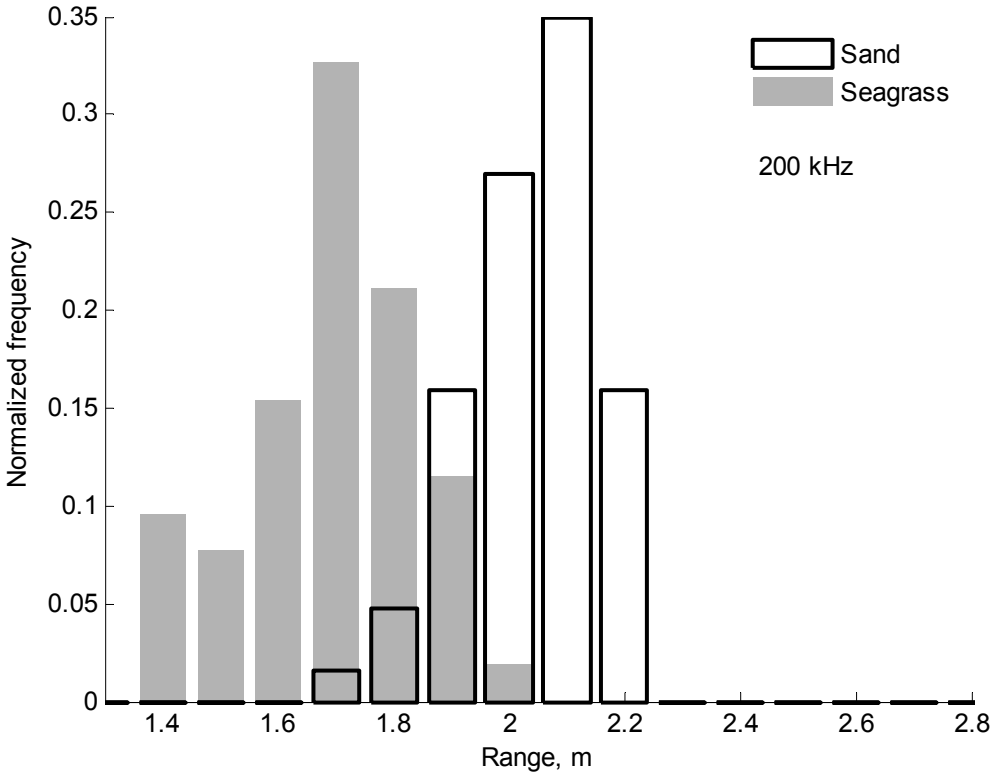

Figure 4-12 Histogram of bottom ranges measured from the front location of the waveform at 200 kHz for sand and two seagrass species combined.

4.2.3 Detection of seagrass canopy

In view of the above observations, the range difference between the "Front" at 200 kHz and the "Max" at 38 kHz, defined as RD in this study, is proposed as a measure for the height of vegetation on seabeds. The "Front" indicated in Figure 4-6 was determined by selecting the first sampled point on the waveform below a selected threshold level. The threshold was assigned at levels approximately 20 dB below the average peak level value of the echo signals and used as a criterion for the computer algorithm to detect the arrival of the first pulse after excluding the initial time interval from the echogram which contains noise from acoustic ringing by the transducer.

From the optical recordings, different habitat types have different surface contours. Even for the same plant on the same bottom location insonified by the same sonar system within the main lobe, it can have different RD values varying

over time due to the plant's waving motion with the currents. As shown in Figure 4-13, the macro algae exhibits the biggest RD variation value reflecting the wide variety of algae sizes and its changing canopy height over time actually observed in the field, while flat surface bottom types such as the sand seem to have smaller RD and RD variation values than other classes. The *Posidonia* seagrasses generally have bigger RD values than the sand bottom.

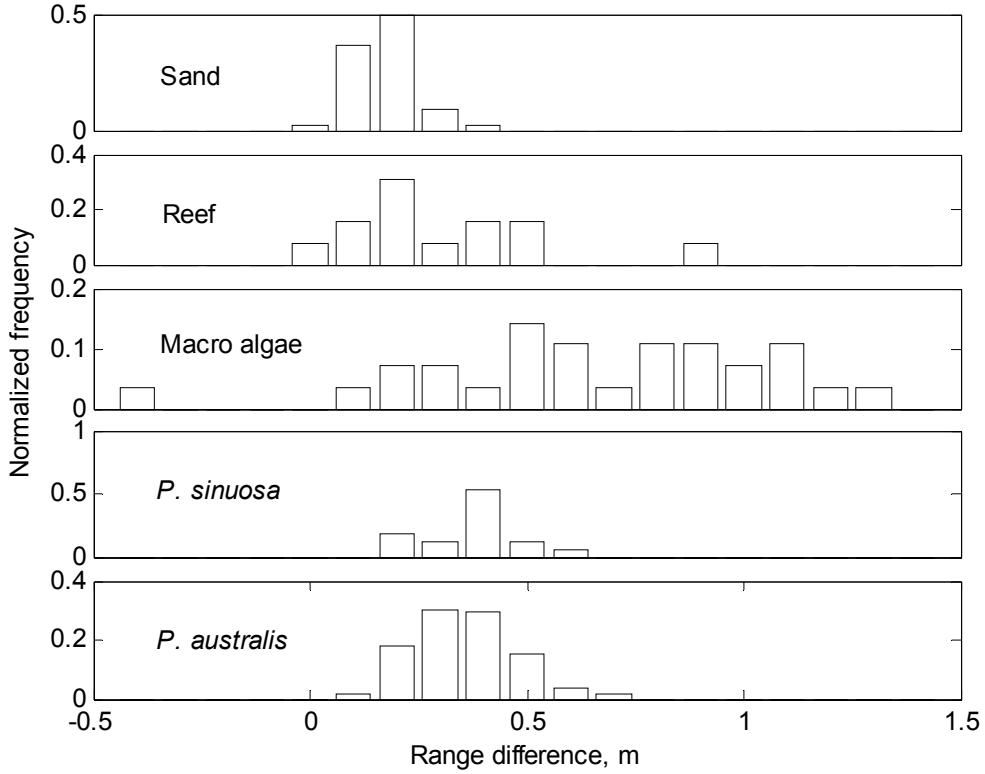

Figure 4-13 Histogram of the RD values for five pure classes where samples were collected from the first field trial.

Further investigation results for the relationship between RD and seagrass canopy height for samples collected from Owen Anchorage and Parmelia Bank at different seasons in 2005 are illustrated in section 4.3.4.

4.3 Owen Anchorage and Parmelia Bank 2005

4.3.1 Sea squirts

In the second field trial, a seafloor densely populated by sea squirts was observed among other habitats. It was not possible to distinguish the bottoms covered by sea squirts from the surrounding mudy seafloor by using the best parameter (EPW) as a sole parameter for classification purposes (see Figure 4-14 for the pure classes and Figure 4-15 for the non-pure classes). The seagrass class has generally higher EPW values different from other non-vegetation classes while the EPW values of the mud class are generally lower. The EPW distribution of the macro algae class overlaps the EPW variations of all other classes. The sea squirts class exhibits EPW values close to the mud class.

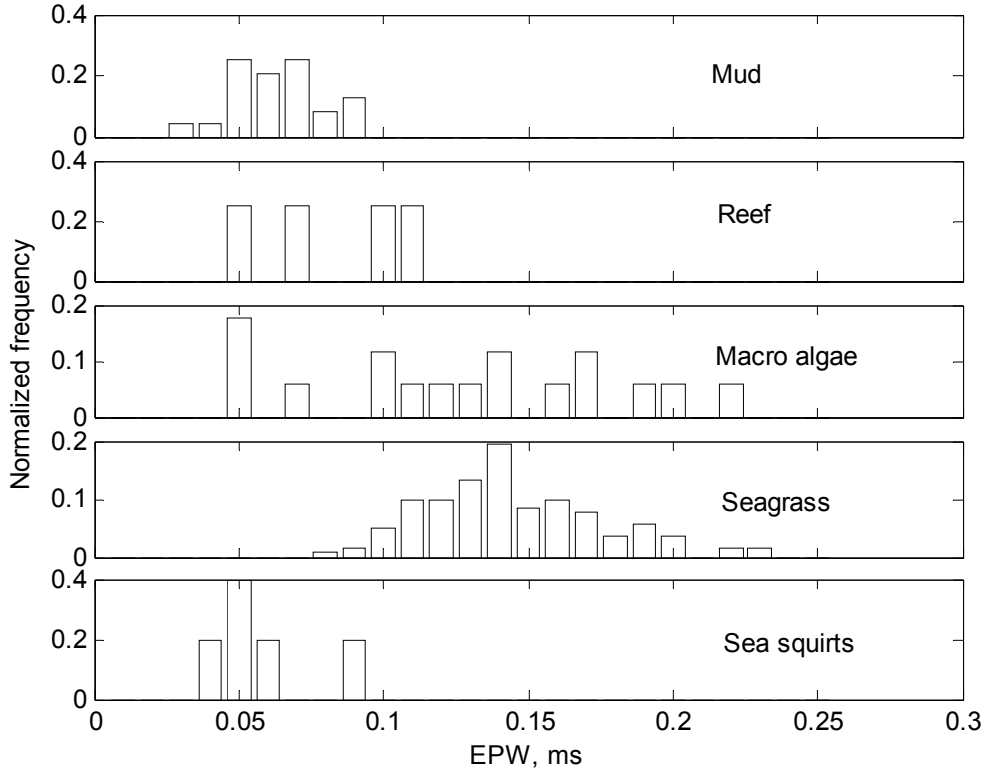

Figure 4-14 Histograms of the EPW of five pure habitat types where samples were collected from the second field trial (cf. Figure 4-7).

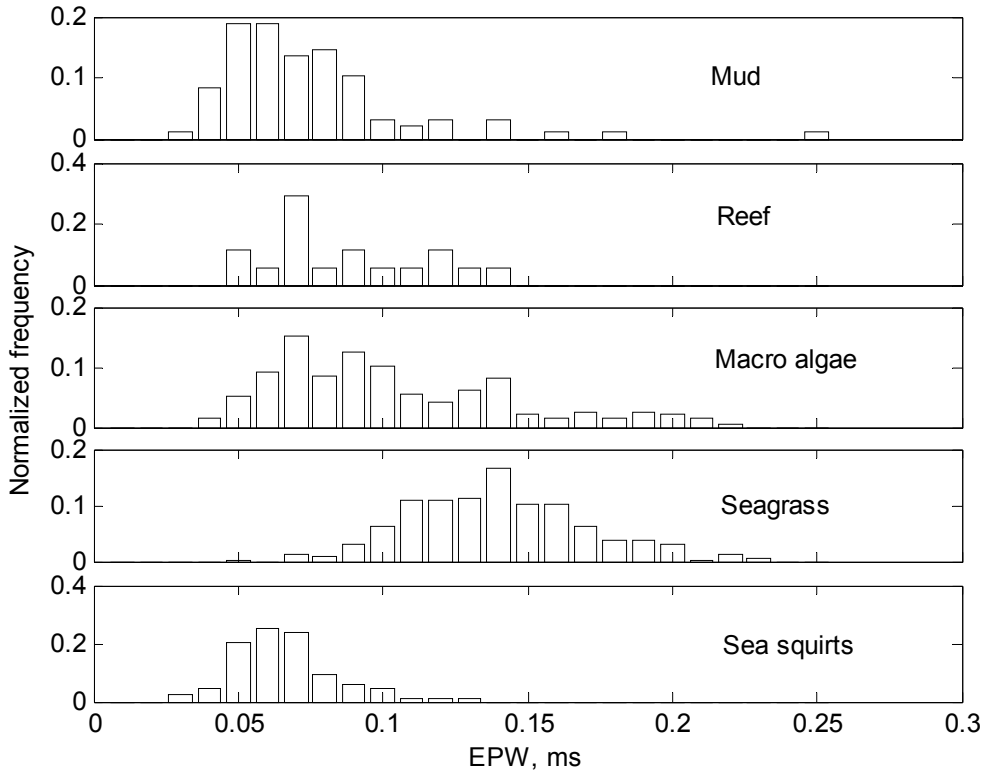

Figure 4-15 Histograms of the EPW of five non-pure habitat types where samples were collected from the second field trial (cf. Figure 4-8).

4.3.2 Classification performance for only sand and seagrass

In the final field trial, sand and the *Amphibolis griffithii* and *Posidonia* seagrass species are the predominant habitats observed in the surveyed area. The quality of the optical recordings did not allow the author to differentiate the *Posidonia* seagrasses into further finer species. The *Posidonia* seagrasses observed in the final field trial were different from those observed in the second field trial. They populated densely in a bigger patchy area but without the row pattern observed in the second field trial. *Amphibolis griffithii* was observed for the first time in this study. Its canopy height was only a few centimetres and the plants were sparsely distributed on the seabed. To understand the characterization ability of the best parameter (EPW) investigated in the previous sections for the echo samples collected in the final field trial, histograms of the EPW values of these two classes are shown in Figure 4-16.

Note: *Posidonia* and *Amphibolis* are combined as a single class due to *Amphibolis*'s too few sample numbers.

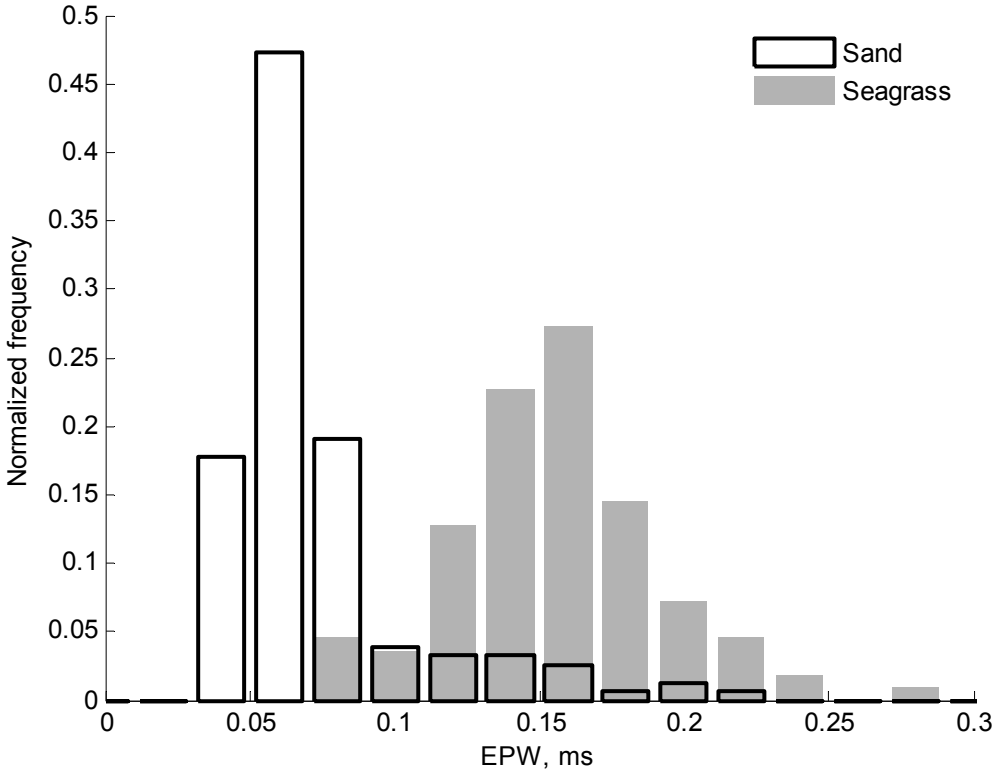

Figure 4-16 Histograms of EPW values of the two pure classes observed in the final field trial (cf. Figure 5-8).

It is seen from Figure 4-16 that the sand and the combined seagrass classes can be distinguished by selecting an EPW threshold below which the samples are classified as sand and as seagrass otherwise. A confusion matrix for all samples of the pure classes derived from an EPW boundary value of 0.12 ms is provided in Table 4-1. The confusion matrices for each particular site are given in Table 4-2, Table 4-3, and Table 4-4. The number in each bracket in the tables indicates the identification accuracy of the acoustic method with the EPW parameter for each class.

Table 4-1 Confusion matrix for all pure class samples collected from all sites of the final field trial based on the EPW boundary value of 0.12 ms (cf. Table 4-5, Table 4-6, Table 4-7, Table 4-8, Table 4-9, and Table 5-2). Note samples of the *Amphibolis griffithii* and *Posidonia* classes are combined as a single class.

Acoustics / Optics	Sand	*Amphibolis* + *Posidonia*
Sand (150)	134 (89%)	16
Amphibolis (3) + *Posidonia* (107)	12	98 (89%)

Table 4-2 Confusion matrix for pure class samples collected at site 1 and 2.

Acoustics / Optics	Sand	*Amphibolis* + *Posidonia*
Sand (0)	0 (100%)	0
Amphibolis (3) + *Posidonia* (74)	8	69 (90%)

Table 4-3 Confusion matrix for pure class samples collected at site 3.

Acoustics / Optics	Sand	*Amphibolis* + *Posidonia*
Sand (0)	0 (100%)	0
Amphibolis (0) + *Posidonia* (30)	3	27 (90%)

Table 4-4 Confusion matrix for pure class samples collected at site 4.

Acoustics / Optics	Sand	*Amphibolis* + *Posidonia*
Sand (150)	134 (89%)	16
Amphibolis (0) + *Posidonia* (3)	1	2 (67%)

Based on the above recognition criterion, the distribution conditions of the three pure classes identified by the optical (left) and acoustic (right) methods at each site are shown in Figure 4-17.

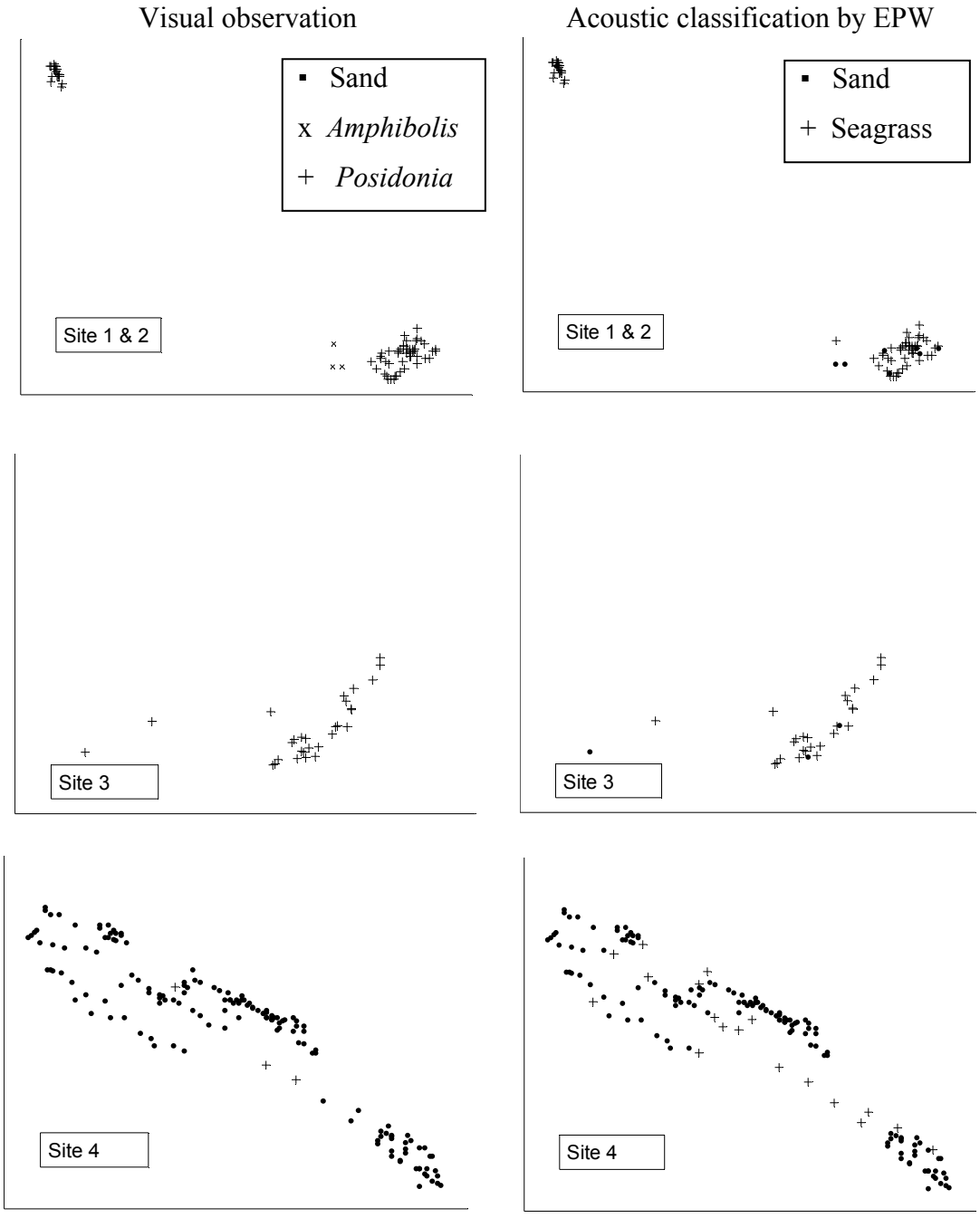

Figure 4-17 Distributions of the pure class samples derived from the classification results made by visual observation (left) and acoustic method with the EPW parameter (right) over sites of the final field trial. Note the coordinates are omitted here.

4.3.3 Dependence of characterization parameters on range

Investigation of the acoustic backscatter dependence on range was carried out by deploying sonar systems at a few discrete ranges in the final ESP field trial. Measurements of the acoustic backscatter of the sand and the seagrass classes were made at different fixed depths. Physical quantity investigated was the surface backscatter strength having been corrected for factors as shown in equation 3-4 (see section 3.5). In calculating the characterization parameters, a fixed sound speed of 1500 m/s was used all the time in this study. Variations of the parameter values against observation ranges are shown in Figure 4-18 and Figure 4-19 for the pure sand and pure seagrass samples respectively. Dashed lines indicate the standard deviations from the best linear fit shown by the solid lines.

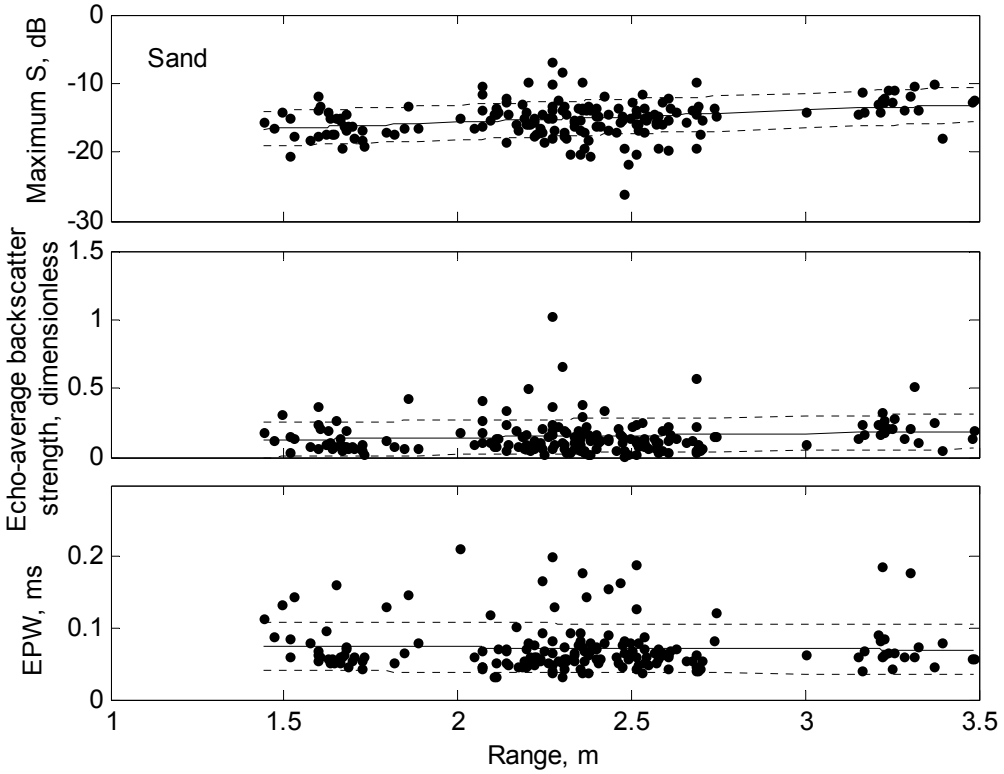

Figure 4-18 Measurements of the characterization parameters versus range to the bottom and their linear fits for pure sand samples collected from the final field trial.

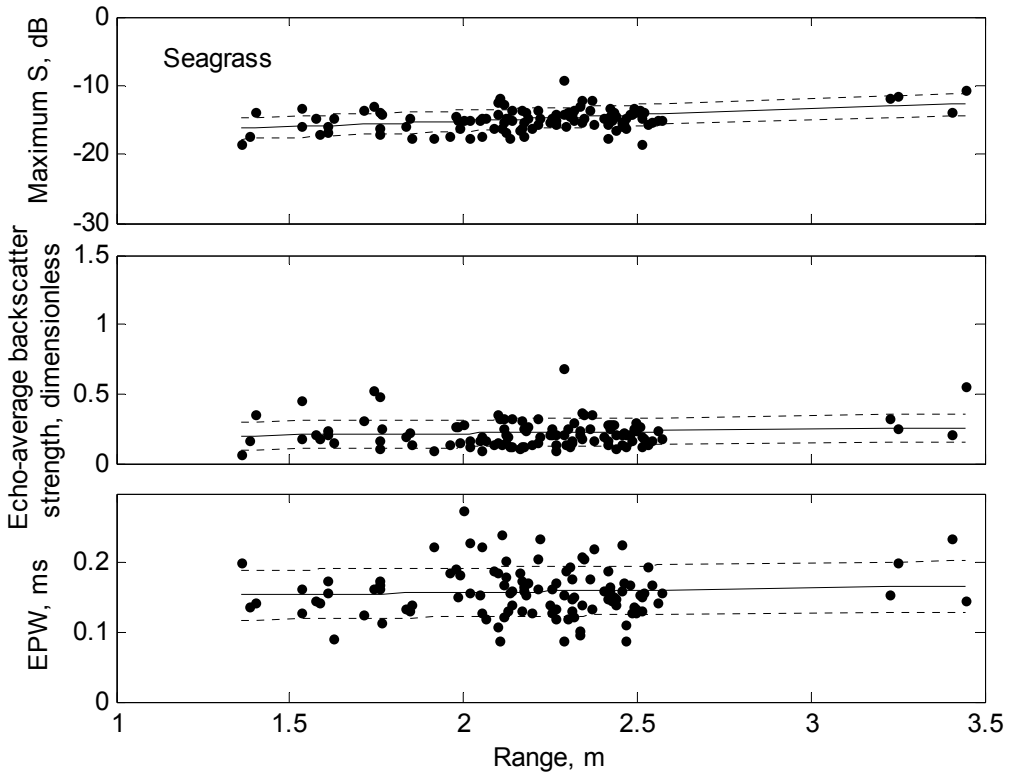

Figure 4-19 Measurements of the characterization parameters versus range to the bottom and their linear fits for pure seagrass samples collected from the final field trial.

Overall, the maximum *S* value shown in both figures appears to slightly increase with range, which is seen in a gentle slope of the linear fit. On the other hand, the echo-average backscatter strength and EPW do not exhibit any noticeable dependence on range for both sand and seagrass. This is an expected result because the seafloor backscatter strength, derived from the backscatter intensity corrected for the transmission loss and insonification area, should be in general range independent and depend mainly on the morphological and physical parameters of the bottom, rather than the geometry of measurement. However, since the observations are made within a very limited range interval (3.5 m) and only very few samples are available at the larger ranges (between 3 and 3.5 m), the range dependence prediction of these parameters at much larger ranges is uncertain.

4.3.4 Range difference (RD) and seagrass canopy height

Based on the above observations investigated in the previous sections, it is reasonable to assume that vegetation such as the *Posidonia* seagrasses would be moderately transparent for acoustic waves at frequencies as low as 38 kHz, but effectively reflective at hundreds of kHz. If such an assumption is appropriate, the seagrass canopy height can be practically determined by comparing the detected bottom ranges at two different frequencies. The criteria for determining the bottom range at the 38 and 200 kHz in different ways have been discussed in sections 4.2.2 and 4.2.3.

The dependence of the RD values measured at the two frequencies on the detected bottom range is shown in Figure 4-20. Dashed lines around each linear fit are the standard deviations above and below the linear approximation. For sand, the average RD is around 0.17 m. For seagrass, the average RD is about 0.43 m. The average seagrass canopy height estimated by subtracting sand's average RD value from seagrass average RD value is about 26 cm, which is smaller than the historical records varying from 35 to 45 cm but is in reasonable agreement with the measurements of the canopy height between 20 and 40 cm observed by the optical system in the ESP project (see sections 2.2.2.1 and 3.3.1.3).

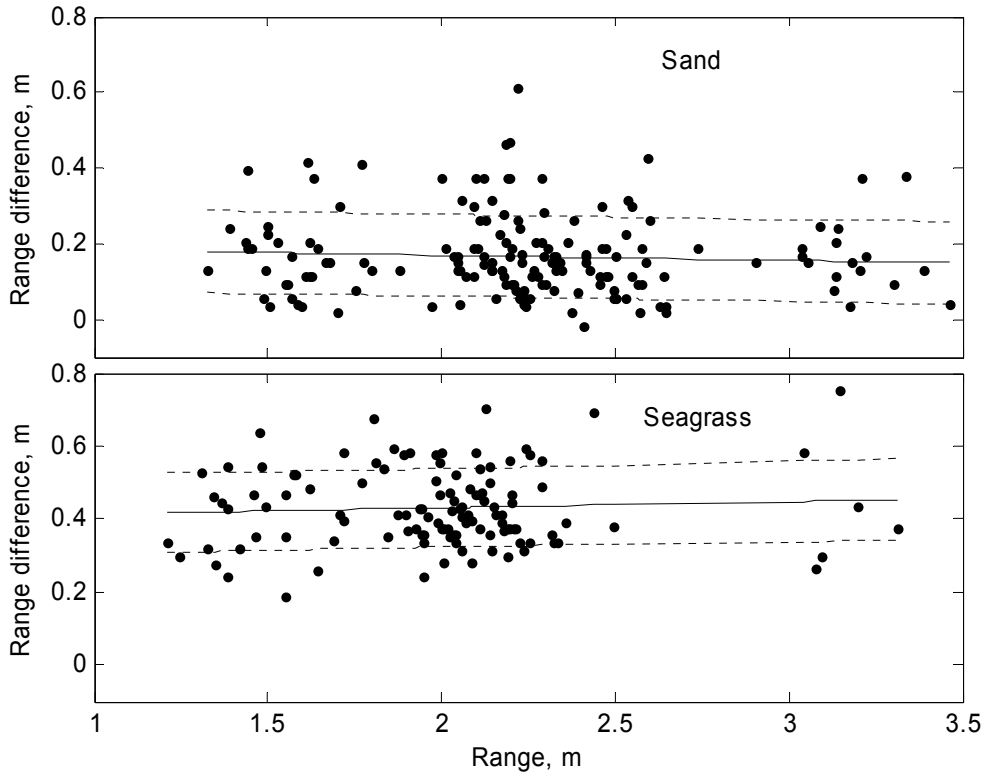

Figure 4-20 RD vs. bottom range and the linear fits for pure sand and seagrass samples collected from the final field trial.

A map of the sand and seagrass samples discriminated according to the EPW parameter over an area at site 4 of the final ESP field trial is given in Figure 4-21. The corrected RD values (after removing the average sand RD value of 0.17 m) are indicated by colours. The frequency distribution of the corrected RD values (seagrass canopy height) for the samples at each site that were classified using the EPW parameter as seagrass, is shown in Figure 4-22.

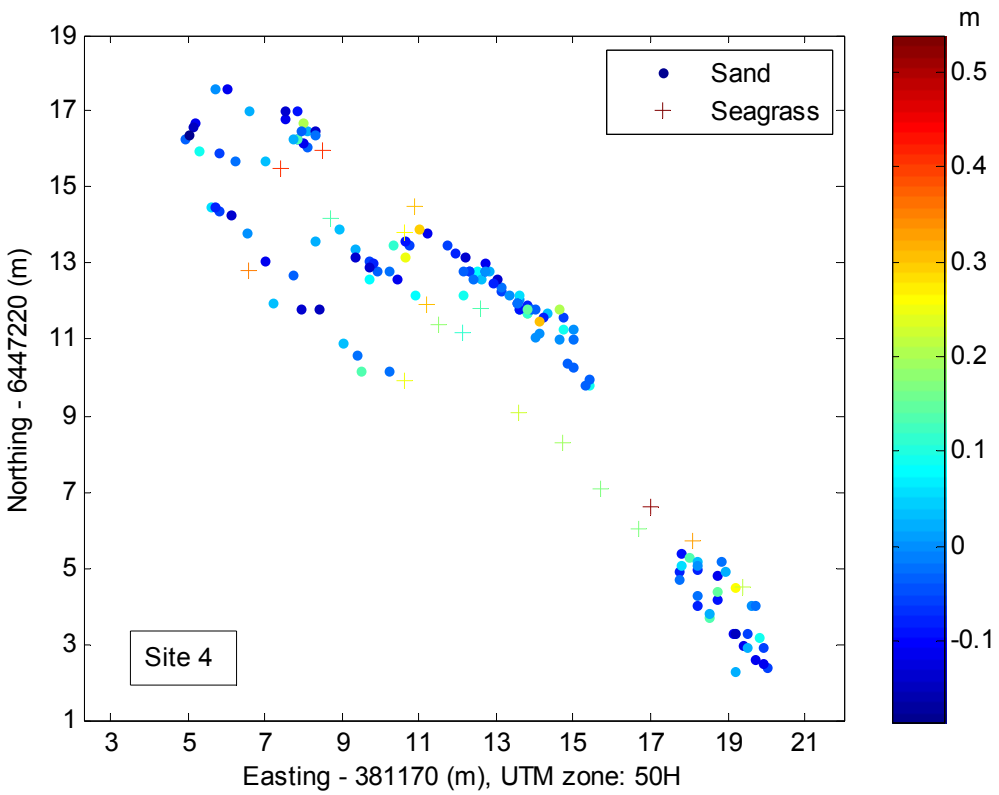

Figure 4-21 Distributions of the sand and seagrass samples classified by EPW with the corrected RD values shown in colour designated for seagrass canopy height at site 4 of the final ESP field trial (cf. Figure 4-30, Figure 4-34, Figure 4-38, Figure 4-46, and Figure 5-10).

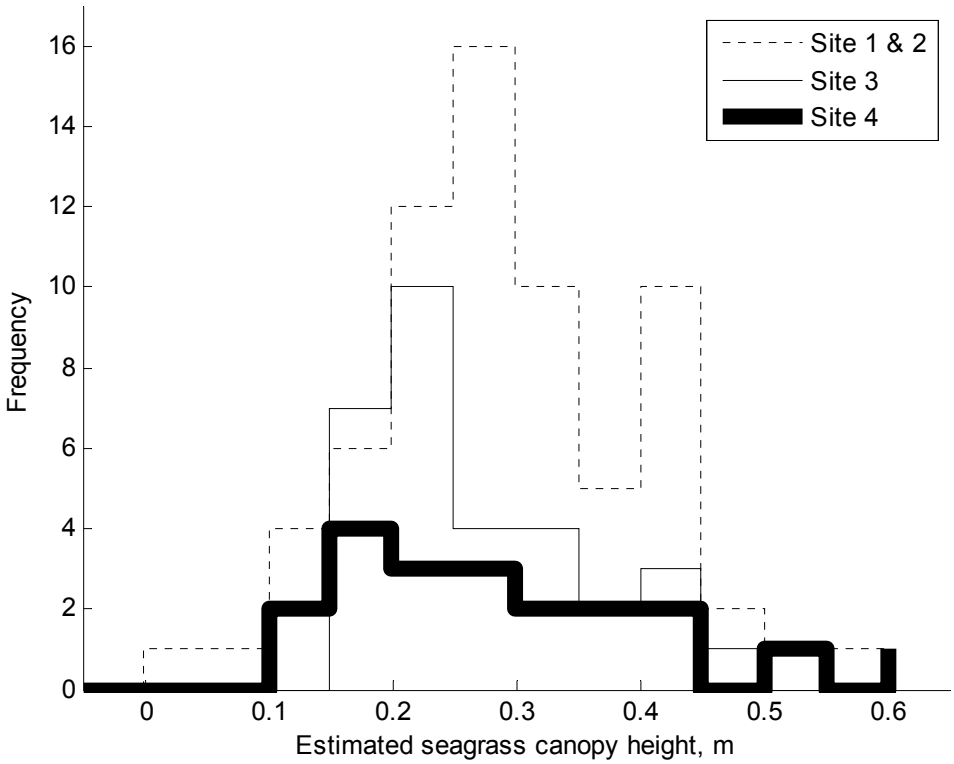

Figure 4-22 Histograms of the estimated seagrass canopy height obtained after removing the average sand RD value of 0.17 m from the RD measured for seagrass at each site of the final ESP field trial.

There is a small amount of outliers of the sand samples which can be observed with large RD values from either Figure 4-20 or Figure 4-21. In rare cases, the 38 kHz waveform of sand samples had several peaks in the first bottom return, such as the one shown in Figure 4-23, where the second peak of the first bottom return has a higher amplitude response than the first one causing an uncommonly large RD value when comparing to the normal RD values. The reason causing such response is uncertain yet.

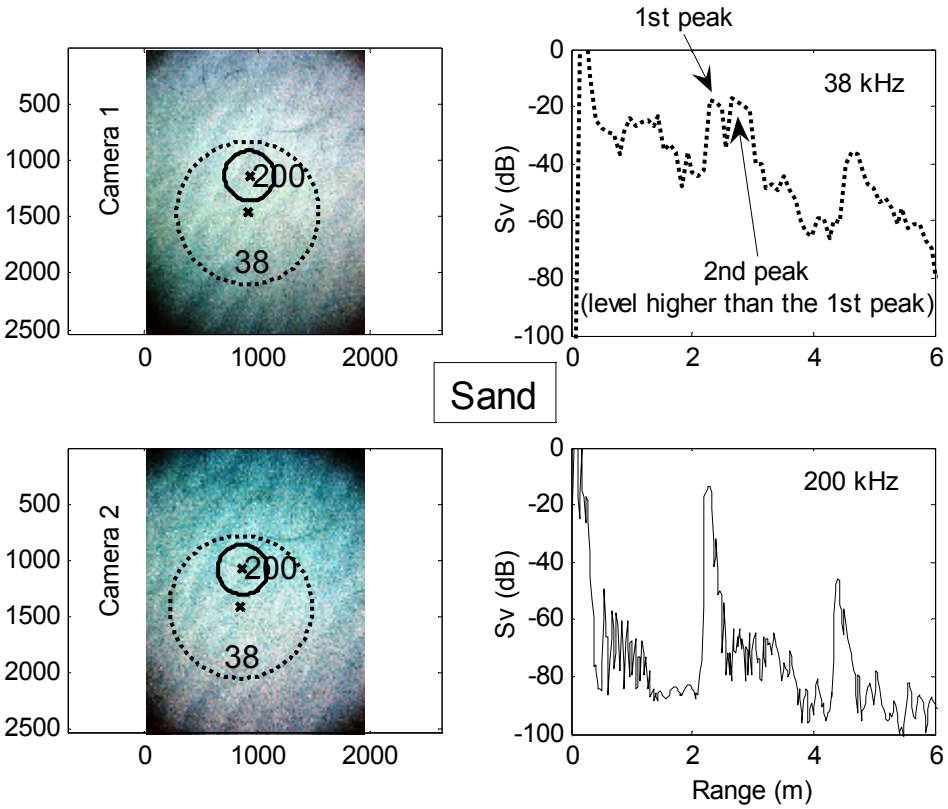

Figure 4-23 An instance of the second peak in the 38-kHz first bottom return from sand which has a higher amplitude than the first one causing an uncommonly large RD value when comparing to the normal RD values.

4.3.5 Differences between dense and sparse dispositions

One of the results obtained by Shenderov through numerical modelling is that the acoustic backscatter level from densely populated algae should be at least two times higher than that from sparse algae (Shenderov 1998). Although seagrass is biologically different from algae, seagrass and algae might be similar in acoustic properties. To examine if there is any similar backscatter tendency on the seagrass, the author investigated the variation of the acoustic backscatter from densely and sparsely disposed *P. sinuosa* seagrasses.

The characteristics compared for the dense and sparse seagrasses were the echo-average backscatter strength and EPW parameters (see sections 4.2.1.2 and 4.2.1.3). The histograms of the two seagrass density conditions for the EPW and

echo-average backscatter strength are shown in Figure 4-24 and Figure 4-25 respectively.

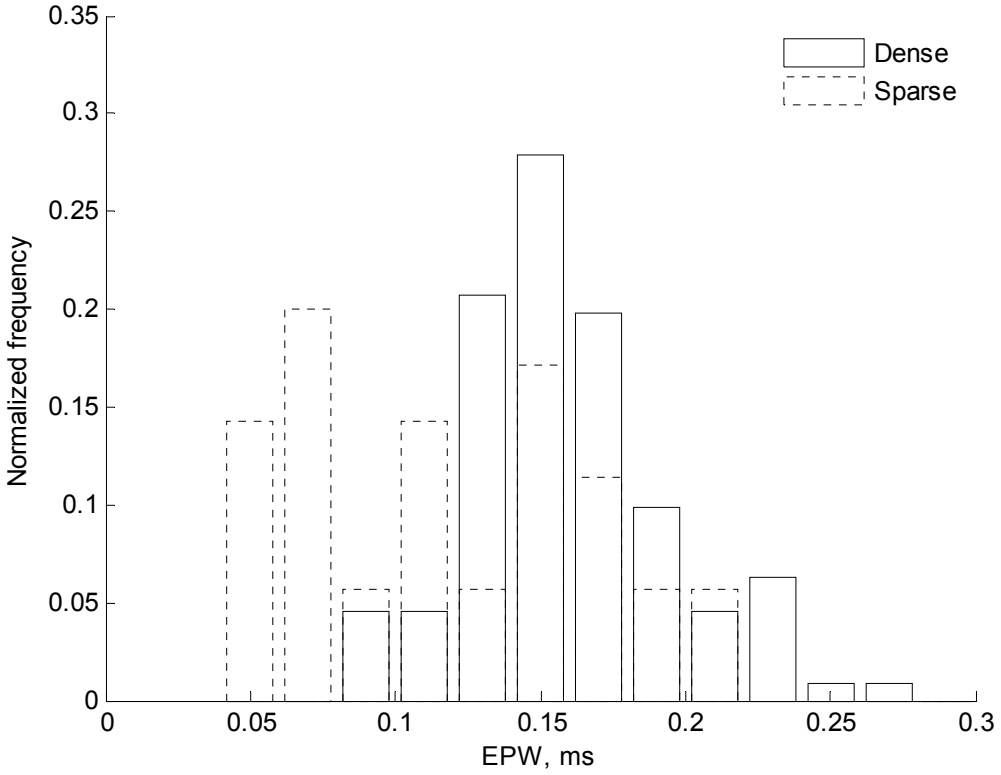

Figure 4-24 Histograms of EPW for the densely and sparsely populated *P. sinuosa* seagrass observed in the final field trial.

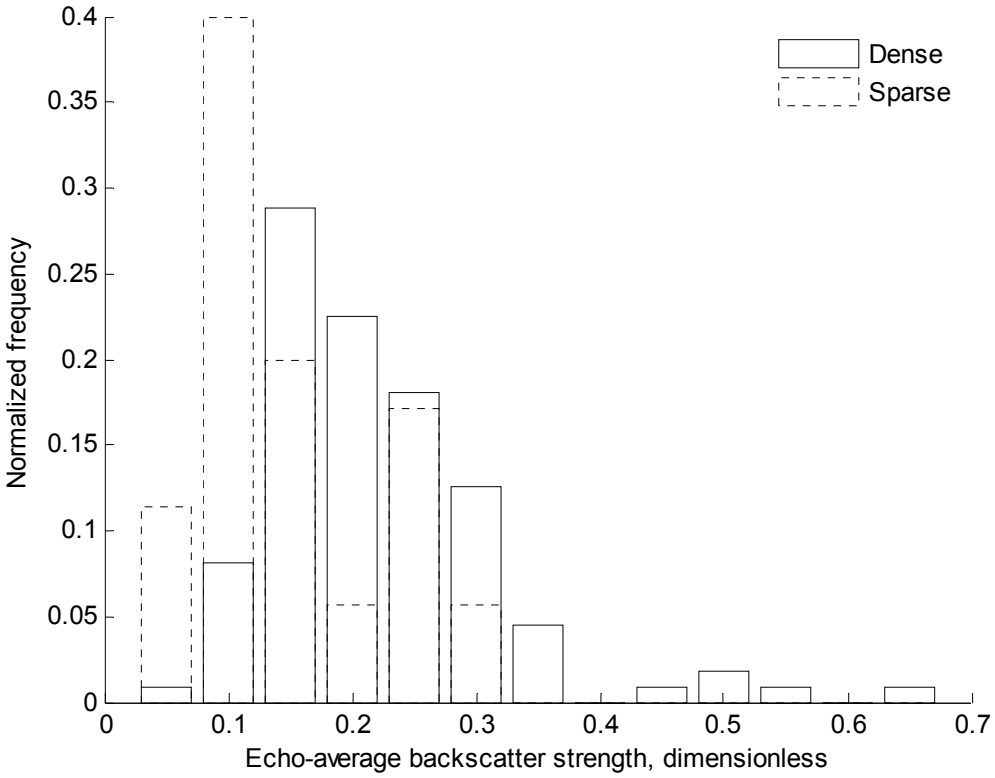

Figure 4-25 Histograms of echo-average backscatter strength for the densely and sparsely populated *P. sinuosa* seagrass samples collected from the final field trial (cf. Figure 4-5).

Because of the large overlap between the histograms shown in Figure 4-24 and Figure 4-25, both EPW and echo-average backscatter strength were unable to completely discriminate the difference between the two seagrass density conditions. Yet, there is some difference between the maximum frequency values of the echo-average backscatter strength for the two seagrass conditions. The echo-average backscatter strength value at the maximum frequency for the dense seagrass is about 0.15 while that for the sparse seagrass is roughly 0.1 in Figure 4-25, and the peak EPW value of the dense seagrass is about two times as large as the sparse one in Figure 4-24 – a tendency observed from the above two figures approaches the model predicted by Shenderov (see section 2.1.3.2 for the discussion of the algae models made by Shenderov). However, considering the variations and overlapping conditions of the above two parameters for the two seagrass density conditions and the fact that the actual number of sparse seagrass samples (35) is far less than that of the dense seagrass (111), a thorough investigation of a larger data set than that used

here would be required in order to make a definite conclusion for whether or not the seagrass cover conditions are distinguishable by the acoustic parameters used here.

4.4 Multivariate approach

Below are the results of multivariate statistical analysis of acoustic signals collected from some distinctive pure habitat types observed in the final ESP field trial. Each first bottom return, which will hereinafter be referred to as an acoustic bottom sample, was processed to obtain a set of statistical values that was used to represent the main features of each sample.

4.4.1 Correlations among statistics

Later in section 4.4.2 and Chapter 5, the same statistics investigated in this section will be used again for comparison purposes. Analysis will be first made for the performance with five statistics only (maximum, mean, standard deviation, skewness, and kurtosis). Later in section 4.4.2.1.2 the EPW parameter will be included in order to understand whether the addition of this parameter improves the classification performance or not.

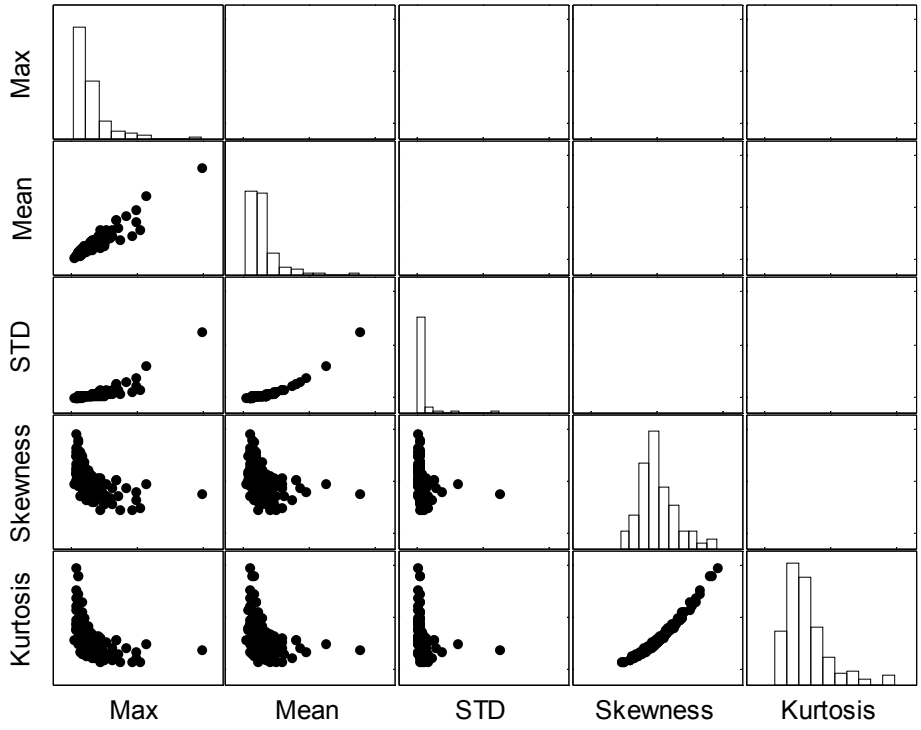

Figure 4-26 Matrix plot of pairs of five statistics derived from the backscatter envelope of the first bottom return from sand class samples collected from the final field trial and their respective distribution histograms on the main diagonal where scales and units are omitted.

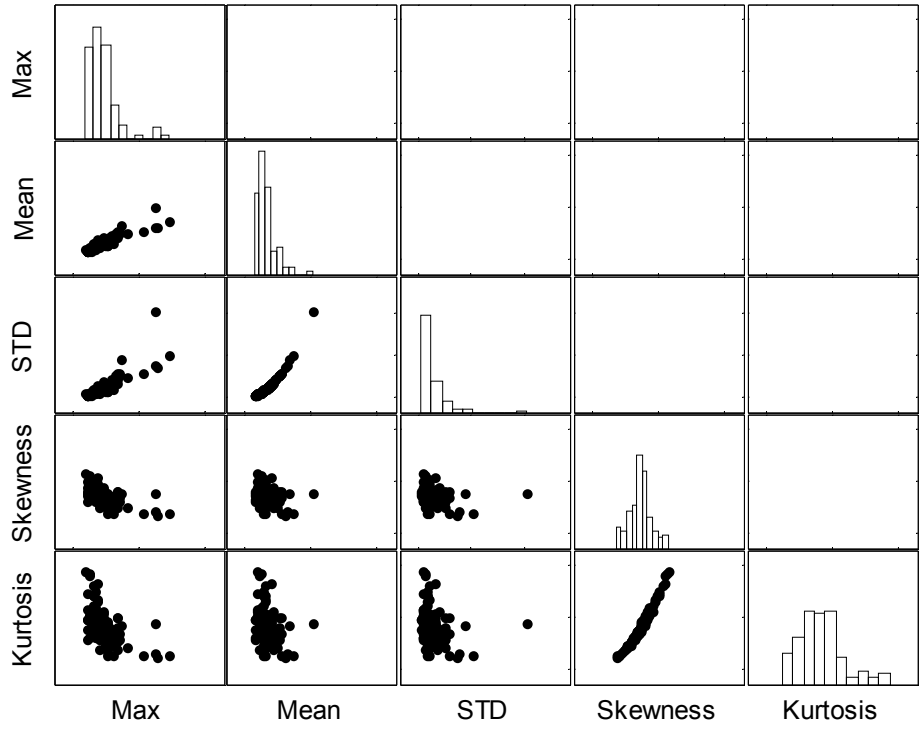

Figure 4-27 Matrix plot of pairs of five statistics derived from the backscatter envelope of the first bottom return from *Posidonia* seagrass class samples collected from the final field trial and their respective distribution histograms on the main diagonal where scales and units are omitted.

To see the general linear relationship between each pair of the five statistics obtained from the data here, we can plot their correlations pair-wisely in a 2-dimensional space to know roughly whether or not any statistical variable has any linear dependence tendency on the other. From matrix plots Figure 4-26 and Figure 4-27 for sand and *Posidonia* seagrass classes respectively, it is obvious that some statistical variables are well correlated to others. For example, pairs like Mean and STD, and Skewness and Kurtosis have comparably stronger linear relationships in strength and direction than others. On the main diagonal of these figures, one can have a rough picture of the distribution conditions of the numbers of samples on the statistical variable values.

To get a rough idea of the characterization abilities of these five statistic variables for the sand and *Posidonia* seagrass classes, histograms of these five statistics derived from the linear scale value of the echo-average backscatter strength are given in Figure 4-28. From the figure, it is seen that some statistics, such as

skewness and kurtosis, demonstrate a better performance with respect to distinguishing the two classes than the other ones. However, since skewness and kurtosis are almost linearly proportional to each other for both sand and seagrass, fewer statistical variables should suffice to provide similar performance for the characterization of the classes involved here. For this reason, Principal Components Analysis (PCA) commonly used in multivariate statistical analysis will be applied to the same data in the next section for extractions of best characterization parameters.

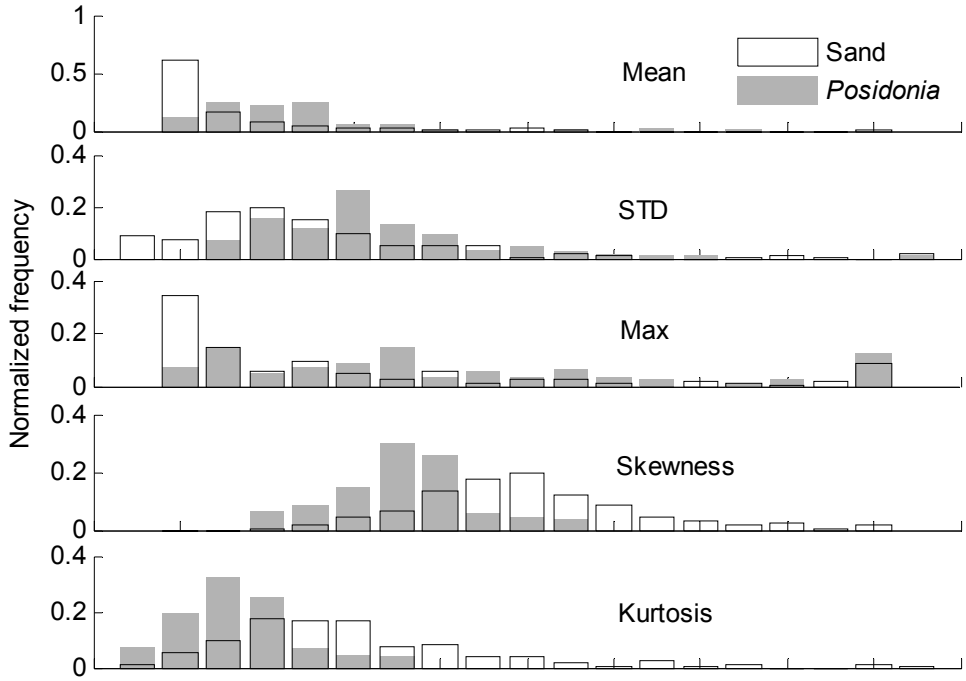

Figure 4-28 Histograms of five statistics derived from the first bottom echoes for sand and *Posidonia* classes obtained from the final field trial where units are omitted here.

To understand the classification abilities of these five statistics, the author picked the skewness variable as an example for this purpose. Obviously the performance of the skewness variable is not better than that of the EPW parameter in classification although skewness is the best parameter among the above statistic variables which can best discriminate the class samples when comparing Figure 4-29 below and Figure 4-16. To quantitatively understand its classification abilities, the author made some investigations and provided the results as shown in Table 4-5 and Figure 4-30.

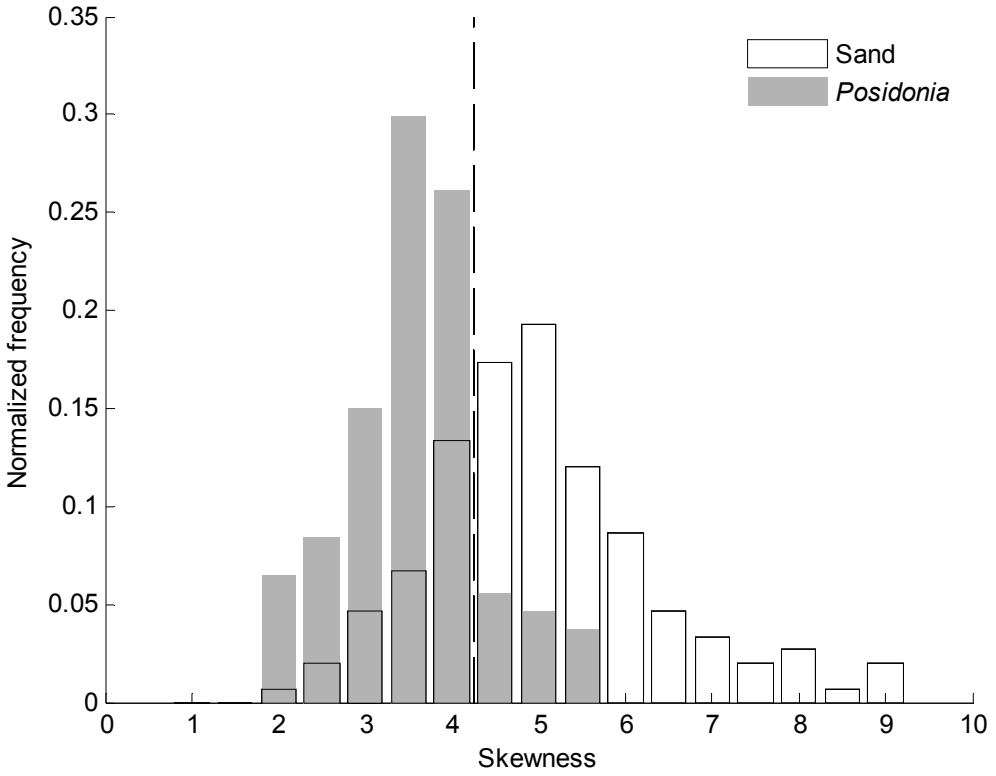

Figure 4-29 Histograms of skewness values of the two pure classes observed in the final field trial with a boundary value of 4.25 used to discriminate the two class samples.

From Figure 4-28 and Table 4-5, it is expected that the other individual statistics might not provide any better abilities than the skewness to discriminate the two class samples involved in this study. To understand the effect after applying the PCA method over the individual statistics in classification performance, the author made some investigations on this problem and provided the results in section 4.4.2.

Table 4-5 Confusion matrix for all pure class samples collected from all sites of the final field trial based on the skewness boundary value of 4.25 (cf. Table 4-1, Table 4-6, Table 4-7, Table 4-8, Table 4-9, and Table 5-2).

Acoustics / Optics	Sand	*Posidonia*
Sand (150)	109 (73%)	41
Posidonia (107)	15	92 (86%)

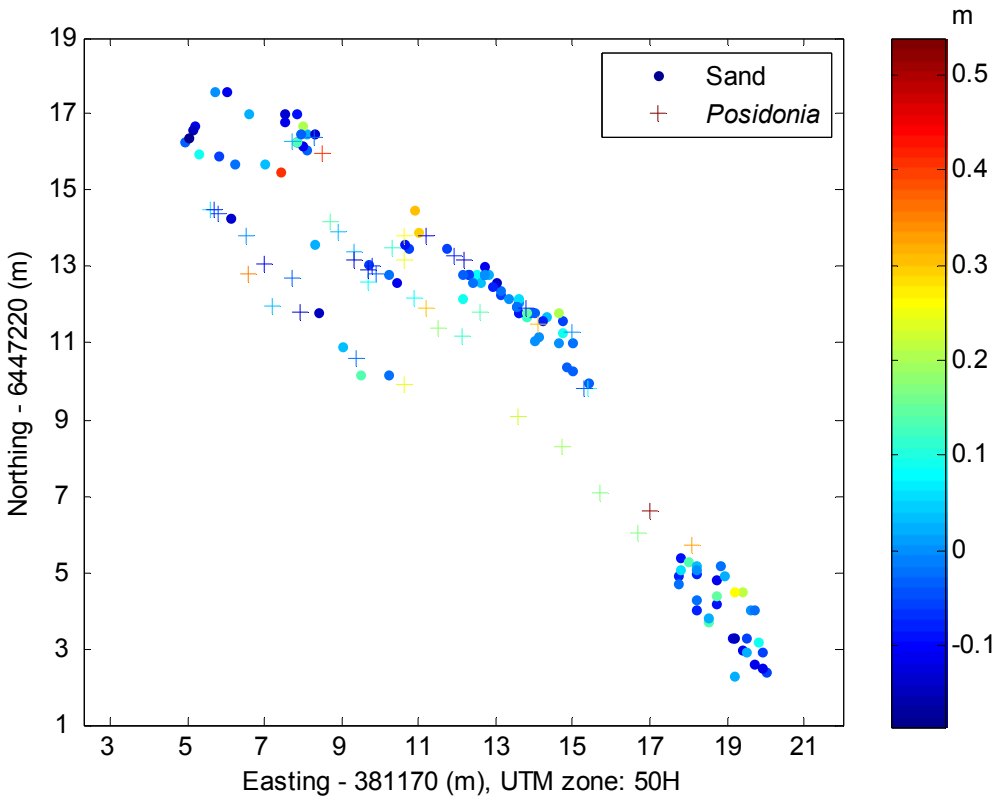

Figure 4-30 Distribution of the sand and *Posidonia* seagrass samples identified by the skewness variable with the corrected RD values shown in colour designated for seagrass canopy height at site 4 of the final ESP field trial (cf. Figure 4-21, Figure 4-34, Figure 4-38, Figure 4-46, and Figure 5-10).

4.4.2 Principal components analysis

Principal Components Analysis is probably one of the most well-known techniques used for reducing the number of parameters needed for modelling variations in natural processes. It is a common multivariate method widely adopted for classification purposes in many scientific areas. The major advantage of PCA is its ability to find the best linear combinations of parameters to use as new orthogonal parameters for the description of data variation. In this case study, the statistical parameters used for characterization, including the EPW, are normalized first with respect to their means and then variations around the mean values are calculated. After this normalization process, the algorithm finds the eigenvectors and

eigenvalues of the covariance matrix from the normalized parameters. Eigenvalues of the covariance matrix represent the contributions of the eigenvectors to the global variations in the new variable space. That is, a higher variance signifies the importance of the eigenvector, which is indicated by a higher eigenvalue. Based on a selection criterion, the eigenvectors with the most significant eigenvalues are selected as the major parameters in place of the original variables for the description of original data variations in the eigenvector space. The major component accounts for the most variability in the data and the succeeding components of smaller eigenvalues account for the remaining variability in descending order.

To examine the abilities of the PCA technique in characterizing the acoustic backscatter from seafloor vegetation, investigations of classification performance in the following subsections were made respectively for when the input parameters were selected from the five statistics only (see section 4.4.2.1.1) and when the EPW parameter was included (see section 4.4.2.1.2).

4.4.2.1 Kaiser's rule

In PCA, it is important to determine the number of principal components (PCs) that contribute most to the variation. Kaiser provided a criterion, called Kaiser's eigenvalue-greater-than-one rule, which defined a threshold of unity for the eigenvalues derived from the variations of normalized parameters (Kaiser 1960). The eigenfunctions with the corresponding eigenvalues exceeding the defined threshold are selected as PCs, while the other eigenfunctions are considered to have negligible effects. The criterion proposed by Kaiser is adopted in this study and used for the following tests.

After the selection of PCs based on Kaiser's rule, a K-means clustering method will be used to partition the samples on the selected PCs space into two clusters representing the sand and *Posidonia* seagrass classes. There are many partitioning options in the K-means method. The basic approach implemented in the K-means is to minimize the sum of distances from each multivariate sample to the clusters' centroid for all clusters. In this case study, it is found that the best partitioning result is obtained by minimizing the so-called "correlation distance", $d(x, y)=1 - corr(x, y)$, where $d(x, y)$ represents the distance between data points x and y

and *corr(x, y)* is the correlation value of *x* and *y* after normalizing data points to zero mean and unit standard deviation within each cluster (Seber 2004).

4.4.2.1.1 Input parameters: Statistics

The variances of the five PCs after normalizing the five statistics as discussed in section 4.4.1 are shown in Figure 4-31. The selection of the first two PCs that have eigenvalues greater than unity based on Kaiser's rule is well demonstrated in this figure.

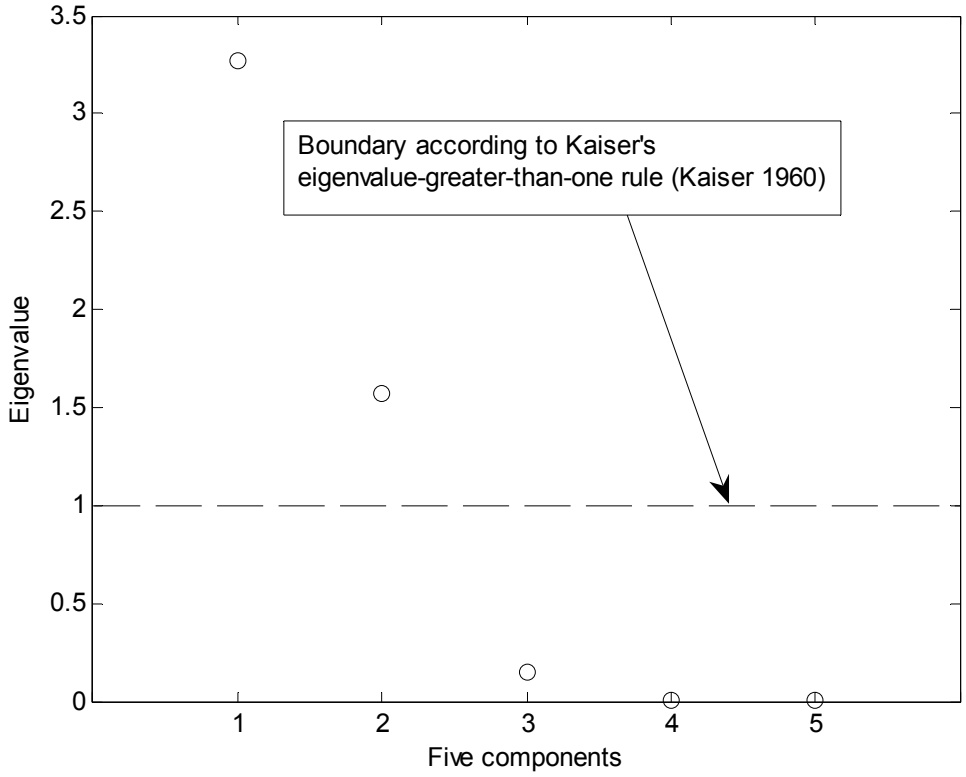

Figure 4-31 Eigenvalues obtained from the five normalized statistics as used in section 4.4. The threshold value for the selection of PCs is based on Kaiser's rule (Kaiser 1960).

Based on Kaiser's rule, a scatter plot of the sand and *Posidonia* seagrass class samples represented by their coefficients in the two PCs space is shown in the upper panel of Figure 4-32. Using K-means, the partitioning result with the two assigned clusters and their respective centroids is shown in the lower panel of Figure 4-32.

Cluster 1 is mainly sand samples and therefore is assigned to sand class while cluster 2 is *Posidonia* seagrass.

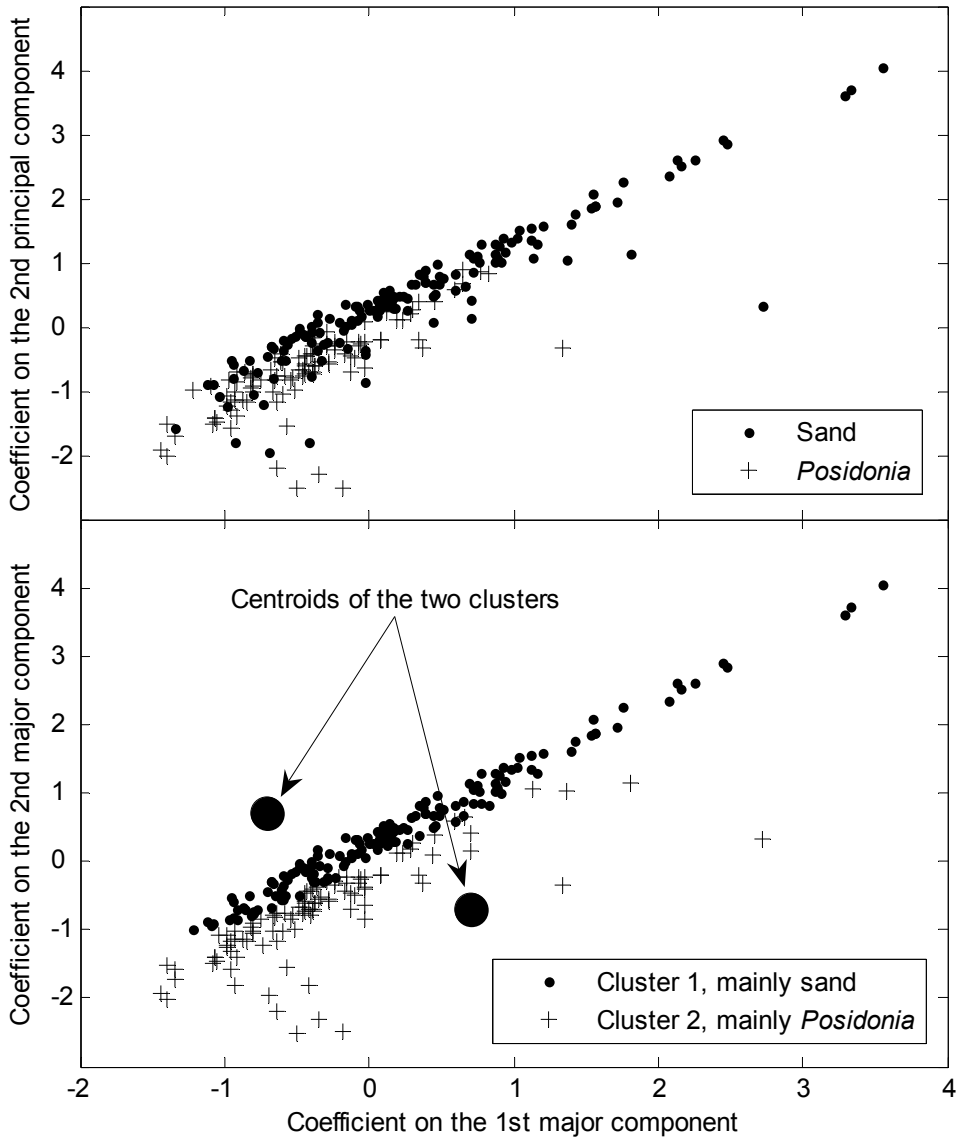

Figure 4-32 Scatter plot of the sand and *Posidonia* class samples on the top-two-PCs space (upper panel) and the partitioning result for two clusters with their respective centroids using K-means (lower panel).

Figure 4-33 shows the misclassification events marked with circles and squares in the selected PCs space determined by the above mentioned method. The confusion matrix in Table 4-6 demonstrates the identification ability of the classification method based on PCA and K-means for partitioning, as discussed above.

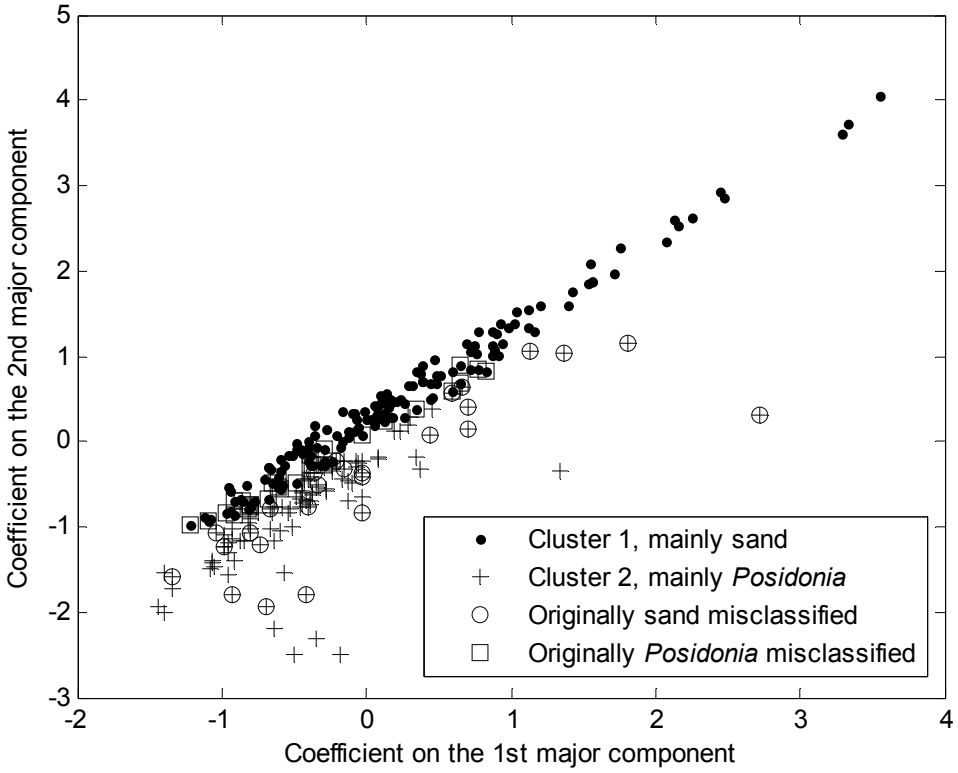

Figure 4-33 Scatter plot of two-cluster data on the top-two-PCs space with the misclassified samples marked by circles and squares.

Table 4-6 Confusion matrix of all the pure sand and *Posidonia* class samples with their statistics as the input parameters for the PCA and partitioned by K-means as discussed in the text for the data collected from the final ESP field trial (cf. Table 4-1, Table 4-5, Table 4-7, Table 4-8, Table 4-9, and Table 5-2).

K-means / Optics	Sand	Posidonia
Sand (150)	124 (83%)	26
Posidonia (107)	30	77 (72%)

As seen from comparing Table 4-6 with Table 4-1 in section 4.3.2, the partitioning result by K-means for the pure sand and *Posidonia* seagrass samples on the selected top-two-PCs space does not have a better performance than that determined by the EPW parameter.

With the same RD value as a measure for the seagrass canopy height as discussed in section 4.3.4, a map of the two-cluster samples identified by the PCA and K-means method at site 4 of the final field trial is provided in Figure 4-34.

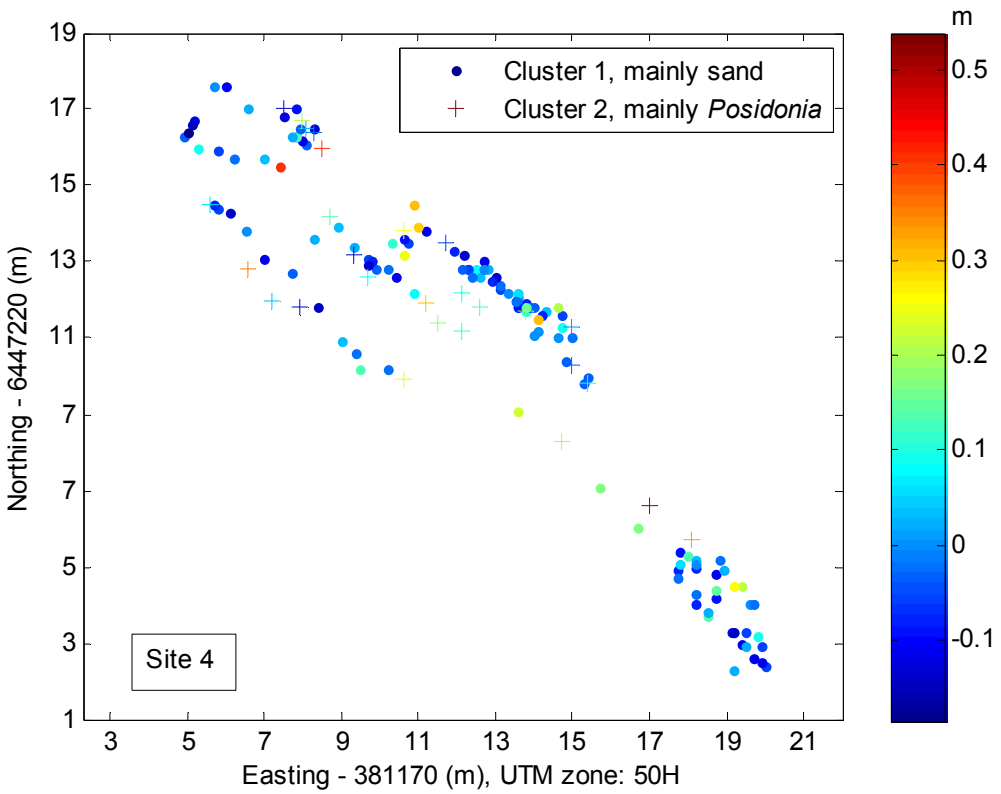

Figure 4-34 Distribution of the sand and seagrass samples identified by the PCA and K-means method with the corrected RD values shown in colour designated for seagrass canopy height at site 4 of the final ESP field trial (cf. Figure 4-21, Figure 4-30, Figure 4-38, Figure 4-46, and Figure 5-10).

The identification capability by the PCs for seagrass is 72% in Table 4-6, which is worse than that (89%) in Table 4-1 identified by the EPW. The poor performance by the PCs used here can be also observed from the inconsistency of the colour-coded representation originally intended for the seagrass canopy height and the poor identification ability given in Figure 4-34.

4.4.2.1.2 Input parameters: Statistics and EPW

Because EPW was found to be the most effective parameter with respect to discrimination of the backscatter features of the sand and seagrass samples in a 1-D space, the EPW was included as one of the input features in the PCA analysis in order to examine possible improvements in classification performance. The eigenvalues of the normalized variations derived from the new set of six parameters after the inclusion of EPW are shown in Figure 4-35. It is obvious by comparing Figure 4-35 against Figure 4-31 that the third component here is more prominent than that calculated for the set of five statistical parameters, although the third component is still below Kaiser's threshold.

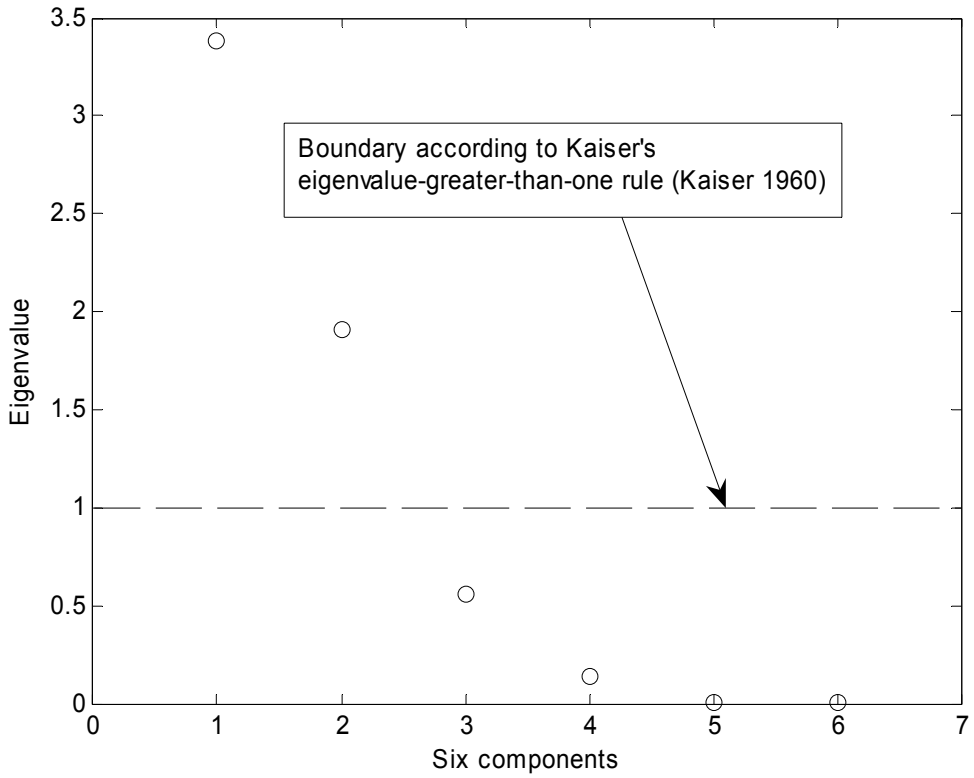

Figure 4-35 Same as Figure 4-31, but with the inclusion of the EPW parameter.

Based on Kaiser's rule, two PCs determined from Figure 4-35 were selected. A scatter plot for the sand and *Posidonia* class samples with their coefficients on the selected PCs space is provided on the upper panel of Figure 4-36. A partitioning result using K-means with two assigned clusters and their respective centroids is shown in the lower panel of Figure 4-36. Cluster 1 is mainly sand samples and

therefore is assigned for sand while cluster 2 is *Posidonia* seagrass. It seems that the two clusters are better separated in the 2-D space than that shown in Figure 4-32.

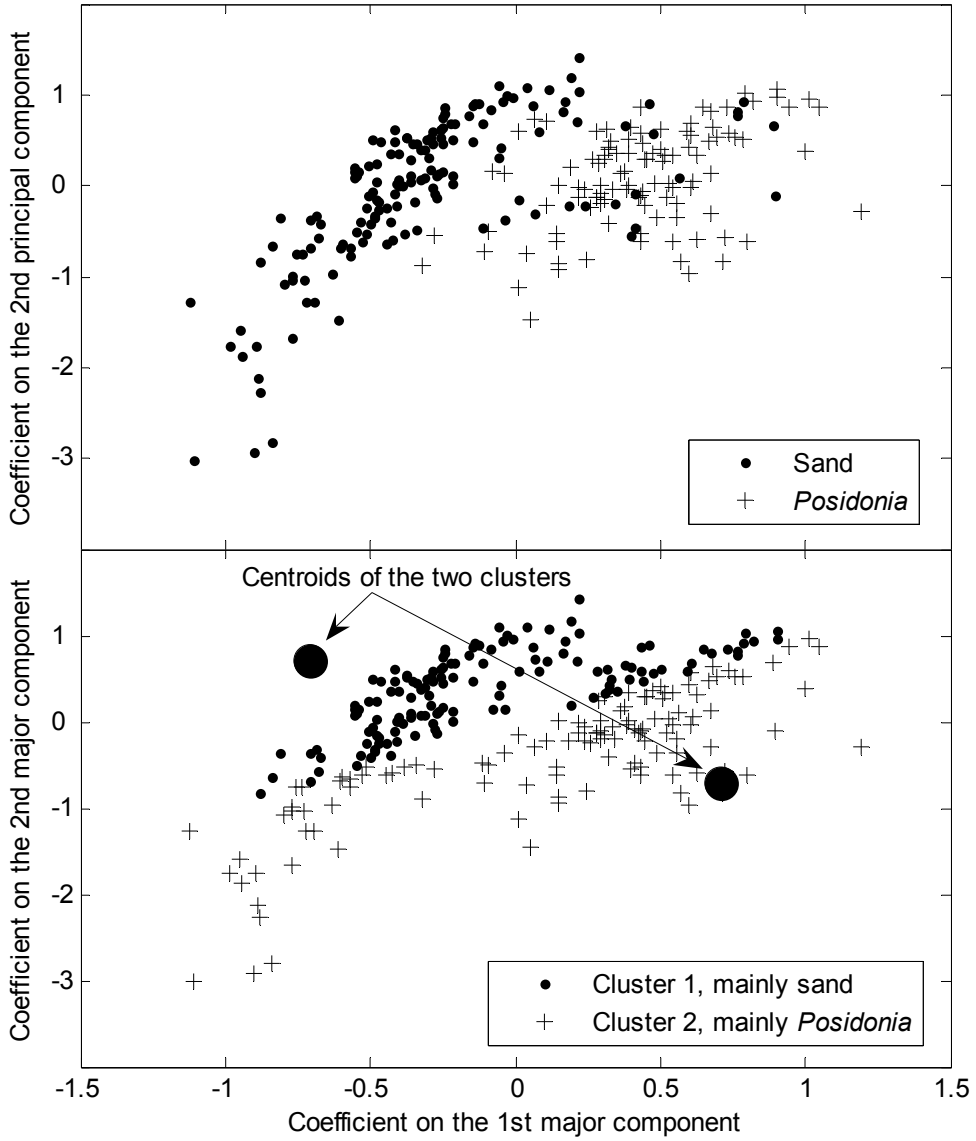

Figure 4-36 Scatter plot of the sand and *Posidonia* class samples on the top-two-PCs space (upper panel) and the partitioning result of two clusters with their respective centroids using K-means (lower panel) resulted from the inclusion of the EPW.

After the inclusion of the EPW, the misclassification events on the top-two-PCs space are shown in Figure 4-37 and the confusion matrix is shown in Table 4-7.

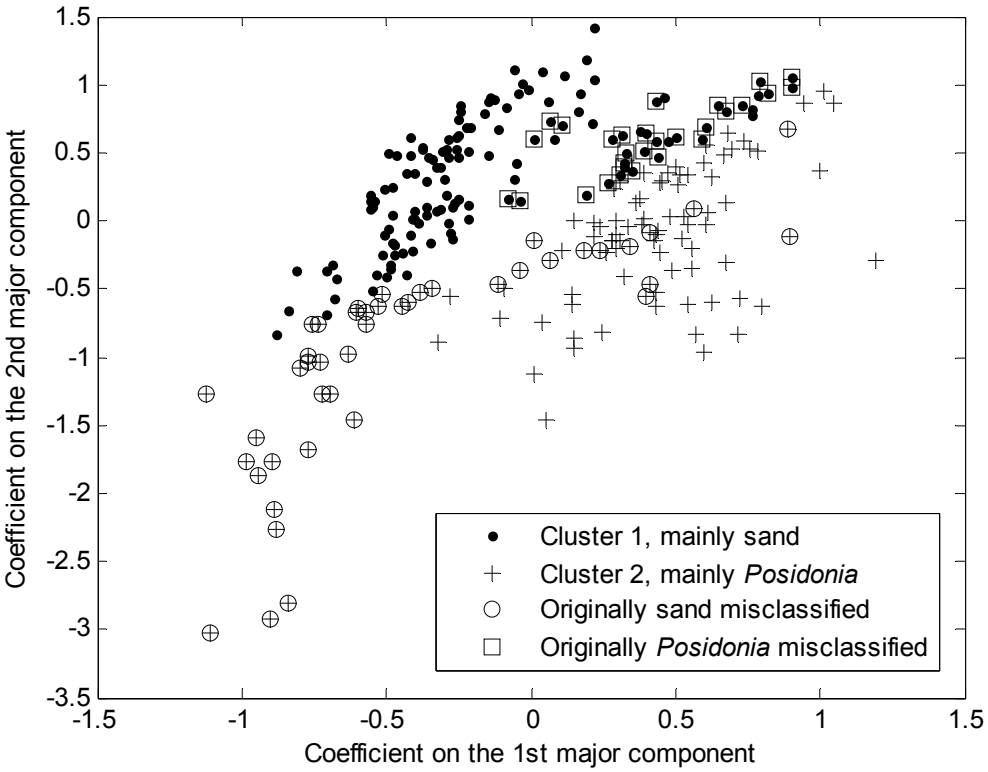

Figure 4-37 Scatter plot of two-cluster data on the top-two-PCs space with the misclassified data points marked by circles and squares after including the EPW.

Table 4-7 Confusion matrix of all the pure sand and *Posidonia* class samples determined by K-means after including the EPW for the data collected from the final ESP field trial (cf. Table 4-1, Table 4-5, Table 4-6, Table 4-8, Table 4-9 and Table 5-2).

K-means / Optics	Sand	Posidonia
Sand (150)	106 (71%)	44
Posidonia (107)	29	78 (73%)

After the inclusion of the EPW, the distribution condition of the two-cluster samples determined by the above mentioned method is shown in Figure 4-38. By comparing the identification accuracy for sand in Table 4-6 (83%) and Table 4-7 (71%), the identification performance for sand after the inclusion of the EPW is surprisingly worse than that without the inclusion of the EPW, which was considered in the previous section. This could be due to the determination algorithm used in the

K-means. However, by comparing Figure 4-34 and Figure 4-38, it seems that most of the seagrass samples with prominent canopy heights are mostly effectively identified when comparing to those in Figure 4-34, which is an improvement in identifying the actual seagrass locations rather than just for the performance measured exclusively only in terms of numbers.

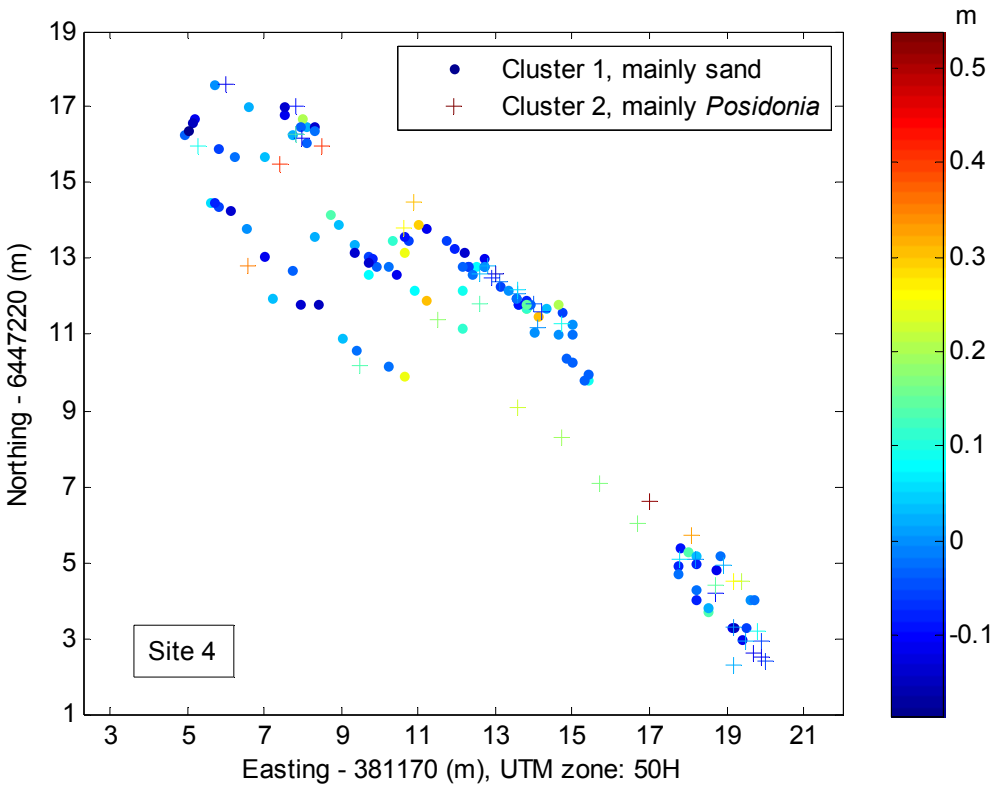

Figure 4-38 Same as Figure 4-34 but after the inclusion of the EPW (cf. Figure 4-21, Figure 4-30, Figure 4-46, and Figure 5-10).

As demonstrated by comparing the results in this section and the previous section, the classification ability combining both PCA and K-means to distinguish samples of the two classes seems to be limited by the clustering algorithm implementd by the K-means, although the input parameters, the five statistics and the EPW, play a critical role to the performance. The statistical method and the PCA are not able to provide acceptable classification results, even though the two pure classes involved here are the most distinctive ones. After the inclusion of the EPW, it is obvious from Figure 4-35 that the third PC contributes more to the global variations when comparing against Figure 4-31. However, since the third component is not selected for the PCs, there is no indication by comparing Table 4-6 and Table 4-7

that the overall recognition ability from the above process is enhanced after the inclusion of the EPW.

Figure 4-39 to Figure 4-42 and Table 4-8 demonstrate results of classification using K-means applied to the first three PCs of the highest eigenvalues.

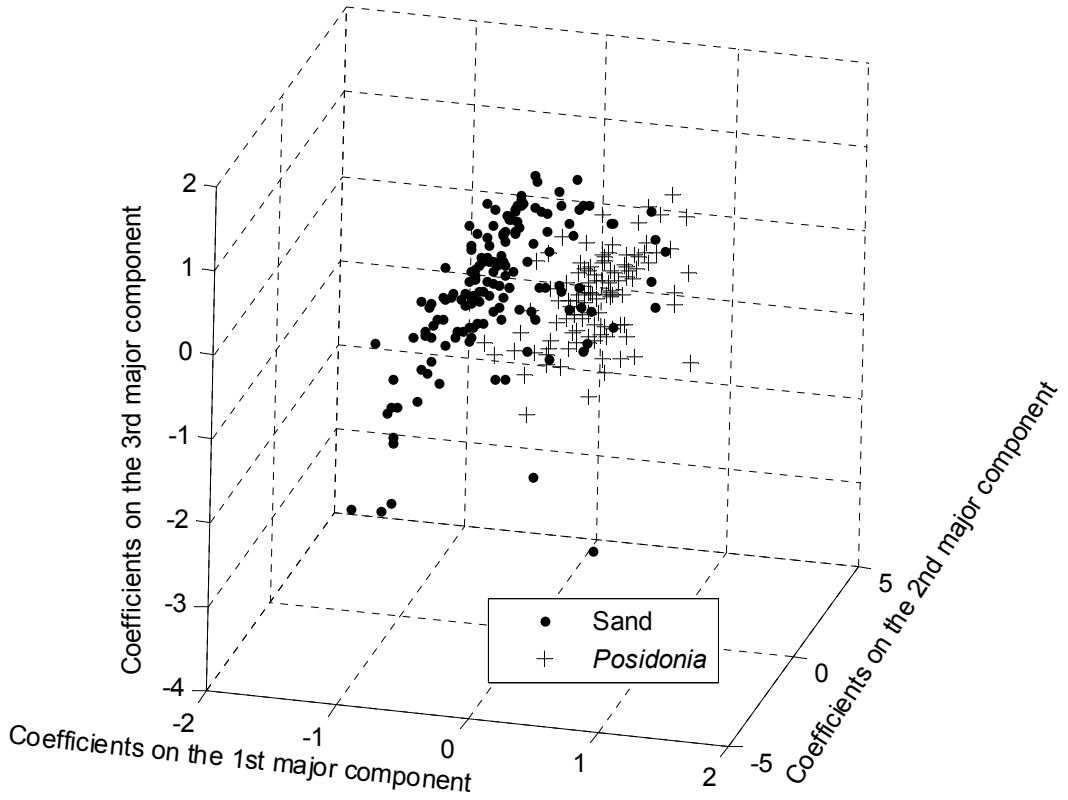

Figure 4-39 Same as the upper panel of Figure 4-36 but after the inclusion of the third PC.

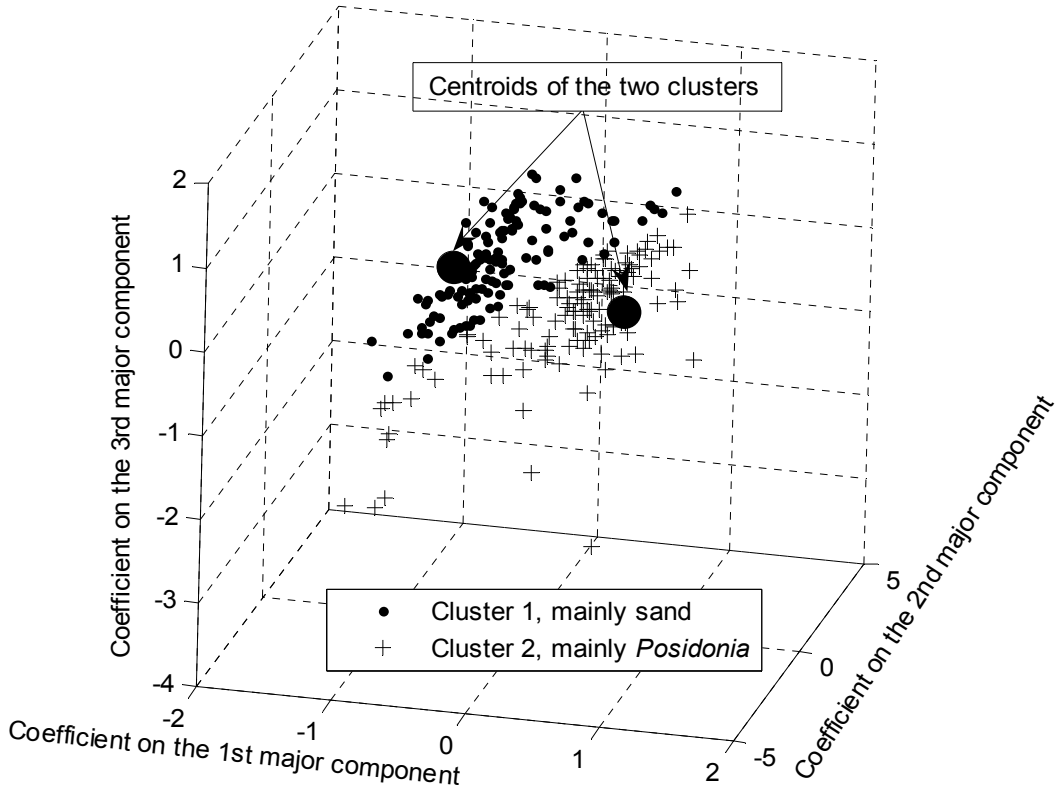

Figure 4-40 Same as the bottom panel of Figure 4-36 but after the inclusion of the third PC.

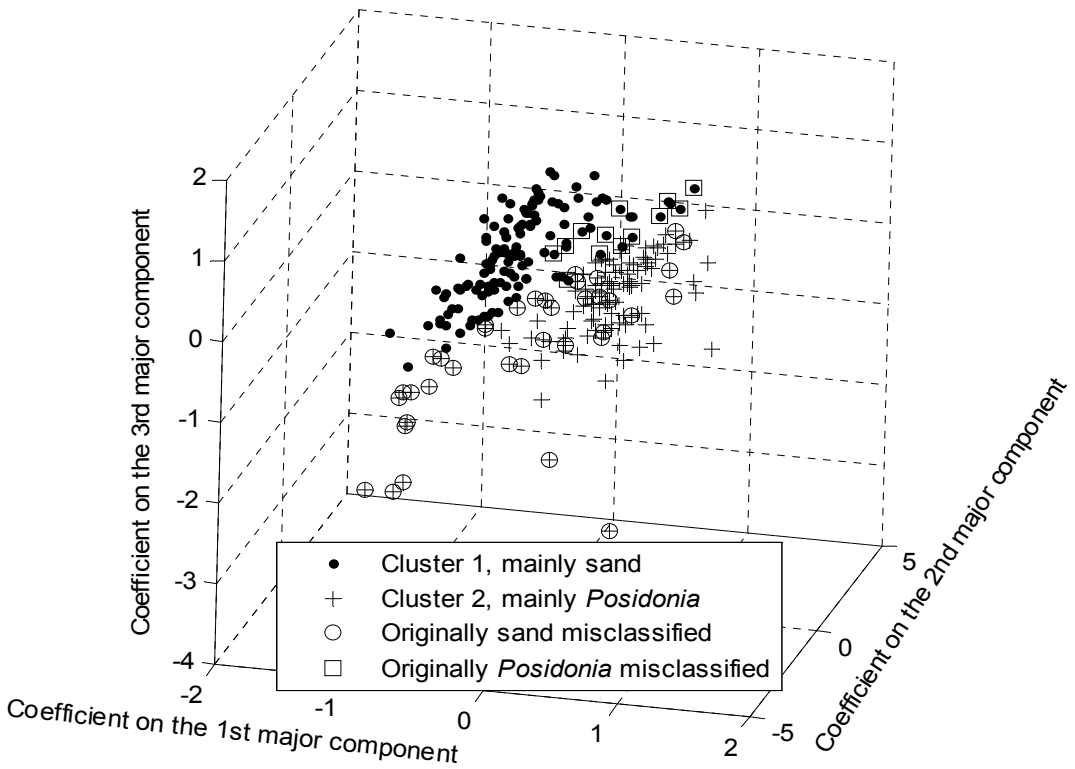

Figure 4-41 Same as Figure 4-37 but after the inclusion of the third PC.

Table 4-8 Confusion matrix of all the pure sand and *Posidonia* class samples determined by K-means after the inclusion of EPW and the third PC for the data collected from the final ESP field trial (cf. Table 4-1, Table 4-5, Table 4-6, Table 4-7, Table 4-9, and Table 5-2).

Optics \ K-means	Sand	Posidonia
Sand (150)	113 (75%)	37
Posidonia (107)	13	94 (88%)

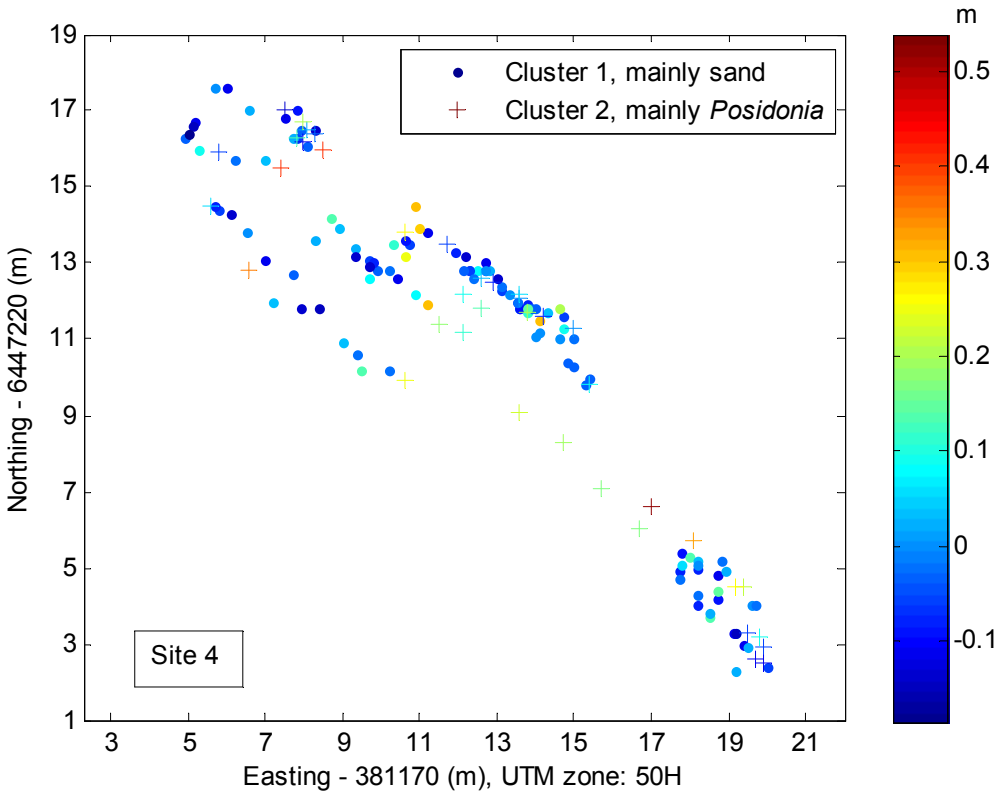

Figure 4-42 Same as Figure 4-38 but after the inclusion of the third PC (cf. Figure 4-21 and Figure 5-10).

After the inclusion of the third PC, the overall performance is enhanced when comparing to the results with only two PCs. However, the classification performance is still worse than that obtained purely by the EPW parameter investigated in sections 4.3.2 and 4.3.4. The PCA is in principle an effective method which can extract new prominent components from the original input parameters for describing the

variation of the data. The unsatisfactory discrimination performance obtained here could be due to the partitioning algorithm employed by the K-means, which is an unsupervised algorithm that does not use any prior knowledge about the actual classes identified unambiguously for training samples. By contrast, the single parameter classification results based on EPW and described in section 4.3.2 relied on a set of training data to determine the optimum discrimination threshold.

4.4.3 Linear discriminant analysis

In the previous sections, the focus of classification has been narrowed down to a two-class problem for the sand and seagrass classes. In history, Fisher has investigated similar problems and proposed a method to differentiate the two plant species, *Iris setosa* and *I. versicolor*, by their characteristics (Fisher 1936). The methodology, which he applied to the taxonomic problem, has been developed nowadays into the so-called linear discriminant analysis (LDA).

LDA is one of the available supervised classification techniques frequently used by researchers for classification problems where the number of classes is determined *a priori*. In LDA, the discriminant function (DF) is a linear combination of the observational variables such as the statistics, PCs, and EPW in this study.

In principle, the DF formed by m observational variables can be expressed by:

$$\sum_{i=1}^{m} w_i V_i \qquad 4\text{-}12$$

where w_i is the weight of the observational variable V_i, denoting its proportional contribution to the variable's discrimination capability for the known classes. With equation 4-12, the description of the training data observed on the m-dimensional space is then transformed to the observation of the data consisting of the same classes by the DF on a one-dimensional space.

For a problem with only two observational variables (m=2), a mixed two-class data set can be segmented into two separated classes based on Fisher's criterion. The criterion proposed by Fisher is the so-call F ratio (Dodge 2008). Its formulation is given by equation 5-1 in section 5.4. The criterion implies the maximum separation between different classes and the minimum dispersion within each class.

From the previous investigation results, we understood that the simple and easily interpretable variables, such as the skewness and EPW, gave above average performance in classifying the sand and seagrass classes. As shown in the upper panel of Figure 4-43, *Zp* is the projection value of point *P* of the two-class samples onto the new axis *Z*, which is called the discriminant score (Goldstein and Dillon 1978; Sharma 1996).

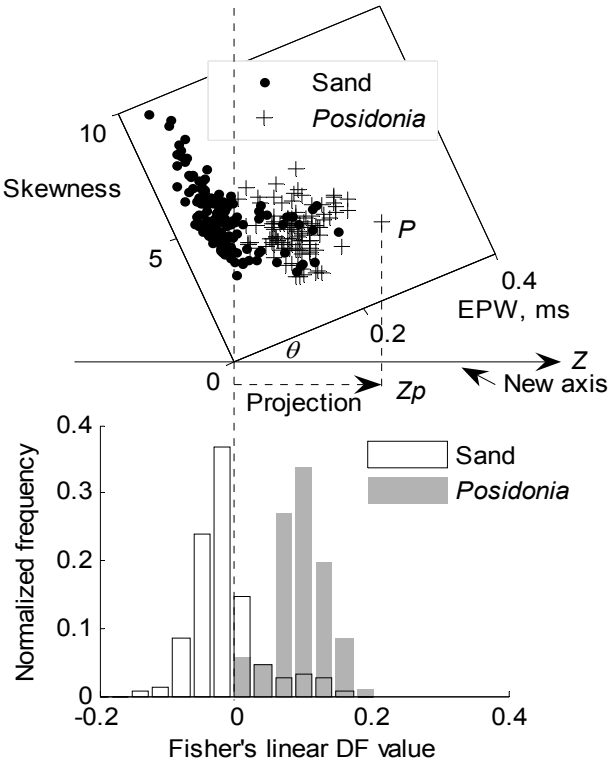

Figure 4-43 Projection value *Zp* of point *P* (upper panel) and histograms (lower panel) of the two classes observed on the new axis *Z* expressed by the DF.

In such a case, equaiton 4-12 can then be expressed as

$$\cos(\theta)\cdot EPW + \sin(\theta)\cdot Skewness \qquad 4\text{-}13$$

where θ denotes the angle between the EPW axis of the two-dimensional space and the new axis *Z*, as shown in the upper panel of Figure 4-43. The DF given by equation 4-13 is referred to as the Fisher's linear DF with the two variables, EPW and skewness.

Each sample lying in the original two-dimensional space at the angle θ relative to the new axis will have its corresponding *z* value, which is the discriminant

score of each individual sample observed on the new axis. A series of angle θ values will then generate a series of F ratio values according to Fisher's criterion, which is plotted in Figure 4-44. The optimization procedure in this case is to find the angle θ at which the F ratio is maximal. There is one angle θ[††††††] which results in the maximum F value.

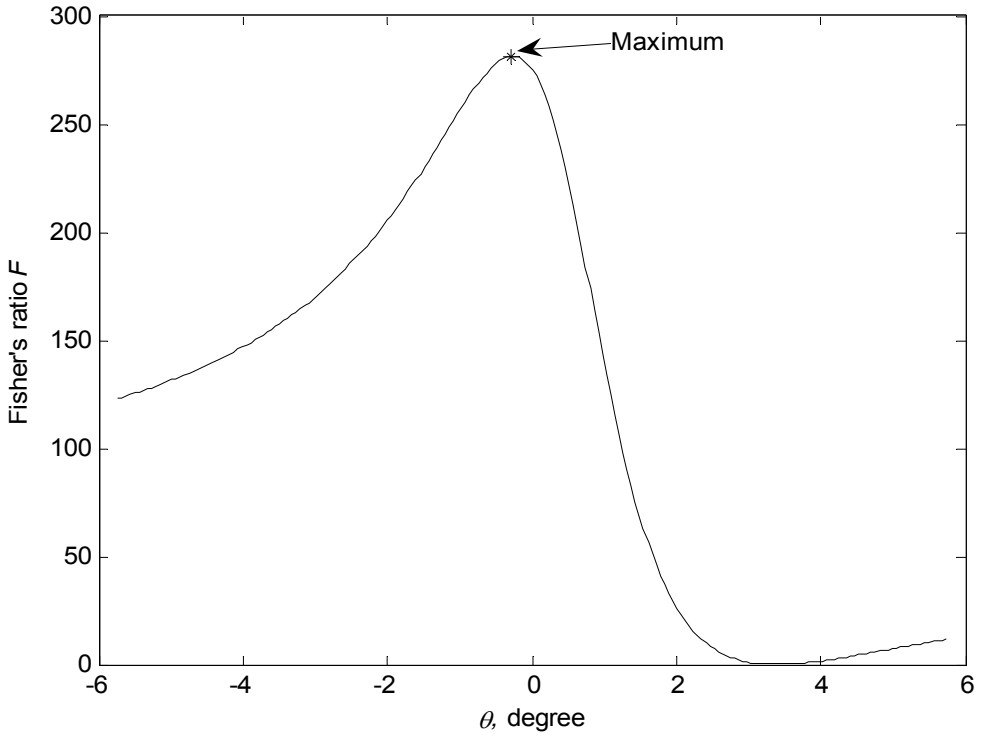

Figure 4-44 Plot of Fisher's ratio F versus angle θ with the maximum F ratio value of 281 at an angle of -0.3 degree pointed by the arrow.

Once the optimal angle θ of the Fisher's linear DF in equation 4-13 is determined, histograms of the DF values of the two classes can finally be plotted, as shown in the lower panel of Figure 4-43. The minimum misclassification rate takes place when the boundary between the two classes of sand and seagrass is set at the optimum DF value of 0.091. Based on the boundary found by LDA, a discrimination result shown in the EPW-skewness space is given in Figure 4-45.

[††††††] The other anlge which gives the same maximum F value is the one obtained by adding 180° to the angle θ.

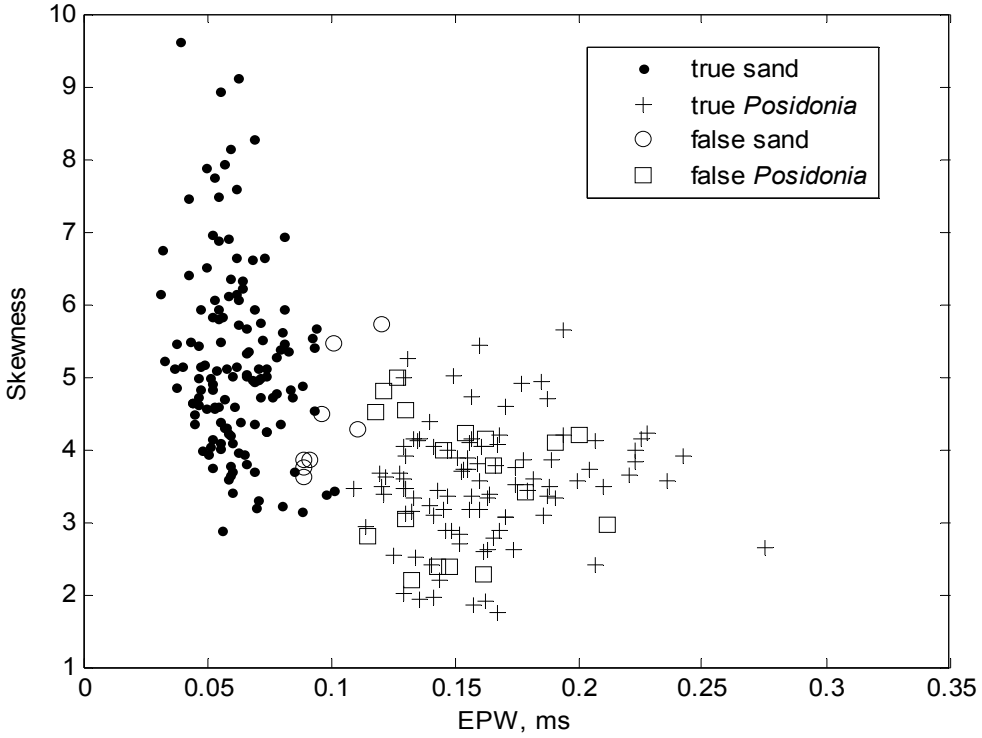

Figure 4-45 A LDA discrimination result for the data collected from the final ESP field trial using Fisher's criterion with an error rate of 0.097.

Table 4-9 Confusion matrix of all the pure sand and *Posidonia* samples determined by LDA with the EPW and skewness variables using Fisher's criterion for the data collected from the final ESP field trial (cf. Table 4-1, Table 4-5, Table 4-6, Table 4-7, Table 4-8, and Table 5-2).

LDA / Optics	Sand	Posidonia
Sand (150)	132 (88%)	18
Posidonia (107)	8	99 (93%)

Table 4-9 contains the confusion matrix of all the pure sand and *Posidonia* samples collected from the final ESP field trial. It is determined by the LDA method with the EPW and skewness variables using Fisher's criterion. By comparing the numbers in Table 4-9 against those in Table 4-1 made by EPW, the identification performance here is marginally worse (88% against 89%) for sand, but is better (93% against 89%) for *Posidonia*.

A map of habitats identified by the LDA method is shown in Figure 4-46 along with the estimated seagrass canopy height. By comparing this figure with all previously shown maps of identified habitat classes, we can conclude that the LDA's identification performance is comparable to or slightly better than that by EPW.

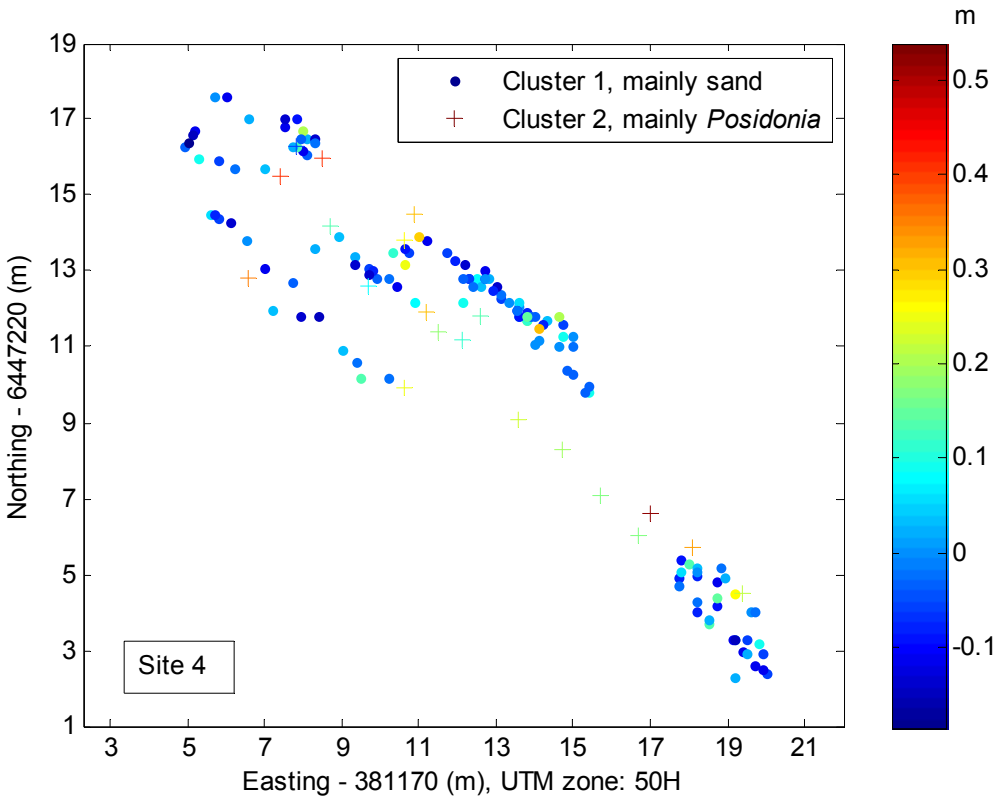

Figure 4-46 Map of the sand and seagrass samples identified by the LDA with the corrected RD values shown in colour designated for seagrass canopy height at site 4 of the final ESP field trial (cf. Figure 4-21, Figure 4-30, Figure 4-34, Figure 4-38, and Figure 5-10).

4.5 Summary

Several parameters have been investigated with respect to their recognition capabilities for the seafloor vegetation. The EPW parameter provided the best performance in differentiating the habitat types when comparing to other parameters, such as the maximum backscatter intensity (see section 4.2.1.1), echo-average backscatter strength (see section 4.2.1.2), and Hurst exponent (see section 4.2.1.4).

Acoustic discrimination for the flat sand seafloor and seagrass meadows by the EPW parameter was particularly successful. However, further differentiation of each of these two major classes into more specific subclasses was not so effective.

A considerable difference between the detected bottom ranges of seagrass meadows measured at 38 and 200 kHz was observed. The echo signal at the lower frequency (38 kHz) was almost insensitive to the presence of seagrass in contrast to the echo signal at 200 kHz. It was found that the 38 kHz echo could be used for detecting the substrate even in the presence of seagrass, which provided the means for estimating the seagrass canopy height by comparing the ranges detected at 38 and 200 kHz (see sections 4.2.2, 4.2.3, and 4.3.4).

The range to the maximum level of acoustic backscatter at 200 kHz did not indicate the true location of the seagrass's canopy. It was found instead that the echo front at 200 kHz was a more appropriate reference point for the detection of seagrass's canopy (see section 4.2.3). However, at some scenarios, the canopy height determined acoustically cannot be groundtruthed by the optical system due to the fact that optical observations of the substrate were obscured by the dense seagrass shoots (see for example Figure 3-14). This is the reason why there is no quantitative comparison of the canopy height made by acoustics and optics in this study.

Sea squirts observed in the second field trial on sand seafloors cannot be discriminated by acoustic means. Possible reasons for this could be due to the poor resolution of the acoustic system when comparing to the physical size of sea squirts and the limited characterization capabilities of the parameters examined.

No obvious range dependence of backscatter characteristics used for seafloor classification has been observed.

Determination of seagrass canopy height based on the bottom detection at two different frequencies was made. Firstly, the seagrass meadows on the seabed were distinguishable from bare sand by the EPW values of acoustic backscatter signal. Estimates of the canopy height were then acquired by the use of the RD value measured at two frequencies. The corrected RD values after subtracting the average sand RD value (0.17 m) gave quite reasonable estimates of the seagrass's canopy height consistent with both historical data and optical observations in this study.

The statistics used in this study were not efficiently capable of differentiating the acoustic signals backscattered from the sand and *Posidonia* seagrass bottoms except the skewness.

From the multivariate approach, when two or three PCs were used for distinguishing the two distinctive classes, the results obtained in section 4.4 with the PCA and K-means methods were still worse than that made by the EPW parameter investigated in sections 4.2 and 4.3.

In the last section, results obtained from the LDA method with the EPW and skewness variables are in general as good as those obtained by the EPW, which shows that LDA is a better discrimination algorithm than the combined PCA and K-means method for the classification problem encountered in this study.

Chapter 5 Application of Genetic Programming

5.1 Study motivation

Genetic Programming (GP) has been explored for its possible applications to marine science in very limited areas of research to date (Chami and Robilliard 2002; Liong, Gautam *et al.* 2002). The author of this thesis was inspired by an effective application case of GP to a diesel engine problem (Sun, Tsung *et al.* 2004), which prompted him to investigate the potential applicability of GP to solve the problems encountered in this study. A preliminary investigation of using GP for classification of acoustic backscatter data has led to some promising results (Tseng 2005; Tseng, Gavrilov *et al.* 2005a; Tseng, Gavrilov *et al.* 2005b). To illustrate the principle and algorithm employed for implementing GP for the problem of classifying acoustic backscatter signals from the seafloor, the author presents in detail its application method in this chapter. Differences between the classification results after the application of GP and other methods presented in the previous chapter can be observed by comparing the GP results given in this chapter with those given in Chapter 4.

Since the principle of GP has been systematically explored and discussed in the literature by some pioneers in the Machine Learning area (Koza 1992; Banzhaf, Nordin *et al.* 1998), a brief introduction of the principle of GP is given in the beginning of this chapter. It is necessary for readers to understand its basic principle in order to fully comprehend the application results illustrated in this chapter. This chapter focuses on the application of the GP approach to the classification problems encountered in this study.

5.2 A novel approach for feature extraction

Traditionally, parameters which were used to characterize different classes of signals were determined by experts according to their experience and detailed studies of the problems involved. Conventional approaches to solve problems are usually adopted. In the conventional case, provision of signal features greatly relies on experts' understanding of the problem.

Is it possible that the determination of characterization parameters can be replaced by machines with artificial intelligence in order to provide solutions for difficult problems or for scenarios where alternative solutions are required? GP provides the potential to answer this question. By modifying the fitness function used in general GP problems, the GP algorithm can be employed to provide capabilities to learn the input signals and give versatile solutions which are comparable in performance to those offered by traditional methods investigated in Chapter 4.

The GP system does not just allow for more ways of combining the input parameters than the linear combinations used in PCA examined in section 4.4.2, but also adopt Darwin's selection principle to check for the optimal way of combining input signal parameters into potential solutions for obtaining the best classification performance. The check process is implemented in each generation by comparing every randomly generated offspring (new parameter randomly generated by combining the input parameters and the operators provided) in performance. After several generations assigned by system programmer, the best performed parameter selected will be generated. In such an approach, it is mainly the randomness and the selection principle which govern the birth of the possibly robust parameters for classification and the way to compare each new parameter's performance with the fitness function provided, which is a difference in concept against the conventional methods.

5.2.1 Supervised training for classification

In signal classification studies, there are usually two common approaches adopted: supervised training and un-supervised training. The adoption of either mode

depends on the attributes of the data acquired. Each acoustic sample obtained in this study was simultaneously collected along with its corresponding optical record. The data acquired in this way provided opportunities for researchers to carry out supervised training of the acoustic data for classification purposes.

Below are the introduction of the GP algorithm and the study results after applying the GP algorithm in showing its adaptive abilities for the classification of acoustic signals extracted from samples collected from the final ESP field trial.

5.3 Introduction of GP

GP, in short, is a paradigm of breeding computer programs according to genetic evolution processes. It can be employed to achieve machine learning abilities by an appropriate design of the algorithm. It is based on Darwin's natural selection principle according to required conditions to breed computer programs for specific purposes. The searching for possible solutions for complex real world problems is replaced by machines with learning abilities.

The study of GP is mainly pioneered by John Koza in investigating machine learning abilities on real world problems where computer programs can adapt themselves to provide improved solutions from one generation into next one (Koza 1992). GP is believed to be evolved from the Genetic Algorithm (GA) developed before 1992 (Holland 1992). GP is now further explored for its principle and applications by many scientists (Banzhaf, Nordin *et al.* 1998; Sette and Boullart 2001; Langdon and Poli 2002), and has evolved into different versions of GP (Downing 2001) and for different purposes (Langdon 1998; Babovic and Keijzer 2000). All in all, GP provides mechanisms for computer programs to evolve themselves from one generation into the next with potentially better performance in solving problems.

It is important to know how GP was applied on tasks for solving problems of interest. Initially GP was investigated for its capabilities on solving small and relatively easy problems. Ideally, the algorithm used in solving simple problems may also be applied to solve a wide range of problems. Whether this was for the proof-of-concept or as a demonstration of GP's capabilities in solving the problems involved, researchers showed that GP can seemingly solve a wide variety of

problems, such as the design of complex structures (e.g., antenna (Comisky, Yu *et al.* 2000)).

Because the implementation of GP requires fast computing machines, it has increasingly become one of the intensely studied disciplines within Genetic and Evolutionary Computation due to nowadays affordable computer prices. Since there have been a variety of problem domains shown to be amenable to the application of GP, it is now intensely explored for its possible applicability to different areas. Studies of GP on issues of optimization, symbolic regression, fitness design, and its possible applications on real world problems have been explored in the annual GECCO (Genetic and Evolutionary Computation COnference) conference promoted by the Special Interest Group on Genetic and Evolutionary Computation (SIGEVO) (SIGEVO 2006).

One of the biggest advantages of adopting machine learning approaches is the provision of possible solutions by the machine itself when human intelligence is not able to provide efficient solutions for the complex real world problems or alternative solutions are necessary. This instance can be easily seen from the well known case study of the artificial ant in the problem of following the Santa Fe Trail (Langdon and Poli 2002). This successful and powerful ability of the machine learning approach has been commercialized and applied on the vehicle dispatching and cargo delivery business (Benyahia and Potvin 1998).

5.3.1 Genetic evolution of computing programs

In GP, a candidate solution or computer program is called an "individual". In each program run, programmers need to assign a set of initial GP parameters in order to implement the GP, including the numbers of generation and population (number of individuals in a generation). In a generation, individuals have variable abilities in solving problems. In order to find individuals which best solve the problem, GP programs (individuals) undergo genetic evolution from one generation into the next with potentially improved performances through selection mechanisms determined by the fitness function. The evolution has to follow Darwin's natural selection principle. In short, only those individuals with above average performance can be selected into the next generation for further GP processes.

Individuals usually undergo three common genetic evolution processes in order to evolve into new individuals. In a new generation, it includes new individuals "randomly" generated by the GP system according to the system settings, along with the "good" individuals selected from the previous generation.

The randomness attribute of the GP algorithm provides all possible appearances of an individual to be generated in a generation. The way which each intermediate generation is filled by the randomly generated individuals mimics nature's strategy for survival. In such an environment controlled by the fitness function and system settings designed by programmers, potential solution programs are expectedly to be generated from a more global solution space rather than from a limited and local one. Through randomness, GP provides survival opportunities for an initial group of candidate programs to evolve into a group of programs with better performance. The best performing program sorted from the final generation is then the best program so far and regarded as the "best-so-far" solution for a problem.

It is also important to note that there is no so-called early rejection problem for individuals to be selected in the GP algorithm. Those individuals which have appeared in an early generation are not necessarily excluded from reappearing in a later generation. Due to GP's randomness property, any individuals are possibly regenerated several times in different generations as long as the GP system does not limit itself in any particular restrictions.

5.3.1.1 Tree-based GP individuals

In classical GP, each GP individual can be represented by a GP-tree, such as the simple GP-tree given in Figure 5-1. In the figure, it is a tree-based expression equivalent to the mathematical function of $(\sqrt{F1}) \times (F2 - F3)$. The operator in the figure can be any mathematical operator or a combination of any operators while F1, F2, and F3 at the terminals can be any real numbers and represent the input parameter values used to characterize different data (different signals in this case study). Hence, each individual is a combination of the numerical values of the input characterization parameters and the mathematical operators.

Ultimately the hope is that the input parameters at the terminals after combining with the operators at the non-terminals can be evolved through the genetic

process into individuals that perform well. In principle, individuals transform the original characterization parameters (terminal nodes) into new variables (new individuals) and map them onto the best-so-far solution space. The performances of the individuals are measured by a fitness function. That is, each individual, by transforming every sample onto a solution space, is a candidate solution. They only differ in their performance in solving problems. After the selection process, the best performing individual in the final generation is selected as the best-so-far solution.

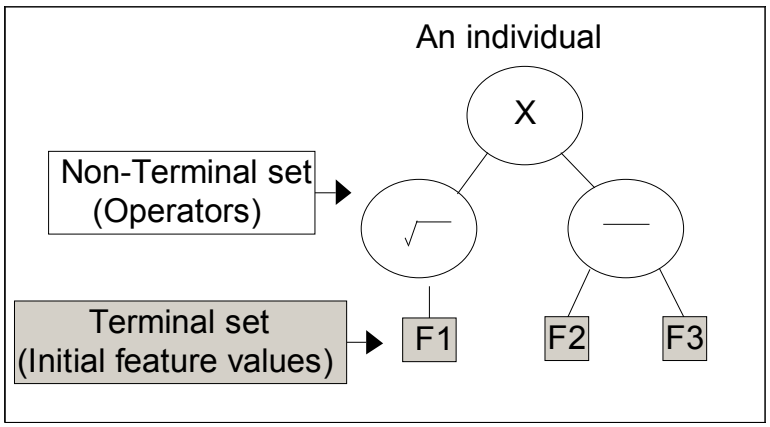

Figure 5-1 A tree-based GP individual expression equivalent to (√F1) x (F2 – F3).

Usually each individual in a generation can undergo any of the following three genetic evolution processes in breeding new individuals.

5.3.1.2 Reproduction

Reproduction is a process of breeding a new individual by producing an exact copy of its parent individual. This reproduction process can be illustrated by the example given in Figure 5-2. As in Figure 5-1, the OP1, OP2, and OP3 in Figure 5-2 are any mathematical operators or any combinations of operators while F1, F2, and F3 are the numeric values of the input parameters.

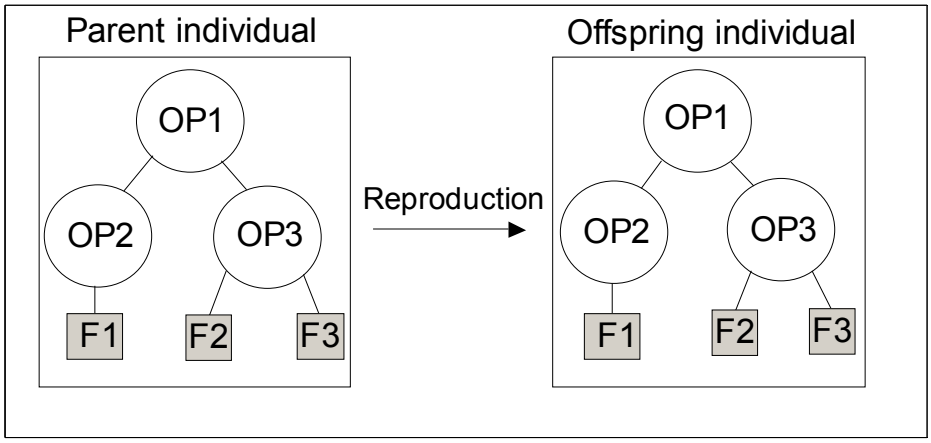

Figure 5-2 A sample genetic evolution process of reproduction.

5.3.1.3 Crossover

Crossover is a process occurring within a pair of individuals. A sub-tree of an individual is replaced by another sub-tree from the other individual in constructing a new individual, and the replaced sub-tree will replace the other sub-tree where it is originally attached on the other individual. A sample process illustrating the crossover operation on a pair of individuals is given in Figure 5-3.

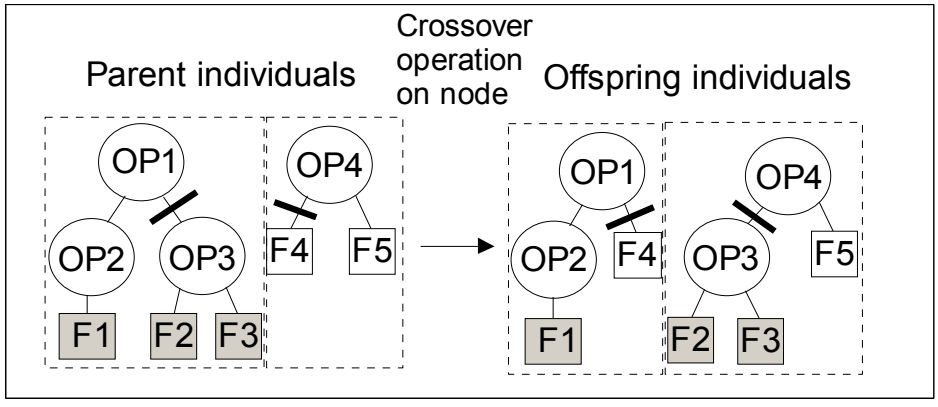

Figure 5-3 A sample genetic evolution process of crossover operating on a node.

5.3.1.4 Mutation

Mutation is a process that can happen either on the non-terminals or on the terminals of a GP-tree. In a sample mutation process given in Figure 5-4, the OPX and OPY on the non-terminals denote some operators while FX and FY on the terminals denote some parameters before and after mutation processes. The possible parameters and operators are limited to those initially provided by the programmer.

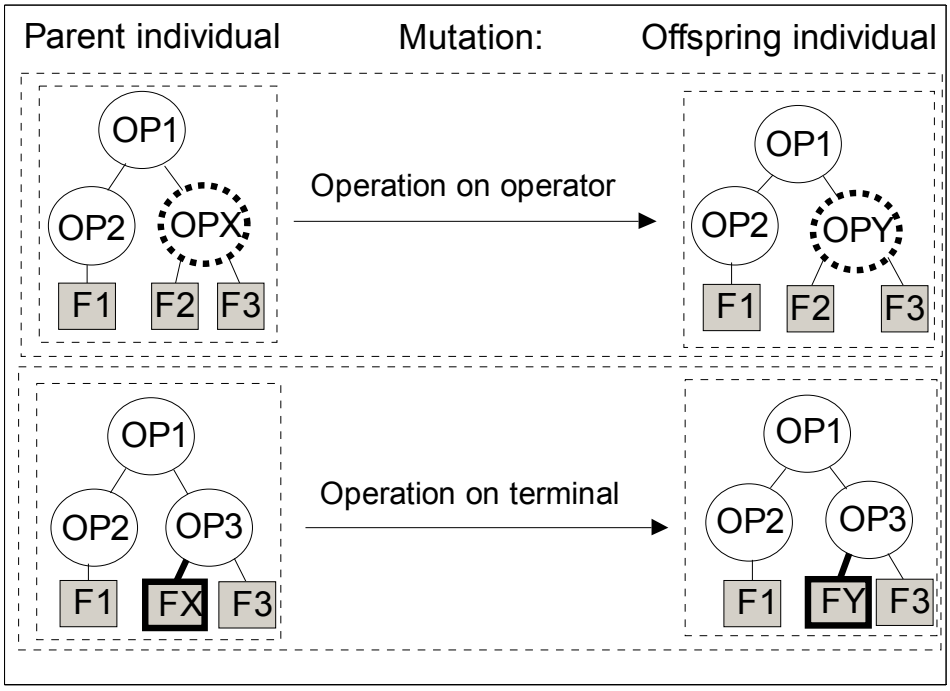

Figure 5-4 Two sample genetic evolution processes of mutation operated on an operator and terminal respectively.

5.3.1.5 Why best-so-far

Scientists frequently need to answer whether the solution found is the best one or not. Are there any better ones existing, and, if so, how to find them? In the search space for the solutions, GP also confronts the same dilemma. The best-so-far solution obtained is basically controlled by the settings of the GP system and by the intrinsic nature of randomness. In principle, the more generations allowed in a GP program run, the more chances are given to the GP system to find better performing

solutions than those found by allowing fewer generations. However, in the search for the top performing solutions, the so-called best one found is still only valid within the search space attempted in that only limited generations are allowed in the GP program run. There are still possibilities that better solutions may exist beyond the search scope. This is why the term, best-so-far, is probably the most appropriate term for referring to the solution found by the GP system.

Another important property of the GP algorithm is that each GP program run cannot be exactly replicated in another program run (Stewart 2004). Different program runs follow different evolutional routes to the final results with similar but unequal solution values. Even if the constraints provided by the GP settings are the same, the evolution process can be dramatically different among different program runs.

There have been many studies focusing on the understanding of factors which may control the GP system and determine the solutions (Koza 1992; Koza 1994; Banzhaf, Nordin *et al.* 1998; Koza, Bennett *et al.* 1999; Banzhaf, Koza *et al.* 2000; Sette and Boullart 2001; Langdon and Poli 2002; Luke and Panait 2002; Koza 2003). Since these are beyond the focus of this study, they will not be discussed here. Interested readers are referred to the above mentioned literature for further studies.

5.4 Design of the Fitness Function for classification

How each individual is assessed and determined by the GP system in order to be selected into the next generation critically depends on the fitness function (FF). Just like creatures in nature are relentlessly selected by their environments according to Darwin's selection principle, FF in GP serves exactly the same role as the "environment" for the GP individuals. Only the best performing individuals can survive from the test of the environment (i.e., FF) and breed "offspring" (new individuals) for new generations.

According to each problem's requirements, the FF can be in a variety of forms. Generally it gives the error rate of individuals in solving problems. Those individuals with lower error rates get higher scores in performance. Through this

assessment mechanism, each individual obtains a score according to its performance in solving problems.

Since GP is more commonly used for optimization problems rather than for classification tasks, the FF commonly employed by the GP community needs to be modified in order to be applicable to this case study.

A group of researchers has investigated the use of GP on similar classification problems with good results (Sun, Tsung *et al.* 2004). Their basic idea is very simple: to decrease the distribution range of each class and increase the separation between different classes in the GP solution space. To explain this point, an example of two separated classes of samples being transformed by a candidate GP individual and mapped onto a 1-dimensional solution space is shown in Figure 5-5. For illustration purposes, the separation between the two classes is represented by their median values and the scattering within each class is represented by the maximum fluctuation. In order to separate these two classes, it is better to increase the distance between the median values of the two classes as far as possible, and to reduce the maximum fluctuations within each class as small as possible.

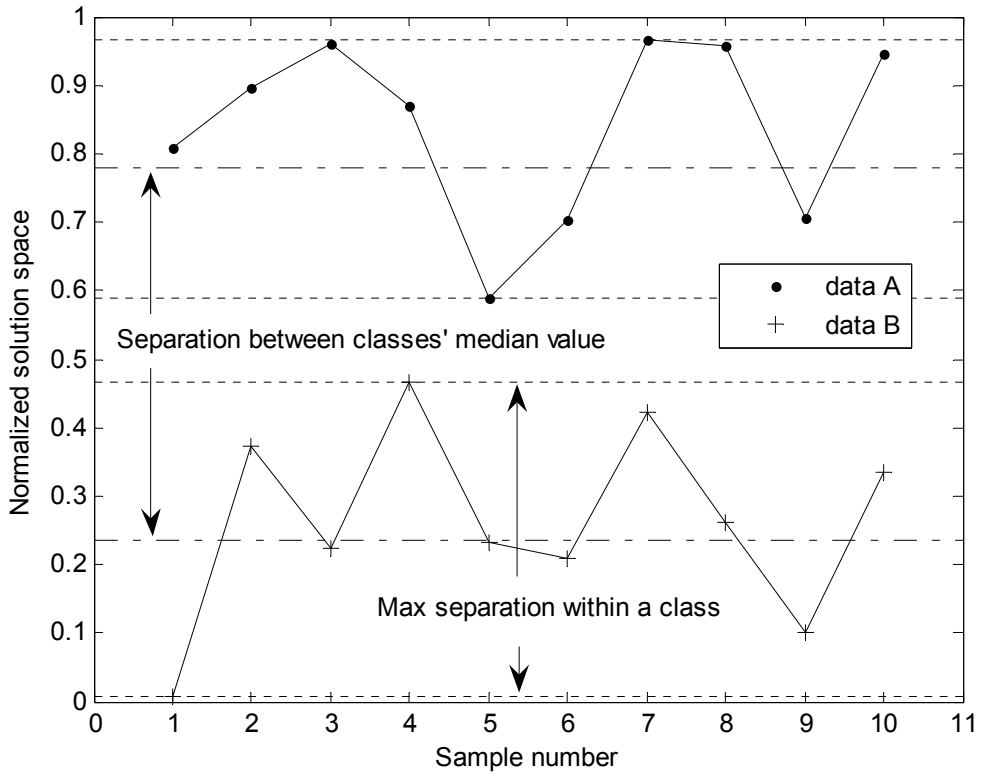

Figure 5-5 An ideal case of two separated classes with their samples being transformed by a candidate GP individual and mapped on a normalized solution space. The separation between different classes' median values and the maximum fluctuation range within each class combined is one of the measures for the performance of the GP individuals.

Unlike the FF used by the previous researchers, the one used in this study is based on the statistical approach suggested by Fisher (Fisher 1936) and advice from Gavrilov and Duncan[‡‡‡‡‡‡]. In Fisher's study, he investigated techniques which can find an optimal linear combination of features to best minimize the misclassification rates of two or more classes of objects in his taxonomic problem. The optimal linear combination of features is then expected to be an effective classifier for classification of objects. Based on Fisher's idea and from a general statistical point of view, the separation of M classes can be measured as:

[‡‡‡‡‡‡] Personal communication with Dr. Alexander Gavrilov and Dr. Alec Duncan of Curtin University on 19th of June 2007 and 16th of January 2008.

$$\frac{S_1^2}{S_2^2} \qquad 5\text{-}1$$

where S_1^2 is the interclass dispersion given by:

$$S_1^2 = \frac{1}{M-1}\sum_{m=1}^{M} N_m \left(\overline{X}_m - \overline{X}\right)^2 ,$$

N_m is the number of samples in class m,

$\overline{X}_m$ is the mean of the samples in class m, and

$\overline{X}$ is the mean of all samples,

and

S_2^2 is the intraclass dispersion given by:

$$S_2^2 = \frac{1}{N-M}\sum_{m=1}^{M} (N_m - 1) s_m^2$$

in which

N is the total number of samples, and

s_m^2 is the dispersion within class m given by:

$$s_m^2 = \frac{1}{N_m - 1}\sum_{n=1}^{N_m} \left(X_n - \overline{X}_m\right)^2 .$$

The fitness function defined by equation 5-1, commonly referred to as the *F* ratio, is to be maximized in order to obtain the maximum separation between samples of different classes and the minimum dispersion within samples of each class.

5.5 A MATLAB toolbox for GP, GPLAB

A free MATLAB toolbox specially made for the study of GP, GPLAB, was used in this study. It can be flexibly amended to adapt to different GP-related studies. Although it was not originally designed for the classification task, it was modified and extended by adding new routines in order to meet the author's study requirements. Using this toolbox, the author carried out an investigation of GP's

abilities with respect to the marine habitat classification task. The complete version of GPLAB, except the modified programs especially written for this study, can be found at:
http://gplab.sourceforge.net/

5.6 Implementation of GP

To compare the classification performance of the GP algorithm with those by the conventional methods discussed in Chapter 4, the data used in this chapter were the same pure sand and *Posidonia* samples investigated in section 4.4, which were collected from Owen Anchorage and Parmelia Bank in the final field trial.

5.6.1 Terminal and non-terminal nodes

In order to keep the input number of parameters the same as those used in Chapter 4 for fair comparison purposes, the five statistics (Max, Mean, STD, Skewness, and Kurtosis) of the pure sand and *Posidonia* seagrass samples are used again as the input values for the GP terminal nodes. As for the non-terminal nodes, they are selected from the common operators: summation, subtraction, multiplication and division. In order to safely run the program, a protected operator referred to as *kozadivide* [§§§§§§] (Koza 1992) is used instead of the common division to prevent dividing by zero errors.

5.6.2 Symbolic regression

To implement the designed GP system for classification, the acoustic data were rearranged to resemble a symbolic regression. Each acoustic sample was pre-processed from the first bottom return to obtain a set of statistical values which was

[§§§§§§] *kozadivide*(x1,x2) returns 1 if x2=0 and x1/x2 otherwise.

used here to represent the main features of each sample. Any solution resulting from the GP system will hence be a result originated from these statistics representing the original samples. The data were then normalized before being used as input parameters for the GP system. In order to distinguish the differences between different classes for the GP system, samples of different classes were assigned with distinctive codes for differentiation purposes in order to undertake symbolic regression.

The GP system initially generates several combinations of the input parameters with the mathematical operators provided. Each combination is evaluated with the fitness function as shown in equation 5-1 which rewards solutions producing similar values for the same class and different values for different classes. The aim is to be able to delimit the regions where each class plots its own values, minimizing the overlap between classes.

Ideally the optimal regression function should map the two pure classes into two separate ranges on a 1-dimensional space, with as small an overlap between the pure sand and *Posidonia* classes as possible. At the same time, space sitting between the two clusters is assumed to represent mixed habitat types or any extra types which are not considered in the algorithm.

The performance of the designed GP system for the classification of the two pure classes with the above defined FF is given below.

5.6.3 Result

The GP-tree representing the best-so-far solution program found by the GP system is shown in Figure 5-6[*******]. On the GP-tree terminals, the X1, X2, X3, X4, and X5 represent respectively the five statistics of the acoustic backscatter signals: maximum, mean, standard deviation, skewness, and kurtosis. Figure 5-7 shows the solution values of the 2-class samples being mapped on a 1-dimensional solution space by the best-so-far solution given in Figure 5-6 after 10 generations.

[*******] The corresponding algebraic formula of the solution found is written as: minus(plus(times(times(X4,X5),X5),kozadivide(minus(kozadivide(X2,X3),plus(times(X5,X2),times(X5,X2))),X5)),plus(minus(X2,times(X4,X5)),kozadivide(X2,X3))).

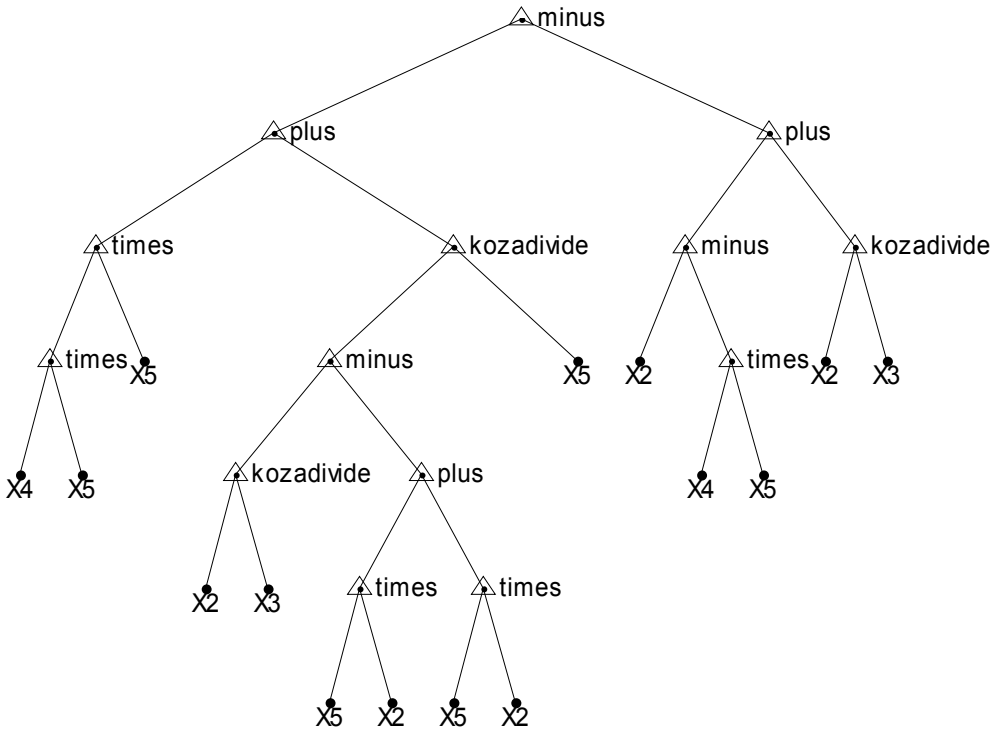

Figure 5-6 The GP-tree of the best-so-far solution found by the GP system with the fitness function given in equation 5-1.

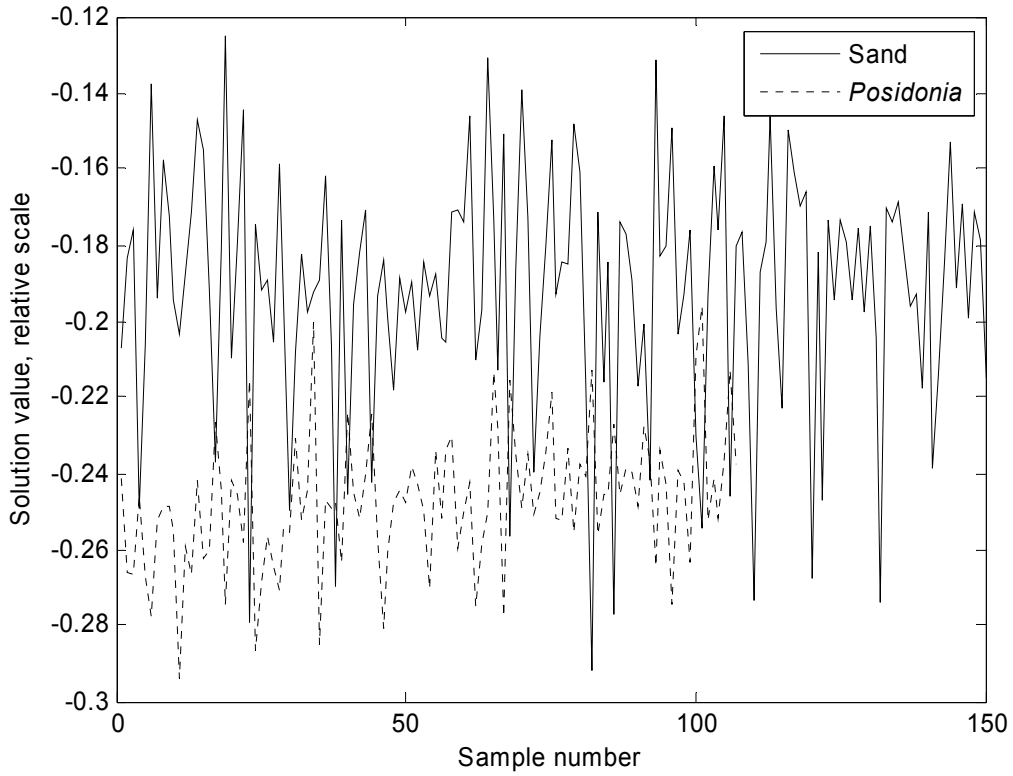

Figure 5-7 Solution values of the 2-class samples after being mapped on a 1-dimensional solution space by the best-so-far solution program for which the statistics at the GP-tree terminals were derived from the same data collected from the final field trial as investigated in section 4.4.

To understand if the implemented GP system has provided any improvement or not in differentiating these two classes against those by the EPW parameter and the statistics investigated in sections 4.3 and 4.4 respectively, Figure 5-7 was replotted as histograms given in Figure 5-8.

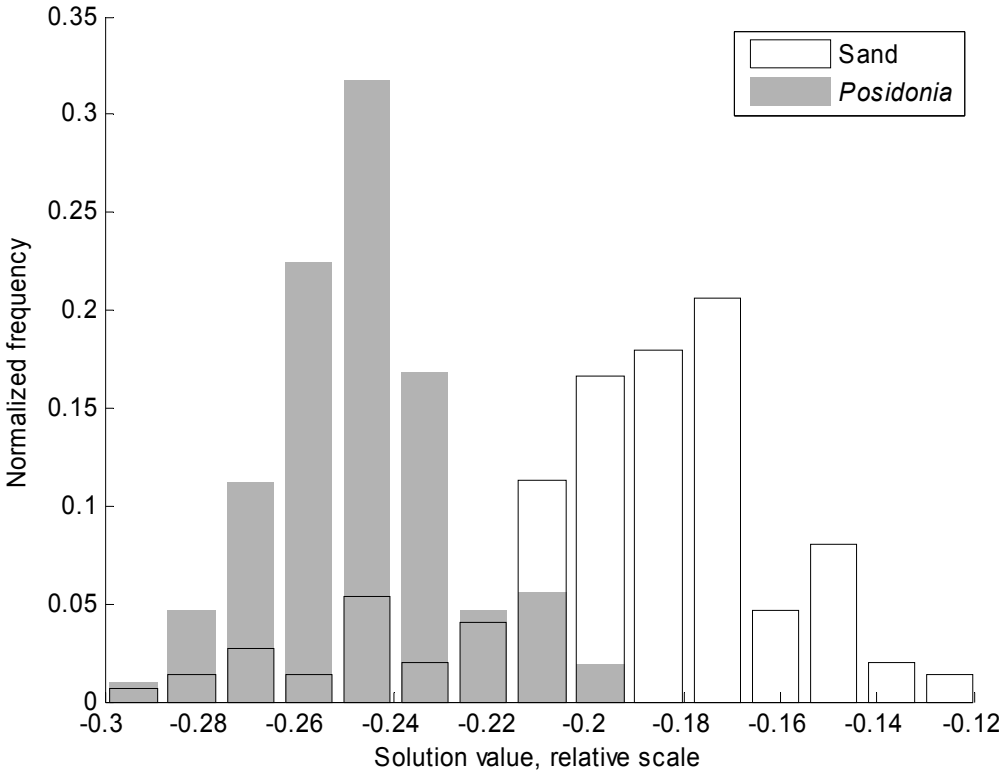

Figure 5-8 Histograms of GP solution values of the 2-class samples as used for Figure 5-7.

By comparing Figure 5-8 against Figure 4-16 and Figure 4-28, it is clear that the GP system is capable of providing comparable discrimination ability to that of the EPW parameter and noticeably better ability than those of the individual statistics discussed in sections 4.3 and 4.4 respectively.

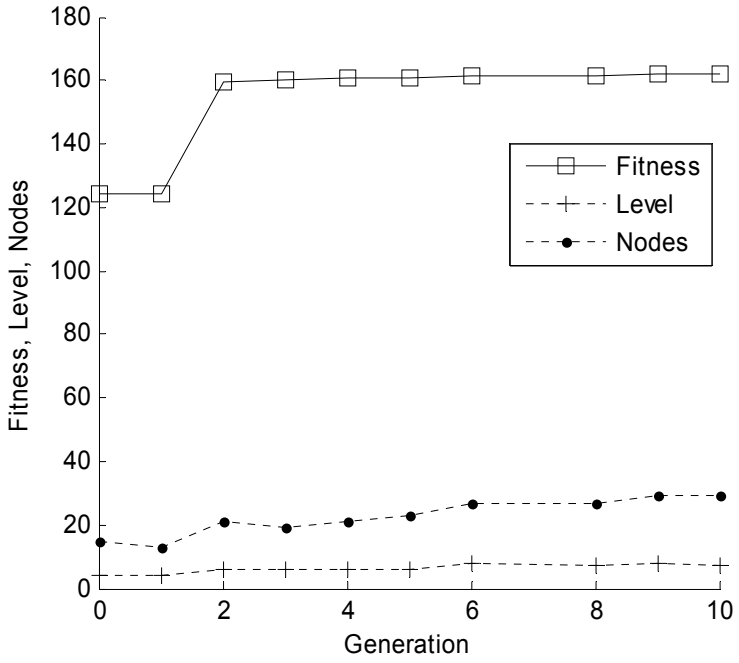

Figure 5-9 Fitness value, number of levels and nodes for the best individuals resulted from each generation vs 10 consecutive generations for the final solution program shown in Figure 5-6. The final fitness value is about 162.1.

The plot in Figure 5-9 shows the progress of the fitness value, tree level (the maximum number of levels from the tree top to the terminals), and number of nodes of the best performing individuals generated in the GP program run. It reveals whether the fitness value of the best individual in each generation increases with the increase of number of levels and nodes in the tree or not. The GP program was controlled by the settings listed in Table 5-1 for the choice of: 1) the first generation to be introduced (Ramped Half-and-half (Koza 1992)), 2) numbers of populations and generations allowed, 3) rates of genetic operations allowed, 4) strategy adopted in selecting individuals when the fitness values are equal (Lexicographic method (Luke and Panait 2002)), and 5) the historical records generating the final best-so-far solution program. For in-depth understandings of each GP parameter used in the GP program run, readers are referred to the literature cited here.

Obviously, it can be found from Figure 5-9 that the fitness value stalled after two generations.

Table 5-1 Major GP parametric settings, main historical parameter values, and characteristics used for finding the GP-tree solution program in Figure 5-6.

Population initialization	Ramped Half-and-half[†††††††] (Koza 1992)
Population size	250 individuals
Generations till solution	10
Crossover rate	0.5
Mutation rate	0.5
Reproduction rate	0.1
Tournament size	25, Lexicographic[‡‡‡‡‡‡‡] (Luke and Panait 2002)
Elitism	none
Best level history	4, 4, 6, 6, 6, 6, 8, 8, 7, 8, 7
Best node history	15, 13, 21, 19, 21, 23, 27, 27, 27, 29, 29
Maximum level history	28, 28, 28, 28, 28, 28, 28, 28, 28, 29, 29, Heavy Dynamic Limit[§§§§§§§] (Silva and Costa 2004)
Solution tree	7 levels, 29 nodes
Originally generated by	Crossover

Based on the boundary value at -0.22 determined from Figure 5-8 for the segmentation of the two-class samples by minimizing the misclassification error rate, a confusion matrix of all the pure sand and *Posidonia* seagrass samples is provided in Table 5-2. Shown in Figure 5-10 is a map of the sand and *Posidonia* seagrass samples identified by the GP solution program given in Figure 5-6. The corrected RD values expressed in colour were independently determined by the method discussed in section 4.3.4.

[†††††††] One of the three basic ways (along with "grow" and "full" methods) to initialize a population of individuals.

[‡‡‡‡‡‡‡] A technique for controlling the significant growth of a GP tree by modifying selection to prefer smaller trees when fitness does not change. By default, the tournament size is 10% of the population size.

[§§§§§§§] An approach for controlling code bloat of a GP tree during the course of a program run.

Table 5-2 Confusion matrix of all the pure sand and *Posidonia* class samples based on the boundary of the GP result determined from Figure 5-8 for the data collected from all four sites of the final ESP field trial in 2005 (cf. Table 4-1, Table 4-5, Table 4-6, Table 4-7, Table 4-8, and Table 4-9).

GP / Optics	Sand	Posidonia
Sand (150)	129 (86%)	21
Posidonia (107)	9	98 (92%)

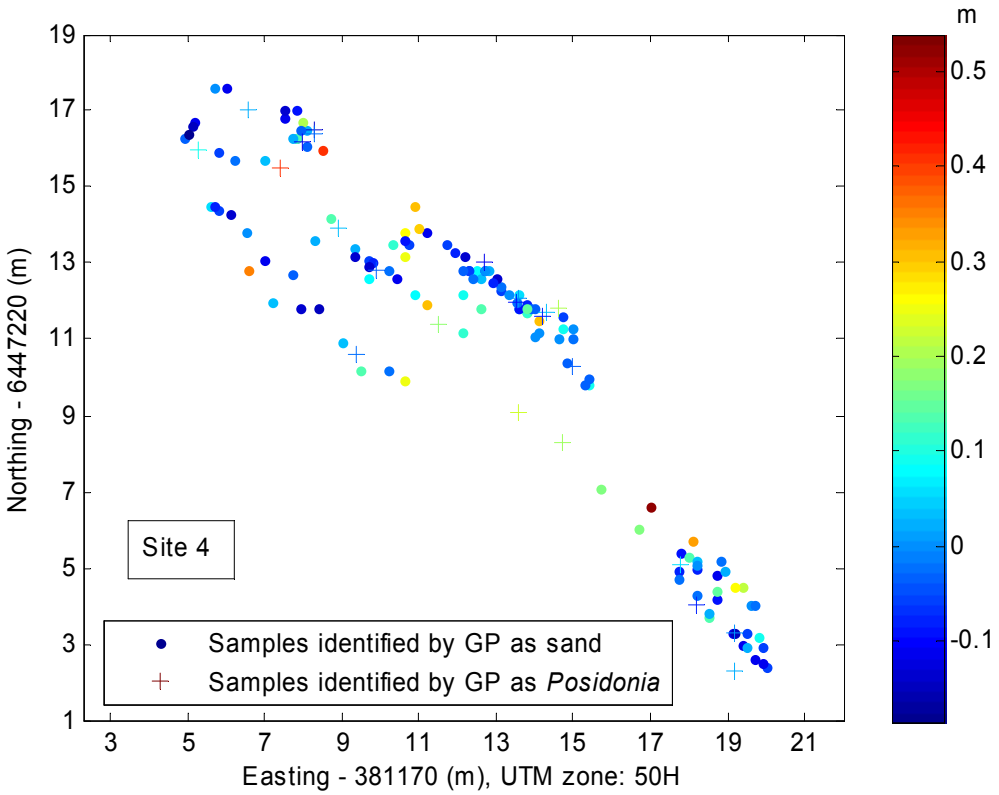

Figure 5-10 Distributions of the sand and seagrass samples classified by the GP result with the corrected RD values shown in colour designated for seagrass canopy height at site 4 of the final ESP field trial (cf. Figure 4-21, Figure 4-30, Figure 4-34, Figure 4-38, and Figure 4-46).

By comparing the confusion matrix given in Table 5-2 against that in Table 4-1 in section 4.3.2 and those confusion matrices in Table 4-6, Table 4-7, Table 4-8, and Table 4-9 in section 4.4, one can conclude that GP is capable of providing

classification performance comparable to that of the EPW parameter and better performance than those resulted from the multivariate approach, except the LDA performance discussed in section 4.4. However, the identification performance for the actual seagrass locations provided by GP is worse than that made by the EPW and LDA.

5.7 Limitations of GP

From the GP results demonstrated in the previous section, it is clear that the classification performance should not just consider accuracy in terms of number only. As shown in Figure 5-10, a few seagrass samples with large canopy height were incorrectly classified as sand samples by the GP method while such case was rarely seen in the result achieved by the EPW as shown in Figure 4-21. Obviously the GP algorithm designed for the classification problem in this study was incapable of avoiding such an irrational mistake although its performance measure in terms of number was not necessarily weaker than those by other methods.

The optimal adjustment of the GP parameters listed in Table 5-1 for a best identification result is one of the focuses (Bäck and Schwefel 1993; Koza, Keane *et al.* 2000; Koza, Keane *et al.* 2005) repeatedly discussed in the annual SIGEVO conference (SIGEVO 2006). To find an optimal combination of the GP parameter setting is a hard research problem. To have a reasonable GP parameter setting, problems like stagnation and code growth (Smith and Harries 1998; Smith 2000; Fernández, Galeano *et al.* 2004; Luke and Panait 2006) are among other key issues on-going hot topics. A universal approach for an optimal GP parameter setting for a good classification result is still unavailable up to date.

In the GP approach, GP systems with the fitness function like that given by equation 5-1 are good for discriminating simple mixing conditions where different classes can be well separated by the GP solution programs after being mapped on a one-dimensional solution space as shown in Figure 5-5. For more complicated mixing scenarios, the mixed classes should be better distinguished in a two- or multi-dimensional solution space.

Theoretically, the more flexibility the GP system offers, the more chances a better solution will be found. In reality, only a limited computational time is allowed. And, the GP system is only allowed to implement its algorithm with limited generations and population sizes.

GP has higher computing power requirements than the other methods considered in this thesis. Its primary advantage is the flexibility it gains from breeding solution programs genetically from its input parameters, but this is diminished by its variable and hard-to-predict behaviours due to its intrinsic randomness.

5.8 Summary

The design of the fitness function as shown in equation 5-1 and the symbolic regression procedure made the GP system a useful tool for breeding solution programs, which are then used as descriptors for differentiating acoustic signals of different attributes. The designed GP system is capable of acting as a supervised training mechanism for the initial input parameters at the GP-tree terminals to genetically evolve into not only acceptable but also as many versatile solution programs as possible for classification purposes. Although the solution programs found by GP were not necessarily superior in capability when comparing to the EPW parameter (see section 4.2.1.3) in distinguishing the data, the proposed GP system was found possessing human-competitive machine intelligence which can provide comparable classification performance against those by the conventional methods.

The GP approach proposed here for classification purposes can be applied to any tasks involving supervised training for signal classification problems. For example, by providing some basic statistics derived from the signals as the GP terminals and following the procedures as described in this chapter, a fair solution program can be safely obtained from each program run and used as a descriptor for characterizing the signals. In other words, the prerequisite for a supervised training requirement is achieved by assigning a symbolic regression process for the GP system to follow and with an appropriate fitness function as a measure to distinguish different classes of signals.

One of the advantages of the GP method proposed here is the availability of solutions without substantial knowledge of the nature of the data involved except some basic statistical properties of the study target. In other words, GP has the flexibility with respect to the selection of operators at the non-terminal nodes and their random combinations of genetic processes applied to every intermediate terminal node, including the initial parameters, in the GP solution tree. Another advantage of using GP for classification is its applicability to very complex systems, where it is very hard to determine the relationship/connection between different observed characteristics, for example when identifying different persons by different features of their faces (Loizides, Slater *et al.* 2001; Bhanu, Yu *et al.* 2004). In this aspect, the GP system proposed here is an effective tool capable of providing alternative and possibly effective solutions for signal classification tasks.

Chapter 6 Discussion

This chapter discusses the results and issues that have been investigated in the previous sections. Comments on the experimental platform developed within the ESP project for the observation of epi-benthos are given in section 6.1. Issues which may have affected the analysis outcomes of the conventional methods are given in section 6.2. The GP issues are discussed in section 6.3.

6.1 The experimental platform: the ESP structure

By using the optical component of the ESP structure, reliable optical recordings were available within limited focus ranges. Clear images were only available between ranges of about 1 and 4 m. Moreover, acoustic recordings collected from ranges smaller than 1.5 m were difficult to process due to the ringing of the sonar head. These limitations reduced the number of useful samples. Those classes with insufficient number of samples were discarded from further investigations. Hence, limitations highlighted above reduced the data processing in this study to limited groups of data rather than on all available data.

A further upgrade of the observation platform will highly enhance its operational capabilities. By improving the way the optical system stored its optical data, the platform can remain longer in time in the water so that more abundant data can be available in each deployment.

Tilting of the ESP structure driven away from the normal incidence direction by currents was considered negligible. However, examination of the optical data still found occasional cases in which the ESP structure was away from the ideal normal incidence direction. Effects that may come from this aspect are unknown.

There were several factors which may affect the quality of the collected data. Due to the limited time windows available in the field and limited hardware resources available to this study, the data set obtained contained only limited samples with serious imbalances both in sample number and in diversity. These restrictions diminished the full potential capabilities of the whole ESP data collection system and hence may have influenced the quality and the scope of diversity of the acquired data for the data analysis requirements. For example, a total number of 1232 collected samples in the first field trial were left with only 435 perfect samples for use while a great portion of the discarded samples were identified useless for several reasons. With this limited and imbalanced data set, analyses of the data were difficult to have fair comparisons between groups of different habitat types. Due to this consideration, compromises were made in the data analysis by restricting the comparisons between data classes with comparable sample numbers. As a result, the accuracy of the conclusions made from this study should be proportional to the number of samples available. Study results from samples scarce in number are considered unreliable. Some of acoustic backscatter characteristics of seafloor vegetation are still poorely investigated and need further experimental and theoretical studies.

6.2 Conventional investigation results

When backscattering was from seagrass meadows or rough seafloors like the macro algae patches, enhanced backscatter level in the "tail", as described in the literature, was observed in this study. Since EPW is by definition an effective measure of the length of the "tail", it was found the most effective parameter capable of differentiating the difference between the sand and seagrass classes (see section 4.2.1.3).

In addition to statistics and EPW, other acoustic parameters such as fractals were investigated for their possible capabilities in characterizing backscatter signals (see section 4.2.1.4). A potential improvement for the use of fractal dimension in classification problems is the adoption of other approaches for the derivation of fractal dimension such as the spectrum inclination or box dimension instead of the approach used here. However, since it was not the author's intention to do an

exhaustive test of all the existing techniques for this problem, other alternative methods or parameters which might have better results than the ones obtained here are not considered in this study. For the parameters investigated in this study, the EPW gives an above average result.

Although the sea squirts had rough contours when comparing to the flat sandy bottoms, they did not exhibit any difference in the acoustic features when comparing against the sand class (see section 4.3.1). This could be due to the reason that the sonar system's best sampling resolution is not good enough to observe the existence of sea squirts on seafloors. Or, the use of the best parameter found (EPW) is still incapable of differentiating the tiny variations between the sea squirts and their surrounding substrates. To understand if there are any detection possibilities for the sea squirts, sonar systems of higher frequencies and higher sampling resolutions might be necessary.

Investigations of the dependence of the characterization parameters on range were made in section 4.3.3. The results indicated that any range dependence was not obvious. The major consideration is that the available data were collected from very limited ranges of observation, between 1 and 4 m. An investigation that can extend to longer ranges than those observed in this study is necessary in order to provide a definite conclusion.

When examining vegetation-covered seabeds, it is a critical issue in assigning a correct reference point on the echo envelopes for the identification of the vegetation's canopy. It was commonly accepted by the marine community that the maximum level was a good reference point for the designation of the study target's position. Investigation results (see section 4.1.3) indicated that the maximum level on the waveform was not an appropriate reference point for the indication of seagrass canopy height at 200 kHz. It is shown in this study that the echo front is a better reference point than the maximum on the echo envelope at this frequency.

RD was found an effective measure which gave acceptable estimate results for the seagrass canopy height after considering the sand's average RD value (see section 4.3.4). However, readers are reminded to understand that the estimated seagrass canopy height varied from around 10 to 50 cm, which should have been affected by the sampling rate of the sonar system at both frequencies. It is also true that the seagrass can move along with the currents so that its canopy height is not a static value but an instantaneous value changing with time.

6.2.1 Strengths and weeknesses of the characterization parameters and techniques used

The derivation of EPW for the characterization of seafloor vegetation was motivated by the evidence of long echo "tail" from seabeds with rough surfaces observed by previous researchers. From this evidence, EPW was hence defined to account for the echo "tail" aspect which in a hope could best describe the study targets. From the comparisons against other techniques in the previous chapters, EPW stands out from other parameters, such as the statistic moments, and characterizes the study targets with an above average discrimination performance. Though good in characterizing simple combinations of different classes, the EPW characteristic is still incapable of differentiating complex mixing types or classes of more than two. There is a need to find other parameters which could account for the acoustic properties of different seafloor types not being correlated with EPW.

LDA was among the multivariate methods which provided the best characterization capability for the two seafloor types investigated in this study. However, to be effective in characterization, the LDA method needs supplying robust input variables, such as the EPW and skewness, in order to derive a new variable as a parameter for distinguishing different classes in an effective way.

6.3 Application of GP algorithm to classification tasks

The investigation of the GP algorithm for this study was driven by the limited abilities of the conventional methods when applied on the classification problems. The study of GP was mainly for its potential abilities for the classification of acoustic backscatter data collected from the assorted habitat types. It is clear from the investigation results as shown in Chapter 5 that the GP system can provide not only versatile but also comparable solutions in performance for classification problems.

GP is totally different in concept from multivariate analyses such as the PCA with K-means or LDA. PCA can extract prominent components from each input parameter and differentiate the variation of the data with the PCs on a multi-dimensional space. However, the combined performance of the final selected PCs is

still limited by each input parameter's ability. There is no way that the performance of the final PCs selected can exceed that combined from all input parameters. The LDA approach also suffers from similar limitations. In contrast, as long as the FF of the GP system is able to provide a good way for the "individual" to genetically evolve into robust offspring, the GP system is capable of providing solutions with reasonable differentiation capabilities, which does not necessarily have to be weaker in performance than that combined from all the input parameters.

Different program runs gave different best-so-far solutions by combining operators and terminal parameters in a variety of forms. Since there is no universal rule to determine the number of the program runs needed to find an optimal solution, the best-so-far solution was selected based on to the solution performance of the testing program runs. Two solutions with similar performance can be derived from drastically different GP-tree forms. This makes it difficult to identify any branches in the GP-tree which are the most prominent roles in solving the classification problems.

The algorithm implemented in the GP system is applicable to any signal classification task as long as the task is under a supervised training condition. The GP algorithm implemented here is capable of providing as many solutions as needed for classifying the signals, which is an advantage inborn in the GP algorithm.

As shown in section 5.6.3, the GP system did not perform efficiently along the generations. The number of nodes and the GP-tree level could get further complicated while fitness has stalled if no appropriate measure is used. How to prevent the program code bloat and improve the efficiency in the GP program runs requires a great deal of understanding of the effects of those GP parameters, which is still under investigations by many researchers (Fernández, Galeano *et al.* 2004; Silva and Costa 2004; Luke and Panait 2006). Since these issues are far beyong the focus of this study, no further information is available from this study.

Chapter 7 Conclusions and Recommendations

This study investigated effective ways for the recognition and assessment of seafloor vegetation by using a single beam echosounder. The optical sub-system of the ESP structure was able to provide photographic pairs for groundtruthing purposes through the synchronization mechanism between the acoustic and optical components. The optical recordings obtained were able to provide support for the identification of the actual habitat type for each corresponding acoustic sample.

Data were mainly collected from shallow coastal waters near the author's study base, Perth, through the ESP project in 2004 and 2005. Measurements were mainly carried over sea bottoms of sandy seafloor, seagrass meadows, and rocky reefs populated with macro algae, corals, and other epi-benthos. Seagrass species of *P. sinuosa* and *P. australis* were the major plant benthos observed on the sandy sea bottoms. They were particularly focused on in this study due to their long term importance as an indicator for the estimate of impacts from natural forces and anthropological activities.

Collected data were firstly built into a database so that acoustic and optical data could be correctly linked. After classifying the acoustic data through the identification of the optical recordings, acoustic samples having been classified into different classes were then investigated for their possible characteristics by a few methods.

Below are the major conclusions and the important observations as a whole obtained from this study. They are divided into three parts: Literature review in section 7.1, Experimental materials in section 7.2, and Data analysis results in section 7.3.

7.1 Literature review

In this study, a detailed survey of the literature review pertinent to this study topic was done. It was systematically studied and discussed in Chapter 2. The study of the literature indicated that the earliest time of the study records of marine benthos by the acoustic methods, especially for seagrass, only began from around 1977 by Colantoni and Zucchini (see (Colantoni and Zucchini 1979)) and around 1980 by Maceina and Shireman (Maceina and Shireman 1980). It started a new page in history in that people started the use of sonar systems for the study of seagrass.

"Shading" and "tail" are the words most often used by the early scientists to describe the seagrass meadows or rough surface seafloors when using sonar systems. These words suggest that the characteristics of the epi-benthos may conceal their acoustic features in the levels after the maximum backscatter level on the echo envelope. When the pulses were backscattered from seagrass meadows or rough surface seafloors, increases of backscatter intensity and elongated duration in time were observed on the tail of the echo envelope.

While the study of animal benthos might be motivated by the needs for fishery, the study of plant benthos by acoustic methods involved a mixture of requirements from not only environmental concerns but also military needs for effective surveillance of explosive mines within seagrass meadows in shallow waters.

Recorded in literature as well are the techniques developed for the classification of acoustic backscatter signals for assorted applications. Among those techniques, PCA is the most revealing and popular one frequently used in the marine acoustic communities. Among the multivariate methods, LDA is the best in deriving the new variable for classification problems. However, none of them can provide perfect results for all cases.

From the literature review, the author was inspired to develop a new algorithm to provide alternative solutions for the classification problem. The study of the GP algorithm proved that the GP system developed here is capable of solving classification problems involving supervised training conditions.

7.2 Experimental materials

- The ESP structure used in this study is an excellent experimental platform for the observation of close range targets in shallow waters and within small areas when real time data observation and monitoring are necessary.
- The unique simultaneous firing mechanism of the ESP structure for both the acoustic and optical systems contributed to a production of a synchronized data set with acoustic and optical samples linked by their firing time for data classification requirements.
- The whole ESP system was quite portable and can be installed on small boats on reasonably calm waters for data collection purposes.
- Due to the design and the available data storage space in the optical system, one disadvantage of the ESP data collection system was the requirement of periodical retrievals of the wet end component back on board in order to download the photographic data and clear the memory space for the next new measurement in the water. This action interrupted the function of continuous observations for some specific targets and could cause difficulties in bringing the ESP structure back to the original observation position.
- Due to the inherent limitations of the optical system, the available operational ranges were limited within very short distances, which subsequently restricted the available acoustic data within very limited ranges. As a result, the investigation of the acoustic backscatter dependence on range seemingly can not provide any definite conclusion for the range dependence concern discussed in section 4.3.3.
- Awareness of the differences of the insonified areas between the 38 and 200 kHz of the EQ60 is important. The acoustic samples obtained by the 200 kHz were collected from a comparatively smaller footprint size than that obtained by the 38 kHz on a wider area surrounding that of the 200 kHz. Due to this difference, each pulse of the 200 kHz was unable to completely reflect what was actually observed by the 38

kHz although the insonified area by the 200 kHz was within that of the 38 kHz and this difference was corrected in the calculation for the acoustic parameters. It should be noted that there were still differences in species compositions and population densities between the two insonified areas of each collected acoustic sample although samples analysed were selected from those that can minimize the impact from the condition mentioned here.

- Uncertainties due to the operational factors in the field such as the tilting of the ESP structure in waters away from the normal incidence configuration were also experienced. Although operations were made over areas where waters were thought as calm as possible, imperfect conditions due to the unforeseen environmental factors were still inevitable and hence could have affected the accuracy of the investigation results. Improvement of a more controllable observation system than the present one is necessary in order to improve the observation result.

7.3 Data analysis results

- There was a difference between the detected ranges by the 38 and the 200 kHz in measuring the targets in the water. For flat sandy seafloors, the differences are negligible. But, for those measured from seagrass meadows or rough seafloors, the differences can be as high as the size of the study targets.
- Statistics showed that the maximum level on the acoustic backscatter waveform at 200 kHz is not an appropriate reference point in indicating the location of the seagrass canopy. When the seagrass canopy heights are comparable to the backscatter wave length, the use of the maximum backscatter strength as an indication of seagrass canopies can lead to misleading results. It is found in this study that the wave front is a better reference point than the maximum on the waveform in referring the seagrass canopy location.

- The RD value investigated in section 4.3.4 was found an effective measure for the seagrass canopy height. Although the error of the estimate of seagrass canopy height by RD may be as high as the number calculated, the estimated mean values for the seagrass canopy height by the use of RD were within a reasonable range and was consistent to both the historical recordings and the observations made by the optical system in this study.
- Fractal analysis on the acoustic backscatter signals was investigated for its possible ability for differentiation purposes. Results showed that this parameter was a poor classifier.
- Among the plant benthos, seagrass was particularly focused on, and exhibited unique acoustic features. As indicated in the article (Lyons and Abraham 1999), there is no easy way that the backscatter strength at vertical incidence can be used to effectively characterize the seagrass. However, it was found in this study that the EPW and RD were capable of providing reasonable estimates for the recognition and assessment of the seafloor vegetation against its sandy background. It is fortunate to know that seagrass only exists on sandy seafloors while live corals only grow on reefs. The understanding of the seagrass's neighbouring background can provide additional assistance for the identification of the seagrass by acoustics.
- Sea squirts were found in the field. They can not be differentiated from their background by the acoustic parameters investigated in this study. The backscatter intensity did not show any differences which can reveal their existence. Based on the understanding of the limited resolution abilities of the sonar systems used in this study and the sparse density and the comparably small size of the sea squirts observed in the field, recommendations for improving acoustic detection of sea squirts might be to use sonar systems with higher resolution capabilities than the one used in this study and to conduct additional complementary measurements using other approaches.
- When comparing the acoustic backscatter intensity between the sparsely and densely populated seagrass meadows as shown in section 4.3.5, the author could not find strong evidence which would prove

the model predicted by Shenderov, although the tendency was consistent with Shenderov's prediction (Shenderov 1998). The considerations were mainly their overlapping conditions given in Figure 4-24 and Figure 4-25 and the imbalance in number of samples between the two population density classes.

- The LDA classification algorithm performed better than the K-means method for the classification problems encountered in this study. However, its performance, like that of other multivariate methods, still strongly depends on the input parameters which should be robust enough for reliable classification result.
- The investigation results showed that the GP method provided advantages over the traditional methods in the affordability of many alternative solutions. The GP method provides a new approach to the classification problem, and is shown in this study that classification problems can be solved by the introduction of GP. For classification problems of more than two classes, it will require a further adjustment of the fitness function instead of the one provided in equation 5-1, in order to accommodate other mixing conditions of different habitat types.

References

Aioi, K., T. Komatsu *et al.* (1998). "The world's longest seagrass, *Zostera caulescens* from northeastern Japan." Aquatic Botany **61**(2): 87-93.

Akal, T. and J. Hovem (1978). "Two-dimensional space series analysis for sea-floor roughness." Marine Geotechnology **3**(2): 171-182.

Andrieux, N., P. Delachartre *et al.* (1995). "Lake-bottom recognition using a wideband sonar system and time-frequency analysis." The Journal of the Acoustical Society of America **98**(1): 552-559.

Atallah, L. and P. J. P. Smith (2003). "Using wavelet analysis to classify and segment sonar signals scattered from underwater sea beds." International Journal of Remote Sensing **24**(21): 4113-4128.

Babovic, V. and M. Keijzer (2000). "Genetic Programming as a model induction engine." Journal of Hydroinformatics **2**(1): 35-60.

Bäck, T. and H.-P. Schwefel (1993). "An overview of evolutionary algorithms for parameter optimization." Evolutionary Computation **1**(1): 1-23.

BAE Systems TAPS technical manual, Introducation**:** page 1.

Banzhaf, W., J. R. Koza *et al.* (2000). "Genetic Programming." IEEE Intelligent Systems and Their Applications **15**(3): 74-84.

Banzhaf, W., P. Nordin *et al.* (1998). Genetic Programming: an introduction: on the automatic evolution of computer programs and its applications, San Francisco, CA: Morgan Kaufmann.

Barton, R. J. and H. V. Poor (1988). "Signal detection in fractional Gaussian noise." IEEE Transactions on Information Theory **34**(5): 943-959.

Bates, C. R. and E. J. Whitehead (2001). "Echoplus measurements in Hopavågen Bay, Norway." Sea Technology **42**: 34-43.

Beaujean, P.-P. J. (1995). Sediment classification of the sea floor using the chirp sonar and the Biot model. Florida Atlantic University.

Bentrem, F. W., J. Sample *et al.* (2002). High-frequency acoustic sediment classification in shallow water. OCEANS '02. **1**: 7-11.

Benyahia, I. and J.-Y. Potvin (1998). "Decision support for vehicle dispatching using Genetic Programming." IEEE Transactions on Systems, Man and Cybernetics, Part A **28**(3): 306-314.

Berkson, J. M. and J. E. Matthews (1983). "Statistical properties of seafloor roughness." Acoustics and the Seabed: 215-223.

Berntsen, B., J. M. Hovem *et al.* (1999). Characterization of the seafloor using normal incidence acoustic backscattered time domain signals from a parametric sonar. OCEANS '99. **1**: 30-36.

Bett, B. J. (2001). "UK Atlantic margin environmental survey: Introduction and overview of bathyal benthic ecology." Continental Shelf Research **21**(8-10): 917-956.

Bhanu, B., J. Yu *et al.* (2004). Feature synthesis using Genetic Programming for face expression recognition. Genetic and Evolutionary Computation – GECCO 2004. K. Deb, R. Poli *et al.* Berlin / Heidelberg, Springer. **3103:** 896-907.

Bilgen, M. and J. H. Rose (1997). "Acoustic backscatter from materials with rough surfaces and finite size microstructure: Theory." The Journal of the Acoustical Society of America **101**(1): 264-271.

BioSonics Inc. (1994). "Use of an acoustic method for mapping seagrass density and location in Narrabeen Lagoon Australia." Retrieved 20/10, 2003, from http://www.biosonicsinc.com/matrix_nodes.cfm?step=2&row_id=2&col_id=4#tag21.

BioSonics Inc. (2001a). "Assessment of digital sonar technology to map eelgrass (*Zostera marina*) in the San Juan Islands." Retrieved 20/10, 2003, from http://www.biosonicsinc.com/doc_library/docs/Roche_Harbor_Report.pdf.

BioSonics Inc. (2001b). "Methods for bottom tracking in aquatic vegetation." Retrieved 20/10, 2003, from http://www.biosonicsinc.com/.

Bozzano, R., L. Castellano *et al.* (1998). Characterization of submerged aquatic vegetation by a sector-scanning sonar. The Fourth European Conference on Underwater Acoustics, Rome. **1**: 159-164.

Bozzano, R., R. Mantovani *et al.* (2002). Backscattering from seagrasses: an experience with a high frequency sector scanning sonar. The Sixth European Conference on Underwater Acoustics, ECUA'2002: 679-684.

Bozzano, R., R. Mantovani *et al.* (1998). Acoustic backscattering from marine vegetation. OCEANS '98, IEEE. **2**: 927-930.

Bozzano, R. and A. Siccardi (1997). Underwater vegetation detection in high frequency sonar images: A preliminary approach. The 9th International Conference on Image Analysis and Processing, Florence, Italy, Springer-Verlag London, UK. **2**: 576-583.

Brandes, H. G., A. J. Silva *et al.* (2001). "Physical and acoustic measurements on cohesionless sediments from the northwest Florida sand sheet." Geophysical Research Letters **28**(5): 823-826.

Brearley, A. and D. I. Walker (1995). "Isopod miners in the leaves of two Western Australian *Posidonia* species." Aquatic Botany **52**(3): 163-181.

Brehmer, P., F. Gerlotto *et al.* (2003). "New applications of hydroacoustic methods for monitoring shallow water aquatic ecosystems: the case of mussel culture grounds." Aquatic Living Resources **16**(3): 333-338.

Brown, C. J., A. Mitchell *et al.* (2005). "Mapping seabed habitats in the Firth of Lorn off the west coast of Scotland: evaluation and comparison of habitat maps produced using the acoustic ground-discrimination system, RoxAnn, and sidescan sonar." ICES Journal of Marine Science **62**(4): 790-802.

Burczynski, J. (2001). "Bottom classification." Retrieved 16/01, 2004, from http://www.biosonicsinc.com/search_doc.cfm?step=3&did=28.

Burczynski, J., J. Hoffman *et al.* (2001). "Use of acoustics for detecting aquatic vegetation." Retrieved 20 October, 2003, from http://www.ices.dk/reports/ftc/2001/joint01.pdf.

Butler, A. and P. Jernakoff (1999). Seagrass in Australia. Collingwood Vic 3006 Australia, CSIRO Publishing.

Caddell, S. E. (1998). "Application of an acoustic sea floor classification system for benthic habitat assessment." Journal of Shellfish Research **17**(5): 1459-1461.

Caiti, A. (2000). "Seafloor properties determination from acoustic backscattering at normal incidence with a parametric source." Journal of Computational Acoustics **8**(2): 365-388.

Cambridge, M. L. (1975). "Seagrasses of south-western Australia with special reference to the ecology of *Posidonia australis* Hook *f.* in a polluted environment." Aquatic Botany **1**: 149-161.

Cambridge, M. L., A. W. Chiffings *et al.* (1986). "The loss of seagrass in Cockburn Sound, Western Australia. II. Possible causes of seagrass decline." Aquatic Botany **24**(3): 269-285.

Cambridge, M. L. and P. J. Hocking (1997). "Annual primary production and nutrient dynamics of the seagrasses *Posidonia sinuosa* and *Posidonia australis* in south-western Australia." Aquatic Botany **59**(3-4): 277-295.

Cambridge, M. L. and J. Kuo (1979). "Two new species of seagrasses from Australia, *Posidonia sinuosa* and *P. angustifolia* (Posidoniaceae)." Aquatic Botany **6**: 307-328.

Cambridge, M. L. and J. Kuo (1982). "Morphology, anatomy and histochemistry of the Australian seagrasses of the genus *Posidonia* Konig (Posidoniaceae) III. *Posidonia sinuosa* Cambridge & Kuo." Aquatic Botany **14**: 1-14.

Cambridge, M. L. and A. J. McComb (1984). "The loss of seagrasses in Cockburn Sound, Western Australia. I. The time course and magnitude of seagrass decline in relation to industrial development." Aquatic Botany **20**(3-4): 229-243.

Carbó, R. and A. C. Molero (1997). "Scattering strength of a *Gelidium* biomass bottom." Applied Acoustics **51**(4): 343-351.

Carle, L., S. Bloomer *et al.* (2004). "Seabed classification and sediment transport on Roberts bank." Hydro International **8**(10): 29-31.

Caruthers, J. W. and C. A. Fisher (2002). Remote sediment classification using acoustical techniques. Mississippi, University of Southern Mississippi.

Cavazza, W., F. Immordino *et al.* (2000). "Sedimentological parameters and seagrasses distributions as indicators of anthropogenic coastal degradation at Monterosso Bay (Ligurian Sea, NW Italy)." Journal of Coastal Research **16**(2): 295-305.

Chakraborty, B., R. Kaustubha *et al.* (2001). "Acoustic seafloor sediment classification using self-organizing feature maps." IEEE Transactions on Geoscience and Remote Sensing **39**(12): 2722-2725.

Chakraborty, B., V. Mahale *et al.* (2007). "Acoustic characterization of seafloor habitats on the western continental shelf of India." ICES Journal of Marine Science **64**(3): 551-558.

Chami, M. and D. Robilliard (2002). "Inversion of oceanic constituents in case I and II waters with Genetic Programming algorithms." Applied Optics **41**(30): 6260-6275.

Chivers, R. C., N. Emerson *et al.* (1990). "New acoustic processing for underway surveying." Hydrographic Journal **56**: 9-17.

Chotiros, N. P., A. P. Lyons *et al.* (2002). "Normal incidence reflection loss from a sandy sediment." The Journal of the Acoustical Society of America **112**(5): 1831-1841.

Chu, D., P. H. Wiebe *et al.* (2000). Measurements of the material properties of live marine organisms and their influence on acoustic scattering. OCEANS 2000, RI, USA. **3**: 1963-1967.

Clarke, J. E. H., B. W. Danforth *et al.* (1997). Areal seabed classification using backscatter angular response at 95kHz. High frequency acoustics in shallow water, Lerici, Italy, NATO SACLANT Undersea Research Centre: 243-250.

Coast Protection Board. (2004). "Seagrasses of South Australia." 2004, from www.environment.sa.gov.au.

Colantoni, P., P. Gallignani *et al.* (1982). "Patterns of *Posidonia oceanica* (L.) Delile beds around the Island of Ischia (Gulf of Naples) and in adjacent waters." Marine Ecology **3**(1): 53-74.

Colantoni, P. and P. Zucchini (1979). "Underwater mapping of *Posidonia Oceanica* prairies around the Ischia island (Naples)." Rapp. Comm. Int. Mer Medit. **25/26**(6): 89-90.

Collier, J. S. and C. J. Brown (2005). "Correlation of sidescan backscatter with grain size distribution of surficial seabed sediments." Marine Geology **214**(4): 431-449.

Comisky, W., J. Yu *et al.* (2000). Automatic synthesis of a wire antenna using genetic programming. Genetic and Evolutionary Computation Conference, Las Vegas, Nevada, USA.

Dalachartre, P., D. Vray *et al.* (1992). Time-frequency analysis applied to sandy bottom echoes. Ultrasonics Symposium, Tucson, AZ. **1**: 345-348.

Davies, J., R. Foster-Smith *et al.* (1997). "Marine biological mapping for environment management using acoustic ground discrimination systems and geographic information systems." Underwater Technology **22**(4): 167-172.

Denbigh, P. N. (1989). "Swath bathymetry: principles of operation and an analysis of errors." IEEE Journal of Oceanic Engineering **14**(4): 289-298.

Di Massa, D. E. and K. F. Bosma (2000). Hydroacoustic measurement of detritus from the Delaware Bay estuary. OCEANS 2000, RI, USA. **3**: 1969-1973.

Dodge, Y. (2008). The concise encyclopedia of statistics. New York, NY, Springer-Verlag Berlin Heidelberg.

Downing, K. L. (2001). "Reinforced Genetic Programming." Genetic Programming and Evolvable Machines **2**(3): 259-288.

Duarte, C. M. (1987). "Use of echosounder tracings to estimate the aboveground biomass of submerged plants in lakes." Canadian Journal of Fisheries and Aquatic Sciences **44**(4): 732-735.

Duarte, C. M. (1991). "Seagrass depth limits." Aquatic Botany **40**(4): 363-377.

Dyer, C., K. Murphy *et al.* (1997). "An experimental study of sediment discrimination using 1st and 2nd echoes." SACLANTCEN Conference Proceedings Series CP-45, High Frequency Acoustics in Shallow Water: 139-146.

Elmore, P. A., M. D. Richardson *et al.* (2005). "Mine burial by scour in shallow seas: Prediction and experiments." Sea Technology **46**(3): 10-15.

Feder, J. (1988). Fractals. New York, Plenum Press.

Fenstermacher, L. E., G. B. Crawford *et al.* (2001). "Enhanced acoustic backscatter due to high abundance of sand dollars, *Dendraster excentricus*." Marine Georesources and Geotechnology **19**(2): 135-145.

Fernández, F., G. Galeano *et al.* (2004). Control of Bloat in Genetic Programming by Means of the Island Model. Lecture Notes in Computer Science : Parallel Problem Solving from Nature - PPSN VIII, Springer Berlin / Heidelberg. **3242:** 263-271.

Fisher, R. A. (1936). "The use of multiple measurements in taxonomic problems." Annals of Eugenics **7**(2): 179-188.

Fodale, M. F., C. R. Bronte *et al.* (2003). "Classification of lentic habitat for sea lamprey (*Petromyzon marinus*) larvae using a remote seabed classification device." Journal of Great Lakes Research **29**(Supplement 1): 190-203.

Fortin, G. R., L. Saint-Cyr *et al.* (1993). "Distribution of submersed macrophytes by echo-sounder tracings in lake Saint-Pierre, Quebec." Journal of Aquatic Plant Management **31**: 232-240.

Foster-Smith, R. L., C. J. Brown *et al.* (2004). "Mapping seabed biotopes at two spatial scales in the eastern English Channel. Part 2. Comparison of two acoustic ground discrimination systems." Journal of the Marine Biological Association of the UK **84**(3): 489-500.

Foster-Smith, R. L. and I. S. Sotheran (2003). "Mapping marine benthic biotopes using acoustic ground discrimination systems." International Journal of Remote Sensing **24**(13): 2761-2784.

Fox, C. G. and D. E. Hayes (1985). "Quantitative methods for analyzing the roughness of the seafloor." Reviews of Geophysics **23**(1): 1-48.

Freeman, S., S. Mackinson *et al.* (2004). "Diel patterns in the habitat utilisation of sandeels revealed using integrated acoustic surveys." Journal of Experimental Marine Biology and Ecology **305**(2): 141-154.

Freitas, R., A. M. Rodrigues *et al.* (2003). "Benthic biotopes remote sensing using acoustics." Journal of Experimental Marine Biology and Ecology **285**: 339-353.

Freitas, R., S. Silva *et al.* (2003). "Acoustic seabed classification of marine habitats: studies in the western coastal-shelf area of Portugal." ICES Journal of Marine Science **60**(3): 599-608.

Galloway, J. L. (2001). Benthic habitat mapping with acoustic seabed classification. OCEANS 2001. **4**: 2642-2644.

Gneiting, T. and M. Schlather. (2003). "Stochastic models that separate fractal dimension and Hurst effect." 2006, from http://www.stat.washington.edu/www/statistician/.

Godlewska, M., A. Swierzowski *et al.* (2004). "Hydroacoustics as a tool for studies of fish and their habitat." International Journal of Ecohydrology and Hydrobiology **4**(4): 417-427.

Goldstein, M. and W. R. Dillon (1978). Discrete discriminant analysis. New York, Wiley.

Gordon, D. M., K. A. Grey *et al.* (1994). "Changes to the structure and productivity of a *Posidonia sinuosa* meadow during and after imposed shading." Aquatic Botany **47**(3-4): 265-275.

Greenstreet, S. P. R., I. D. Tuck *et al.* (1997). "An assessment of the acoustic survey technique, RoxAnn, as a means of mapping seabed habitat." ICES Journal of Marine Science **54**(5): 939-959.

Hamilton, L. J. (2001). Acoustic seabed classification systems. DSTO. Fishermans Bend, DSTO Aeronautical and Maritime Research Laboratory.

Hamilton, L. J., P. J. Mulhearn *et al.* (1999). "Comparison of RoxAnn and QTC-View acoustic bottom classification system performance for the Cairns area, Great Barrier Reef, Australia." Continental Shelf Research **19**(12): 1577-1597.

Hastings, H. M. and G. Sugihara (1993). Fractals: A user's guide for the natural sciences. Oxford, Oxford University Press.

Hastings, K., P. Hesp *et al.* (1995). "Seagrass loss associated with boat moorings at Rottnest Island, Western Australia." Ocean & Coastal Management **26**(3): 225-246.

Hausdorff, F. (1918). "Dimension und äußeres Maß." Mathematische Annalen **79**(1-2): 157-179.

Heald, G. J. and N. G. Pace (1996). An analysis of 1st and 2nd backscatter for seabed classification. 3rd European Conference on underwater acoustics, Heraklion, Crete, Foundation for research and technology - Hellas. **2**: 649-654.

Hermand, J.-P. (2004a). Acoustic remote sensing of photosynthetic activity in seagrass beds. Handbook of Scaling Methods in Aquatic Ecology: Measurement, Analysis, Simulation. L. Seuront and P. G. Strutton. Florida, CRC Press LLC**:** Chapter 5, 65-96.

Hermand, J.-P. (2004b). Photosynthesis of seagrasses observed in situ from acoustic measurements. OCEANS '04. **1**: 433-437.

Hermand, J.-P., P. Nascetti *et al.* (1998). Inversion of acoustic waveguide propagation features to measure oxygen synthesis by *Posidonia oceanica*. OCEANS '98. **2**: 919-926.

Hermand, J.-P., P. Nascetti *et al.* (1999). "Inverse acoustical determination of photosynthetic oxygen productivity of *Posidonia* seagrass." SACLANTCEN Memoranda Retrieved 20/10, 2003, from http://www.saclantc.nato.int/abstracts/sm/sm366.html.

Hoffman, J. C., J. Burczynski *et al.* (2002). "Digital acoustic system for ecosystem monitoring and mapping: assessment of fish, plankton, submersed aquatic vegetation, and bottom substrata." Retrieved 20/10, 2003, from http://www.biosonicsinc.com/.

Holland, J. H. (1992). "Genetic Algorithms." Scientific American **267**(1): 66-72.

Howell, K. L., D. S. M. Billett *et al.* (2002). "Depth-related distribution and abundance of seastars (Echinodermata: Asteroidea) in the Porcupine Seabight and Porcupine Abyssal Plain, N.E. Atlantic." Deep Sea Research Part I: Oceanographic Research Papers **49**(10): 1901-1920.

Humborstad, O.-B., L. Nottestad *et al.* (2004). "RoxAnn bottom classification system, sidescan sonar and video-sledge: spatial resolution and their use in assessing trawling impacts." ICES Journal of Marine Science **61**(1): 53-63.

Hundley, A. and K. Denning (1994). Report on the use of an acoustic method for mapping seagrass density and location, Unpublished report by Offshore Scientific Services Pty Ltd**:** 11.

Hundley, A., K. Zabloudil *et al.* (1994). A review of acoustic application for Marine Resource Examination and Monitoring. The Sixth Pacific congress on marine science & technology, Townsville, James Cook University of North Queensland.

Hurst, H. E. (1951). "Long-term storage capacity of reservoirs." Transactions of the American Society of Civil Engineers **116**: 770-808.

Hurst, H. E. (1952). The Nile: a general account of the river and the utilization of its waters. London, Constable.

Hutin, E., Y. Simard *et al.* (2005). "Acoustic detection of a scallop bed from a single-beam echosounder in the St. Lawrence." ICES Journal of Marine Science **62**(5): 966-983.

Isakovich, M. A. (1969). "Wave scattering from a statistically rough surface." Trudy Akusticheskogo Instituta AN SSSR (in Russian) **5**: 152-251.

Ivakin, A. N. (1998). Models for seafloor roughness and volume scattering. OCEANS '98. **1**: 518-521.

Jackson, D. R. and K. B. Briggs (1992). "High-frequency bottom backscattering: roughness versus sediment volume scattering." The Journal of the Acoustical Society of America **92**(2, Part 1): 962-977.

Jackson, D. R., D. P. Winebrenner *et al.* (1986). "Application of the composite roughness model to high-frequency bottom backscattering." The Journal of the Acoustical Society of America **79**(5): 1410-1422.

Jernakoff, P. and J. Nielsen (1998). "Plant-animal associations in two species of seagrasses in Western Australia." Aquatic Botany **60**(4): 359-376.

Johnson, J. T. (2002). "A numerical study of scattering from an object above a rough surface." IEEE Transactions on Antennas and Propagation **50**(10): 1361-1367.

Johnson, J. T. and R. J. Burkholder (2004). "A study of scattering from an object below a rough surface." IEEE Transactions on Geoscience and Remote Sensing **42**(1): 59-66.

Jordan, A., M. Lawler *et al.* (2005). "Seabed habitat mapping in the Kent Group of islands and its role in marine protected area planning." Aquatic Conservation: Marine and Freshwater Ecosystems **15**(1): 51-70.

Kaiser, H. F. (1960). "The application of electronic computers to factor analysis." Educational and Psychological Measurement **20**: 141-151.

Keiffer, R. S. and J. C. Novarini (2000). "A time domain rough surface scattering model based on wedge diffraction: Application to low-frequency backscattering from two-dimensional sea surfaces." The Journal of the Acoustical Society of America **107**(1): 27-39.

Kendrick, G. A., M. J. Aylward *et al.* (2002). "Changes in seagrass coverage in Cockburn Sound, Western Australia between 1967 and 1999." Aquatic Botany **73**(1): 75-87.

Kendrick, G. A., J. Eckersley *et al.* (1999). "Landscape-scale changes in seagrass distribution over time: a case study from Success Bank, Western Australia." Aquatic Botany **65**(1-4): 293-309.

Kendrick, G. A., B. J. Hegge *et al.* (2000). "Changes in seagrass cover on Success and Parmelia Banks, Western Australia between 1965 and 1995." Estuarine, Coastal and Shelf Science **50**(3): 341-353.

Kendrick, G. A., M. Waycott *et al.* (1997). Two Peoples Bay seagrass study. University of Western Australia. (Unpublished report).

Keulen, M. v. and M. A. Borowitzka (2003). "Seasonal variability in sediment distribution along an exposure gradient in a seagrass meadow in Shoalwater Bay, Western Australia." Estuarine, Coastal and Shelf Science **57**(4): 587-592.

Kirkman, H. (1985). "Community structure in seagrasses in southern Western Australia." Aquatic Botany **21**(4): 363-375.

Kirkman, H. (1997). Seagrasses of Australia. Australia: State of the environment technical paper series (Estuaries and the sea). Department of the Environment. Canberra.

Kirkman, H. (1999). "Pilot experiments on planting seedlings and small seagrass propagules in Western Australia." Marine Pollution Bulletin **37**(8-12): 460-467.

Kirkman, H. and J. Kirkman (2000). "Long-term seagrass meadow monitoring near Perth, Western Australia." Aquatic Botany **67**(4): 319-332.

Kirkman, H. and J. Kuo (1990). "Pattern and process in southern Western Australian seagrasses." Aquatic Botany **37**(4): 367-382.

Kloser, R. J., N. J. Bax *et al.* (2001). "Remote sensing of seabed types in the Australian South East Fishery; development and application of normal incident acoustic techniques and associated 'ground truthing'." Marine and Freshwater Research **52**(4): 475-489.

Komatsu, T., C. Igarashi *et al.* (2003). "Use of multi-beam sonar to map seagrass beds in Otsuchi Bay on the Sanriku Coast of Japan." Aquatic Living Resources **16**(3): 223-230.

Komatsu, T. and K. Tatsukawa (1998). "Mapping of *zostera marina* L. beds in Ajino Bay, Seto Inland Sea, Japan, by using echo-sounder and global positioning systems." Journal de Recherche Oceanographique **23**(2): 39-46.

Kostylev, V. E., R. C. Courtney *et al.* (2003). "Stock evaluation of giant scallop (*Placopecten magellanicus*) using high-resolution acoustics for seabed mapping." Fisheries Research **60**(2-3): 479-492.

Koza, J. R. (1992). Genetic Programming: on the programming of computers by means of natural selection. Boston, MA, MIT Press.

Koza, J. R. (1994). "Genetic Programming as a Means for Programming Computers by Natural-Selection." Statistics and Computing **4**(2): 87-112.

Koza, J. R. (2003). Genetic programming: Automatic synthesis of topologies and numerical parameters. Handbook of Metaheuristics. K. G. Glover FW. **57:** 83-104.

Koza, J. R., F. H. Bennett *et al.* (1999). Genetic programming as a Darwinian invention machine. Genetic Programming. **1598:** 93-108.

Koza, J. R., M. A. Keane *et al.* (2005). Human-competitive automated engineering design and optimization by means of genetic programming. Evolutionary Algorithms and Intelligent Tools in Engineering Optimization**:** 294-321.

Koza, J. R., M. A. Keane *et al.* (2000). "Automatic creation of human-competitive programs and controllers by means of Genetic Programming." Genetic Programming and Evolvable Machines **1**(1): 121-164.

Kuo, J. (1978). "Morphology, anatomy and histochemistry of the Australian seagrasses of the genus *Posidonia* könig (Posidoniaceae). I. Leaf blade and leaf sheath of *Posidonia australis* Hook. *f*." Aquatic Botany **5**: 171-190.

Kuo, J. (1993). "Root anatomy and rhizosphere ultrastructure in tropical seagrasses." Australian Journal of Marine and Freshwater Research **44**(1): 75-84.

Kuo, J. and M. L. Cambridge (1978). "Morphology, anatomy and histochemistry of the Australian seagrasses of the genus *Posidonia* könig (Posidoniaceae). II. Rhizome and root of *Posidonia australis* Hook. *f*." Aquatic Botany **5**: 191-206.

Kuo, J., H. Iizumi *et al.* (1990). "Fruit anatomy, seed-germination and seedling development in the Japanese seagrass *Phyllospadix* (Zosteraceae)." Aquatic Botany **37**(3): 229-245.

Kuo, J. and H. Kirkman (1990). "Anatomy of viviparous seagrasses seedlings of *Amphibolis* and *Thalassodendron* and their nutrient supply." Botanica Marina **33**(1): 117-126.

Kuo, J. and A. J. McComb (1989). Seagrass taxonomy, structure and development. Biology of seagrasses. A treatise on the biology of seagrasses with special reference to the Australian region. A. W. D. Larkum, A. J. McComb *et al.* Amsteredam, Elsevier**:** 6-73.

Lambert, D. N., D. J. Walter *et al.* (1998). Developments in acoustic sediment classification. OCEANS '98. **1**: 26-31.

Langdon, W. B. (1998). Genetic Programming and Data Structures: Genetic Programming + Data Structures = Automatic Programming! Massachusetts, Springer.

Langdon, W. B. and R. Poli (2002). Foundations of Genetic Programming, Springer.

Langeland, K. A. (1996). "*Hydrilla verticillata* (L.F.) Royle (Hydrocharitaceae), "The perfect aquatic weed"." Castanea **61**(3): 293-304.

Lee, K.-S., F. T. Short *et al.* (2004). "Development of a nutrient pollution indicator using the seagrass, *Zostera marina*, along nutrient gradients in three New England estuaries." Aquatic Botany **78**(3): 197-216.

Lee Long, W. J., L. J. McKenzie *et al.* (1998). Preliminary evaluation of an acoustic technique for mapping tropical seagrass habitats. G. B. R. M. P. Authority. Townsville**:** 29.

Legendre, P. (2002). Acoustic seabed classification methodology: a user's statistical comparison. Montréal, Université de Montréal**:** 17.

Libicki, C., K. W. Bedford *et al.* (1989). "The interpretation and evaluation of a 3-Mhz acoustic backscatter device for measuring benthic boundary layer sediment dynamics." The Journal of the Acoustical Society of America **85**(4): 1501-1511.

Linton, D. M. and G. F. Warner (2003). "Biological indicators in the Caribbean coastal zone and their role in integrated coastal management." Ocean & Coastal Management **46**(3-4): 261-276.

Liong, S.-Y., T. R. Gautam *et al.* (2002). "Genetic programming: A New paradign in rainfall runoff modeling." Journal of the American Water Resources Association **38**(3): 705.

Liu, J.-Y., C.-F. Huang *et al.* (2002). "Acoustic plane-wave scattering from a rough surface over a random fluid medium." Ocean Engineering **29**: 915-930.

Liu, J.-Y., S.-H. Tsai *et al.* (2004). "Acoustic wave reflection from a rough seabed with a continuously varying sediment layer overlying an elastic basement." Journal of Sound and Vibration **275**(3-5): 739-755.

Loizides, A., M. Slater *et al.* (2001). Measuring facial emotional expressions using genetic programming. 6th World Conference on Soft Computing in Industrial Applications, on the World Wide Web.

Luke, S. and L. Panait (2002). Lexicographic parsimony pressure. GECCO 2002: The Genetic and Evolutionary Computation Conference, New York, Morgan Kaufmann Publishers: 829-836.

Luke, S. and L. Panait (2006). "A comparison of bloat control methods for Genetic Programming." Evolutionary Computation **14**(3): 309-344.

Lyons, A. P. and D. A. Abraham (1999). "Statistical characterization of high-frequency shallow-water seafloor backscatter." The Journal of the Acoustical Society of America **106**(3): 1307-1315.

Lyons, A. P. and E. Pouliquen (1998). "Measurements of high-frequency acoustic scattering from seabed vegetation." The Journal of the Acoustical Society of America **103**(5): 2934.

Lyons, A. P., E. Pouliquen *et al.* (1998). "The impact of anisotropic roughness on acoustic interaction with the seafloor." The Journal of the Acoustical Society of America **104**(3): 1812.

MacArthur, L. D. and G. A. Hyndes (2001). "Differential use of seagrass assemblages by a suite of odacid species." Estuarine, Coastal and Shelf Science **52**(1): 79-90.

Maceina, M. J. and J. V. Shireman (1980). "The use of a recording fathometer for determination of distribution and biomass of *hydrilla*." Journal of Aquatic Plant Management **18**: 34-39.

Mackinson, S., K. Turner *et al.* (2005). "Using acoustics to investigate changes in efficiency of a sandeel dredge." Fisheries Research **71**(3): 357-363.

Madsen, J. A. (2004). Benthic and sub-benthic mapping of Delaware's coastal areas for natural resource management – Pilot study. Newark, University of Delaware**:** 51.

Magorrian, B., M. Service *et al.* (1995). "An acoustic bottom classification survey of strangford-lough, Northern-Ireland." Journal of the marine biological association of the United Kingdom **75**(4): 987-992.

Mandelbrot, B. (1967). "How long is the coast of Britain? Statistical self-similarity and fractional dimension." Science **156**(3775): 636-638.

Mandelbrot, B. B. (1984). Les objets fractals: forme, hasard et dimension. Paris, Flammarion.

Mandelbrot, B. B. and J. A. Wheeler (1983). "The Fractal Geometry of Nature." American Journal of Physics **51**(3): 286-287.

Marba, N., R. Santiago *et al.* (2006). "Seagrass (*Posidonia oceanica*) vertical growth as an early indicator of fish farm-derived stress." Estuarine Coastal and Shelf Science **67**(3): 475-483.

Marbà, N. and D. I. Walker (1999). "Growth, flowering, and population dynamics of temperate Western Australian seagrasses." Marine Ecology-Progress Series **184**: 105-118.

Masini, R. J., J. L. Cary *et al.* (1995). "Effects of light and temperature on the photosynthesis of temperate meadow-forming seagrasses in Western Australia." Aquatic Botany **49**(4): 239-254.

McCarthy, E. M. and B. Sabol (2000). Acoustic characterization of submerged aquatic vegetation: military and environmental monitoring applications. OCEANS 2000, RI, USA. **3**: 1957-1961.

McKenzie, L. J. (1994). "Seasonal changes in biomass and shoot characteristics of a *Zostera capricorni* Aschers. Dominant meadow in Cairns Harbour, northern Queensland." Australian Journal of Marine and Freshwater Research **45**(7): 1337-1352.

McMahon, K. and D. I. Walker (1998). "Fate of seasonal, terrestrial nutrient inputs to a shallow seagrass dominated embayment." Estuarine, Coastal and Shelf Science **46**(1): 15-25.

Medwin, H. and C. S. Clay (1998). Fundamentals of acoustical oceanography, Academic Press.

Michalopoulou, Z.-H., D. Alexandrou *et al.* (1994). "Application of a maximum likelihood processor to acoustic backscatter for the estimation of seafloor roughness parameters." The Journal of the Acoustical Society of America **95**(5): 2467-2477.

Miner, S. P. (1993). Application of acoustic hydrosurvey technology to the mapping of eelgrass (*Zostera marina*) distribution in Humboldt bay, California. Coastal Zone '93: The eighth Symposium on Coastal and Ocean Management, New Orleans, Louisiana. **3**: 2429-2442.

Molz, F. J., H. H. Liu *et al.* (1997). "Fractional Brownian motion and fractional Gaussian noise in subsurface hydrology: A review, presentation of fundamental properties, and extensions." Water Resources Research **33**(10): 2273-2286.

Moreno, A., P. Siljestrom *et al.* (1998). Benthic phanerogam species recognition in side scan sonar images: importance of the sensor direction. The Fourth European Conference on Underwater Acoustics, Rome, Italy, CNR-IDAC. **1**: 173-178.

Moreton Bay Waterways and Catchments Partnership. (2002). "*Lyngbya* management strategy." from http://www.epa.qld.gov.au/register/p00540aa.pdf.

Moyer, R. P., B. Riegl *et al.* (2005). "Assessing the accuracy of acoustic seabed classification for mapping coral reef environments in South Florida (Broward County, USA)." Revista de Biologia Tropical **53**(Supplement 1): 175-184.

Naidu, K. S. and E. M. Seward (2003). The use of acoustic ground discrimination as a precursor to the estimation of shellfish abundance. OCEANS 2003. **5**: P2736-P2738.

NOAA Coastal Services Center. (2005). "Managing a nuisance aquatic plant." Retrieved 24 April, 2006, from http://www.csc.noaa.gov/crs/rs_apps/issues/sb_ulva.htm.

Noel, C., C. Viala *et al.* (2006). "Acoustic characterization of underwater vegetations." Retrieved 22 August, 2006, from http://www.tvt.fr/.

Novarini, J. C. and J. W. Caruther (1998). "A simplified approach to backscattering from a rough seafloor with sediment inhomogeneities." IEEE Journal of Oceanic Engineering **23**(3): 157-166.

Ogilvy, J. A. (1987). "Wave scattering from rough surfaces." Reports on Progress in Physics **50**: 1553-1608.

Ogilvy, J. A. (1991). Theory of wave scattering from random rough surfaces. Bristol, Adam Hilger.

Orłowski, A. (1984). "Application of multiple echoes energy measurements for evaluation of sea bottom type." Oceanologia **19**: 61-78.

Orr, M. H. and D. C. Rhoads (1982). "Acoustic imaging of structures in the upper 10 cm of sediments using a megahertz backscattering system: Preliminary results." Marine Geology **46**(1-2): 117-129.

Pace, N. G., K. S. Al-Hamdani *et al.* (1985). "Range dependence of normal incidence acoustic backscatter from a rough surface." The Journal of the Acoustical Society of America **77**(1): 101-112.

Paling, E. I. and A. J. McComb (2000). "Autumn biomass, below-ground productivity, rhizome growth at bed edge and nitrogen content in seagrasses from Western Australia." Aquatic Botany **67**(3): 207-219.

Paling, E. I., M. van Keulen *et al.* (2001). "Mechanical seagrass transplantation in Western Australia." Ecological Engineering **16**(3): 331-339.

Panda, S., L. R. LeBlanc *et al.* (1994). "Sediment classification based on impedance and attenuation estimation." The Journal of the Acoustical Society of America **96**(5 I): 3022-3035.

Pasqualini, V., C. Pergent-Martini *et al.* (1998). "Mapping of *Posidonia oceanica* using aerial photographs and side scan sonar: application off the Island of Corsica (France)." Estuarine, Coastal and Shelf Science **47**: 359-367.

Peters, E. E. (1994). Fractal market analysis: applying Chaos theory to investment and Economics, J. Wiley & Sons New York.

Phillips, R. C. and E. G. Meñez (1988). "Seagrasses." Smithsonian contributions to the marine sciences **34**: 85-89.

Piazzi, L., S. Acunto *et al.* (2000). "Mapping of *Posidonia* oceanica beds around Elba Island (western Mediterranean) with integration of direct and indirect methods." Oceanologica Acta **23**(3): 339-346.

Pinn, E. H. and M. R. Robertson (1998). "The effect of bioturbation on RoxAnn®, a remote acoustic seabed discrimination system." Journal of the Marine Biological Association of the United Kingdom **78**(3): 707-715.

Pinn, E. H. and M. R. Robertson (2001). "Further analysis of the effect of bioturbation by *Nephrops norvegicus* (L.) on the acoustic return of the RoxAnn(TM) seabed discrimination system." ICES Journal of Marine Science **58**(1): 216-219.

Pinn, E. H. and M. R. Robertson (2003). "Effect of track spacing and data interpolation on the interpretation of benthic community distributions derived from RoxAnn™ acoustic surveys." ICES Journal of Marine Science **60**(6): 1288-1297.

Pinn, E. H., M. R. Robertson *et al.* (1998). "Broad-scale benthic community analysis in the Greater Minch Area (Scottish west coast) using remote and nondestructive techniques." International Journal of Remote Sensing **19**(16): 3039-3054.

Pouliquen, E. and X. Lurton (1992). Sea-bed identification using echosounder signal. European Conference on Underwater Acoustics, Luxembourg, Elsevier Applied Science: 535-538.

Preston, J. M., D. R. Parrott *et al.* (2003). Sediment classification based on repetitive multibeam bathymetry surveys of an offshore disposal site. OCEANS 2003. **1**: 69-75.

Richardson, M., P. Valent *et al.* (2001). NRL Mine Burial Experiments. The Second Australian-American Joint Conference on Technologies of Mine Countermeasures, Sydney, Australia.

Riegl, B. M., R. P. Moyer *et al.* (2005). "Determination of the distribution of shallow-water seagrass and drift algae communities with acoustic seafloor discrimination." Revista de Biologia Tropical **53**(Supplement 1): 165-174.

Riegl, B. M., S. J. Purkis *et al.* (2005). "Distribution and seasonal biomass of drift macroalgae in the Indian River Lagoon (Florida, USA) estimated with acoustic seafloor classification (QTCView, Echoplus)." Journal of Experimental Marine Biology and Ecology **326**(1): 89-104.

Sabol, B. (2002). "Hydrographic surveying in dense aquatic vegetation. Digital signal processing for improved bottom tracking." Hydro International **6**(5): 7-9.

Sabol, B., D. J. Shafer *et al.* (2005). "Dredging effects on eelgrass (*Zostera marina*) in a New England small boat harbor." Journal of Marine Environmental Engineering **8**(1): 57-81.

Sabol, B. M. (1984). Development and use of the Waterways Experiment Station 's hydraulically operated submersed aquatic plant sampler. Ecological Assessment of Macrophyton: Collection, Use and Meaning of Data. W. M. Dennis and B. G. Isom. Philadelphia, ASTM International**:** 46-57.

Sabol, B. M. (2005). "An explicit approach to detecting and characterizing submersed aquatic vegetation using a single-beam digital echosounder." The Journal of the Acoustical Society of America **118**(3): 1908.

Sabol, B. M. and J. Burczinski (1998). Digital echo sounder system for characterizing vegetation in shallow-water environments. The Fourth European Conference on Underwater Acoustics, Rome. **1**: 165-171.

Sabol, B. M., J. Burczynski *et al.* (2002). Advanced digital processing of echo sounder signals for characterization of very dense submersed aquatic vegetation. Aquatic Plant Control Research Program. US Army Corps of Engineers. Washington, DC, US Army Corps of Engineers**:** 18.

Sabol, B. M. and S. A. Johnston (2001). Innovative techniques for improved hydroacoustic bottom tracking in dense aquatic vegetation. Aquatic Plant Control Research Program. Washington, DC, U.S. Army Corps of Engineers**:** 16.

Sabol, B. M. and R. E. Melton Jr. (1995). Development of an automated system for detection and mapping of submersed aquatic vegetation with hydroacoustic and global positioning system technologies, report 1 - The Submersed Aquatic Vegetation Early Warning System (SAVEWS) - System description and user's guide (Version 1.0).

Sabol, B. M., R. E. Melton, Jr. *et al.* (2002). "Evaluation of a digital echo sounder system for detection of submersed aquatic vegetation." Estuaries **25**(1): 133-141.

Sabol, B. M. and R. M. Stewart (2005). Automated hydroacoustic mapping of submersed aquatic vegetation: Application in Lake St. Clair. International Association for Great Lakes Research, 2205 Commonwealth Boulevard Ann Arbor MI 48105 USA.: 105.

Schlagintweit, G. E. O. (1993). Real-time acoustic bottom classification for hydrography a field evaluation of RoxAnn. OCEANS '93, Victoria, BC, Canada. **3**: III/214-III/219.

Schneider, P., J. Burczynski *et al.* (2001). Results from submerged aquatic plant assessment using digital echosounder technique. ICES.

Seaman, R., M. Finkbeiner *et al.* (2000). Application of single-beam acoustics to macro-algae bloom management. OCEANS 2000, Providence, RI. **3**: 1703-1705.

Seber, G. A. F. (2004). Multivariate observations. Hoboken, N.J., Wiley-Interscience.

Self, R. F. L., P. A'Hearn *et al.* (2001). "Effects of macrofauna on acoustic backscatter from the seabed: Field manipulations on West Sound, Orcas Island, Washington, U.S.A." Journal of Marine Research **59**(6): 991-1020.

Sette, S. and L. Boullart (2001). "Genetic programming: principles and applications." Engineering Applications of Artificial Intelligence **14**(6): 727-736.

Sharma, S. (1996). Applied multivariate techniques. New York, J. Wiley.

Shenderov, E. L. (1998). "Some physical models for estimating scattering of underwater sound by algae." The Journal of the Acoustical Society of America **104**(2): 791-800.

Shono, K., T. Komatsu *et al.* (2004). Integrated hydro-acoustic survey scheme for mapping of sea bottom ecology. OCEANS '04. **1**: 423-427.

Siccardi, A. and R. Bozzano (2000). A test at sea for measuring acoustic backscatter from marine vegetation. Experimental acoustic inversion methods for exploration of the shallow water environment. A. Caiti, J. Hermand *et al.* Dordrecht, Kluwer Academic Publishers**:** 145-160.

Siccardi, A., R. Bozzano *et al.* (1997). Seabed vegetation analysis by a 2 MHz sonar. OCEANS '97. **1**: 344-350.

SIGEVO (2006). Special interest group on genetic and evolutionary computation.

Silberstein, K., A. W. Chiffings *et al.* (1986). "The loss of seagrass in cockburn sound, Western Australia. III. The effect of epiphytes on productivity of *Posidonia australis* Hook. f." Aquatic Botany **24**(4): 355-371.

Siljeström, P., A. Moreno *et al.* (2002). "Selectivity in the acoustic response of *Cymodocea nodosa* (Ucria) Ascherson." International Journal of Remote Sensing **23**(14): 2869-2876.

Siljeström, P. A., J. Rey *et al.* (1996). "Characterization of phanerogam communities (*Posidonia oceanica* and *Cymodocea nodosa*) using side-scan-sonar images." ISPRS Journal of Photogrammetry and Remote Sensing **51**(6): 308-315.

Silva, S. and E. Costa (2004). Dynamic limits for bloat control.

Simons, J. D., T. M. Soniat *et al.* (1992). "An improved method for mapping oyster bottom using a global positioning system and an acoustic profiler." Journal of Shellfish Research **11**(2): 431-436.

Simrad EQ60 Technical specifications**:** page 1.

Siwabessy, P. J. W. (2001). An investigation of the relationship between seabed type and benthic and bentho-pelagic biota using acoustic techniques. Curtin University of Technology.

Siwabessy, P. J. W., Y.-T. Tseng *et al.* (2004). Seabed habitat mapping in coastal waters using a normal incident acoustic technique. Acoustics 2004, Transportation Noise and Vibration - The New Millennium, Gold Coast, Australia, Australian Acoustical Society: 187-192.

Smith, G. F., D. G. Bruce *et al.* (2001). "Remote acoustic habitat assessment techniques used to characterize the quality and extent of oyster bottom in the Chesapeake Bay." Marine Geodesy **24**(3): 171-189.

Smith, G. F. and K. N. Greenhawk (1998). "Shellfish benthic habitat assessment in the Chesapeake Bay: Progress toward integrated technologies for mapping and analysis." Journal of Shellfish Research **17**(5): 1433-1437.

Smith, N. M. and D. I. Walker (2002). "Canopy structure and pollination biology of the seagrasses *Posidonia australis* and *P. sinuosa* (Posidoneaceae)." Aquatic Botany **74**(1): 57-70.

Smith, P. W. H. (2000). Controlling code growth in Genetic Programming. Advances in Soft Computing, De Montfort University, Leicester, UK, Physica-Verlag: 166–171.

Smith, P. W. H. and K. Harries (1998). "Code growth, explicitly defined introns, and alternative selection schemes." Evolutionary Computation **6**(4): 339-360.

Sotheran, I. S., R. L. Foster-Smith *et al.* (1997). "Mapping of marine benthic habitats using image processing techniques within a raster-based geographic information system." Estuarine, Coastal and Shelf Science **44**(Supplement A): 25-31.

Spratt, J. D. (1989). "The distribution and density of eelgrass, *Zostera marina*, in Tomales Bay, California." California Fish and Game **75**(4): 204-212.

Stanton, T. K. (1984). "Sonar estimates of seafloor microroughness." The Journal of the Acoustical Society of America **75**(3): 809-818.

Stanton, T. K. (1985). "Echo fluctuations from the rough seafloor: Predictions based on acoustically measured microrelief properties." The Journal of the Acoustical Society of America **78**(2): 715-721.

Stanton, T. K., D. Chu *et al.* (1991). "Estimating unresolved roughness from echo amplitude fluctuations." The Journal of the Acoustical Society of America **90**(4): 2231.

Stent, C. J. and S. Hanley (1985). "A recording echo sounder for assessing submerged aquatic plant populations in shallow lakes." Aquatic Botany **21**(4): 377-394.

Stewart, R. (2004). Genetic Programming: Computers that program themselves. Williams College. 7. (Lecture material, CSCI 373 Artificial Intelligence).

Sun, R., F. Tsung *et al.* (2004). "Combining bootstrap and genetic programming for feature discovery in diesel engine diagnosis." International Journal of Industrial Engineering-Theory Applications and Practice **11**(3): 273-281.

Taylor, J. A., C. E. Vincent *et al.* (1998). Three-dimensional sediment transport measurements by acoustics (TRIDISMA). OCEANS '98. **2**: 1108-1114.

Tęgowski, J. (2002). Acoustical recognition of the bottom sediments in the southern Baltic Sea. 3rd European Congress on Acoustics, Forum Acusticum 2002, Sevilla, España.

Tęgowski, J. (2005). "Acoustical classification of the bottom sediments in the southern Baltic Sea." Quaternary International **130**(1): 153-161.

Tęgowski, J., N. Gorska *et al.* (2003). "Statistical analysis of acoustic echoes from underwater meadows in the eutrophic Puck Bay (southern Baltic Sea)." Aquatic Living Resources **16**: 215-221.

Thomas, T. R., B. G. Rosen *et al.* (1999). "Fractal characterisation of the anisotropy of rough surfaces." Wear **232**(1): 41-50.

Thorne, P. D. and D. M. Hanes (2002). "A review of acoustic measurement of small-scale sediment processes." Continental Shelf Research **22**(4): 603-632.

Thorne, P. D., P. J. Hardcastle *et al.* (1998). Application of acoustics for measuring nearbed sediment processes: an integrated approach. OCEANS '98. **1**: 438-441.

Thorne, P. D., P. J. Hardcastle *et al.* (1994). "On the use of acoustics for measuring shallow water suspended sediment processes." IEEE Journal of Oceanic Engineering **19**(1): 48-57.

Thorsos, E. I. (1988). "The validity of the Kirchhoff approximation for rough surface scattering using a Gaussian roughness spectrum." The Journal of the Acoustical Society of America **83**(1): 78-92.

Thorsos, E. I., K. L. Williams *et al.* (2001). "An overview of SAX99: acoustic measurements." IEEE Journal of Oceanic Engineering **26**(1): 4-25.

Tseng, Y.-T. (2005). Settings of Genetic Programming toward the improvement of acoustic classification performance for different seafloor conditions. Underwater Acoustic Measurements, Crete, Greece. **3**: 1099-1104.

Tseng, Y.-T., A. N. Gavrilov *et al.* (2005a). Classification of acoustic backscatter from marine macro-benthos. Boundary influences in high frequency, shallow water acoustics, Bath, UK: 263-270.

Tseng, Y.-T., A. N. Gavrilov *et al.* (2005b). Implementation of Genetic Programming toward the improvement of acoustic classification performance for different seafloor habitats. OCEANS '05 - Europe, Brest, France. **1**: 634-639.

US Army Engineer Research and Development Center. (2005). "Submersed Aquatic Vegetation Early Warning System (SAVEWS)." from http://www.erdc.usace.army.mil/pls/erdcpub/!www_fact_sheet.PRODUCT_PAGE?ps_product_numb=112825&tmp_Main_Topic=&page=All.

van der Heijden, L. A. M., V. Claessen *et al.* (1983). "Influence of vegetation on acoustic properties of soils." Oecologia **56**(2 - 3): 226-233.

van Keulen, M. (2005). "The Western Australian seagrass web page." from http://wwwscieng.murdoch.edu.au/centres/others/seagrass/index.html.

Walker, D. I., K. A. Hillman *et al.* (2001). "Ecological significance of seagrasses: Assessment for management of environmental impact in Western Australia." Ecological Engineering **16**(3): 323-330.

Walker, D. I., R. J. Lukatelich *et al.* (1989). "Effect of boat moorings on seagrass beds near Perth, Western Australia." Aquatic Botany **36**(1): 69-77.

Walker, D. I. and A. J. McComb (1988). "Seasonal variation in the production, biomass and nutrient status of *Amphibolis antarctica* (Labill.) Sonder ex Aschers. and *Posidonia australis* Hook.f. in Shark Bay, Western Australia." Aquatic Botany **31**(3-4): 259-275.

Walker, D. I. and A. J. McComb (1992). "Seagrass degradation in Australian coastal waters." Marine Pollution Bulletin **25**(5-8): 191-195.

Walter, D. J., D. N. Lambert *et al.* (2002). "Sediment facies determination using acoustic techniques in a shallow-water carbonate environment, Dry Tortugas, Florida." Marine Geology **182**(1-2): 161-177.

Walter, D. J., D. N. Lambert *et al.* (1997). "Mapping sediment acoustic impedance using remote sensing acoustic techniques in a shallow-water carbonate environment." Geo-Marine Letters **17**(4): 260-267.

Weron, R. (2002). "Estimating long-range dependence: finite sample properties and confidence intervals." Physica A: Statistical Mechanics and its Applications **312**(1-2): 285-299.

White, W. H., A. R. Harborne *et al.* (2003). "Using an acoustic ground discrimination system to map coral reef benthic classes." International Journal of Remote Sensing **24**(13): 2641.

Wilding, T. A., M. D. J. Sayer *et al.* (2003). "Factors affecting the performance of the acoustic ground discrimination system RoxAnn(TM)." ICES Journal of Marine Science **60**(6): 1373-1380.

Wildish, D. J., G. B. J. Fader *et al.* (1998). "The acoustic detection and characteristics of sublittoral bivalve reefs in the Bay of Fundy." Continental Shelf Research **18**(1): 105-113.

Wood, N. and P. Lavery (2000). "Monitoring seagrass ecosystem health - The role of perception in defining health and indicators." Ecosystem Health **6**(2): 134-148.

Woods, A. (2004). Epibenthic scattering project, milestone report I: experimental design report. Curtin University of Technology. 18. (Unpublished work).

Wright, L. D., D. B. Prior *et al.* (1987). "Spatial variability of bottom types in the lower Chesapeake Bay and adjoining estuaries and inner shelf." Estuarine, Coastal and Shelf Science **24**(6): 765-784.

From the author's words:

"Every reasonable effort has been made to acknowledge the owners of copyright material. I would be pleased to hear from any copyright owner who has been omitted or incorrectly acknowledged."

Appendices

Appendix A Areal acoustic studies of seagrasses or algae in the world, showing the key research members, the major acoustic devices, and the frequencies used for the study targets. (Note: On first column, the "T or E" under the column represents the attribute of the studies, Theoretical or Experimental, while "T & E" represents both.)[********]

A	Group	Key persons	Acoustic devices	kHz	Study targets	Ref
E	Australia	Hundley	N/A	N/A	N/A	(Hundley and Denning 1994; Hundley, Zabloudil *et al.* 1994)
		Lee Long McKenzie Roder Hundley	Sidescan	420	*H. ovalis* *H. pinifolia* *H. uninervis* *Z. capricorni* *C. serrulata*	(Lee Long, McKenzie *et al.* 1998)
		Jordan Lawler Halley Barrett	Single beam: SIMRAD ES60&EK60 Furuno 600L	120 200	*H. australis* *Z. tasmanica* *P. australis*	(Jordan, Lawler *et al.* 2005)
E	Canada	Duarte	Sitex-Honda HE-356	50	Macrophytes	(Duarte 1987)
		Fortin Saint-Cyr Leclerc	Single beam: Raytheon DE-719	208	*Potamogeton* *Vallisneria* *Nitella* sp.	(Fortin, Saint-Cyr *et al.* 1993)

[********] Table is spanned into three pages and continued on next two pages.

A	Group	Key persons	Acoustic devices	kHz	Study targets	Ref
E	France	Pasqualini Pergent-Martini Clabaut Pergent	Sidescan	N/A	*P. Oceanica*	(Pasqualini, Pergent-Martini *et al.* 1998)
E	Italy	Colantoni	Single beam: Sidescan:	3.5 N/A	*Posidonia*	(Colantoni and Zucchini 1979; Colantoni, Gallignani *et al.* 1982)
		Bozzano Siccardi	Sector Scan: ST2000	2000	*P. Oceanica*	(Siccardi, Bozzano *et al.* 1997; Bozzano, Castellano *et al.* 1998; Bozzano, Mantovani *et al.* 1998; Siccardi and Bozzano 2000; Bozzano, Mantovani *et al.* 2002)
		Lyons Pouliquen	Normal incidence	8 40	*P. Oceanica*	(Lyons and Pouliquen 1998)
			Oblique incidence	30 40 80 90 110		
		Piazzi Acunto Cinelli	Sidescan	100 500	*P. Oceanica*	(Piazzi, Acunto *et al.* 2000)

A	Group	Key persons	Acoustic devices	kHz	Study targets	Ref
E	Japan	Shono Komatsu Sato Koshinuma Tada	Sidescan: Klein 3000	130 445	*Z. caulescens* *Z. asiatica*	(Shono, Komatsu *et al.* 2004)
			Multibeam: Seabat 9001	455		
T & E	Poland	Tęgowski Gorska Klusek	Single beam: BioSonics DT4200	208	Macro algae *Pilayella* sp.	(Tęgowski, Gorska *et al.* 2003)
E	Spain	Siljestrom Rey Moreno	Sidescan: Klein 595	100 500	*P. Oceanica* *C. nodosa*	(Siljeström, Rey *et al.* 1996; Moreno, Siljestrom *et al.* 1998; Siljeström, Moreno *et al.* 2002)
		Carbó Molero	Single beam: IA-100 Raytheon V700 Ulvertech 295	102 201 527	*Gelidium*	(Carbó and Molero 1997)
T	Russia	Shenderov	N/A	N/A	Macro algae	(Shenderov 1998)
E	UK	Stent Hanley	Single beam: Seafarer	N/A	*E. canadensis*	(Stent and Hanley 1985)

A	Group	Key persons	Acoustic devices	kHz	Study targets	Ref
	USA	Maceina Shireman	Single beam: Raytheon DE-719	208	*Vallisneria* *Hydrilla* *Lyngbya*	(Maceina and Shireman 1980)
		Spratt	Lowrance Truline LRG-1510	N/A	*Z. marina*	(Spratt 1989)
		Miner	N/A	N/A	*Z. marina*	(Miner 1993)
		BioSonics Sabol McCarthy Burczinski	Single beam: DT4000 DT6000 Klein 2000 Sidescan: Klein 2000	420 208 100 500	Eelgrass *Z. capricorni* *V. Americana* *T. testufinum* *S. filiforme* *H. wrightii* *Z. marina* *Z. noltii*	(Sabol and Melton Jr. 1995; Sabol and Burczinski 1998; McCarthy and Sabol 2000; BioSonics Inc. 2001b; BioSonics Inc. 2001a; Burczynski, Hoffman *et al.* 2001; Sabol and Johnston 2001; Sabol 2002; Sabol, Burczynski *et al.* 2002; Sabol, Melton *et al.* 2002; Sabol 2005)
		Seaman Finkbeiner Worthy	RoxAnn Groundmaster	200	Macro algae *Ulva*	(Seaman, Finkbeiner *et al.* 2000)
		Riegl Moyer Dodge Morris Virnstein	Single beam: Suzuki TGN60-50H-12L Suzuki TGW50-200-10L	50 200	Seagrass Macro algae	(Riegl, Moyer *et al.* 2005; Riegl, Purkis *et al.* 2005)

Appendix B A system block diagram made by the ESP project member, Dr. Alec J. Duncan, showing the detailed components and data flow directions of the whole ESP data collection system.

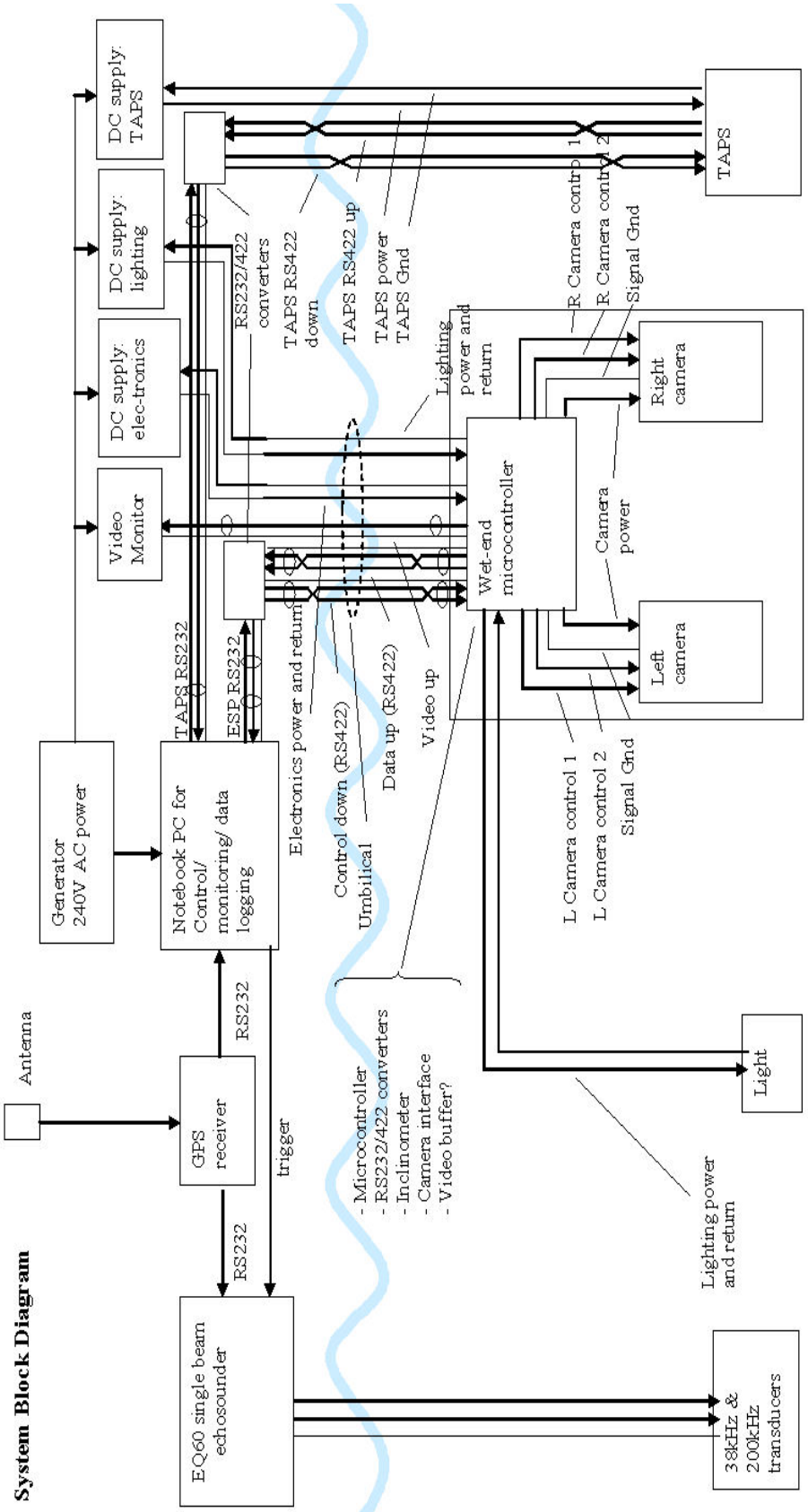

Appendix C Schematic diagram of the wet end micro-controller made by Mr. Andrew Woods.

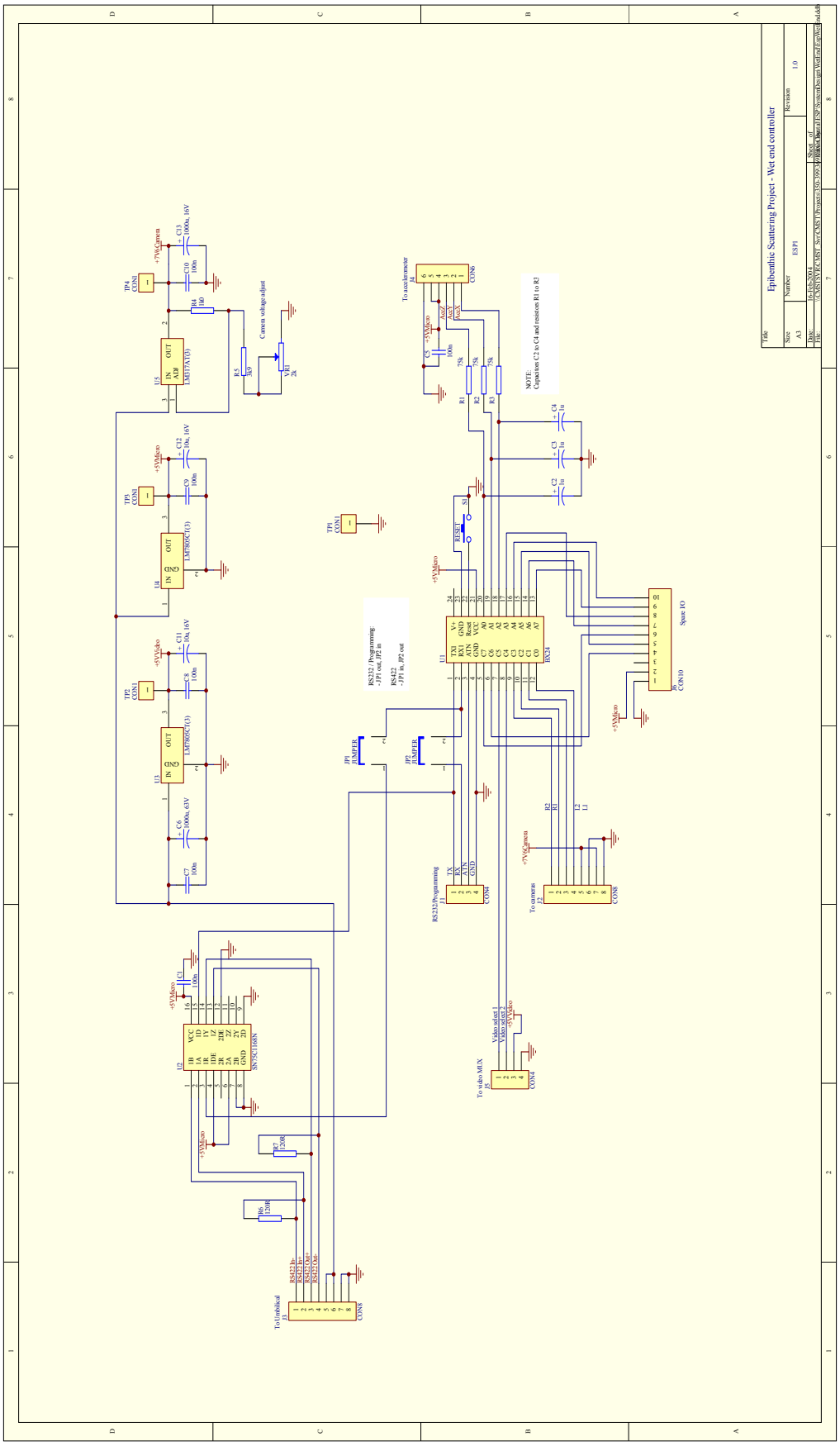

Appendix D Beam patterns of the EQ60 at the 38 kHz Longitudinal, 38 kHz Transverse, and 200 kHz from SIMRAD's product specifications.

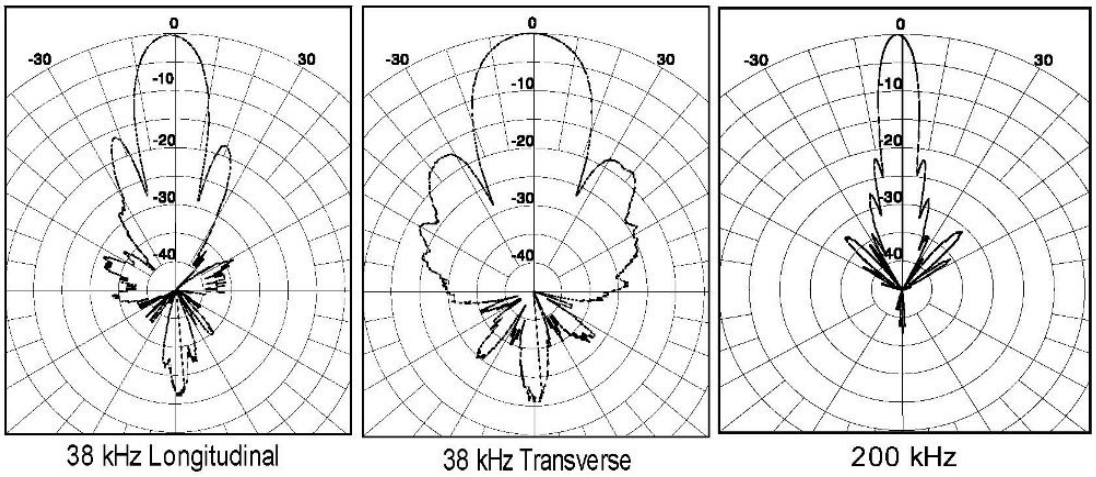

(This page intentionally left blank.)